University of Alberta
Department of Civil &
Environmental Engineering

Structural Engineering Report No. 251

EFFECT OF LOADING ANGLE ON THE BEHAVIOUR OF FILLET WELDS

by

Kam Deng

Gilbert Y. Grondin

and

Robert G. Driver

June, 2003

Effect of Loading Angle on the Behaviour of Fillet Welds

by

Kam Deng

Gilbert Y. Grondin

and

Robert G. Driver

Structural Engineering Report 251

Department of Civil and Environmental Engineering
University of Alberta
Edmonton, Alberta, Canada

June 2003

ABSTRACT

The fillet weld design equation in the North American standards predicts that fillet weld strength increases as the angle between the weld axis and the loading direction increases. An increase of up to 50% is predicted as the loading direction increases from zero (longitudinal welds) to 90 degrees (transverse welds). However, because the results upon which the equation is based were obtained from tests of specimens prepared using shielded metal arc welding, a process that generally produces fillet welds with relatively high toughness levels, the equation may not be suitable for welds deposited using other welding processes. Therefore, the effect of toughness on fillet weld strength and ductility was investigated. Tests were conducted on longitudinal and transverse fillet welds and fillet welds oriented at 45° to the loading direction. The specimens were prepared using the flux cored arc welding process, a process more commonly used in high production shop welding, and filler metals with and without a specified toughness. Higher toughness was found to improve fillet weld ductility and to decrease longitudinal fillet weld strength. A reliability analysis of the test data collected in this test program and a number of other test program indicated that the current North American design equation provides a sufficient safety index.

ACKNOWLEDGEMENTS

This research project was funded by the American Institute of Steel Construction and the Natural Sciences and Engineering Research Council of Canada.

The work presented in this report was conducted with the assistance of Mr. Anthony Ng, Mr. Logan Callele, and Mr. Cameron Franchuk, MSc students, and Mr. Mohammad Behbahanifard, PhD student in the Department of Civil and Environmental Engineering, University of Alberta.

TABLE OF CONTENTS

LIST OF TABLES

LIST OF FIGURES

LIST OF SYMBOLS

$A_{fracture}$	Measured fracture surface area of the weld (mm^2)
A_{throat}, A_w	Theoretical throat area of the weld (mm^2)
d	Average measured weld leg size (mm)
MPL	The main plate leg is the fillet weld leg that is on the main plate of the specimen (mm)
LPL	The lap plate leg is the fillet weld leg that is on the lap plate of the specimen (mm)
P	The applied load resisted by one weld (kN)
P_u	Maximum applied load (kN)
V_G	Coefficient of variation for the measured-to-nominal theoretical throat area of the weld
V_{M1}	Coefficient of variation for the measured-to-nominal ultimate tensile strength of the filler metal
V_{M2}	Coefficient of variation for the measured-to-predicted ultimate shear strength of the filler metal
V_P	Coefficient of variation for the test-to-predicted weld capacity
V_R	Coefficient of variation for the resistance of the weld
P_θ	Fillet weld strength loaded at an angle θ to the weld axis (kN)
X_u, F_{EXX}	Nominal ultimate tensile strength of the filler metal (MPa)
α_R	Coefficient of separation
β	Reliability index
Δ_f	Fillet weld deformation at weld fracture (mm)
Δ_u	Fillet weld deformation at ultimate load (mm)
θ	Angle between the axis of the fillet weld and the direction of the applied load (degrees)
ρ_G	Bias coefficient for the theoretical weld throat area
ρ_{M1}	Bias coefficient for the ultimate tensile strength of the filler metal
ρ_{M2}	Bias coefficient for the ultimate shear strength of the filler metal
ρ_P	Mean test-to-predicted weld capacity
ρ_R	Bias coefficient for the resistance of the weld

τ_u	Measured ultimate shear strength for the fillet weld (MPa)
ϕ , ϕ_w	Weld resistance factor
Φ_β	Adjustment factor for the weld resistance factor

1. INTRODUCTION

1.1 Background

The influence of the angle between the axis of a fillet weld and the direction of the applied load on fillet weld strength and ductility is recognised by both North American steel design standards, CSA–S16–01 (CSA 2001) and AISC (1999). The fillet weld design equations in the two standards predict that fillet weld strength increases as the loading angle increases. In the extreme case where the load is applied perpendicular to the weld axis, the weld strength is 50% higher than the weakest case where the load is applied parallel to the weld axis.

Both design equations are based on the expression proposed by Lesik and Kennedy (1990), which is a simplified version of the original relationship developed by Miazga and Kennedy (1989) using the results from their experimental program. This test program included lap-spliced fillet weld specimens prepared with shielded metal arc welding (SMAW) using one electrode type that had no toughness requirement. However, this welding process is not commonly used in industry for high production welding and tends to produce welds with higher toughness levels than the more prevalent flux-cored arc welding (FCAW) process. For these reasons, and the fact that the toughness of the filler metal used in Miazga and Kennedy's study was not measured, the strength levels attainable by fillet welds loaded in different directions must be investigated. Therefore, additional tests on fillet welds of different measured toughness levels are required in order to determine the effect of toughness on fillet weld behaviour and ensure that the strength improvements recognised by the design provisions are not actually dependent on weld toughness.

1.2 Objectives and Scope

This research project has been separated into three phases, and the overall objective was to determine whether or not the toughness level of the filler metal affects the strength and ductility of fillet welds. In Phase I, described in Ng *et al*. (2002, 2003), transverse welds were investigated, and the effect of several parameters on the strength and ductility of fillet welds was assessed. This report presents Phase II of the research program. Specifically, the effect of weld metal toughness and filler metal classification on the strength and ductility of welds loaded in other directions in addition to the transverse case was examined. Phase III will examine the behaviour of welded connections fabricated with a combination of weld orientations to investigate the effect of the difference in weld ductilities on connection strength.

To achieve the objectives of the second phase, an experimental program consisting of 18 lap-spliced fillet weld specimens was conducted. Nine of these specimens were fabricated with longitudinal welds, and the other nine were fabricated with welds that were oriented at 45° to the loading direction. The specimens were prepared using the FCAW process with electrodes of three different filler metal classifications, namely, E70T-4, E70T-7, and E71T8-K6. The first two filler metals have no toughness requirement while the last one has a toughness requirement of 20 J at –29°C (AWS 1998). The results from three sets of transverse specimens tested in Phase I were also used in this investigation. The fabricator of these specimens and the manufacturer of the filler metals used for their fabrication were the same as the ones used in this phase, providing a direct comparison with fillet welds of different orientations. For completeness, the results from three SMAW specimens from Phase I prepared with the same filler metal type used by Miazga and Kennedy were also included for general comparisons. All results were analysed and compared with the data available in other studies. The applicability of the current design equations to fillet welds made with the three FCAW filler metal types studied was assessed by comparing the predictions with the experimental results and by evaluating the safety index to gauge the level of safety being provided by the design equations.

1.3 Units Used in Report

Although SI units were adopted in this paper, the AWS classification, which is in imperial units, was used to refer to the filler metals. This exception was made because the AWS classification is more commonly used than the equivalent CSA designation. A description of this classification system for SMAW and FCAW electrodes is given in Figures 1.1 and 1.2, respectively.

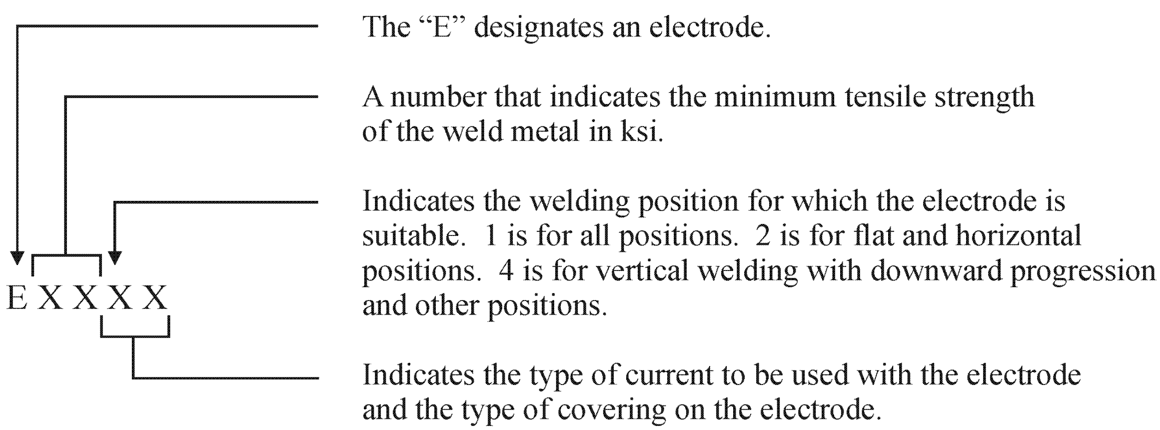

Figure 1.1 – AWS Classification System for Carbon Steel Electrodes for SMAW (AWS 1991)

E X X T - X M

- The “E” designates an electrode.
- A number that indicates the minimum tensile strength of the weld metal in one-tenths of a ksi.
- Indicates the welding position for which the electrode is suitable. 0 is for flat and horizontal positions only. 1 is for all positions.
- The “T” indicates that the electrode is a flux-cored electrode.
- A number that refers to the usability of the electrode.
- An “M” designator indicates that the electrode is classified using 75-80% argon/balance CO_2 shielding gas. When the “M” designator does not appear, it signifies that either the shielding gas used for classification is CO_2 , or that the electrode is a self-shield electrode.

(a) AWS Classification System for Carbon Steel Electrodes

E X X T X - K X

- The “E” designates an electrode.
- A number that indicates the minimum tensile strength of the weld metal in one-tenths of a ksi.
- Indicates the welding position for which the electrode is suitable. 0 is for flat and horizontal positions only. 1 is for all positions.
- The “T” indicates that the electrode is a flux-cored electrode.
- A number that refers to the usability of the electrode.
- Indicates the chemical composition of the weld metal. The “K” is the designator for the group of electrodes which produce weld metals of several different chemical compositions.
- A number that indicates the chemical composition of the weld metal.

(b) AWS Classification System for Low-Alloy Steel Electrodes

Figure 1.2 – AWS Classification System for FCAW Filler Metals (AWS 1995, 1998)

2. LITERATURE REVIEW

2.1 Introduction

When designing fillet welds, two modes of failure must be considered: failure of the base metal and failure of the weld metal. To prevent the former failure mode, the main consideration is the strength of the base metal. However, the capacity of the weld metal is dependent upon the angle between the axis of the weld and the line of action of the applied load. Several studies have shown that as this angle increases, the weld strength increases and the ductility decreases. Therefore, the strength of transverse welds and longitudinal welds represent the upper and lower bounds, respectively, of weld strength. Until relatively recently the effect of the loading angle on fillet weld strength has been ignored by the Canadian standard, and the design of fillet welds has been conservatively based on longitudinal weld strength, irrespective of the weld orientation. This approach allows higher safety margins against failure for weld orientations that tend to fracture in a less ductile manner.

The effect of the loading angle on weld strength has been recognised by the Canadian standard only since the 1994 edition of CAN/CSA–S16.1–94 (CSA 1994). The equation in the design provisions that accounts for this factor is based on research conducted by Miazga and Kennedy (1986, 1989) and Lesik and Kennedy (1988, 1990). However, the standard also permits the designer to disregard the effect of the loading angle. This conservative approach is still used by the American specification (AISC 1999) although the equation incorporating the dependence of weld strength on loading angle is provided as an alternative design method in Appendix J2.4.

The following sections summarise the experimental research programs that have been performed over the last few decades concerning the effect of loading angle on fillet weld behaviour, including those that have led to the equations used in the North American design standards. The literature review focuses on the studies of concentrically loaded joints, although there have also been investigations on eccentrically loaded connections such as the ones by Butler *et al*. (1974), Dawe and Kulak (1974), Swannell (1981*a*, 1981*b*), and Sanaei and Kamtekar (1988). Examples of the theoretical research available on this subject, which are not reviewed here, are Kato and Morita (1974), Kamtekar (1982, 1987), Kennedy and Kriviak (1984), Neis (1985), and Iwankiw (1997).

2.2 Research on the Effect of Loading Angle on Fillet Weld Behaviour

2.2.1 Archer et al. (1959)

Two transverse and two longitudinal weld specimens were included in a test program of eccentrically loaded fillet welds by Archer *et al.* (1959). The welds were approximately 6 mm in size, and no indication was given of the welding process used. The limited test results showed that the transverse welds were 56% stronger than the longitudinal welds.

2.2.2 *Higgins and Preece (1969)*

Higgins and Preece (1969) performed 168 tension tests on longitudinal and transverse fillet welds deposited by shielded metal arc welding (SMAW). The main objective of their research program was to develop simple criteria for the allowable working stress for any combination of weld metal and base metal strength. They also assessed the extent to which weld metal dilution with the base metal affected weld strength. The nominal electrode tensile strengths ranged from 413 MPa to 758 MPa, and the base metal tensile strengths ranged from 410 MPa to 895 MPa. The failure plane for longitudinal welds was reported to occur at an angle less than 45° to the plane of the main plate, while for transverse welds, the angle was much smaller. Specific values for these angles are not reported in their paper. The deformation experienced by the longitudinal welds was observed to reach up to 10% of the weld length. Results indicated that the influence of weld dilution was less than expected; whether a high-strength electrode was deposited on a significantly weaker base metal or on a matching base metal made only a small difference on welded joint resistance. Furthermore, the strength of a weld made with a low-strength electrode on a high-strength steel was found to be almost the same as the weld strength resulting from the same electrode used with a matching base metal. A comparison between the safety factors for longitudinal and transverse welds made with E70XX filler metal gives an average transverse to longitudinal weld stress ratio of 1.57. Higgins and Preece reported that a decrease in the factor of safety also resulted from an increase in weld size.

2.2.3 *Butler and Kulak (1971)*

Butler and Kulak (1971) tested 23 specimens with 6.4 mm fillet welds loaded in tension at 0^o, 30^o, 60^o, and 90^o to the weld axis. All the test specimens were prepared using the SMAW process. The test results were used to incorporate the effect of load direction on fillet weld behaviour in their model for designing eccentrically loaded welded connections. Weld deformations were recorded until the attainment of the ultimate load. As the loading angle became larger, they observed that the weld strength increased and the weld deformation capacity decreased, resulting in a 44% difference in strength and 75% difference in deformation at ultimate load between 6.4 mm transverse and longitudinal fillet welds.

2.2.4 *Clark (1971)*

Clark (1971) also tested fillet welds loaded at 0^o, 30^o, 60^o, and 90^o with respect to the weld axis. The filler metal classification and base metal grade were not reported. The load vs. deformation data from these tests were generally similar to those obtained by Butler and Kulak (1971). From an assessment of the load deformation curves, Clark suggested that transverse welds possess sufficient ductility to allow the strength of commonly sized joints to be taken as the sum of the individual weld strengths. The results showed an increase in strength of approximately 70% as the angle between the direction of load and the weld axis changed from 0° to 90°.

2.2.5 Swannell and Skewes (1979)

As part of the development of an ultimate load prediction model for the design of welded brackets, Swannell and Skewes (1979) derived simplified load vs. deformation curves for 6.4 mm fillet welds oriented at each of 0°, 30°, 60°, and 90° relative to the loading angle. The simplified curves were developed from plots of actual weld response obtained from compression tests on more than 19 weld coupons produced by SMAW. It is not clear from their paper how many valid test results were obtained from their test program since the number of specimens with weld defects is not reported. The welds were deposited over-sized with several passes and then machined to the desired leg length. Three additional sets of four transverse weld specimens were also tested to investigate the effect of weld size on weld strength. Each set was fabricated using welds with one of three leg sizes: 4.5 mm, 6.4 mm, and 7.9 mm. These results suggested that smaller welds have a higher unit strength than larger welds. The reported difference in unit strength between similarly sized longitudinal and transverse fillet welds was 18% to 25%.

2.2.6 Mansell and Yadav (1982)

Mansell and Yadav (1982) examined the results of transverse and longitudinal fillet weld tests, performed by students at the University of Melbourne, to investigate the failure mechanisms of welds. The weld throat sizes ranged from 4 mm to 7 mm. Data from the shielded metal arc specimens verified that welds loaded transversely are stronger than those loaded longitudinally and that increasing the weld size decreases the weld unit strength.

2.2.7 Pham (1983a, 1983b)

Pham (1983a, 1983b) assessed the effect of weld size and welding process on the strength of fillet welds. Transverse welds on cruciform specimens and longitudinal welds on Werner specimens were produced with flux-cored arc welding (FCAW) and submerged arc welding (SAW) processes for testing. Nominal weld sizes of 6 mm, 10 mm, and 16 mm were investigated. The FCAW electrode used had a typical Charpy V-notch impact value of 60 J at 0°C while the SAW electrode used is a general purpose wire. Most of the cruciform specimens fractured in the heat affected zone, while some fractured at the throat. In the FCAW Werner specimens, all failures occurred along the weld throat. The failure loads exceeded the expected capacity considerably due to oversized welds and over-strength wires and showed that the true capacity is mainly a function of the actual throat size, which includes weld penetration and reinforcement. Both the transverse and longitudinal welds exhibited similar trends with respect to weld size. However, while the FCAW fillets on both specimen types showed that weld strength decreased markedly for welds with throats of up to 8 mm in size (leg size of 11.3 mm), with no further reduction for larger welds, the SAW fillets showed that weld strength decreased more gradually over the entire range of the weld sizes studied. The FCAW longitudinal welds displayed higher ductility than the SAW welds, but the reverse was observed for the transverse welds. Ductility also increased with longitudinal weld size for the size range tested; however, the opposite was again observed in the cruciform specimens. Ratios of the longitudinal to transverse weld strengths were determined by comparing the results of the cruciform specimens to those of the Werner specimens. For the FCAW welds, the ratio ranged from 1.39 to 1.55 while for the SAW welds, it ranged from 1.53 to 2.00.

2.2.8 McClellan (1989)

McClellan (1989) performed 96 tests on 6.4 mm and 9.5 mm longitudinal and transverse fillet welds deposited through FCAW. The test specimens were made with high-strength, low-alloy steel plates commonly used in ship structures. Two FCAW electrodes were investigated, namely, MIL-T71T1-HY and MIL-101-TC/TM. These electrodes have a toughness requirement of 27 J at -29°C and 81 J at -51°C, respectively. Weld stress was calculated by dividing the test load by the weld length and the theoretical weld throat determined from weld leg measurements. Fracture surface angles ranged from 42° to 48° for longitudinal fillets and 20° to 25° for transverse fillets. The transverse to longitudinal weld strength ratio averaged 1.51 and 1.39 for the MIL-T71T1-HY and the MIL-101-TC/TM electrodes, respectively.

2.2.9 Miazga and Kennedy (1989)

Miazga and Kennedy (1989) reported the results from 42 fillet weld double lap-spliced test specimens loaded at angles varying from 0^o to 90^o, in 15^o increments. The two weld sizes tested were 5 mm and 9 mm deposited using SMAW with an E7014 weld electrode, which has no specified toughness. The 5 mm welds were deposited in one pass, while the 9 mm welds were laid in three passes. The results showed that the average fracture angle decreased from 49° to 14° as the loading angle increased from 0° to 90°. The ratio of the transverse weld stress to the longitudinal weld stress was 1.28 for the 5 mm welds and 1.60 for the 9 mm welds, with an average of 1.43 for all specimens. Based on the measured data and a free body diagram of a fractured weld, they developed an expression that related weld strength to the loading angle. The transverse to longitudinal strength ratio predicted by this expression is 1.50.

2.2.10 Lesik and Kennedy (1990)

Lesik and Kennedy (1990) formulated a simplified version of the strength equation proposed by Miazga and Kennedy (1989). The equation takes the following form:

$$P_\theta = 0.67\, \phi_w\, A_w\, X_u\, (1.00 + 0.50 \sin^{1.5} \theta) \qquad [2.1]$$

where P_θ is the weld strength when loaded at an angle θ to the weld axis, 0.67 is the shear to tensile strength ratio for weld metal, A_w is the weld area calculated at the throat, X_u is the nominal tensile strength of the filler metal, and ϕ_w is the resistance factor. This equation was later adopted, with a resistance factor of 0.67, by the Canadian design standard CAN/CSA–S16.1–94 (CSA 1994). It deviates from the expression proposed by Miazga and Kennedy by no more than 1.5% and retains the transverse to longitudinal weld strength ratio of 1.50.

2.2.11 Bowman and Quinn (1994)

Bowman and Quinn (1994) investigated the effect of weld size and weld root opening (see Figure 2.1) on weld behaviour. A total of 18 transverse and longitudinal fillet weld specimens prepared using the SMAW process were tested. Three weld sizes (6.4 mm, 9.5 mm, and 12.7 mm) and two weld root opening sizes (1.6 mm ($\frac{1}{16}$"), and 3.2 mm ($\frac{1}{8}$")) were investigated. The smaller root gap, 1.6 mm, is the maximum opening size allowed by the AWS Structural Welding Code (AWS 2002) before the weld leg length must be increased by the size of the opening or before the contractor is required to show that the weld has the required effective throat. The test specimens were prepared using an E7018 welding electrode, which is a low hydrogen electrode. They reported that the angle of failure for transversely and longitudinally loaded specimens was 18° and 58°, respectively. The fillet weld transverse to longitudinal strength ratio ranged from 1.3 to 1.7 for specimens with no weld root opening. The observed strength ratio for the specimens with a weld root opening varied from 1.2 to 1.4.

In the transverse weld specimens, no strong effect of weld size on weld strength was observed. The 12.7 mm fillet welds showed only a 4.5% lower unit strength than that of the 6.4 mm welds. This was not the case for the longitudinal welds. The large longitudinal fillets showed a significant decrease in unit strength compared to the small fillet size. The authors argued that the difference in strength could be partially attributed to the profile of the weld, indicating that the small welds had more convexity than the large welds. The transverse welds were less affected by this factor because the failure surface was closer to the fusion face.

2.2.12 Ng et al. (2002)

Ng *et al.* (2002) investigated the strength and ductility of transverse fillet welds. The objective of the research was to expand the work of Miazga and Kennedy (1986) on transverse welds to include welds produced using the FCAW process and filler metals of different classifications. A total of 102 weld tests were conducted to investigate the effect of the following parameters: filler metal classification, both with and without a toughness requirement; flux-cored versus shielded metal arc welding; weld size and number of passes; weld electrode manufacturer; steel fabricator; low temperature; and weldment geometry (lapped vs. cruciform splice). Weld toughness, weld size, electrode manufacturer, and fabricator were all found to be influential parameters on weld strength. Weld toughness, weld size, root notch orientation, and testing temperature were all found to be influential on weld ductility. It was found that the equation proposed by Lesik and Kennedy (1990) gives a safe prediction of the capacity of transverse fillet welds. The resistance factors used in the CSA and AISC specifications provides a safety index greater than 4.5.

2.3 Summary

A considerable amount of research has been conducted on fillet welds loaded at various angles to the weld axis. Researchers generally agree that weld strength increases with increases in the loading angle. Reports of the strength ratio between transverse and longitudinal fillet welds range from 1.2 to 2.0. Although there is a large quantity of test data, most of the experimental research employed SMAW to prepare the specimens. This welding process is not widely used for production welding and tends to produce welds that are tougher than welds prepared by more common shop processes such as FCAW. Two investigations studied fillets deposited by FCAW, but the electrodes used for the projects have a required toughness. Consequently, there are no results for welds with low toughness levels. Because the effect of weld toughness on weld strength is unclear, further research on fillet welds is required, with filler metal toughness as the main variable of study.

A recent research project at the University of Alberta has looked into the effect of weld toughness and welding process on the strength and ductility of transverse fillet welds (Ng *et al*. 2002). This work needs to be extended to fillet welds loaded at other angles.

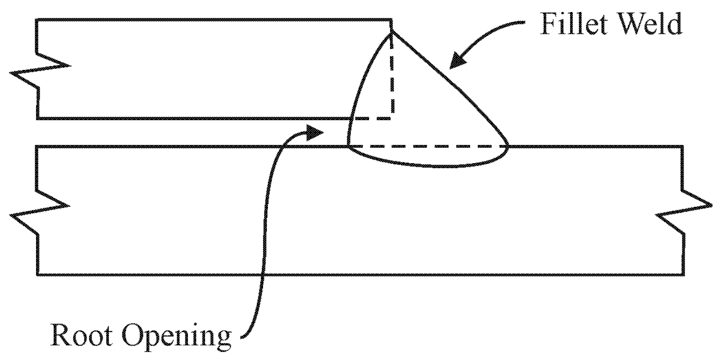

Figure 2.1 – Opening at the Weld Root (Bowman and Quinn 1994)

3. EXPERIMENTAL PROGRAM

3.1 Introduction

The literature review conducted as part of this research has shown that most studies concerning the effect of loading angle on the behaviour of fillet welds used the shielded metal arc welding (SMAW) process for specimen fabrication. However, SMAW can produce welds that are tougher than equivalent welds formed by more widely used welding processes such as flux-cored arc welding (FCAW) and gas-shielded metal arc welding (GMAW). Therefore, a study of the effect of weld metal toughness on the strength and behaviour of fillet welds was initiated to verify the applicability of the current design equation for a broad range of weld metal toughness (Ng *et al*. 2002). This research program has so far investigated the effect of several variables on the strength and behaviour of transverse fillet welds. These variables include filler metal classification and manufacturer, welding process, fabricator, test temperature, and root notch orientation. Since all the work up to this point has been conducted on transverse fillet welds, an extension of this experimental program was therefore designed to determine the effect of weld toughness on the behaviour of fillet welds loaded at other angles. FCAW was chosen to prepare three sets of fillet weld specimens, each with a different angle between the weld axis and the loading direction. The weld orientations studied are 0°, 45°, and 90°. Filler metals both with and without a specified toughness were selected and the fracture toughness, determined from Charpy tests, was measured for each filler metal. A control group of three transverse weld specimens prepared with SMAW was also included. These latter tests and the other transverse fillet weld tests presented in this report were conducted in the first phase of the program presented in Ng *et al*. (2002).

3.2 Filler Metal

Three FCAW filler metals were selected for this study: two with no specified toughness, E70T-4 and E70T-7, and one with a toughness requirement of 20 J at –29°C, E71T8-K6. The SMAW filler metal used in this investigation, E7014, has no toughness requirement and is the same electrode type that was used by Miazga and Kennedy (1989). As determined from a previous investigation (Ng *et al*. 2002), the selected filler metals provide a wide range of weld metal toughness. All the flux-cored wires used in this test program were manufactured by Hobart Brothers Corporation while the SMAW electrodes were manufactured by the Lincoln Electric Company. The filler metals of the same classification were obtained from the same spool. Further information regarding the flux-cored filler metals is presented in Table 3.1.

3.3 Base Metal

All plates used for the transverse weld specimens met the requirements of CAN/CSA–G40.21–98 grade 350W (CSA 1998) and ASTM A572 grade 50 (ASTM 2000) steel. All the plates used for the longitudinal and 45-degree weld specimens conformed to the specifications of CAN/CSA G40.21–98 Grade 300W steel. Four different plate thicknesses were used in the fabrication of the specimens: 15.9 mm, 25.4 mm, 31.8 mm, and 50.8 mm. In order to minimise the sources of variation in the test results, plates of the same thickness were obtained from the same heat, except for the 25.4 mm plates. The 25.4 mm plate used for the fabrication of the transverse weld specimens and the one used for the fabrication of the longitudinal and 45-degree weld specimens came from different heats.

3.4 Specimen Design

All specimens were fabricated as double lap-spliced joints (Figures 3.1 to 3.3) with 12.7 mm fillet welds oriented at one of three angles with respect to the loading direction: 0°, 45°, and 90°. The first phase of the test program included two weld sizes: 6.4 mm and 12.7 mm (Ng *et al*. 2002). Only one of the two sizes (12.7 mm) studied in the first phase of the project was chosen for investigation in order to reduce the number of specimens. Because numerous studies (Higgins and Preece 1969; Swannell and Skewes 1979; etc.), including Phase I of the present research program, have shown that weld strength decreases with increasing weld size, the larger weld size was selected to be conservative. For each weld orientation, three specimens were fabricated with each flux-cored electrode classification listed in Table 3.1. Three additional transverse weld specimens were prepared with the SMAW process for a total of 30 specimens. All plates were made sufficiently thick to allow fracture to occur in the welds, but they were not designed to prevent yielding before fracture. The test matrix summarising this information is shown in Table 3.2.

The welds at one end of each specimen were reinforced to force failure to occur at the other end, thus reducing the amount of instrumentation required. The welds that were not reinforced are referred to in the following as the "test welds." The transverse and 45-degree welds were reinforced by depositing three additional weld passes after the specimens had been received from the fabricators. The longitudinal welds were reinforced through the design of the specimens as described below.

Transverse fillet weld specimens of the same filler metal classification were designed to be fabricated together in one assembly. An extra 100 mm was added to the width of the assembly to avoid including the weld starts and stops within the test specimens. Three specimens, with weld lengths of 76 mm, were later cut from the assembly. Figure 3.1 shows a typical assembly for the transverse weld specimens.

The 45-degree specimens were designed to be fabricated individually with the aid of run-on and run-off tabs as illustrated in Figure 3.2. The 54 mm width was chosen to produce the same weld length as the transverse fillet welds.

The longitudinal weld specimens were also fabricated individually but, due to the specimen design, only one run-off tab was required (Figure 3.3b). Unlike the other specimen types, the two main plates were placed against one another with no gap in between, an arrangement that allowed for continuous welds on each side of the splice plates. These fillets would later be separated into test welds and reinforced welds. The reinforced welds were of the same size as the test welds, but their length was twice the test weld length of 51 mm. The longitudinal test welds were made shorter than the transverse and 45-degree fillets in order to keep the weight of the test specimens at a reasonable level so that the specimens could be lifted into the testing machine manually.

3.5 Specimen Designation

A system for identifying the specimens has been developed that separates the specimens, by weld orientation, into three series. Each series is further divided into groups (also called assemblies), which consist of three nominally identical specimens, according to the electrode type involved in specimen production. The assembly designations are composed of a letter and a number. The letter identifies the series to which the assembly belongs, and the number is the number of the assembly itself. The specimen designation consists of the assembly designation followed by a dash and a number ranging from one to three. A typical specimen designation is illustrated in Figure 3.4. The assembly numbers for the transverse welds are not consecutive because the designations that were used in Phase I have been retained.

3.6 Specimen Fabrication

The SMAW specimens were fabricated by Waiward Steel Fabricators Ltd., while the FCAW specimens were fabricated by Supreme Steel Ltd. All welding was performed in the horizontal position, and the welds were deposited in three passes. Before welding, the plates were ground free of mill scale in the area to be welded. The welding procedures used were within the specifications of the filler metal manufacturer and are shown in Appendix A.

3.7 Ancillary Test Specimens

3.7.1 Base Metal Tension Tests

The base metals chosen for this project are considered to match the selected electrode classifications, and thus their exact material properties are not expected to significantly affect the fillet weld behaviour. Nevertheless, tension coupon tests were performed on the 350W plates. Three coupons for each of the two thicknesses were cut. The tension tests were conducted in a MTS 1000 testing machine following the procedure given in ASTM A370-97 (ASTM 1997). The strains were measured over a 50 mm gauge length using an electronic extensometer. No tension coupons were prepared for the three 300W plates.

3.7.2 Chemical Analysis of Weld Metal

A chemical analysis of the filler metals was performed in accordance with the appropriate AWS specification (AWS 1991, 1995, 1998) for each filler metal. The chemical pads for the analysis were prepared by Waiward Steel Fabricators Ltd. for the first phase of this test program (Ng *et al*. 2002).

3.7.3 Weld Metal Tension Tests

For each filler metal, two weld metal tension coupons were prepared and tested in accordance with the AWS specifications (AWS 1991, 1995, 1998). As for the base metal tension coupon tests, a MTS 1000 universal testing machine was used for the testing, and the strains were measured over a 50 mm gauge length using an electronic extensometer.

3.7.4 Charpy V-Notch Impact Tests

Charpy V-notch specimens for each filler metal were machined from the same assemblies from which the weld metal tension coupons were produced. Following the instructions prescribed by the AWS specifications (AWS 1991, 1995, 1998), the specimens were tested at three different temperatures: -29°C, 21°C, and 100°C. The -29°C temperature is the temperature at which filler metal E71T8-K6 has a toughness requirement of 20 J.

3.7.5 Diffusible Hydrogen Tests

The spools of flux-cored weld wire had been in storage for several months before they were used for specimen fabrication. In order to confirm that the amount of diffusible hydrogen in these filler metals was still within acceptable levels, diffusible hydrogen tests were performed. Filler metals E70T-7 and E71T8-K6 were chosen for testing. Because all the wires were stored under the same conditions, E70T-4 was expected to possess hydrogen levels similar to those of the analysed wires. The samples were prepared using the same welding procedures employed during specimen fabrication and were tested according to the specifications given in ISO standard 3690 (ISO 2000).

3.8 Test Specimen Preparation

After the specimens were received in the laboratory, they were inspected for weld quality, and the following adjustments were made to prepare them for testing. On the transverse and 45-degree weld specimens, the end that appeared to contain the lower quality welds was reinforced, and the run-on and run-off tabs were sawn off. On the longitudinal weld specimens, two cuts per weld were made to separate the test weld from the remaining weld sections. One cut was required where the weld bridged the two main plates, and another was required at the run-off tab (Figure 3.3b).

Before testing, several measurements were performed to characterise the test welds. The two weld legs were measured at 10 mm intervals along the weld length with a caliper. At these same locations, measurements of the weld profile made at 45º were taken using an adjustable fillet weld gauge (Figure 3.5). Two additional weld size measurements were made for the transverse welds at the locations shown in Figure 3.5. The actual length of each weld was also recorded. Summaries of the mean weld dimensions are given in Tables 3.3 to 3.5. The complete data set and the plots of the weld profiles are reported in Appendix B.

Linear variable differential transformers (LVDTs) were mounted on the specimens using custom mounting brackets designed to measure deformation within the leg dimension of the fillet welds (Figure 3.6). Two hardened steel anchors used to support one end of the mounting bracket were set in two light punch marks made on the base plates at the toe of the welds (Figures 3.7a and 3.7b). The punch marks ensured that the two hardened steel anchors of the LVDT brackets remained in place during the test. The rear of each bracket had two rollers to stabilize the assembly while at the same time eliminating longitudinal restraint. On the longitudinal weld specimens, the punch marks were made near the edge of the run-off tab, which had been sawn apart from the test weld (Figure 3.7c).

The gauge length used to calculate strain in the transverse weld specimens was taken as the average weld leg size measured at the two punch mark locations. For the 45-degree welds, the gauge length was taken as this average multiplied by the sine of 45° to obtain the weld dimension parallel to the loading direction. The displacement measurements for the longitudinal welds were either made over the full length of the test welds or over the gap between the run-off tab and the splice plate. The gauge length used for strain calculations was taken as the average weld leg size.

3.9 Instrumentation and Test Setup

The tests were conducted in a universal testing machine with a capacity of 1750 kN, and all displacement and load measurements were collected electronically through a data acquisition system. The behaviour of the welds was monitored throughout the test by using LVDTs and a LabView® program to display the plots of the load and deformation.

The arrangement of the instrumentation for each specimen type is depicted in Figure 3.6. On both the transverse and 45-degree weld specimens, LVDTs were placed at approximately 5 mm to 10 mm from the edges of the specimens at each test weld, giving a total of four sets of weld deformation measurements per specimen. Two additional LVDTs were required for the longitudinal weld specimens because two different weld deformations were measured. One was the shear deformation, and the other was the overall elongation of the welds. If the plates remained elastic during the tests, the magnitude of the shear deformation and the overall weld length deformation should be almost identical. However, if the base plate yields, a significant difference between the two sets of readings would be expected. These LVDTs were located on top of the run-off tab rather than directly on the main plate as shown in the Figure 3.6c. The shear deformation, measured across the gap between the run-off tabs and the lap plates, was monitored by one LVDT on each face of the specimen. The LVDT was located at the specimen mid-width in order to capture the average shear deformation of both welds on one face. Two additional LVDTs on each face measured the overall deformation of the four welds.

All weld deformations were monitored using LVDTs with a nominal linear range of 5 mm. The actual linear range and the calibration factor were obtained for each LVDT before testing. The LVDTs were oriented parallel to the direction of the load in all cases.

Because the thickness of the lap plate in the longitudinal and transverse weld specimens was not large enough to meet the LVDT probes, small tabs were mounted on the test specimens as shown in Figures 3.6a and 3.6c to reach the probes. Although the lap plate thickness of the 45-degree weld specimens presented no such difficulty, tabs were nevertheless needed to prevent slippage of the probe along the angled plate surface. These tabs were glued into position as shown in Figure 3.6b once the natural resting point of the probes on the lap plate surface was determined.

3.10 Testing Procedure

To install a specimen into the testing machine, the end with the reinforced welds was first inserted into the top grips, centred, and secured within the grips. The specimen was then aligned vertically before clamping the bottom grips onto the main plate. To ensure that the grips were fully engaged, the machine crosshead was adjusted to remove any slack between the grips and the specimen. Figure 3.8 shows a typical test setup.

The tests were conducted using stroke control. Several static points were taken throughout the tests of each specimen.

Data was collected until the first weld fractured. After that point, the loading valve was closed to allow safe removal of the instrumentation, and loading was continued until complete separation of the specimen into two pieces. This last step facilitated the removal of the specimens from the testing machine.

3.11 Fracture Information

After testing, the fractured specimens were photographed, and further information was collected from the weld fracture surface. All measurements were taken at the same locations marked previously for the leg size measurements. The width of the fracture surface, from the weld face to the root, was measured with an electronic caliper. Since fracture exposes the weld root, the size of the weld shear leg, including weld penetration, was also measured with a caliper. The angle between the weld shear leg on the main plate and the fracture surface (see Figure 3.9) was measured using a vernier bevel protractor. Once all measurements were completed, some fracture surfaces were selected to be cut and examined using a scanning electron microscope to determine the mode of failure.

Table 3.1 – Flux-Cored Wire Information

AWS Classification	Proprietary Designation	Spool Lot Number	Wire Diameter (mm)
E70T-4	Fabshield 4	04-24-250C 54208B0661	2.38
E70T-7	Fabshield 7027	S222729-014 F00836-001	2.38
E71T8-K6	Fabshield 3Ni1	S226625-029 E11187-001	1.98

Table 3.2 – Test Matrix

Filler Metal Classification	E7014	E70T-4			E70T-7			E71T8-K6		
Weld Orientation	90° †	0°	45°	90° †	0°	45°	90° †	0°	45°	90° †
Number of Specimens	3	3	3	3	3	3	3	3	3	3
Number of Charpy Tests	3 x 2	3 x 2			3 x 2			3 x 2		
Number of Material Tension Tests	2	2			2			2		

† Specimen results also reported in Ng *et al*. (2002)

Table 3.3 – Mean Weld Dimensions for Transverse Weld Specimens

Specimen Designation	Front Face						Back Face					
	Shear Leg (mm)	Tension Leg (mm)	45° Measurements			Weld Length (mm)	Shear Leg (mm)	Tension Leg (mm)	45° Measurements			Weld Length (mm)
			Upper (mm)	Throat (mm)	Lower (mm)				Upper (mm)	Throat (mm)	Lower (mm)	
T20-1	13.4	14.2	4.7	9.8	5.6	75.8	13.3	13.7	4.9	10.3	6.3	75.8
T20-2	12.8	13.2	4.0	9.2	5.1	76.0	13.4	14.6	4.7	9.6	5.8	75.9
T20-3	13.3	14.1	5.4	10.1	5.5	76.0	13.9	13.6	4.3	9.4	5.6	76.2
T22-1	9.4	10.6	3.6	7.8	3.2	76.2	11.1	11.9	4.8	9.2	4.2	76.1
T22-2	10.3	10.0	3.3	8.0	3.6	76.1	10.8	11.5	4.9	9.0	4.0	76.1
T22-3	11.1	10.1	3.4	8.4	4.2	76.0	10.1	11.6	4.4	8.5	3.3	76.1
T26-1	12.4	11.6	4.8	9.5	4.9	76.0	13.2	10.6	3.7	9.0	4.8	76.3
T26-2	12.4	11.9	4.9	9.5	5.0	75.9	12.7	11.2	4.4	9.2	4.8	76.1
T26-3	13.0	11.7	4.6	9.3	5.1	76.2	13.0	11.6	4.4	9.3	5.0	76.2
T32-1	12.3	11.2	4.1	8.8	4.3	76.0	12.2	12.7	4.8	8.9	4.4	76.2
T32-2	11.4	11.7	4.4	9.1	4.6	76.1	12.1	12.7	4.7	9.0	4.7	76.1
T32-3	10.5	12.9	5.0	8.7	4.1	76.0	12.2	11.8	4.4	9.0	4.6	76.1

Table 3.4 – Mean Weld Dimensions for 45-Degree Weld Specimens

Specimen Designation	Front Face				Back Face			
	Shear Leg (mm)	Tension Leg (mm)	45^o Meas. (mm)	Weld Length (mm)	Shear Leg (mm)	Tension Leg (mm)	45^o Meas. (mm)	Weld Length (mm)
F1-1	11.3	10.8	8.7	73.7	11.8	11.0	8.6	72.5
F1-2	9.9	9.5	7.1	71.0	10.9	9.7	7.4	73.4
F1-3	9.5	10.0	8.0	71.7	11.1	10.4	8.3	74.0
F2-1	9.5	10.1	7.6	71.8	9.9	11.4	7.6	70.8
F2-2	10.7	11.2	8.1	72.7	10.3	11.0	8.2	71.0
F2-3	9.3	11.0	7.5	70.6	11.0	11.0	8.1	75.6
F3-1	10.0	12.3	8.8	70.2	10.5	13.4	8.8	71.1
F3-2	10.3	10.7	7.6	71.8	9.5	11.5	7.6	72.7
F3-3	9.2	12.6	7.6	72.1	9.5	13.0	8.6	70.1

Table 3.5 – Mean Weld Dimensions for Longitudinal Weld Specimens

Specimen	Front Face								Back Face							
	Weld 1		Weld 2		45° Measurement		Weld Length		Weld 3		Weld 4		45° Measurement		Weld Length	
Designation	MPL† (mm)	LPL‡ (mm)	MPL† (mm)	LPL‡ (mm)	Weld 1 (mm)	Weld 2 (mm)	Weld 1 (mm)	Weld 2 (mm)	MPL† (mm)	LPL‡ (mm)	MPL† (mm)	LPL‡ (mm)	Weld 3 (mm)	Weld 4 (mm)	Weld 3 (mm)	Weld 4 (mm)
L1-1	10.6	11.4	8.7	9.4	5.9	7.2	49.6	50.6	10.5	10.6	10.0	11.0	8.4	7.6	49.3	47.9
L1-2	11.3	11.5	11.7	10.4	7.8	7.8	49.9	50.0	11.0	9.6	10.9	9.4	7.6	7.4	50.4	49.6
L1-3	10.8	11.5	9.4	10.7	8.0	6.9	48.3	50.8	10.8	10.1	10.3	10.4	7.6	7.3	49.5	49.5
L2-1	10.9	12.0	10.7	11.4	9.2	8.2	48.0	49.7	10.8	11.3	11.6	11.2	8.0	7.3	49.6	49.5
L2-2	10.3	11.0	10.0	10.1	6.9	6.8	48.9	50.0	12.3	11.0	9.8	11.6	7.7	6.5	49.9	48.9
L2-3	11.2	11.9	9.8	11.2	9.0	7.3	49.8	49.8	10.5	11.8	10.5	11.0	8.2	7.9	46.6	49.2
L3-1	10.0	11.9	10.3	10.8	9.1	9.7	49.3	50.5	9.8	10.7	9.0	10.7	8.0	8.2	48.9	50.1
L3-2	9.5	12.2	9.7	11.4	7.6	6.8	48.3	49.6	9.6	12.0	10.0	11.1	8.3	7.4	50.3	49.2
L3-3	9.3	11.3	11.7	11.5	7.5	8.9	50.9	51.1	10.7	10.2	9.7	9.8	8.6	8.2	52.1	50.2

† Main Plate Leg – Size of the weld leg on the main plate.

‡ Lap Plate Leg – Size of the weld leg on the lap plate.

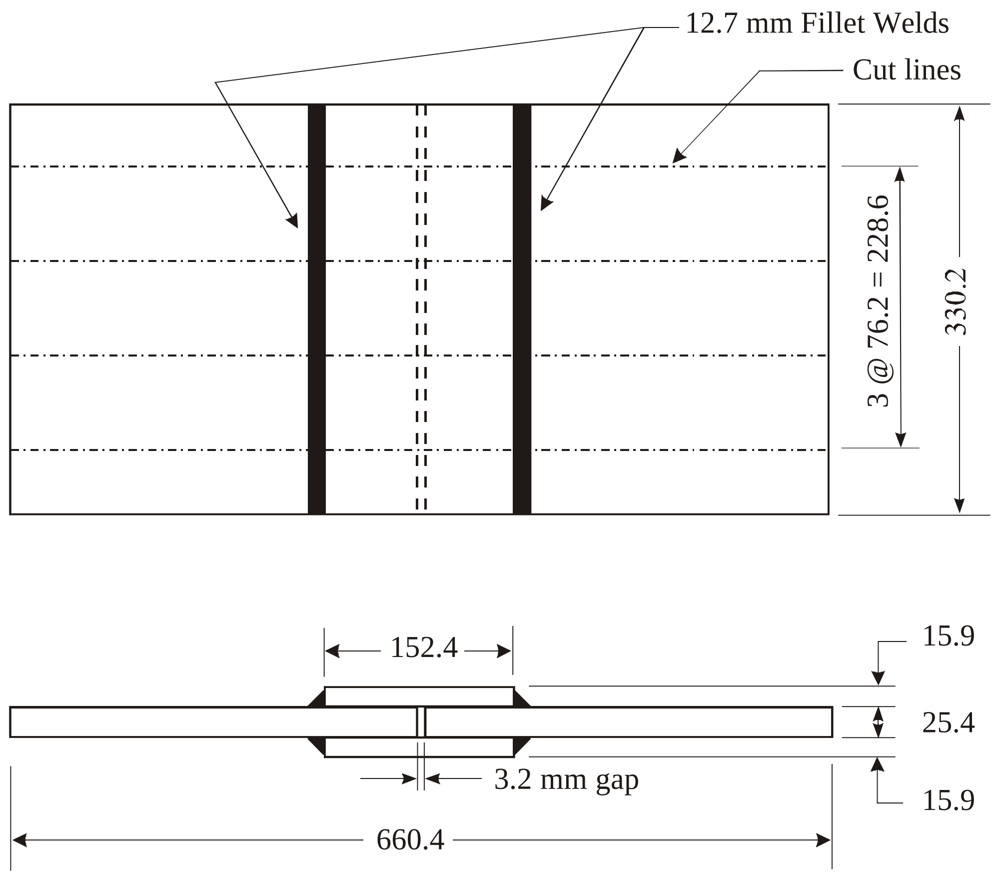

Figure 3.1 – Transverse Fillet Weld Specimens (Ng *et al*. 2002)

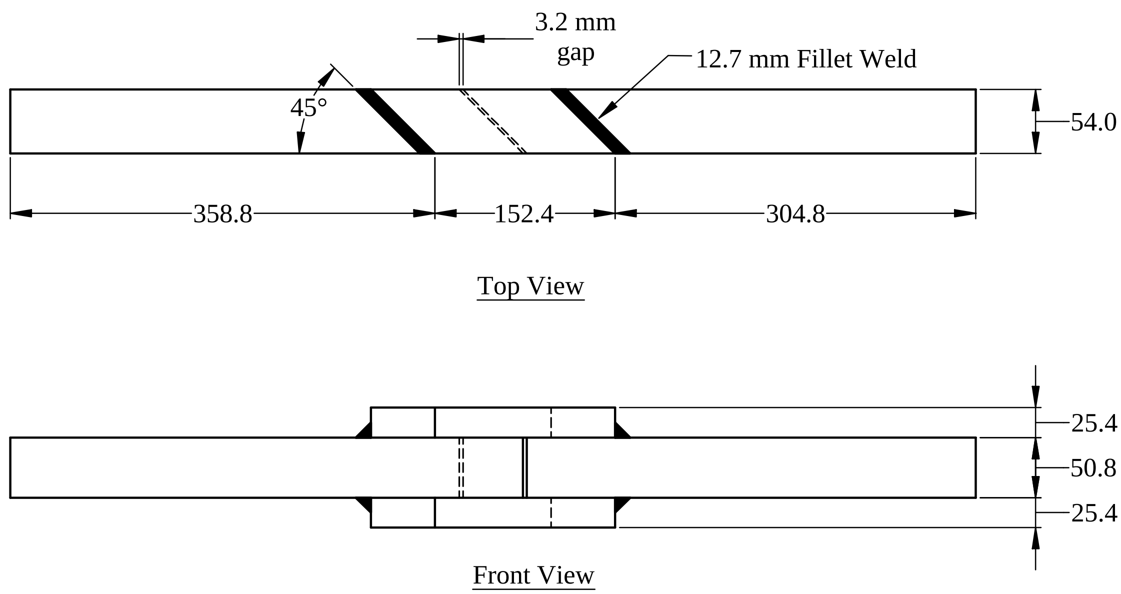

a) 45-Degree Fillet Weld Specimens

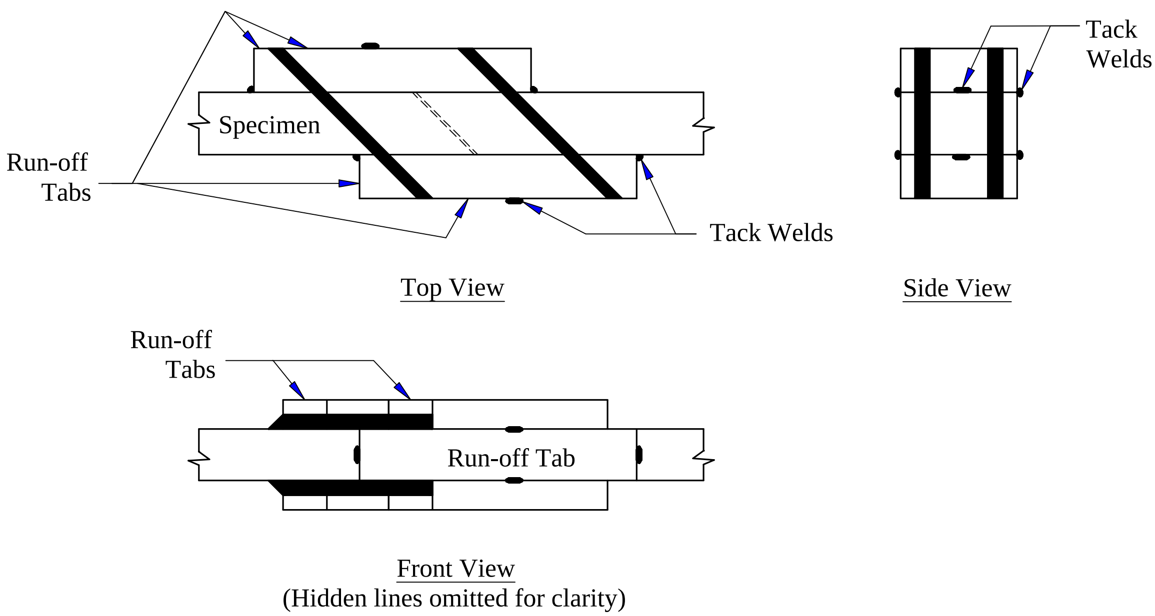

b) Run-Off Tab Details

Figure 3.2 – 45-Degree Fillet Weld Specimens and Run-Off Tab Details

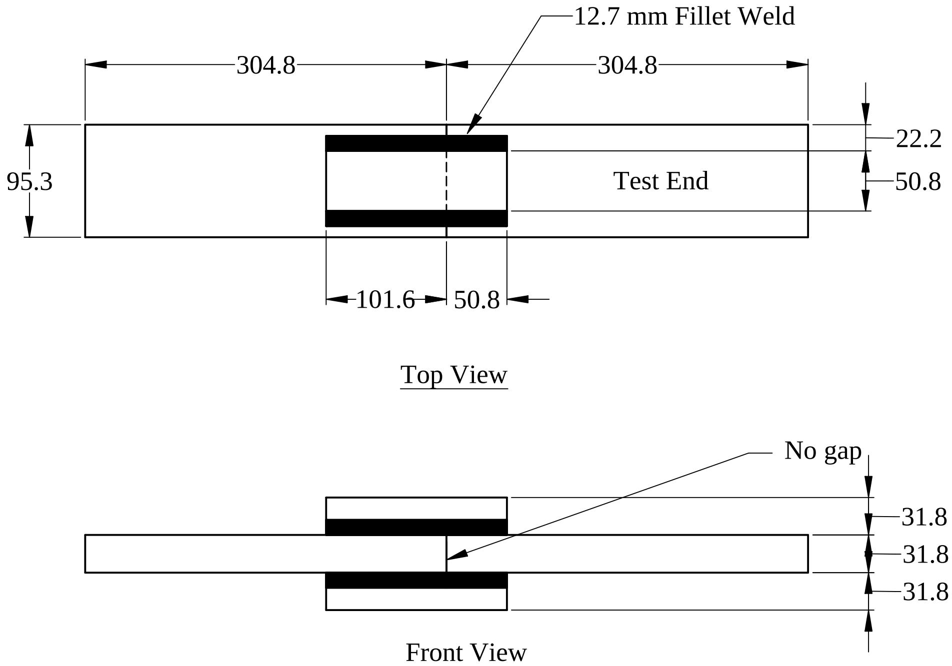

a) Longitudinal Fillet Weld Specimens

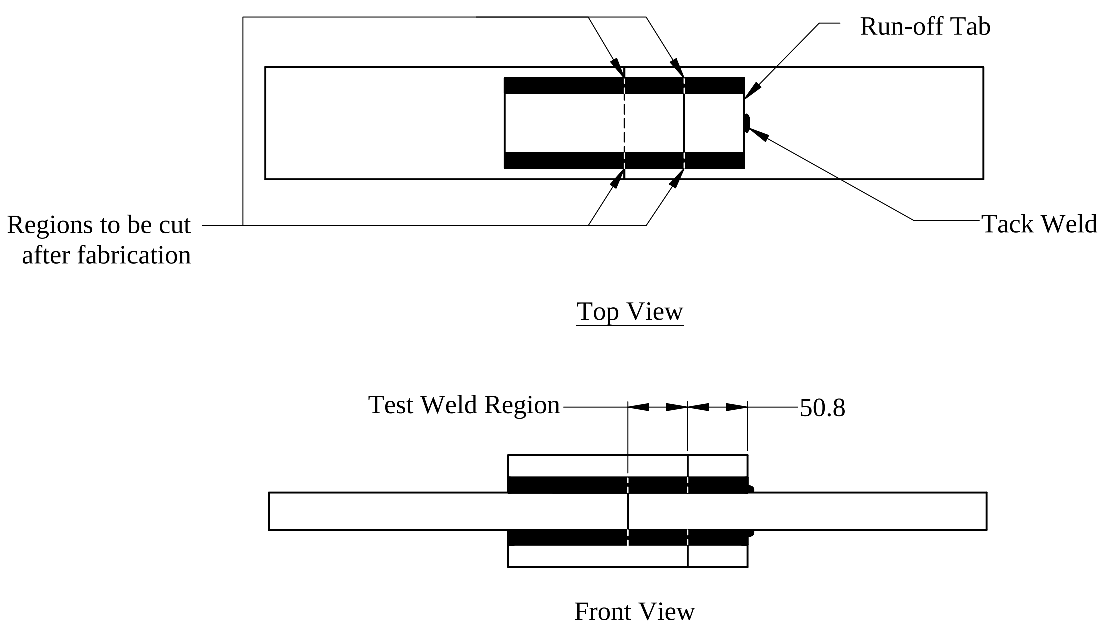

b) Run-Off Tab Details

Figure 3.3 – Longitudinal Fillet Weld Specimens and Run-Off Tab Details

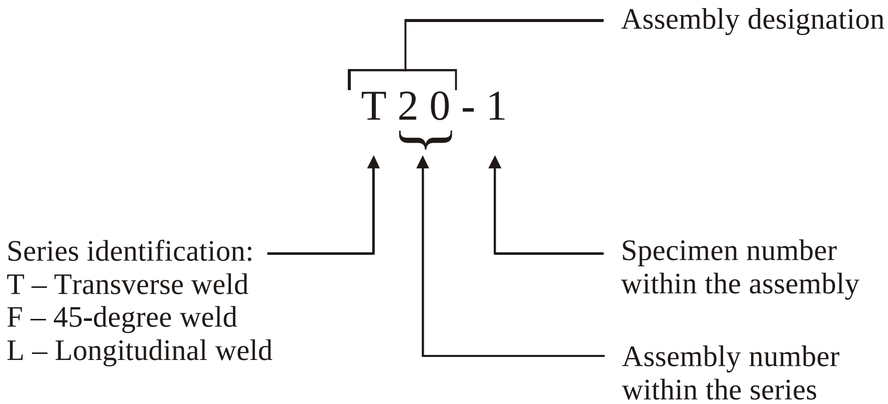

Figure 3.4 – Typical Specimen Designation

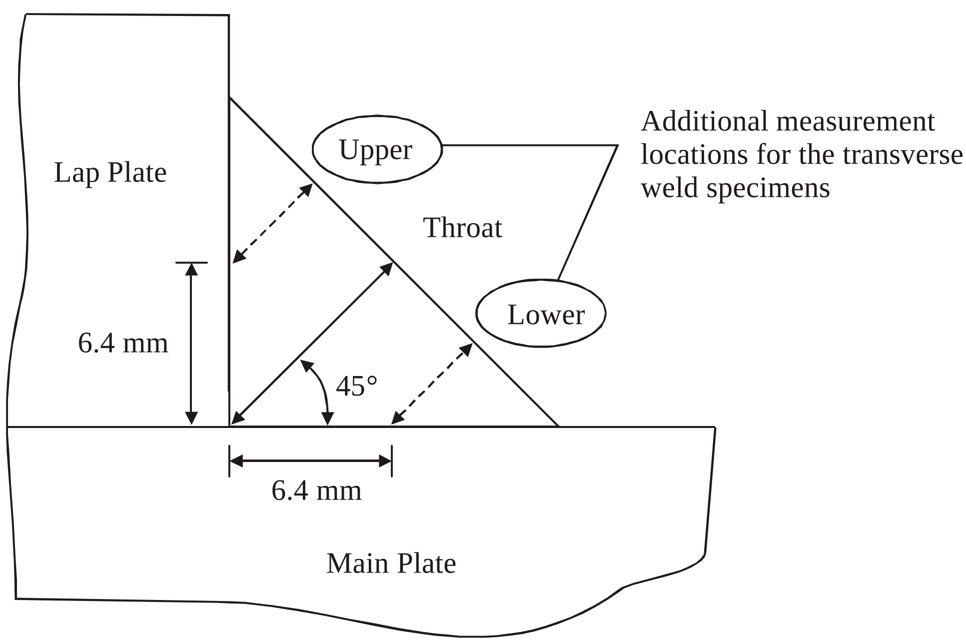

Figure 3.5 – Fillet Weld Measurements Made at 45º

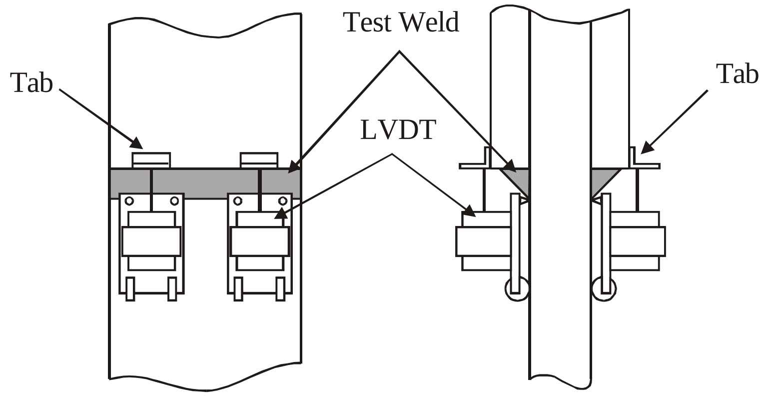

a) Transverse Fillet Weld Specimen

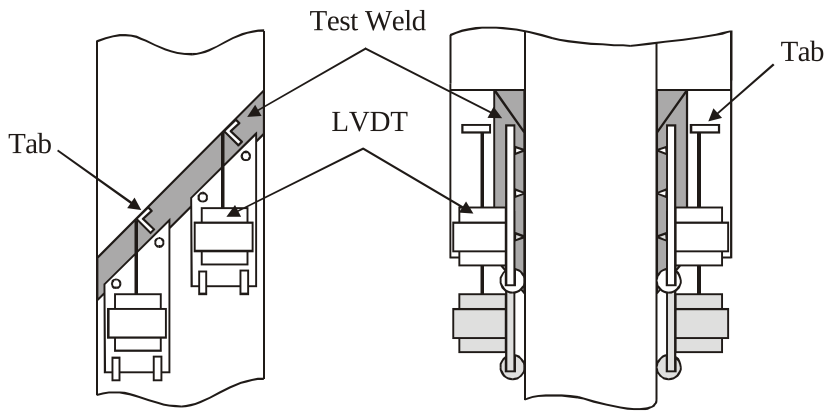

b) 45-Degree Fillet Weld Specimen

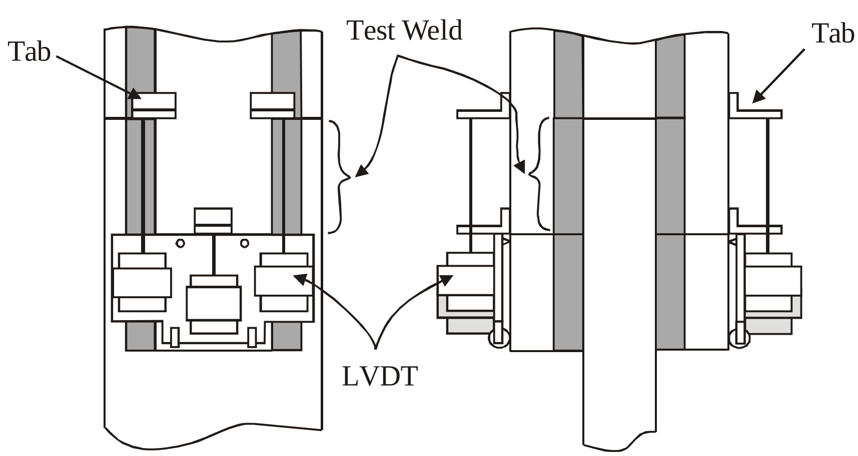

c) Longitudinal Fillet Weld Specimen

Figure 3.6 – Arrangement of Instrumentation on Each Specimen Type

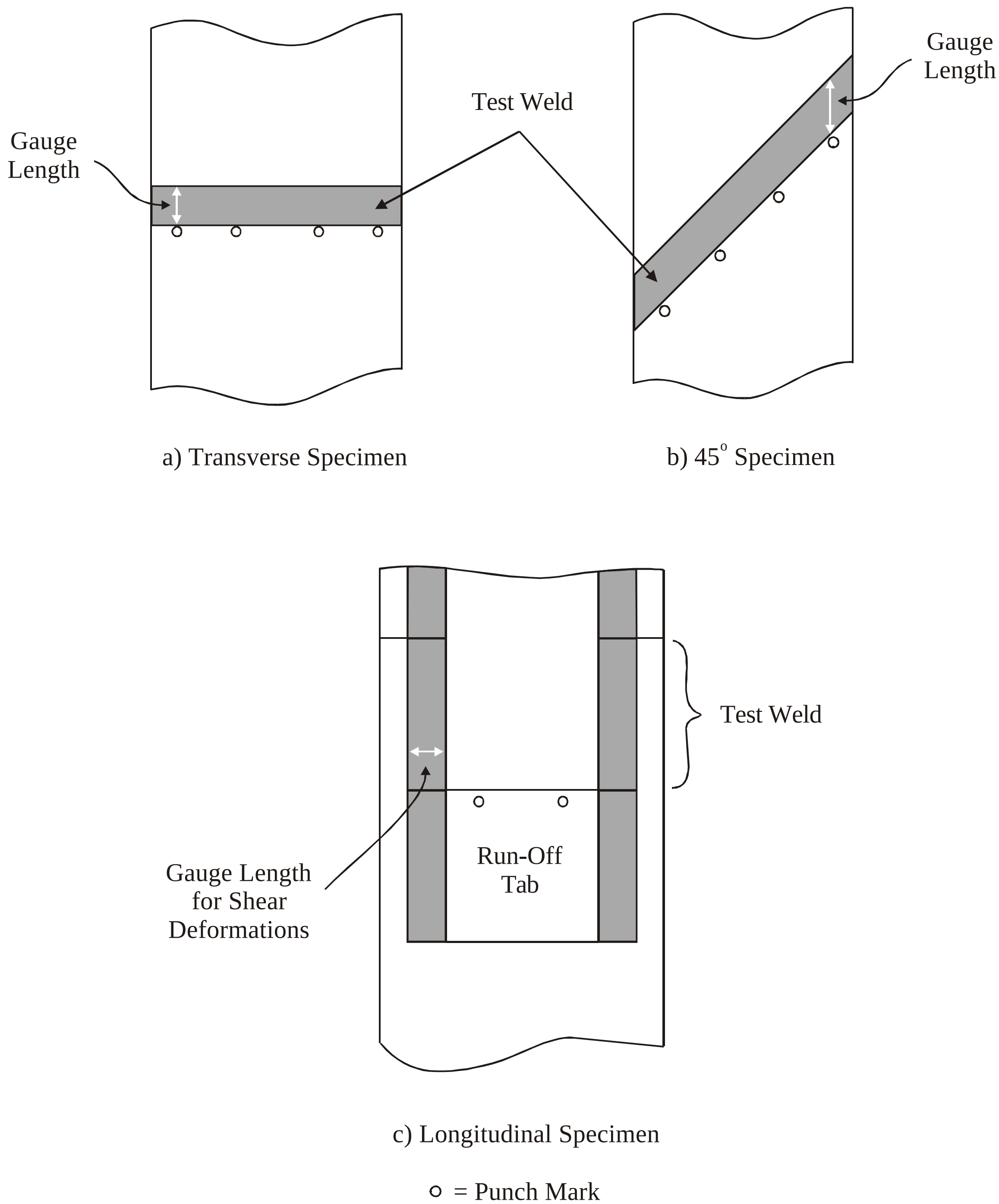

Figure 3.7 – Location of Punch Marks Used to Position the Instrumentation

Figure 3.8 – Typical Test Setup

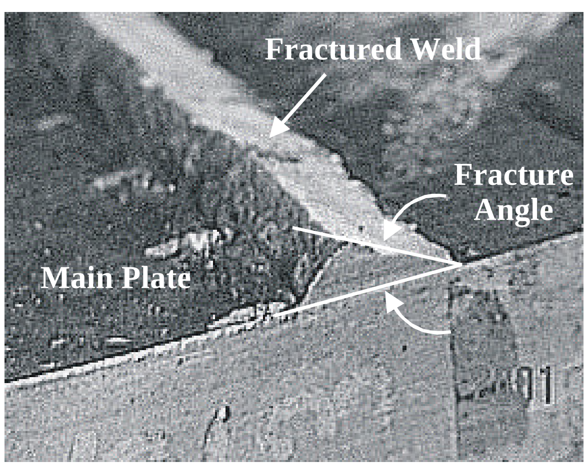

Figure 3.9 – Fracture Angle Measurement

4. TEST RESULTS

4.1 Ancillary Test Results

The results of ancillary tests for the base metal and weld metal are reported in the following. They are also published in Ng *et al*. (2002), except for the results from the diffusible hydrogen tests.

4.1.1 Base Metal Tension Tests

The mean mechanical properties of the base metal are presented in Table 4.1. Two entries appear for the 25.4 mm plates because the plate used for fabrication of the longitudinal and 45-degree weld specimens and the plate used for the transverse weld specimens originated from different heats. The material properties for the plates used in the transverse weld specimens were obtained from tension coupon tests, whereas the material properties for the remaining plates were obtained from mill certificates, as noted in the table.

Two tension coupons were tested from each of the two plate thicknesses used for the transverse weld specimens. Negligible variation in the stress vs. strain curves was observed between coupons from the same source plate. The yield strength was obtained using the 0.2% offset method. Except for the plates for which the results from the mill certificates are reported, Table 4.1 lists static values of the yield and tensile strengths. The properties of the tested coupons conformed to the specifications for CAN/CSA G40.21–98 Grade 350W steel, while those plates for which only mill certificate results are available conformed to the specifications for CAN/CSA G40.21 Grade 300W steel. The detailed test data and the graphs of the load deformation curves are given in Appendix C.

4.1.2 Weld Chemical Analysis

The results of the chemical analysis are reported in Table 4.2. All values fell within the limits prescribed in the AWS standard to which each electrode classification belongs (AWS 1995, 1998). As expected, the filler metal with a toughness requirement has higher nickel content and lower aluminum content.

4.1.3 Weld Metal Tension Tests

Table 4.3 summarises the mean results of the weld metal tension coupon tests. The test results for each coupon and the stress vs. strain curves are presented in Appendix C. All weld assemblies from which the coupons were cut were prepared by Supreme Steel except for the assemblies made with the E7014 and E70T-7 filler metals, which were prepared by Waiward Steel Fabricators Ltd. The static yield strengths were determined using the 0.2% offset method.

The specifications to which these tension coupon test results must conform are AWS A5.1-91, AWS A5.20-95, and AWS A5.29-98 (AWS 1991, 1995, 1998). The minimum yield strengths for the SMAW filler metal and the three FCAW filler metals are 399 MPa and 400 MPa, respectively. The minimum tensile strengths for the SMAW filler metal and the three FCAW filler metals are 482 MPa and 480 MPa, respectively. There is also a maximum allowed tensile strength of 620 MPa specified for the FCAW filler metal with a toughness requirement. The minimum elongation for the SMAW filler metals is 17%, while the minimum elongation for the FCAW filler metals with and without a toughness requirement are 20% and 22%, respectively. The mean results indicate that the properties of all the electrodes met these requirements. However, there were two individual results that were slightly lower than the specified minimum values. The elongation of one E70T-4 coupon and the yield strength of one E71T8-K6 coupon were, respectively, 0.9% and 5 MPa below the minimum.

These tests showed that the degree of over-strength is notably higher in the FCAW filler metals without specified toughness than in the SMAW filler metal or the FCAW filler metal with a toughness requirement. The weld metals in the former category were approximately 30% stronger than the minimum requirement of 480 MPa. The strengths of the other two weld metal types, in comparison, were within 10% of the nominal value.

4.1.4 Charpy V-Notch Impact Tests

The Charpy V-notch impact test results are shown in Table 4.4. The impact energy of weld metal E71T8-K6 met the minimum toughness requirement of 27 J at -29°C set by the AWS standard (AWS 1998). By comparing the mean energy absorption for the various filler metals, the following observations can be made. The two flux-cored filler metals with no toughness requirement had similar toughness levels, as the difference in their means was only 3 J. Also, the results verify that the impact energy of flux-cored wires with a toughness requirement was higher than the impact energy of flux-cored wires without a toughness requirement; the means for the E71T8-K6 wire were at least four times as high as the means for the E70T-4 and E70T-7 wires. The test results further demonstrate that SMAW filler metals with no toughness requirement produce welds of larger impact energies than FCAW filler metals with no toughness requirement; the mean results for the E7014 filler metal were at least 1.5 times the mean results for the E70T-4 and E70T-7 filler metal.

4.1.5 Diffusible Hydrogen Tests

According to AWS A5.29-98 (AWS 1998), flux-cored electrodes typically produce welds with hydrogen levels of less than 16mL/100grams. Therefore, this limit is used as a measure of the acceptability of the weld filler metal after a long storage period. As indicated by the results shown in Table 4.5, the hydrogen levels in all the weld deposits tested were either below or at the limit specified.

4.2 Fillet Weld Test Results

One of the observations from the tests that affects the processing of the data is the fact that the stress level in the specimen base plates was within the elastic range except for the transverse weld specimens. According to the plate stress calculations, which included shear lag allowance in accordance with CSA–S16–01 (CSA 2001), the plates in six of the nine longitudinal weld specimens should have shown signs of yielding at the maximum test loads. However, examination of these specimens revealed no such signs. The discrepancy between the conclusions derived from the observations and the calculations might have been caused by the approximate nature of the shear lag provision or the possibility that the yield stress of the plate was higher than the value reported on the mill certificate.

A summary of the other results from the fillet weld tests is presented in Table 4.6. In most specimens, the test welds did not all fracture simultaneously. Because the loading becomes eccentric after the first fracture occurrence, this summary displays the means of the results corresponding to only those welds that failed first. The means were calculated with the data from the three specimens of each assembly. Test specimen F3-3 failed at one of the reinforced welds; hence, the values shown for assembly F3 represent the mean of two, rather than three, tests. The data for the individual specimens are tabulated in Appendix D, and the stress vs. strain response curves are given in Appendix E. The results for the transverse weld assemblies have also been presented elsewhere (Ng *et al*. 2002). A brief discussion of the results given in Table 4.6 is provided in the following sections.

4.2.1 Test-to-Predicted Ratio

As an indication of the accuracy of the weld strength equation used in the Canadian standard, the test-to-predicted ratio was calculated for the test specimens. The mean ratio for each assembly is given in Table 4.6. The form of the strength equation has already been presented in Section 2.2.10 as Equation 2.1 but is shown again here for convenience:

$$P_\theta = 0.67\, \phi_w\, A_w\, X_u\, (1.00 + 0.50 \sin^{1.5} \theta) \qquad [2.1]$$

The theoretical strengths were determined using a performance factor of unity and using a throat area based on measured leg sizes and the weld tensile strength determined from weld metal coupon tests.

Because it was observed that the measured strength for half of the filler metals was significantly higher than the nominal value, a second test-to-predicted ratio was calculated using the nominal weld strength (480 MPa for all the filler metals used in this program). Comparison of this ratio with the first one gives an indication of the amount of additional safety that could be provided by the over-strength of the weld metal.

Both ratios indicate that Equation 2.1 is conservative for all the specimens tested. The overall mean ratio based on measured weld strength is 1.36, with maximum and minimum values of 1.71 and 1.01, respectively. The overall mean ratio based on nominal weld strength is 1.62, with maximum and minimum values of 1.96 and 1.09, respectively.

4.2.2 *Weld Fracture Stress*

The weld stress at fracture shown in Table 4.6 was calculated with the assumption that the two test welds shared the applied load equally. The stress was determined using two different areas: the measured fracture surface area and the theoretical throat area. The theoretical throat area was calculated based on the mean measured leg sizes of the welds and therefore does not include the additional area due to root penetration and weld face reinforcement. The fracture surface area, however, accounts for both quantities and consequently is often the larger of the two values. On average, this fact caused the stresses calculated with the nominal throat area to be 27% higher than the stresses determined based on the fracture surface area.

4.2.3 *Weld Strain*

Both the mean strain at ultimate load and at weld fracture are given in the Table 4.6. The overall mean fracture strains were 0.169, 0.103, and 0.311 for the transverse, 45-degree, and longitudinal welds, respectively.

For the 45-degree and transverse weld specimens, the strains were calculated by dividing the deformation measurements from the LVDTs by the corresponding gauge length. For the longitudinal specimens, the only strain given is the shear strain; the longitudinal strain was not determined because the deformation experienced by the welds was mostly due to shear since the base plates did not yield as discussed subsequently. The shear strain was calculated by dividing the mean of the two overall deformation measurements on one face by the mean of the main plate shear leg measurements. These deformations could be used to determine the shear strain because the base plates remained elastic. By averaging the two overall deformation measurements on one face of the test specimen, the effect of any in-plane specimen rotation on the displacement values is minimized. To quantify the observation that the overall and shear displacements were essentially the same, a comparison between the two deformation measurements was made by taking the ratio of the shear displacement values to the average of the two overall displacement values taken on the same specimen face. The mean ratio was 1.09 with a standard deviation of 0.077 and a coefficient of variation of 0.071. Although the types of measurements were similar, the overall deformations were preferred for the calculations because these measurements might have been slightly more accurate due to differences in the actual linear range among the LVDTs. This range was smaller in the LVDTs measuring the shear deformations across the gap between the splice plate and the run-off tab. In some cases, the deformations measured in the test welds exceeded the limits of those LVDTs.

4.2.4 *Fracture Angle*

The mean measured angles of the weld fracture surface for each assembly are given in Table 4.6. The mean fracture angle for all specimens of each series were 14°, 28°, and 32° for the transverse, 45-degree, and longitudinal welds, respectively.

In general, there were two locations in which weld fracture tended to occur: at the interface between weld passes and at the shear leg. Six of the 12 transverse weld specimens fractured at the interface between the weld passes, while three failed at the shear leg. Three had non-uniform failure planes, containing a combination of fracture at the shear leg and failure at some other location in the weld. Six 45-degree and eight longitudinal welds failed between the weld passes. The remaining welds (three 45-degree and one longitudinal weld) had fracture surfaces that ran partially along the interface between the weld passes and partially along the weld tensile leg. Figure 4.1 depicts two typical non-uniform fracture surfaces.

Table 4.1 – Base Metal Mechanical Properties

Nominal Plate Thickness (mm)	Number of Specimens	Mean Yield Strength (MPa)	Mean Tensile Strength (MPa)	Mean Modulus of Elasticity (MPa)	Mean Elongation (%)	Steel Grade (CSA G40.21–98)
15.9	2	347	466	201 400	38	350W
25.4	2	386	538	201 600	41	350W
25.4†	—	326	499	—	27	300W
31.8†	—	305	503	—	32	300W
50.8†	—	345	462	—	33	300W

† No tension coupon tests performed; values obtained from mill certificates.

Table 4.2 – Chemical Analysis of Filler Metals

AWS Classification	Weight (%)									
	C	Mn	Si	P	S	Ni	Cr	Mo	V	Cu	Al
E7014	0.092	0.260	0.369	0.015	0.0130	0.070	0.055	0.069	0.0200	0.039	<0.010
E70T-4	0.345	0.295	0.057	0.010	0.0036	0.024	<0.030	<0.050	0.0034	0.016	1.350
E70T-7	0.313	0.379	0.065	0.009	0.0032	0.017	0.340	<0.050	0.0046	0.019	1.110
E71T8-K6	0.106	0.806	0.088	0.015	0.0043	0.442	0.030	<0.050	0.0052	0.019	0.392

Table 4.3 – Weld Metal Tension Coupon Test Results

AWS Classification	No. of Specimens	Mean Static Yield Strength (MPa)	Mean Static Tensile Strength (MPa)	Mean Modulus of Elasticity (MPa)	Mean Elongation (%)
E7014†	2	452	520	210 700	21.7
E70T-4	2	472	631	198 600	22.3
E70T-7†	2	468	605	200 800	23.1
E71T8-K6	2	402	493	207 400	28.4

† Test assembly prepared by Waiward. All other assemblies prepared by Supreme Steel.

Table 4.4 – Charpy V-Notch Specimen Test Results

AWS Classification	-29°C			21°C			100°C		
	Energy (J)	Energy (J)	Mean (J)	Energy (J)	Energy (J)	Mean (J)	Energy (J)	Energy (J)	Mean (J)
E7014†	18	23	20	58	79	68	81	77	79
E70T-4	9	8	9	15	18	16	57	47	52
E70T-7†	7	5	6	16	15	16	49	56	52
E71T8-K6	57	34	45	178	220	199	218	205	212

† Test assembly prepared by Waiward Steel Fabricator. All other assemblies prepared by Supreme Steel.

Table 4.5 – Diffusible Hydrogen Test Results

	Weld Wire				
	E70T-7†	E70T-7†	E70T-7	E71T8-K6	E71T8-K6
Hydrogen Content (mL/100g)	10	11	9	10	16

† 35V was used instead of the 26V used in the fillet weld specimen preparation.

Table 4.6 – Summary of Fillet Weld Specimen Test Results

Assembly Designation	AWS Classification	Mean Ultimate Load, P_u (kN)	Test/Predicted Ratio		Mean Ultimate P/A_{throat} (MPa)	Mean $P/A_{fracture}$ (MPa)	Mean Strain at P_u	Mean Fracture Strain	Mean Fracture Angle (^{o})
			Measured Weld Strength	Nominal Weld Strength					
T20	E7014	870	1.15	1.25	602	477	0.146	0.164	14
T22	E70T-4	936	1.34	1.76	849	488	0.133	0.149	0
T26	E70T-7	1063	1.35	1.70	822	666	0.198	0.202	23
T32	E71T8-K6	1038	1.61	1.66	799	634	0.254	0.264	19
F1	E70T-4	765	1.35	1.77	738	569	0.095	0.101	22
F2	E70T-7	825	1.54	1.94	808	594	0.122	0.128	35
F3	E71T8-K6	740	1.60	1.65	687	583	0.131	0.156	28
L1	E70T-4	744	1.17	1.54	496	476	0.160	0.242	32
L2	E70T-7	812	1.35	1.69	545	475	0.143	0.272	27
L3	E71T8-K6	731	1.51	1.56	500	402	0.185	0.472	32

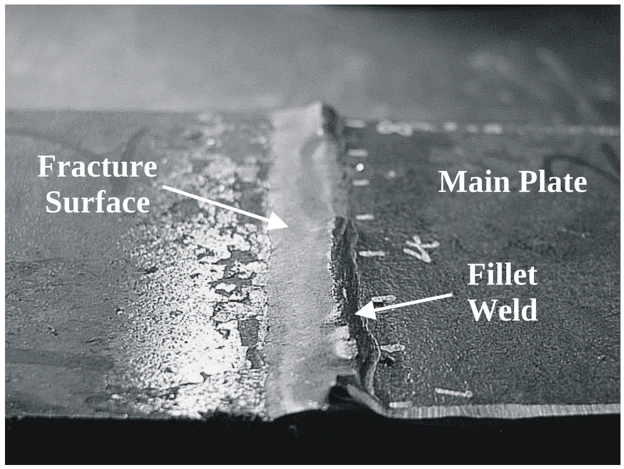

a) Transverse Fillet Weld

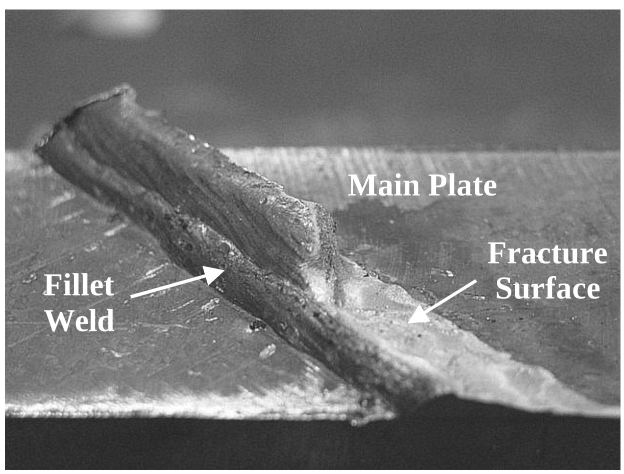

b) 45-Degree Fillet Weld

Figure 4.1 – Typical Non-uniform Weld Fracture Surfaces

5. ANALYSIS AND DISCUSSION

5.1 Introduction

The analysis of the fillet weld test results is presented in this chapter. In particular, the influence of filler metal classification, filler metal toughness, and orientation of load upon fillet weld behaviour are examined. Comparison of the results with those of other researchers, particularly Miazga and Kennedy (1989), and with the predictions of the current North American design equations is presented. An evaluation of the level of safety provided by these design equations is also presented.

5.2 Weld Strength and Ductility

The effect of filler metal classification and toughness on weld behavior, weld strength, and ductility has been plotted for different directions of loading. These plots are shown in Figures 5.1 to 5.3. Two plots are presented in each figure. One plot compares the results between welds of each filler metal classification. The other plot compares the results between welds made with filler metals without a toughness requirement and those made with filler metals with a toughness requirement. Each data point shows the mean value and the range of the test results for the specimen types indicated.

5.2.1 Effect of Filler Metal Classification and Toughness

The Charpy V-notch impact test results (Section 4.1.4) show that the FCAW filler metal with a toughness requirement and the SMAW filler metal without a toughness requirement had toughness levels at 21°C of up to 12 and four times, respectively, the toughness levels of FCAW electrodes without a toughness requirement. The weld metal tension coupon test results indicated that such significant differences in filler metal toughness do influence weld strength and ductility. These tests showed that the tensile strength of the filler metals with no specified toughness were all within 5% of each other but were 1.2 to 1.3 times the tensile strength of the filler metal with a toughness requirement. The coupon tests also showed that the filler metals with no toughness requirement had a fracture strain of approximately 80% that of the FCAW filler metal with a toughness requirement. However, weld metal tension coupons are not always a reliable representation of actual fillet weld behaviour due to such influences as the number of weld passes and restraint from the base plates.

In the following sections, the effect of filler metal classification and toughness level for each weld orientation is examined using the fillet weld specimen test results. Filler metals E70T-7 and E70T-4 were grouped in order to assess the effect of weld toughness. Both the weld stresses based on the theoretical throat area (calculated using the measured weld leg sizes) and on the fracture surface area were considered. The analysis was performed on the fillet weld specimens prepared with FCAW only because for the SMAW process, only one type of electrode was used and only transverse welds were studied.

5.2.1.1 Effect on Fillet Weld Strength

Figures 5.1 and 5.2 compare the strengths of fillet welds according to filler metal classification, toughness, and weld orientation. In Figure 5.1a, all the ranges of the transverse welds overlap, and the means are similar. There is only a 6% difference between the highest and lowest mean. These observations indicate that filler metal classification does not have a significant effect on the strength of transverse welds. The same is also true regarding weld toughness; it does not have a significant effect on the strength of transverse welds (Figure 5.1b). However, Figure 5.2a, which presents the stress at fracture calculated using the measured fracture surface area, appears to support the converse conclusion. This figure shows that the E70T-4 welds were at least 30% lower in strength than the welds of the other two filler metal classifications.

In order to determine the source of the inconsistency between the observations from Figures 5.1 and 5.2, other failure information for the E70T-4 specimens must be considered. The fracture angle of these specimens indicates that the welds failed at the shear leg, thereby providing a significantly larger surface area than specimens that failed near the weld throat. Therefore, the E70T-4 transverse weld stresses plotted in Figure 5.2a actually represent the weld shear strength and cannot be directly compared to the strengths of the E70T-7 and E71T8-K6 transverse welds, which failed near the weld throat under combined shear and tension. They can, however, be compared with the strengths of the longitudinal welds since the longitudinal welds also failed in shear. Figure 5.2a shows that the mean strength for the E70T-4 transverse welds is very similar to the mean strength for the longitudinal welds with no toughness requirement. Consequently, Figures 5.1 and 5.2 do not provide conflicting information; they both support the conclusion that neither filler metal classification nor toughness level has a significant effect on transverse fillet weld strength.

The reason that E70T-4 welds failed at the shear leg rather than nearer the throat might be explained by the amount of weld face reinforcement. Excess weld face reinforcement can lower the fracture angle, and the measured weld profiles presented in Appendix B show that the amount of reinforcement was larger in the E70T-4 weld specimens than in the other specimens.

The plots of the 45-degree weld specimen strengths calculated on the theoretical throat area (Figure 5.1) show that the mean strengths are within 15 percent of each other and the test data ranges overlap, indicating that electrode classification does not have a significant effect on weld strength. The mean strengths for the E70T-4 and E71T8-K6 weld specimens were 91% and 85%, respectively, of the strength of the E70T-7 specimens, which displayed the highest strength of the three electrode classifications. Figure 5.2 shows that if the root penetration and face reinforcement are accounted for, the mean strength of the three electrode classifications fall within 4% of each other.

Therefore, it can be concluded that the filler metal classification and toughness level have negligible effect on weld strength.

The longitudinal weld strengths calculated using the theoretical throat area (Figure 5.1) indicate that the E70T-7 welds were approximately 10% stronger than the welds from the other two electrodes. Again, once the root penetration and face reinforcement are considered, the mean strength of the E70T-4 and E70T-7 specimens become very close as shown in Figure 5.2a. However, using the fracture surface area to calculate the strength increases the difference between the welds with and without a toughness requirement as shown in Figure 5.2b. The mean strength of the welds without a toughness requirement is 18% higher than that of the welds with a toughness requirement.

In summary, the results show that neither filler metal classification nor toughness level has a significant effect on transverse and 45-degree weld strength. However, longitudinal welds with a toughness requirement do have lower strengths than longitudinal welds with no toughness requirement. These observations are not consistent with the observations of Phase I where it was concluded that welds made from filler metals with a toughness requirement have a somewhat higher strength than welds made from filler metals without a toughness requirement. An explanation for these inconsistencies is that one additional FCAW filler metal with a toughness requirement was included in Phase I, and the measured tensile strength for this electrode was 21% higher than the measured tensile strength of the filler metal with a toughness requirement studied in the present phase. In Phase I, if the results of only the E71T8-K6 welds were compared with the results of the welds with no toughness requirement, the observations would have been the same as in this phase.

5.2.1.2 Effect on Weld Ductility

The strain at fracture was used as a measure of ductility of the welds. The strain was obtained by dividing the measured deformation by the gauge length over which the deformation was measured, namely, the weld leg size times the sine of the angle between the axis of the weld and the line of action of the applied load.

The effect of filler metal classification and toughness on ductility can be assessed from Figure 5.3. The figure indicates that there is a consistent trend between weld ductility and filler metal classification for all three weld orientations investigated in this program. The E70T-4 welds were the least ductile and the E71T8-K6 welds were the most ductile as indicated in Figure 5.3a. The ratio between the mean fracture strains of the welds made with filler metals without a toughness requirement (E70T-4 and E70T-7) ranges from 1.12 to 1.35. Electrode classification, therefore, appears to have a notable effect on fillet weld ductility. In Phase I, however, the mean fracture strain of the transverse E70T-4 welds was somewhat higher than the mean fracture strain of the E70T-7 welds, which is opposite to what is observed here. This inconsistency is attributable to the difference in the number of test results involved in each phase; approximately ten times as many E70T-4 and E70T-7 fillet weld test results were analysed in the first phase, which allows for more reliable comparisons. Morever, the fracture strains of the Phase II E70T-4 transverse welds are close to the mean value of the Phase I E70T-4 weld strains, but the fracture strains of assembly T26 (the assembly to which the Phase II E70T-7 transverse welds belong) are the highest among all the Phase I E70T-7 weld fracture strains.

The ratios between the mean fracture strains of the welds for which the filler metals have a toughness requirement to those made with the filler metals for which there is no toughness requirement are 1.51, 1.37, and 1.84 for the transverse, 45-degree, and longitudinal welds, respectively. These are shown in Figure 5.3b. The superior ductility shown by the welds with a toughness requirement was also observed in the weld metal coupon tests. Therefore, it is concluded that welds with higher toughness levels are more ductile than welds with lower toughness levels. This conclusion is consistent with the observations from Phase I where only transverse welds were studied.

5.2.2 Effect of Weld Orientation

Both Figures 5.1 and 5.2 show that there is a distinct decrease in weld strength as the weld orientation approaches the longitudinal case. The apparent discrepancy between the E70T-4 welds and the other welds within the transverse weld test specimens has been explained in Section 5.2.1.1.

According to the stress vs. strain curves of Miazga and Kennedy (1989), the fracture strains among fillet welds of different orientations vary and there is no obvious general trend between fracture strain and loading angle. The same conclusions can be reached using the data presented by Butler and Kulak (1971). However, the mean fracture shear strain of their longitudinal welds was about four times as high as the mean fracture strain of their transverse and 45-degree welds. Similar observations can be made from the test results presented herein, as illustrated in Figure 5.3. There is no general trend showing an increase or decrease in fracture strain with loading angle, but the strain at fracture for the longitudinal welds is significantly higher than strain at fracture for the other two weld orientations. For the filler metals without a toughness requirement, the mean fracture strain of the longitudinal welds was 1.5 and 2.3 times as high as the mean fracture strains of the transverse and 45-degree welds, respectively. For the fillets with a toughness requirement, the mean fracture strain of the longitudinal welds was 1.8 and 3.0 times as high as the mean fracture strains of the transverse and 45-degree welds, respectively. There was also a much larger difference between the strain at ultimate load and the strain at weld fracture for the longitudinal welds. The mean ratio between the fracture strain and the strain at ultimate load is 2.0 for these welds compared to less than 1.1 for the other two weld orientations.

The response of the weld could be measured in terms of either deformation or strain. As described above, strains have been used initially because this normalizes the effect with respect to weld size and the effect of weld orientation on the gauge length. Others have used fracture deformation, and when this is done the work of Butler and Kulak (1971), Clark (1971), Swannell and Skewes (1979), and Lesik and Kennedy (1990) indicate that weld ductility increases as the loading angle decreases. In Figure 5.4, the weld orientation is plotted with the weld fracture deformations normalised with the measured average leg size on the main plate. As expected, the normalised longitudinal weld deformations are significantly higher than those of the other weld orientations. However, the mean normalised deformations of the transverse welds are up to 22% higher than the mean normalised deformations of the 45-degree welds. The discrepancy between the current and earlier research may have been caused by the difference between the stress levels of the base plates: the transverse weld specimen plates yielded whereas the 45-degree weld specimen plates did not. The yielding of the transverse weld specimen base plates could have influenced the weld ductility by affecting the amount of restraint on the weld provided by the plate. Since there were no specimens in which all parameters were the same except for plate yielding, the effect of plate yielding on weld behaviour cannot be assessed directly. Another possibility is that the transverse weld deformation measurements might have captured a significant amount of plate deformation since there was a small gap between the toe of the fillet weld and the punch marks within which the LVDT brackets were anchored.

Miazga and Kennedy (1989) observed that the fracture angle tends to increase as the loading angle decreases, and this is generally the case here as well. The mean weld fracture angles were 14°, 28°, and 30° for the transverse, 45-degree, and longitudinal welds, respectively.

5.3 Fracture Surface Observations

Fracture surfaces of welds of each orientation were examined under a scanning electron microscope in order to collect more information about the weld failure modes. In the selection of the specimens to be examined, favour was given to the welds that displayed non-typical behaviour. Photomicrographs of some of these surfaces are shown in Figures 5.5 to 5.10, and more fracture surfaces are depicted in Appendix F. All photos reveal that fracture mostly occurred by microvoid coalescence, confirming the results from the diffusible hydrogen tests that the FCAW filler metals were not embrittled by hydrogen despite their long storage period before specimen fabrication.

The fracture surface of a typical transverse weld made with the filler metal with a toughness requirement is presented in Figure 5.5. These welds displayed the highest fracture strains of the transverse weld series. The elongated microvoids on the fracture surface indicate that the failure was indeed ductile.

Two of the three 45-degree weld specimens examined also had fracture surfaces with elongated microvoids, an example of which is shown in Figure 5.6. Inclusions at the weld root were found in specimen F1-2 (Figure 5.7), which might explain why the fracture strain of this weld was up to 27% lower than the fracture strains of the other two welds of the same electrode type. The third 45-degree weld specimen examined was prepared with the filler metal with a specified toughness. The 3 mm long segment of the fracture surface examined showed approximately 70% cleavage fracture (Figure 5.8). In addition, some porosity was observed near the weld root. Despite these indications of predominately brittle fracture, the fracture strain was still higher than that of the welds without a toughness requirement.

For the longitudinal welds, one specimen of each filler metal type was chosen for fracture surface examination. Figure 5.9 shows the fracture surface of a typical weld made from the filler metal with a specified toughness. The microvoids are elongated, indicating ductile shear fracture as expected. However, the fracture surfaces of the two welds made from the filler metals with no specified toughness contained mostly equiaxed microvoids. This unexpected observation might partially be explained by the lack of fusion at the weld root found in both weld samples (Figure 5.10). Because the behaviour of these two welds are representative of the welds of their respective assemblies, either the lack of fusion did not adversely affect the weld strength and ductility or all the longitudinal welds with no specified toughness were of the same quality.

5.4 Comparison with Other Studies

The fillet weld strength, ductility, and fracture angle results from this research were compared with the results from other studies. The comparisons were predominantly made with the work of Miazga and Kennedy (1989) because the weld design equations in both North American standards are based on their research. In addition, given that Phase I and other studies have shown that weld size has a significant effect on fillet weld behaviour, only the results for those welds that were laid with a similar number passes as was used in the present study are discussed.

The FCAW weld strengths from this research and the SMAW weld strengths from Miazga and Kennedy were normalised with the longitudinal fillet weld strength before comparing the two data sets. The data were normalised because it is the ratio between the strength of fillets loaded at an angle and the strength of fillets loaded longitudinally that is of interest. The weld stresses of Miazga and Kennedy's specimens used for this comparison were calculated by dividing the ultimate load by the theoretical throat area, which was calculated using the average leg measurements of all the test welds on one specimen. This average is the only information given in their paper concerning these measurements. The weld stresses of the present research were calculated using the theoretical throat area as described in Section 4.2.2. The mean weld strength of each transverse and 45-degree weld assembly were divided by the mean strength of the longitudinal weld assembly made with the same filler metal type.

As shown in Table 5.1, there is reasonable agreement among the weld strength ratios of the present research. The overall ratios are 1.60 and 1.46 for the normalised transverse and 45-degree weld strengths, respectively, which accords well with the corresponding ratios of 1.60 and 1.32 given in Miazga and Kennedy. These observations indicate that filler metal toughness and welding process have no discernable effect on the improvement of weld strength with increasing loading angle.

Comparisons of the weld deformation results with the predicted deformations at the ultimate load and at weld fracture are presented in Figure 5.11. The predicted values were determined from the following empirical expressions presented by Lesik and Kennedy (1990) for determining normalised deformations:

$$\frac{\Delta_u}{d} = 0.209(\theta + 2)^{-0.32} \tag{5.1}$$

$$\frac{\Delta_f}{d} = 1.087(\theta + 6)^{-0.65} \tag{5.2}$$

Δ_u and Δ_f are the weld deformations at ultimate load and weld fracture, respectively; d is the average measured weld leg size; and θ is the weld orientation. These equations were developed based on the deformation results of Miazga and Kennedy. The experimental deformations plotted in the figure have been divided by the average leg size of the weld that had fractured, which yields values that are just slightly different from the weld strains reported elsewhere in this report for the transverse and longitudinal fillets but are about 40% higher than the weld strains for the 45-degree fillets (recall that the strains for the 45-degree welds were obtained by dividing the deformation by the leg size times sine 45˚. The normalised deformations of all transverse and 45-degree welds at ultimate load are well above the predicted values. However, the normalised deformations of only three of the nine longitudinal welds meet or exceed the predictions. All normalised deformations at fracture exceed the predicted values, including those of the longitudinal welds.

Table 5.2 compares the mean fracture angles with those reported in Miazga and Kennedy (1989), McClellan (1989), Bowman and Quinn (1994), and the predictions of the empirical equation developed by Miazga and Kennedy. Except for the longitudinal welds, there is general agreement with the results of these studies. The lower mean fracture angle of the longitudinal welds might have been due to a difference in the location of the interface between the weld passes; observations made by Bowman and Quinn and in the present research (see Section 4.2.4) indicate that these welds tend to fail at this location.

Miazga and Kennedy, however, stated that the longitudinal failure surface on their specimens crossed the weld pass interface and occurred near the weld throat.

5.5 Comparison with Design Standard Predictions

The ability of the CSA–S16–01 fillet weld design equation (Equation 2.1) to predict the test results is examined in this section. The examination was performed by comparing the experimental results to the predicted values of the weld strength ratios and the specimen capacities.

According to the design equation, the factor by which the transverse and 45-degree weld strengths are greater than longitudinal weld strength is 1.50 and 1.30, respectively. These compare reasonably well with the weld strength ratios determined from the weld stresses calculated on the theoretical throat area. As shown in Table 5.1, the experimental transverse to longitudinal weld strength ratios are 1.71, 1.51, and 1.60 for the E70T-4, E70T-7, and E71T8-K6 welds, respectively. The experimental 45-degree to longitudinal weld strength ratios are 1.49, 1.48, and 1.37 for the E70T-4, E70T-7, and E71T8-K6 welds, respectively.

Test-to-predicted ratios, tabulated in Appendix D, for each specimen were determined with the predicted capacities calculated by two different methods, as discussed in Section 4.2.1. Method 1 used the nominal weld strengths and method 2 used the measured weld strengths. The difference between the two sets of ratios reflects the amount of safety that filler metal over-strength provides. All ratios were greater than unity, indicating that the predictions were conservative in every case. The graphs presented in Figure 5.12, in which the test and predicted capacities are compared, give an overall impression of the safety margin provided by the design equation for these specimens. Like the test-to-predicted ratios, they were created using the two different predicted capacities. The diagonal lines represent the test-to-predicted ratio of unity. Closest to these lines are the SMAW welds, whose mean values were the lowest of all the specimens, with ratios of 1.25 and 1.15 obtained by methods 1 and 2, respectively. For the FCAW specimens, method 1 produced ratios that were reasonably consistent within each series. The exception was the 45-degree welds where the test-to-predicted ratio of the E71T8-K6 assembly was more than 10% lower than the ratios of the other two assemblies. The overall mean test-to-predicted ratios are 1.71, 1.78, and 1.60 for the transverse, 45-degree, and longitudinal weld series, respectively.

When the test-to-predicted ratios were determined with the measured weld strengths, the various degrees of filler metal over-strength caused greater differences in the ratios within each specimen series. Because the actual strength of the E71T8-K6 filler metal was within 3% of the nominal value compared to approximately 30% for the other filler metals, the test-to-predicted ratios calculated by method 2 tend to be the highest for the E71T8-K6 specimens. The following are the mean values of these ratios for the E70T-4, E70T-7, and E71T8-K6 assemblies: 1.34, 1.35, and 1.61, respectively, for the transverse welds; 1.35, 1.54, and 1.60, respectively, for the 45-degree welds; and 1.17, 1.35, and 1.51, respectively, for the longitudinal welds.

5.6 Reliability Analysis

In order to obtain a statistical evaluation of the level of safety provided by the North American standards, the safety index, β, was determined for the fillet weld design equations of both standards using the test results of this study. The traditional target safety index for connections is 4.5; therefore, the design equations can be considered adequate when the evaluated indices are at least that high. The CSA–S16–01 (CSA 2001) equation has already been introduced in Sections 2.2.10 and 4.2.1. The AISC (AISC 1999) specification uses basically the same equation, except for the resistance factor and the weld shear strength. It is:

$$P_\theta = 0.60\,\phi\,A_w\,F_{EXX}\,(1.00 + 0.50\sin^{1.5}\theta) \qquad [5.3]$$

The resistance factor, ϕ, used in the AISC equation is 0.75. A_w is the theoretical weld throat area, F_{EXX} is the nominal tensile strength of the filler metal (equivalent to X_u), and θ is the angle between the weld axis and the direction of loading.

The procedure outlined by Lesik and Kennedy (1990) was used to determine the magnitude of the safety index, β, provided by the current North American design equations. The safety index can be determined from the following equation for the resistance factor, ϕ, which was originally proposed by Galambos and Ravindra (1978):

$$\phi = \Phi_\beta\,\rho_R\,e^{-\beta\alpha_R V_R} \qquad [5.4]$$

The coefficient of separation, α_R, was set to 0.55 as suggested by Galambos and Ravindra. The values of ϕ are 0.67 and 0.75 for the CSA–S16–01 and AISC design equations, respectively. The factor Φ_β is an adjustment factor that modifies ϕ when β is not equal to the safety index used for the evaluation of the load factors, which is normally 3.0. An equation developed by Franchuk *et al*. (2002) was used to calculate this factor:

$$\Phi_\beta = 0.0062\beta^2 - 0.131\beta + 1.338 \qquad [5.5]$$

The bias coefficient for resistance, ρ_R, is obtained from:

$$\rho_R = \rho_G\,\rho_{M1}\,\rho_{M2}\,\rho_P \qquad [5.6]$$

where ρ_G is the mean ratio of the measured-to-nominal values for the theoretical throat area, ρ_{M1} is the mean ratio of the measured-to-nominal ultimate tensile strength for the weld metal, and ρ_{M2} is the quotient between the measured and predicted shear strengths. The measured shear strength was taken as the strength of the longitudinal weld specimens calculated on the theoretical throat area while the predicted values were calculated by multiplying the appropriate shear factor (0.67 for CSA–S16–01 and 0.60 for AISC specifications) by the measured tensile strength from the weld metal coupons. Although the longitudinal weld stress determined using the measured fracture surface area is the actual measured shear strength, the weld stress determined using the theoretical throat area was used instead because the design equation assumes that longitudinal welds fail at the theoretical throat. The professional factor, ρ_P, is the mean test-to-predicted capacity ratio calculated as:

$$\rho_P = \text{Mean}\left(\frac{\text{Test Capacity}}{A_{throat} \times \tau_u \times \left(1.00 + 0.50\sin^{1.5}\theta\right)}\right) \qquad [5.7]$$

A_{throat} in Equation 5.7 is the theoretical weld throat area calculated using the measured fillet leg size. The term τ_u is the measured shear strength of the weld. It is equivalent to the terms $0.67X_u$ or $0.60F_{EXX}$ used in the design equations of both design standards. As explained above, the measured shear strength was obtained from the test results of the longitudinal weld specimens.

The last term in the expression for ϕ (Equation 5.4) is the coefficient of variation, V_R, for the resistance. This value is determined from

$$V^2{}_R = V^2{}_G + V^2{}_{M1} + V^2{}_{M2} + V^2{}_P \qquad [5.8]$$

where each variable is the associated coefficient of variation for the bias coefficients described above.

In order to provide a broad view of the safety level provided by the design equations, the reliability analysis was carried out for four different specimen groups:

1. the FCAW transverse weld specimens;
2. the 45-degree weld specimens;
3. the longitudinal weld specimens; and
4. all the specimens from Miazga and Kennedy (1989), Ng *et al.* (2002), and the present research.

A separate analysis was performed for the FCAW specimens of each weld orientation (the first three groups) to allow a comparison among the levels of safety that the design equations provide for each weld orientation. Because the samples sizes of these three groups are small, the results are not as reliable as the results for the fourth group where all the specimens were considered.

The values of ρ_G and V_G for each group were determined using the test results from the specimens of Miazga and Kennedy (1989), Ng *et al*. (2002), and Phase II. The bias coefficient for weld metal tensile strength and the associated coefficient of variation, ρ_{M1} and V_{M1}, for each group were obtained from Lesik and Kennedy (1990) because they analysed a much larger number of weld metal tension coupon tests than was conducted in this research. For the groups considering the Phase II specimens by weld orientation (groups 1 to 3), ρ_{M2} was obtained from the Phase II longitudinal weld results. However, because the sample size of these specimens is too small to provide a representative coefficient of variation, V_{M2} was taken from the work of Lesik and Kennedy. For the group combining all the specimens from the three test programs (group 4), the values of ρ_{M2} and V_{M2} calculated by Lesik and Kennedy were used. The professional factor and the associated coefficient of variation, ρ_P and V_P, were evaluated using the following values of τ_u: 411 MPa for the E7014 welds, 496 MPa for the E70T-4 welds, 545 MPa for the E70T-7 welds, 608 MPa for the E70T7-K2 welds (the second FCAW filler metal with a toughness requirement tested in Phase I), and 506 MPa for the E71T8-K6 welds. The τ_u value for the E7014 welds was calculated from the Miazga and Kennedy longitudinal weld test results, while the remaining values were determined from the Phase II longitudinal weld tests. Because no longitudinal weld specimens were prepared with the E70T7-K2 filler metal, the τ_u value for the E70T7-K2 welds was obtained by multiplying the τ_u value for the E71T8-K6 welds by 1.20. This number is the ratio between the mean tensile strengths of the E70T7-K2 and the E71T8-K6 filler metals measured from the Phase I weld metal tension coupon tests.

Table 5.3 summarises the above data and the calculated safety indices for the CSA-S16-01 and AISC design equations. The safety index, β, is the same for both standards because the products of the respective resistance factors and shear coefficients are identical. The safety index for each specimen group is greater than 4.5, the traditional target value for connections. The longitudinal welds show the lowest safety index at 5.6, while the 45-degree FCAW specimens show the highest safety index at 7.5. The safety index obtained from the combined specimens of Miazga and Kennedy (1989), Ng *et al*. (2002), and the present research is 4.9, which is marginally higher than the overall safety index of 4.8 reported in Ng *et al*. strictly for transverse specimens.

Table 5.1 – Comparison of Weld Strength Ratios with Miazga and Kennedy (1989)

Weld Strength Ratio	Miazga and Kennedy (1989)	Present Research			
	9 mm Weld	E70T-4 Weld	E70T-7 Weld	E71T8-K6 Weld	Overall Ratio
90° / 0°	1.60	1.71	1.51	1.60	1.60
45° / 0°	1.32	1.49	1.48	1.37	1.46

Table 5.2 – Mean Fracture Angle Comparison with Other Studies

Loading Angle (°)	Miazga & Kennedy (1989) (°)	McClellan (1989) (°)	Bowman & Quinn (1994) (°)	Present Research (°)	Predicted Fracture Angle (M&K Equation) (°)
90	19	20 - 25	16	14	15
45	21	—	—	28	24
0	49	42 - 48	56	30	45

Table 5.3 – Safety Indices

CSA–S16–01				
	Phase II 90° Specimens	Phase II 45° Specimens	Phase II 0° Specimens	Miazga and Kennedy (1989), Phases I and II Specimens
Sample Size	9	8	9	145
ρ_G V_G	0.977 0.112	0.977 0.112	0.977 0.112	0.977 0.112
ρ_{M1} V_{M1}	1.123 0.077	1.123 0.077	1.123 0.077	1.123 0.077
ρ_{M2} V_{M2}	1.434 0.121	1.434 0.121	1.434 0.121	1.248 0.121
ρ_P V_P	1.069 0.060	1.403 0.088	0.944 0.036	1.142 0.175
ρ_R V_R	1.682 0.192	2.208 0.203	1.485 0.186	1.564 0.253
β	**6.2**	**7.5**	**5.6**	**4.9**

AISC 1999				
	Phase II 90° Specimens	Phase II 45° Specimens	Phase II 0° Specimens	Miazga and Kennedy (1989), Phases I and II Specimens
Sample Size	9	8	9	145
ρ_G V_G	0.977 0.112	0.977 0.112	0.977 0.112	0.977 0.112
ρ_{M1} V_{M1}	1.123 0.077	1.123 0.077	1.123 0.077	1.123 0.077
ρ_{M2} V_{M2}	1.602 0.121	1.602 0.121	1.602 0.121	1.394 0.121
ρ_P V_P	1.069 0.060	1.403 0.088	0.944 0.036	1.142 0.175
ρ_R V_R	1.878 0.192	2.465 0.203	1.658 0.186	1.746 0.253
β	**6.2**	**7.5**	**5.6**	**4.9**

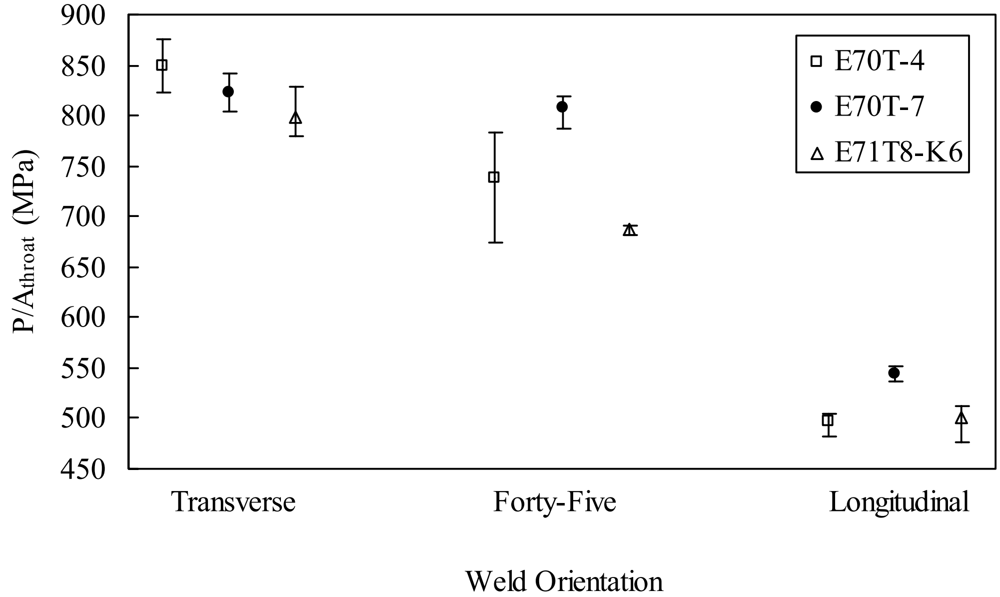

(a) Effect of Filler Metal Classification and Weld Orientation on Weld Strength

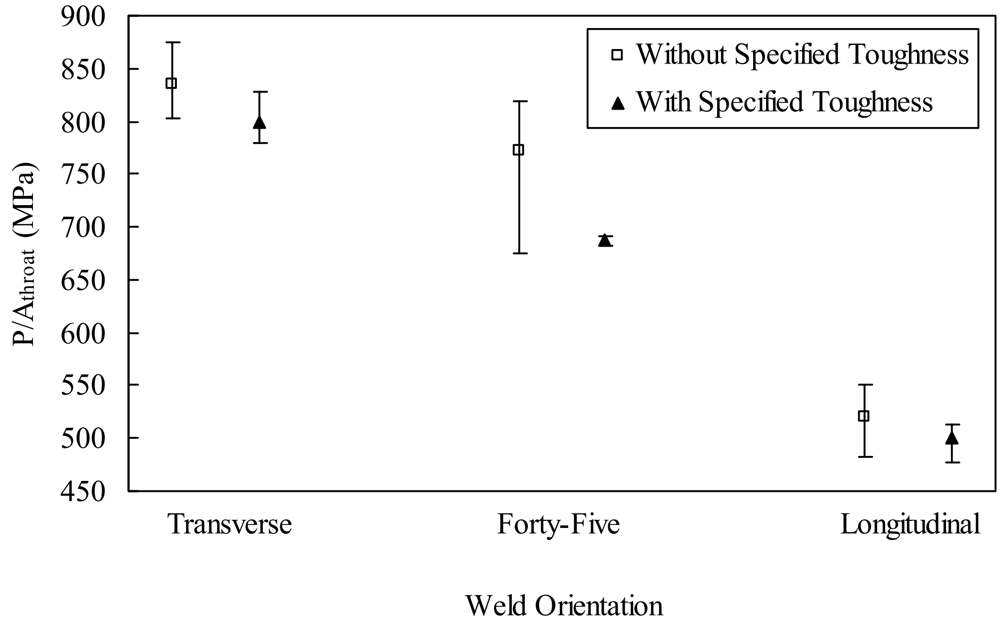

(b) Effect of Filler Metal Toughness and Weld Orientation on Weld Strength

Figure 5.1 – Effect of Weld Metal Classification, Filler Metal Toughness, and Weld Orientation on Fillet Weld Strength Calculated Using the Theoretical Throat Area

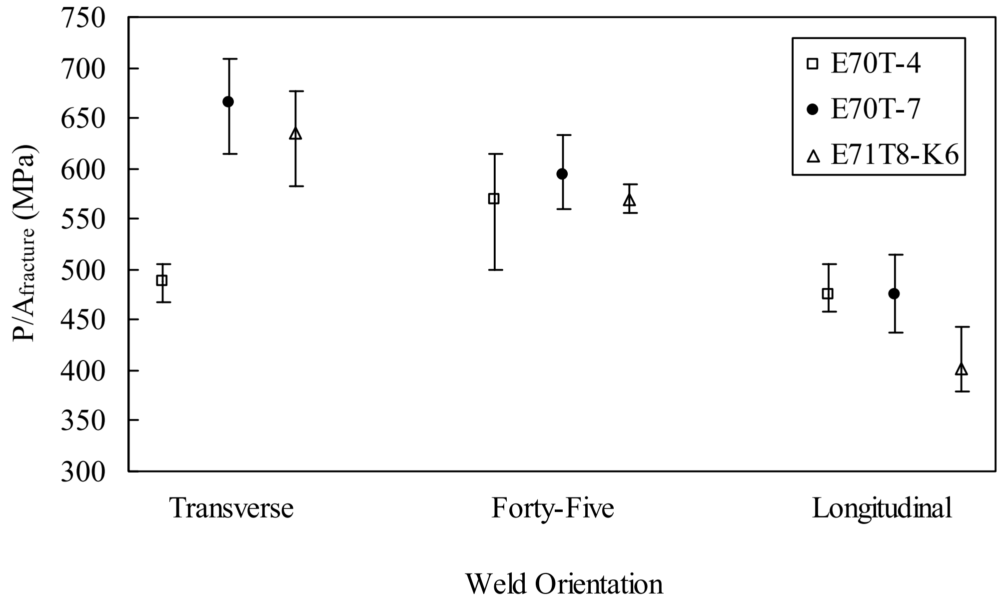

(a) Effect of Filler Metal Classification and Weld Orientation on Weld Strength

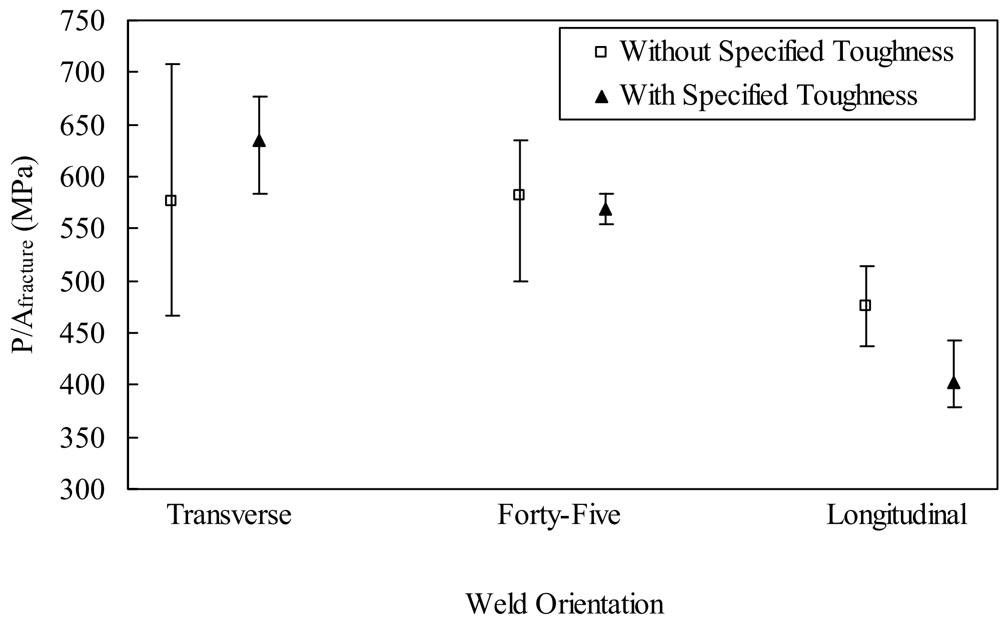

(b) Effect of Filler Metal Toughness and Weld Orientation on Weld Strength

Figure 5.2 – Effect of Weld Metal Classification, Filler Metal Toughness, and Weld Orientation on Fillet Weld Strength Calculated Using the Fracture Surface Area

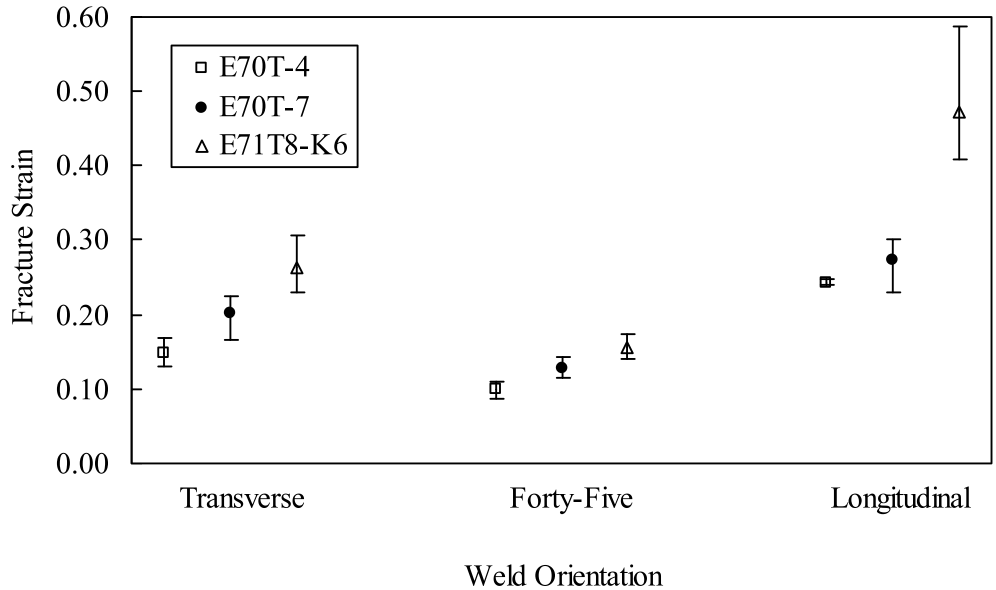

(a) Effect of Filler Metal Classification and Weld Orientation on Weld Ductility

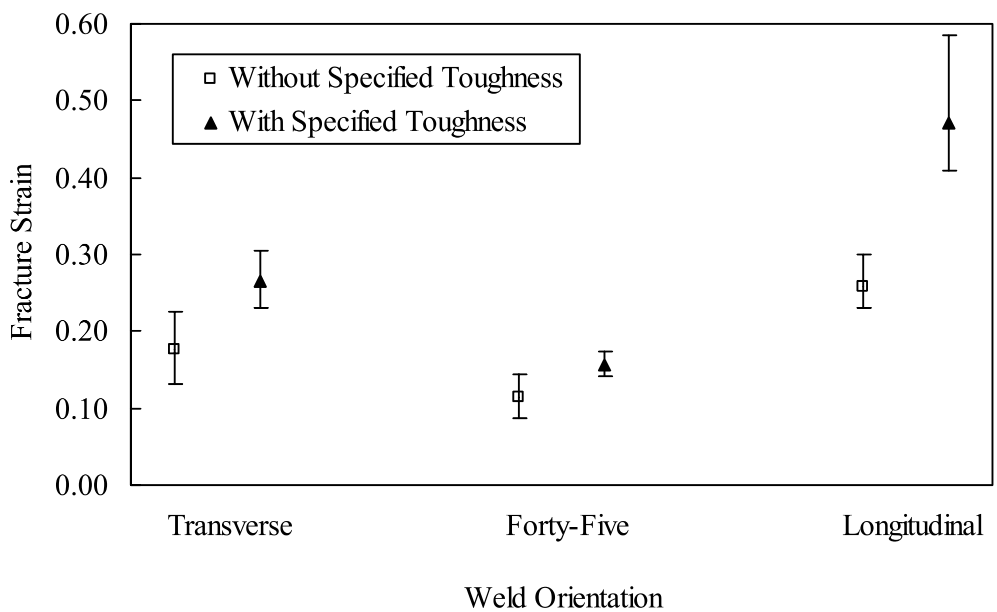

(b) Effect of Filler Metal Toughness and Weld Orientation on Weld Ductility

Figure 5.3 – Effect of Filler Metal Classification, Filler Metal Toughness, and Weld Orientation on Fillet Weld Ductility

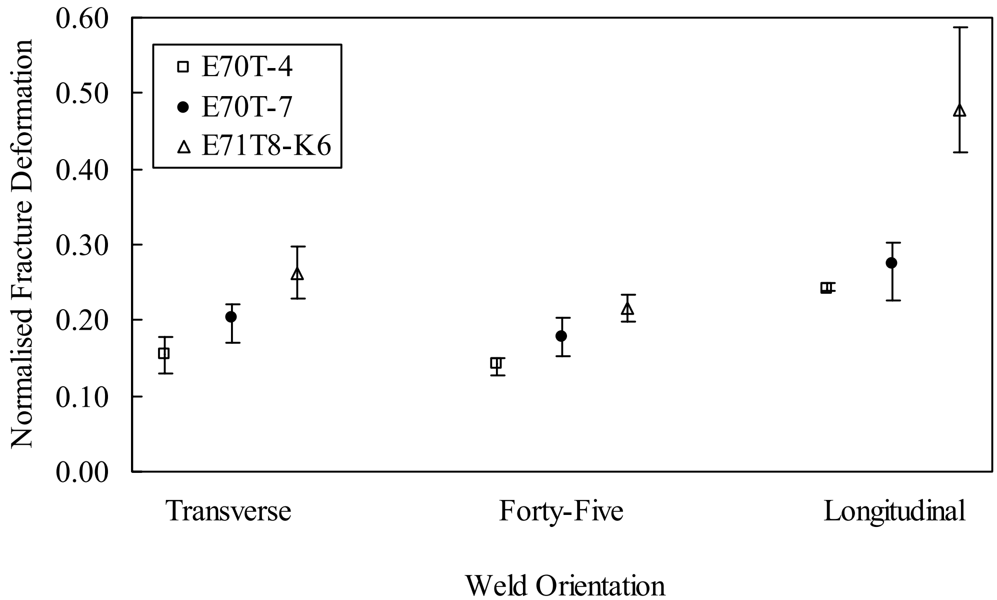

Figure 5.4 – Effect of Weld Orientation on Weld Fracture Deformation Normalised with the Average Measured Leg Size

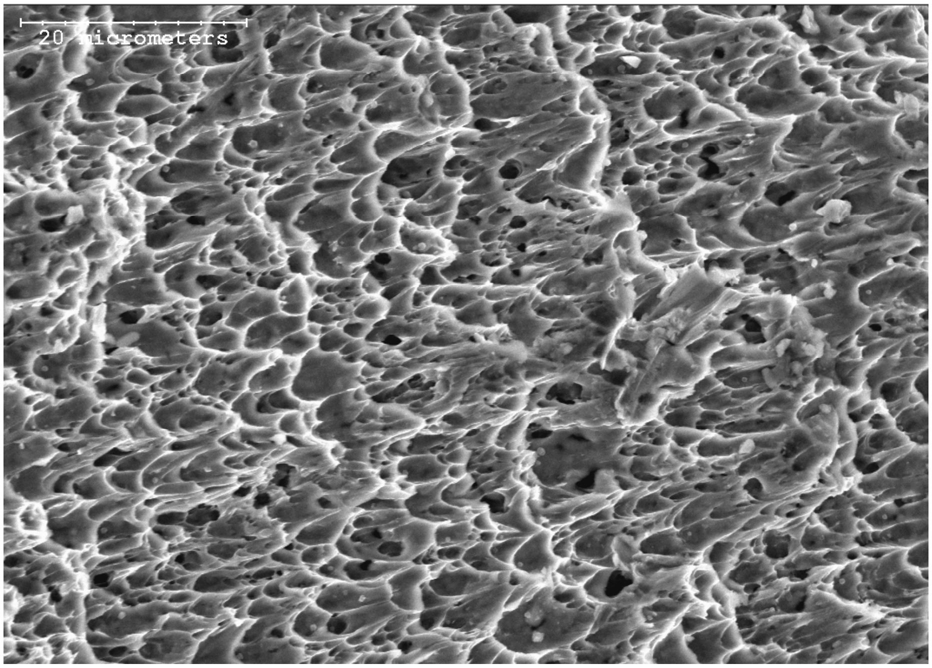

Figure 5.5 – Elongated Microvoids on Transverse Weld Specimen T32-2 Fracture Surface

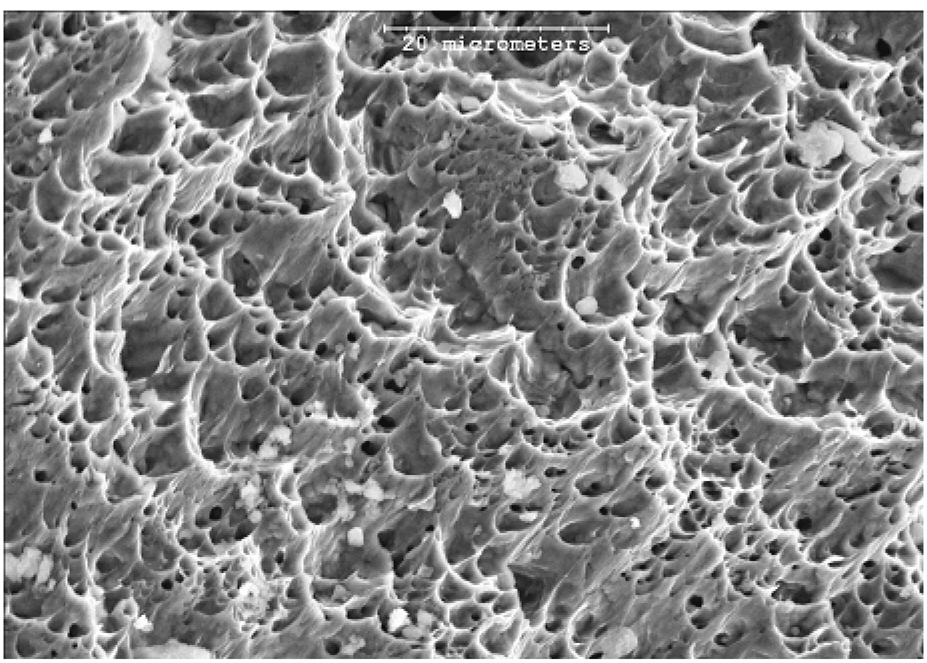

Figure 5.6 – Microvoid Coalescence on 45-Degree Weld Specimen F2-1 Fracture Surface

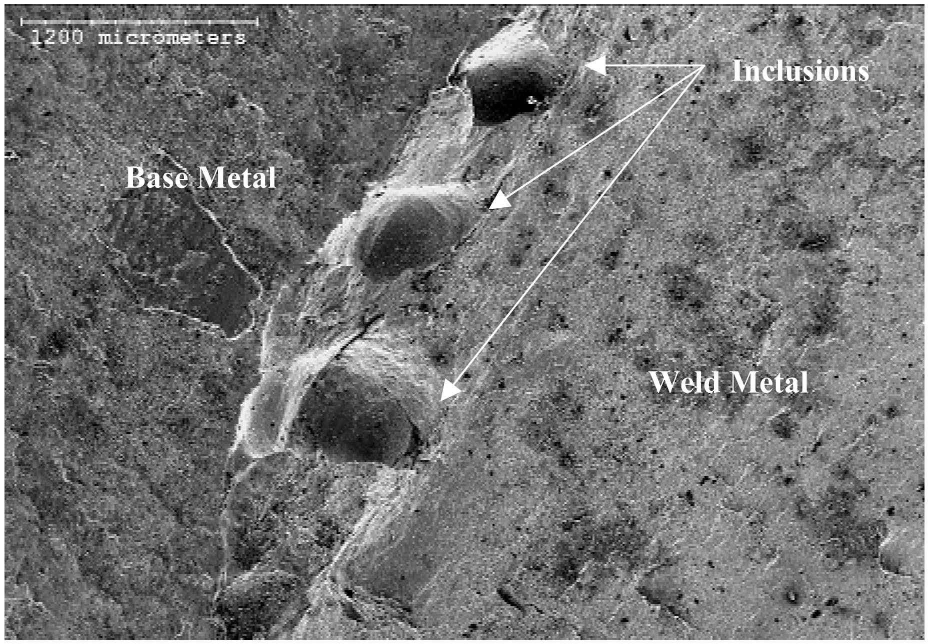

Figure 5.7 – Inclusions at the Weld Root of 45-Degree Weld Specimen F1-2

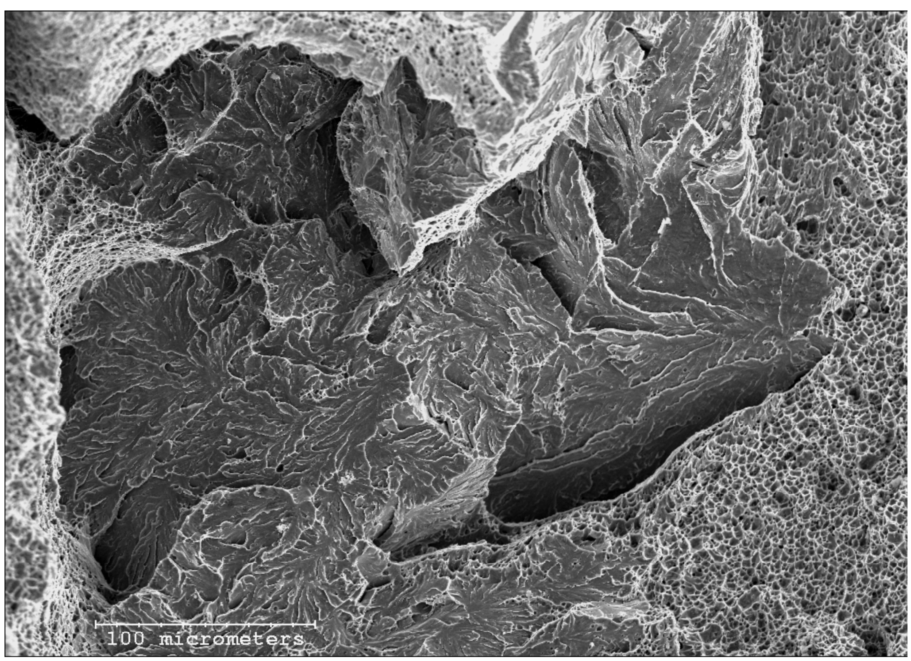

Figure 5.8 – Cleavage Fracture Surface of 45-Degree Weld Specimen F3-1

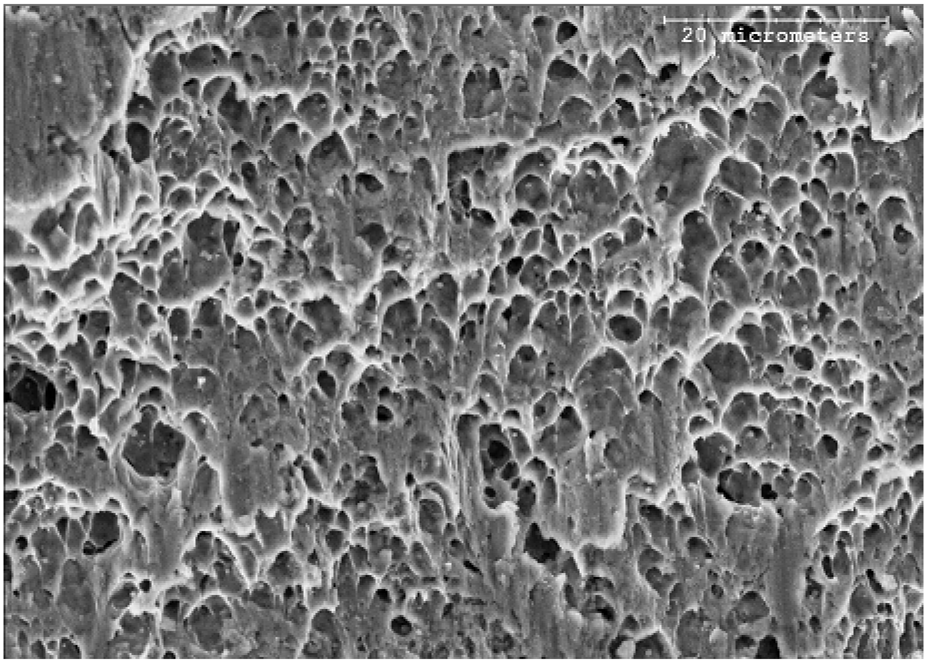

Figure 5.9 – Microvoid Coalescence on Longitudinal Weld Specimen L3-1 Fracture Surface

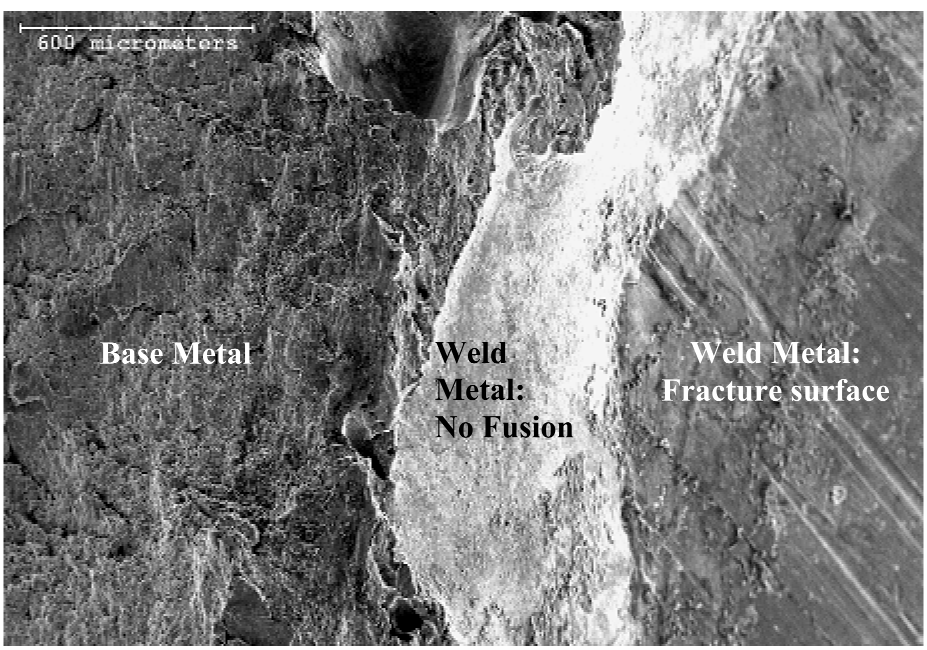

Figure 5.10 – Lack of Fusion at the Weld Root of Longitudinal Weld Specimen L1-2

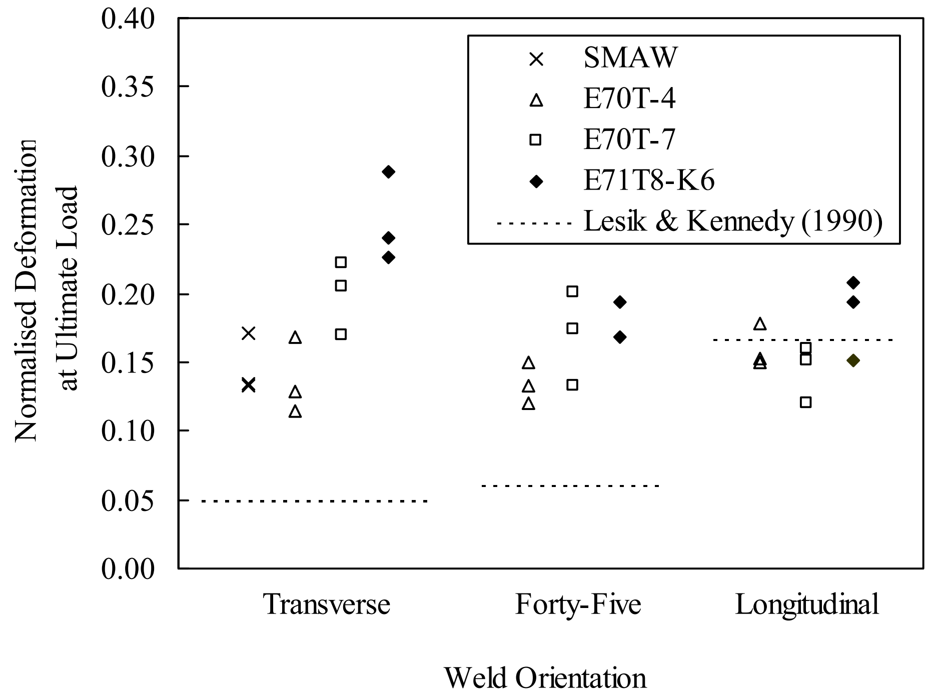

(a) Fillet Weld Ductility at Ultimate Load

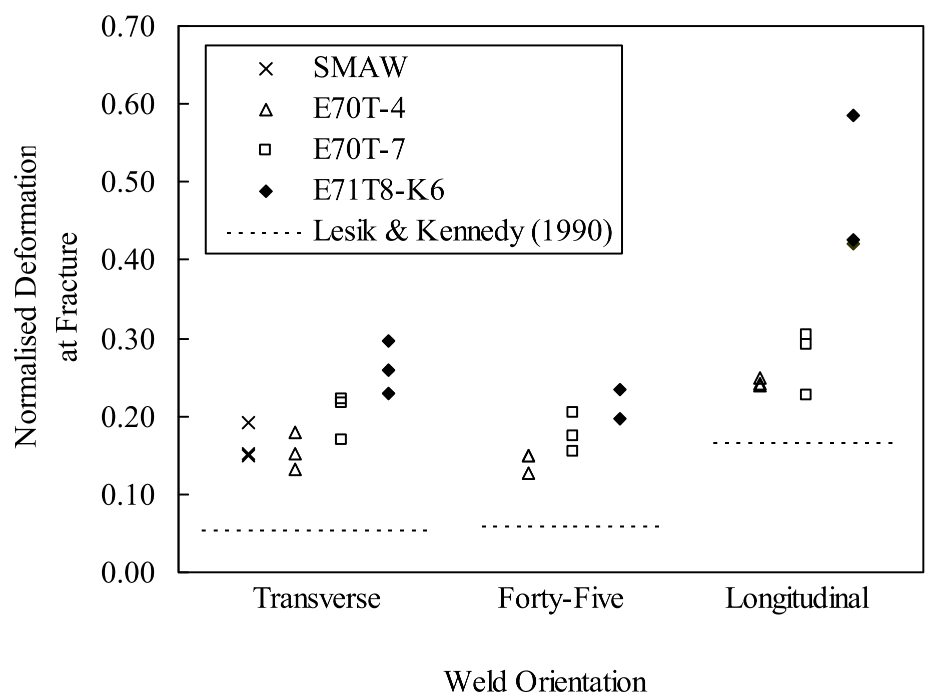

(b) Fillet Weld Ductility at Fracture

Figure 5.11 – Comparison of Fillet Weld Ductility with Predicted Ductility Values

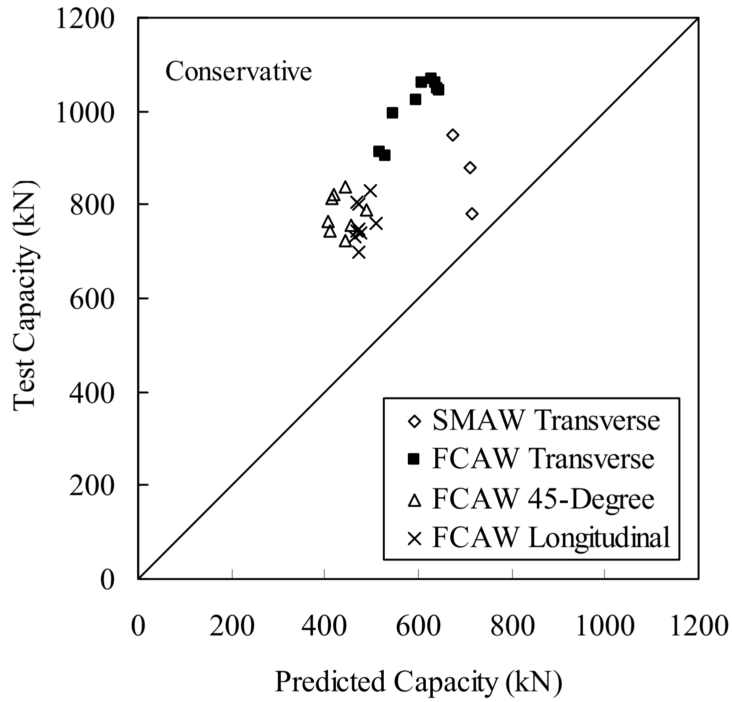

(a) Predicted Capacity Using Nominal Weld Strength

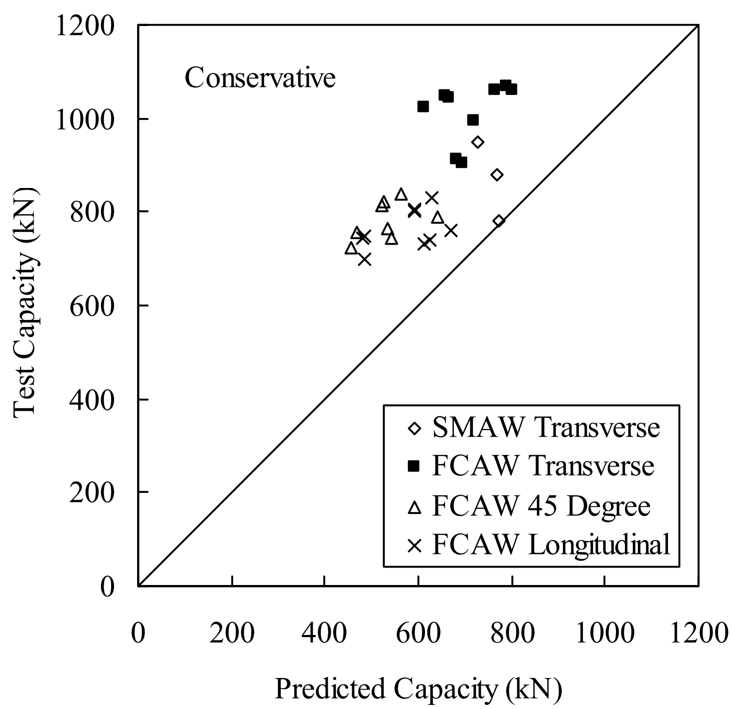

(b) Predicted Capacity Using Measured Weld Strength

Figure 5.12 – CSA–S16–01 (CSA 2001) Test vs. Predicted Capacity

6. SUMMARY AND CONCLUSIONS

6.1 Summary

Over the last few decades, many studies have been conducted to examine the strength and behaviour of fillet welds. However, no tests have been carried out on fillet welds that have been made with low toughness filler metal. Most of the studies used shielded metal arc welding (SMAW) for specimen fabrication, a process that can produce welds that are tougher than those of welding processes more commonly used for high production welding. Because the North American fillet weld design equations are based upon the behaviour of SMAW test specimens, the significant increase in weld strength recognised by these standards as the loading angle increases might not be suitable for low toughness welds. Therefore, an experimental program was conducted to investigate the effect of filler metal toughness on fillet weld behaviour.

The first phase of this test program included only transverse fillet welds. The variables in the first phase included filler metal classification (both filler metals with a toughness requirement and some without were tested); electrode manufacturer; fabricator; weld size; root notch orientation; and test temperature (Ng *et al*. 2003).

The second phase, which formed the basis of the work presented herein, examined the effect of filler metal classification and toughness on the strength and ductility of fillet welds loaded at different angles with respect to their longitudinal axis. The results of this phase were reported herein and were obtained from 30 lap-spliced specimens with 12.7 mm fillet welds. A welding process that is commonly used in high production welding, namely, fluxed-cored arc welding (FCAW), was used to prepare 27 of these specimens. The specimens were loaded in different directions with respect to the weld axis: 0°, 45°, and 90°. Two FCAW filler metals with no specified toughness (E70T-4, E70T-7) and one with a specified toughness (E71T8-K6) were chosen for the study. The other three specimens were control specimens prepared using the SMAW process. In order to determine the toughness levels obtained from FCAW and SMAW, Charpy V-notch impact tests were conducted on specimens prepared using each electrode classification.

The analysis of the effect of the filler metal classification, filler metal toughness, and fillet weld orientation was performed by comparing the weld stresses, fracture strains, and normalised deformations calculated from the test data. The weld stresses were determined using two different methods: one method accounted for the weld face reinforcement and root penetration and the other used the theoretical throat area determined from the measured weld leg sizes.

Comparison of the results of this study with those of previous studies and with the provisions of the North American steel design standards were also made. The adequacy of the current design equations was determined by evaluating the test-to-predicted ratios and by performing a reliability analysis.

6.1 Conclusions

The following conclusions are based on the analysis of the test results:

1. There is a significant difference in toughness levels between the FCAW filler metal selected for this program with a toughness requirement and those without. At 21°C, the mean Charpy V-notch impact energy for the filler metal with a toughness requirement was 12 times the mean impact energy for the filler metals without a toughness requirement. The SMAW filler metal, E7014, which has no toughness requirement, is also notably tougher than the FCAW filler metals without a toughness requirement. The mean measured energy absorption for the E7014 electrode was four times the mean results for the E70T-4 and E70T-7 electrodes at 21°C.

2. Filler metal classification and toughness level have little effect on the strength of transverse and 45-degree fillet welds. However, the longitudinal fillet welds made with the filler metal with a specified toughness had a lower mean strength than the longitudinal fillet welds with no specified toughness. The converse was observed in Phase I of this project because an electrode with a toughness requirement and a significantly higher tensile strength than the one used in the current phase of the program was included in Phase I.

3. As observed in the first phase of the test program, fillet welds prepared using a filler metal with a toughness requirement were more ductile than fillet welds prepared using filler metals without a toughness requirement. The mean fracture strains of the welds with a toughness requirement were 51%, 37%, and 84% higher than the fracture strains of the welds without a toughness requirement for the transverse, 45-degree, and longitudinal welds, respectively.

4. When weld fracture strain was used as the measure of weld ductility, there was no obvious relationship between weld orientation and weld ductility. However, the ductility of the longitudinal welds was notably higher than the ductility of the 45-degree and transverse welds. The mean fracture strains of the longitudinal welds were 1.79 and 3.02 times the mean fracture strains of the transverse and 45-degree welds, respectively.

5. Previous research by Butler and Kulak (1971), Clark (1971), Swannell and Skewes (1979), and Lesik and Kennedy (1990) has shown that weld deformations increase with decreasing loading angle. As expected, the normalised longitudinal weld deformations were higher than the normalised transverse and 45-degree weld deformations. However, the transverse welds deformed up to 22% more than the

45-degree welds. This unexpected behaviour may have been caused by the different state of stress created in the 45-degree welds and the transverse welds; the main plates in the transverse weld specimens yielded before weld fracture whereas the main plates in the 45-degree weld specimens remained elastic.

6. The weld fracture angle, defined as the angle between the fracture surface and the main plate, was observed generally to increase with a decrease in loading angle. The mean fracture angles were 14°, 28°, and 30° for the transverse, 45-degree, and longitudinal welds, respectively.

7. Photomicrographs of eight of the nine fracture surfaces examined showed microvoid coalescence, which indicates ductile failure. The other fracture surface contained approximately 70% cleavage fracture and it belonged to a 45-degree weld with a toughness requirement. However, the 3 mm sample length that was examined may not have been representative of the entire 50 mm long fracture surface because, despite the amount of cleavage fracture, the weld fracture strain of this weld was still among the highest of the 45-degree welds.

8. Except for six longitudinal weld specimens, the normalised weld deformations at ultimate load were at least as high as the values predicted by the equation proposed by Lesik and Kennedy (1990). All normalised deformations at weld fracture exceeded the values predicted by the Lesik and Kennedy equation.

9. The ratios between the ultimate strength of the welds loaded at an angle and the strength of the welds loaded longitudinally were comparable with the weld strength ratios determined by Miazga and Kennedy (1989). They also compared well with the ratios predicted by the CSA-S16–01 (CSA 2001) fillet weld design equation. The mean experimental transverse to longitudinal weld strength ratios were 1.71, 1.51, and 1.60 for the E70T-4, E70T-7, and E71T8-K6 welds, respectively, as compared with a predicted value of 1.50. The mean experimental 45-degree to longitudinal weld strength ratios were 1.49, 1.48, and 1.37 for the E70T-4, E70T-7, and E71T8-K6 welds, respectively, as compared with a predicted value of 1.30.

10. The weld capacities predicted by the CSA–S16–01 (CSA 2001) design equation are conservative for all specimens. The SMAW specimens had the lowest test-to-predicted ratios, 1.25 and 1.15, for predictions made using the nominal and measured weld strengths, respectively. The mean test-to-predicted ratios calculated with the nominal weld strengths for the FCAW specimens (all three electrode classifications combined) were reasonably consistent. These were 1.71, 1.78, and 1.60 for the transverse, 45-degree, and longitudinal weld series, respectively. When the test-to-predicted ratios are calculated using the measured weld strengths, those for the welds without a toughness requirement decreased substantially because of the amount of weld metal over-strength. The mean test-to-predicted ratios for the E70T-4, E70T-7,

and E71T8-K6 assemblies were 1.34, 1.35, and 1.61, respectively, for the transverse welds; 1.35, 1.54, and 1.60, respectively, for the 45-degree welds; and 1.17, 1.35, and 1.51, respectively, for the longitudinal welds.

11. For each of the three weld orientations, the reliability analysis showed that both North American fillet weld design equations provide a level of safety that exceeds the desired safety index of 4.5 for connections. The safety index determined from all the specimen results from Phases I and II and from Miazga and Kennedy (1989) was 4.9.

6.2 Recommendations for Future Research

The present research has helped expand the knowledge regarding fillet weld behaviour, but the results also presented further questions that could be answered by future work in the following areas:

1. Contrary to expectations, the transverse welds were observed to have larger deformations than the 45-degree welds. Because the main plates of the transverse weld specimens yielded while those of the 45-degree weld specimens did not, part of the explanation could be the possibility that yielding might have had an impact on weld ductility. An investigation of whether or not the stress level of the base plate affects the behaviour of fillet welds should be conducted.

2. The longitudinal welds tested in this project were only 50 mm long, which may not be representative of longer welds. Therefore, longitudinal welds longer than 50 mm should be tested to determine the relationship between weld length and weld strength.

3. All of the welds tested in Phases I and II were isolated. Because of the stark differences in behaviour observed for the different weld orientations, additional specimens should be tested that investigate the overall behaviour of joints with weld groups with combinations of orientations.

REFERENCES

AISC, 1999. "Load and Resistance Factor Design Specification for Structural Steel Buildings." American Institute of Steel Construction, Chicago, IL.

Archer, F. E., H. K. Fischer, and E. M. Kitchen, 1959. "Fillet Welds Subjected to Bending and Shear." Civil Engineering and Public Works Review, Vol. 54, No. 634, pp. 455-458.

ASTM, 2000. "Standard Specification for High-Strength Low-Alloy Columbium-Vanadium Structural Steel." A572/A572M-00, American Society for Testing and Materials, Philadelphia, PA.

ASTM, 1997. "Standard Test Methods and Definitions for Mechanical Testing of Steel Products," A370-97a, American Society for Testing and Materials, Philadelphia, PA.

AWS, 2002. "Structural Welding Code—Steel." 18th Edition, ANSI/AWS D1.1/D1.1M:2002, Miami, FL.

AWS, 1998. "Specification for Low-Alloy Steel Electrodes for Flux Cored Arc Welding," ANSI/AWS A5.29-98, American Welding Society, Miami, FL.

AWS, 1995. "Specification for Carbon Steel Electrodes for Flux Cored Arc Welding," ANSI/AWS A5.20-95, American Welding Society, Miami, FL.

AWS, 1991. "Specification for Carbon Steel Electrodes for Shielded Metal Arc Welding," ANSI/AWS A5.1-91, American Welding Society, Miami, FL.

Bowman, M. D. and B. P. Quinn, 1994. "Examination of Fillet Weld Strength." Engineering Journal, AISC, Vol. 31, No. 3, pp. 98-108.

Butler, L. J., and G. L. Kulak, 1971. "Strength of Fillet Welds as a Function of Direction of Load." Welding Journal, Welding Research Council, Vol. 36, No. 5, pp. 231s-234s.

Butler, L. J., S. Pal, and G. L. Kulak, 1972. "Eccentrically Loaded Welded Connections." Journal of the Structural Division, ASCE, Vol. 98, ST5, May, pp. 989-1005.

Clark, P. J., 1971. "Basis of Design for Fillet-Welded Joints Under Static Loading." Proceedings, Conference on Improving Welded Product Design, The Welding Institute, Vol. 1, pp. 85-96.

CSA, 2001. "Limit States Design of Steel Structures." CSA S16-01, Canadian Standards Association, Rexdale, ON.

CSA, 1998. “General Requirements for Rolled or Welded Structural Quality Steel/Structural Quality Steel.” CAN/CSA G40.20/G40.21-98, Canadian Standards Association, Etobicoke, ON.

CSA, 1994. “Limit States Design of Steel Structures.” CSA S16.1-94, Canadian Standards Association, Rexdale, ON.

Dawe, J.L. and G.L. Kulak, 1972. “Welded Connections under Combined Shear and Moment.” Journal of the Structural Division, Proceedings of the ASCE, Vol. 100, No. ST4, pp. 727-741.

Franchuk, C. R., R. G. Driver, and G. Y. Grondin, 2002. “Block Shear Behaviour of Coped Steel Beams,” Structural Engineering Report 244, Department of Civil and Environmental Engineering, University of Alberta, Edmonton.

Galambos, T.V., and M. K. Ravindra, 1978. “Properties of Steel for Use in LRFD,” Journal of the Structural Division, ASCE, Vol. 104, No. ST9, Sept., pp. 1459-1468.

Higgins, T. R. and F. R. Preece, 1969. “Proposed Stresses for Fillet Welds in Building Construction.” Engineering Journal, AISC, Vol. 6, No. 1, pp. 16-20.

ISO, 2000. “Welding and Allied Processes – Determination of Hydrogen Content in Ferritic Arc Weld Metal.” ISO 3690:2000, International Organization for Standardization, Geneva, Switzerland.

Iwankiw, N. R., 1997. “Rational Basis for Increased Fillet Weld Strength.” AISC Engineering Journal, Vol. 34, No.2, pp. 68-71.

Kamtekar, A. G., 1987. “The Strength of Inclined Fillet Welds.” Journal of Constructional Steel Research, Vol. 7, No. 1, pp. 43-54.

Kamtekar, A. G., 1982. “A New Analysis of the Strength of Some Simple Fillet Welded Connections.” Journal of Constructional Steel Research, Vol. 2, No. 2, pp. 33-45.

Kato, B. and K. Morita, 1974. “Strength of Transverse Fillet Welded Joints.” Welding Journal, Welding Research Supplement, Vol. 53, No. 2, pp. 59s-64s.

Kennedy, D. J. L and G. J. Kriviak, 1984. “The Strength of Fillet Welds Under Longitudinal and Transverse Shear: a Paradox.” Canadian Journal of Civil Engineering, Vol. 12, pp. 226-231.

Lesik, D. F. and D. J. L. Kennedy, 1990. "Ultimate Strength of Fillet Welded Connections Loaded in Plane." Canadian Journal of Civil Engineering, Vol. 17, No. 1, pp. 55-67.

Lesik, D. F., and D. J. L. Kennedy, 1988. "Ultimate Strength of Eccentrically Loaded Fillet Welded Connections," Structural Engineering Report 159, Department of Civil Engineering, University of Alberta, Edmonton, AB.

Mansell, D. S. and A. R. Yadav, 1982. "Failure Mechanisms in Fillet Welds." Proceedings of Eighth Australasian Conference on Mechanics of Structures and Materials, ACMSM 8, pp. 25.1-25.6.

McClellan, R. W., 1989. "Evaluation of Fillet Weld Shear Strength of FCAW Electrodes." Welding Journal, Vol. 68, No. 8, pp. 23-26.

Miazga, G. S. and D. J. L. Kennedy, 1989. "Behaviour of Fillet Welds as a Function of the Angle of Loading." Vol. 16, No. 4, pp. 583-599.

Miazga, G. S., and D. J. L. Kennedy, 1986. "Behaviour of Fillet Welds as a Function of the Angle of Loading." Structural Engineering Report 133, Department of Civil Engineering, University of Alberta, Edmonton, AB.

Neis, Vernon, 1985. "New Constitutive Law for Equal Leg Fillet Welds." Journal of Structural Engineering, Vol. 111, No. 8, pp. 1747-1759.

Ng, A. K. F., K. Deng, G.Y. Grondin, and R.G. Driver, 2003. "Behavior of Transverse Fillet Welds: Experimental Program." Paper submitted for publication in the Engineering Journal, American Institute of Steel Construction.

Ng, A. K. F., R. G. Driver, and G. Y. Grondin, 2002. "Behaviour of Transverse Fillet Welds." Structural Engineering Report 245, Department of Civil and Environmental Engineering, University of Alberta, Edmonton.

Pham, L, 1983*a*. "Co-ordinated Testing of Fillet Welds Part 1—Cruciform Specimens." Australian Welding Research, Vol. 12, pp. 16-25.

Pham, L, 1983*b*. "Co-ordinated Testing of Fillet Welds Part 2—Werner Specimen." Australian Welding Research, Vol. 12, pp. 54-60.

Sanaei, E. and A. G. Kamtekar, 1988. "Experiments on Some Arbitrarily Loaded fillet Welds." Welding Journal, Welding Research Supplement, Vol. 67, No. 5, pp. 103s-109s.

Swannell, P, 1981*a*. "Rational Design of Fillet Weld Groups." Journal of the Structural Division, ASCE, Vol. 107, No. ST5, pp. 789-802.

Swannell, P., 1981*b*. "Weld Group Behavior." Journal of the Structural Division, ASCE, Vol. 107, No. ST5,, pp. 803-815.

Swannell, P. and I. C. Skewes, 1979. "The Design of Welded Brackets Loaded In-Plane: Elastic and Ultimate Load Techniques—AWRA Report P6-8-77." Australian Welding Research, Vol. 7, pp. 28-59.

APPENDIX A

Welding Procedures Specification

Appendix A – Welding Procedure Specifications

All the fillet weld specimens were prepared by Supreme Steel Ltd. except for the three SMAW specimens, which were prepared by Waiward Steel Fabricators Ltd. The welding was performed in the horizontal position. The nominal leg size of the fillets was 12.7 mm, which was achieved using three passes. The E70T-4 and E71T8-K6 weld assemblies from which the weld metal tension coupons and Charpy V-Notch specimens were cut were prepared by Supreme Steel while the E7014 and E70T-7 weld assemblies from which they were cut were prepared by Waiward.

Two separate welding procedures are provided for the Supreme Steel specimens, one for the transverse specimens (Table A1) and another for the 45-degree and longitudinal specimens (Table A2). There are two specifications for this fabricator because the transverse specimens were all fabricated earlier in Phase I of the project. Table A1 shows only the portion of the original specifications prepared by Supreme Steel that correspond to the transverse specimens analysed in Phase II. In any case, the specifications for the welds made of the same filler metal are the same regardless of the weld orientation.

Table A1 – Welding Procedure Specifications for 90° Specimens from Supreme Steel

Supreme Steel Data Sheet

Date: 18-Oct-01
Job: 1072
Project: AISC - University of Alberta Fillet Weld Project

Personnel: Welder - Ed Homeniuk (Supreme Steel)
QA/Engineer - Todd Collister (Supreme Steel)

Conditions: Standard Shop Conditions

Material: See Waiward Steel for material specifications and other information

Equipment:

Welding Machine	Wire Feeder
Lincoln Electric	Lincoln Electric
Model - DC-600	LN-7 Wire Feeder
Code - W383-1	Code - 9168
Type - K1288M	Serial No.- 186030
Serial No.- 292309	Input voltage 115 50/60 Hz current 2.0 Amps

Notes: -Best welds on same side were choosen based on visual inspection
-Other side of plate was reinforced with small fillet weld
-Groove welded specimen were welded with a maintained temperature of 150 degrees celcius
-Temperature of plate was monitored with a temperature crayon

Specimen	Mark	Producer	Filler Metal	Class	Polarity	Stick-out	Wire speed	Amps.	Volts	Date
1/2" fillet	T4-H-S	Hobart	Fabshield 4	E70T-4	DC+	2.5"	225	350	29	21-Aug
Groove	T4-H-S	Hobart	Fabshield 4	E70T-4	DC+	2.5"	225	350	29	21-Aug
1/2" fillet	T7-H-S	Hobart	Fabshield 7027	E70T-7	DC-	1.5"	170	350	26	16-Oct
Groove	T7-H-S	Hobart	Fabshield 7027	E70T-7	DC-	1.5"	170	350	26	17-Oct
1/2" fillet	T8-K6-H-S	Hobart	Fabshield 3Ni1	E71T8-K6	DC-	.75"	180	330	24	18-Oct
Groove	T8-K6-H-S	Hobart	Fabshield 3Ni1	E71T8-K6	DC-	.75"	180	330	24	18-Oct

Table A2 – Welding Procedure Specifications for 45° and 0° Specimens from Supreme Steel

Supreme Steel Data Sheet

Date: 14-Mar-02
Job: 1201
Project: AISC - University of Alberta Fillet Weld Project- Phase II

Personnel: Welder - Ed Homeniuk
QA/Engineer - Todd Collister

Conditions: Standard Shop Conditions

Material: ASTM A572-Grade 50

Equipment:

Welding Machine	**Wire Feeder**
Lincoln Electric	Lincoln Electric
Model - DC-600	LN-7 Wire Feeder
Code - W383-1	Code - 9168
Type - K1288M	Serial No.- 186030
Serial No.- 292309	Input voltage 115 50/60 Hz current 2.0 Amps

Notes: -Best welds on same side were choosen based on visual inspection
-Other side of plate was reinforced with small fillet weld
-Temperature of plate was monitored with a temperature crayon

Specimen	Mark	Producer	Filler Metal	Class	Wire dia.	Polarity	Stick-out	Wire speed	Amps.	Volts
45° 1/2" fillet	T4-H-S	Hobart	Fabshield 4	E70T-4	3/32"	DC+	2.5"	225	350	29
45° 1/2" fillet	T4-H-S	Hobart	Fabshield 4	E70T-4	3/32"	DC+	2.5"	225	350	29
45° 1/2" fillet	T4-H-S	Hobart	Fabshield 4	E70T-4	3/32"	DC+	2.5"	225	350	29
45° 1/2" fillet	T7-H-S	Hobart	Fabshield 7027	E70T-7	3/32"	DC-	1.5"	170	350	26
45° 1/2" fillet	T7-H-S	Hobart	Fabshield 7027	E70T-7	3/32"	DC-	1.5"	170	350	26
45° 1/2" fillet	T7-H-S	Hobart	Fabshield 7027	E70T-7	3/32"	DC-	1.5"	170	350	26
45° 1/2" fillet	T8-H-S	Hobart	Fabshield 3Ni1	E71T8-K6	5/64"	DC-	.75"	180	330	24
45° 1/2" fillet	T8-H-S	Hobart	Fabshield 3Ni1	E71T8-K6	5/64"	DC-	.75"	180	330	24
45° 1/2" fillet	T8-H-S	Hobart	Fabshield 3Ni1	E71T8-K6	5/64"	DC-	.75"	180	330	24
Longit. 1/2" fillet	T4-H-S	Hobart	Fabshield 4	E70T-4	3/32"	DC+	2.5"	225	350	29
Longit. 1/2" fillet	T4-H-S	Hobart	Fabshield 4	E70T-4	3/32"	DC+	2.5"	225	350	29
Longit. 1/2" fillet	T4-H-S	Hobart	Fabshield 4	E70T-4	3/32"	DC+	2.5"	225	350	29
Longit. 1/2" fillet	T7-H-S	Hobart	Fabshield 7027	E70T-7	3/32"	DC-	1.5"	170	350	26
Longit. 1/2" fillet	T7-H-S	Hobart	Fabshield 7027	E70T-7	3/32"	DC-	1.5"	170	350	26
Longit. 1/2" fillet	T7-H-S	Hobart	Fabshield 7027	E70T-7	3/32"	DC-	1.5"	170	350	26
Longit. 1/2" fillet	T8-H-S	Hobart	Fabshield 3Ni1	E71T8-K6	5/64"	DC-	.75"	180	330	24
Longit. 1/2" fillet	T8-H-S	Hobart	Fabshield 3Ni1	E71T8-K6	5/64"	DC-	.75"	180	330	24
Longit. 1/2" fillet	T8-H-S	Hobart	Fabshield 3Ni1	E71T8-K6	5/64"	DC-	.75"	180	330	24

Table A3 – Welding Procedure Specifications for Specimens from Waiward

Filler Metal: Lincoln E7014

Pass #	Class	Dia.	Polarity	Wire Feed Speed	Amperage	Volts	Travel Speed
1-3	E7014	5/32	DC-	N/A	170	—	10

Weld Details

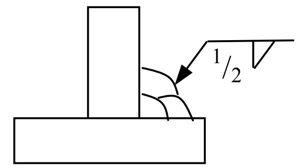

Filler Metal: Lincoln E7014

Pass #	Class	Dia.	Polarity	Wire Feed Speed	Amperage	Volts	Travel Speed
1-26	E7014	5/32	DC-	N/A	170	—	10

Weld Details

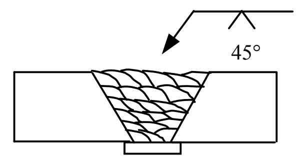

Filler Metal: Fabshield 7027 Stick-out: 1.5”

Pass #	Class	Dia.	Polarity	Wire Feed Speed	Amperage	Volts	Travel Speed
1-10	E70T-7	3/32	DC-	214	410	28.5	13-15

Weld Detail

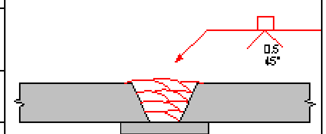

Note: All speeds are inches/min.

APPENDIX B

Weld Measurements and Weld Profiles

Appendix B – Weld Measurements and Weld Profiles

This appendix contains the fillet weld measurements and plots of the weld profiles. The measurements for the transverse welds are also presented in Ng *et al*. (2002).

The tables shown provide all the weld measurements made before and after testing. The pre-test measurements include the size of the two weld legs, which were obtained at 10 mm intervals along the weld length, and the actual weld length. In addition, measurements of the weld profile, oriented at an angle of 45° to the main plate, were performed at three different points on the weld face cross-section in order to better characterise the profile. However, in the case of the 45-degree welds and longitudinal welds, such measurements were made at only the point near the weld throat because the specimen configurations caused difficulties in obtaining reasonably accurate measurements at the other points on the weld face. The weld sizes and the 45° measurements were collected at the same points along the weld length. The locations of the latter measurements on the weld face are shown in Figure B1.

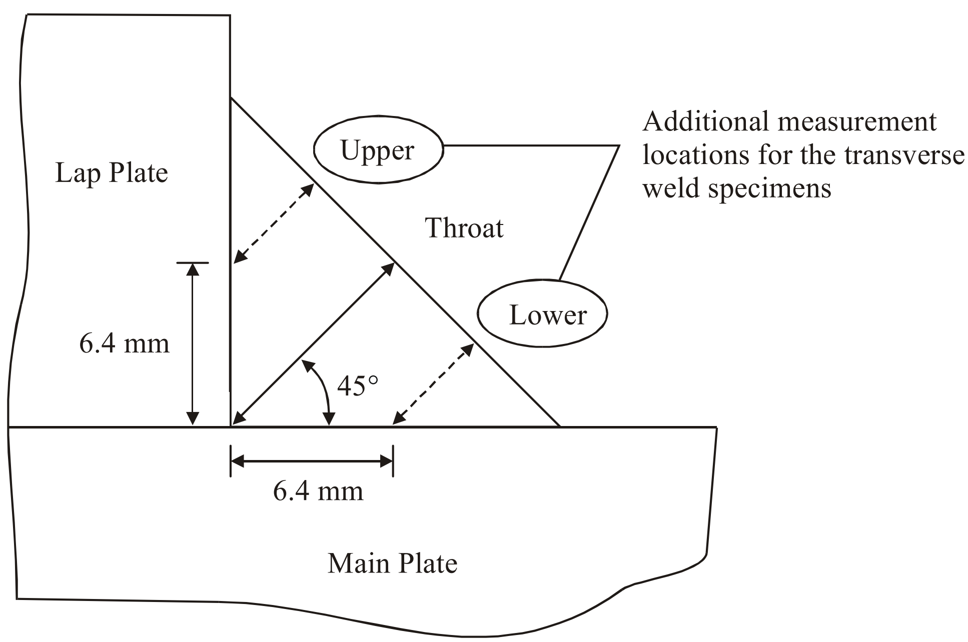

Figure B1 – Fillet Weld Measurements Made at 45º

After weld fracture, measurements of the fracture surface, fracture surface angle, and the weld shear leg on the main plate (called Shear Leg After Fracture) were made for each weld that fractured first. The location of these measured components on the fractured weld is shown in Figure B2. All measurements were taken at the same locations along the weld length as the locations at which the pre-test measurements were made.

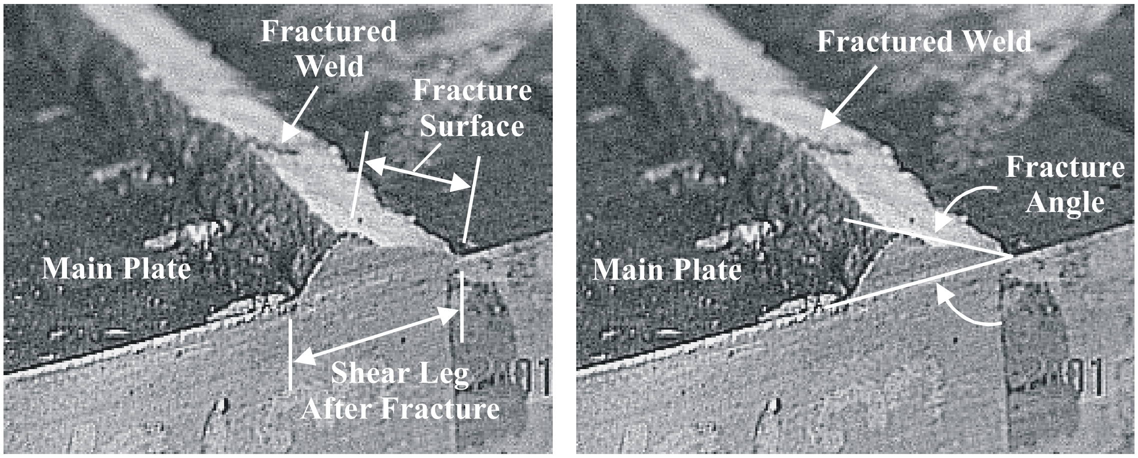

Figure B2 – Post-Test Fillet Weld Measurements

The Weld Root Penetration values were calculated from the difference between the Shear Leg measurement made before testing and the Shear Leg After Fracture measurement made after testing.

The gauge lengths used for determining weld strains are presented in Table B31. The values for the transverse and 45-degree welds are the means of the two gauge length measurements made at each LVDT location as described in Section 3.8. The values for the longitudinal welds are the means of the weld shear legs on the main plate.

Table B1 – Weld Measurements for Specimen T20-1

Meas. Number	Pre-Test Weld Measurements												Post-Test Weld Measurements			
	Front Face						Back Face						Failure Face			
	Shear Leg (mm)	Tension Leg (mm)	45° Measurements Upper (mm)	45° Measurements Throat (mm)	45° Measurements Lower (mm)	Weld Length (mm)	Shear Leg (mm)	Tension Leg (mm)	45° Measurements Upper (mm)	45° Measurements Throat (mm)	45° Measurements Lower (mm)	Weld Length (mm)	Shear Leg After Fracture (mm)	Fracture Surface (mm)	Weld Root Penetration (mm)	Fracture Angle (°)
1	13.1	13.6	4.5	9.5	4.8	75.9	13.4	12.5	4.5	10.2	6.0	75.8	14.5	9.3	1.4	29
2	12.9	14.7	4.4	9.7	5.2	75.8	12.2	13.1	4.2	10.0	5.9	75.8	15.2	9.4	2.2	30
3	13.0	14.2	4.5	9.7	5.4	75.9	12.5	13.4	4.2	9.8	5.9	75.8	14.9	9.6	1.9	31
4	13.0	14.2	4.7	9.8	5.9	75.8	12.9	13.9	4.8	10.0	5.9	75.8	16.3	11.0	3.3	24
5	13.6	14.3	5.0	10.2	6.0	75.8	13.3	14.2	4.8	10.2	6.2	75.8	16.3	10.3	2.7	27
6	13.5	13.8	4.8	9.8	6.0		13.5	14.6	5.3	10.6	6.4		15.8	10.4	2.3	25
7	13.9	13.9	4.8	9.7	5.9		14.7	13.9	6.1	11.0	7.1		16.1	10.4	2.2	26
8	14.6	15.0	4.8	10.2	5.9		14.0	14.1	5.0	10.6	6.8		18.1	10.6	3.5	23
Mean	**13.4**	**14.2**	**4.7**	**9.8**	**5.6**	**75.8**	**13.3**	**13.7**	**4.9**	**10.3**	**6.3**	**75.8**	**15.9**	**10.1**	**2.4**	**27**

Table B2 – Weld Measurements for Specimen T20-2

Meas. Number	Pre-Test Weld Measurements												Post-Test Weld Measurements			
	Front Face						Back Face						Failure Face			
	Shear Leg (mm)	Tension Leg (mm)	45° Measurements Upper (mm)	45° Measurements Throat (mm)	45° Measurements Lower (mm)	Weld Length (mm)	Shear Leg (mm)	Tension Leg (mm)	45° Measurements Upper (mm)	45° Measurements Throat (mm)	45° Measurements Lower (mm)	Weld Length (mm)	Shear Leg After Fracture (mm)	Fracture Surface (mm)	Weld Root Penetration (mm)	Fracture Angle (°)
1	13.0	13.1	3.7	9.0	4.9	76.0	13.9	14.5	4.7	9.5	5.7	75.9	14.2	14.2	1.2	0
2	13.1	12.5	3.7	9.0	5.1	76.0	13.4	14.9	4.5	9.4	5.6	75.9	13.5	13.5	0.4	29
3	12.9	13.0	3.7	8.9	4.8	75.9	13.2	14.5	4.8	9.5	5.7	75.9	13.3	13.3	0.4	26
4	12.6	13.1	4.0	9.2	5.1	76.0	13.1	15.2	4.7	9.7	5.9	76.0	13.5	13.5	0.9	0
5	12.4	13.6	4.2	9.2	5.1	76.0	13.1	14.2	4.8	9.7	5.7	75.9	13.3	13.3	1.0	0
6	12.5	14.0	4.0	9.2	5.2		13.2	14.3	4.7	9.5	5.9		13.3	13.3	0.8	0
7	13.2	13.0	4.0	9.4	5.2		13.5	14.8	4.7	9.8	6.0		14.3	14.3	1.1	0
8	12.7	13.1	4.5	9.5	5.1		13.5	14.7	4.8	9.8	6.0		14.2	14.2	1.5	0
Mean	**12.8**	**13.2**	**4.0**	**9.2**	**5.1**	**76.0**	**13.4**	**14.6**	**4.7**	**9.6**	**5.8**	**75.9**	**13.7**	**13.7**	**0.9**	**7**

Table B3 – Weld Measurements for Specimen T20-3

Meas. Number	Pre-Test Weld Measurements												Post-Test Weld Measurements			
	Front Face						Back Face						Failure Face			
	Shear Leg (mm)	Tension Leg (mm)	45° Measurements Upper (mm)	45° Measurements Throat (mm)	45° Measurements Lower (mm)	Weld Length (mm)	Shear Leg (mm)	Tension Leg (mm)	45° Measurements Upper (mm)	45° Measurements Throat (mm)	45° Measurements Lower (mm)	Weld Length (mm)	Shear Leg After Fracture (mm)	Fracture Surface (mm)	Weld Root Penetration (mm)	Fracture Angle (°)
1	12.2	14.3	4.4	9.7	4.9	75.9	13.9	13.3	4.0	9.4	5.1	76.2	13.6	13.6	1.4	0
2	13.1	14.2	4.7	10.0	5.2	76.0	13.9	13.4	4.0	9.2	5.4	76.2	14.7	14.7	1.6	0
3	13.6	14.3	5.1	10.8	6.0	76.0	13.6	13.8	4.5	9.5	5.6	76.2	15.1	15.1	1.5	0
4	13.8	15.0	6.1	11.7	7.0	76.0	14.3	14.0	4.2	9.5	5.6	76.1	13.6	13.6	-0.2	0
5	14.0	13.8	6.7	10.0	6.8	76.1	13.7	13.5	4.5	9.8	5.9	76.2	15.6	14.9	1.6	0
6	13.2	13.9	5.5	9.7	4.9		13.8	13.1	4.2	9.5	5.9		15.3	9.8	2.1	20
7	13.4	13.3	5.3	9.4	4.8		13.9	13.7	4.4	9.5	5.7		15.3	8.8	1.8	20
8	13.4	14.0	5.3	9.2	4.4		14.1	13.6	4.4	9.0	5.4		15.3	9.1	1.9	20
Mean	**13.3**	**14.1**	**5.4**	**10.1**	**5.5**	**76.0**	**13.9**	**13.6**	**4.3**	**9.4**	**5.6**	**76.2**	**14.8**	**12.4**	**1.5**	**7**

Table B4 – Weld Measurements for Specimen T22-1

Meas. Number	Pre-Test Weld Measurements												Post-Test Weld Measurements			
	Front Face						Back Face						Failure Face			
	Shear Leg (mm)	Tension Leg (mm)	45° Measurements Upper (mm)	45° Measurements Throat (mm)	45° Measurements Lower (mm)	Weld Length (mm)	Shear Leg (mm)	Tension Leg (mm)	45° Measurements Upper (mm)	45° Measurements Throat (mm)	45° Measurements Lower (mm)	Weld Length (mm)	Shear Leg After Fracture (mm)	Fracture Surface (mm)	Weld Root Penetration (mm)	Fracture Angle (°)
1	9.8	10.0	3.4	7.8	3.2	76.3	10.3	11.3	4.4	9.2	4.0	76.1	12.2	12.2	2.4	0
2	9.5	10.9	3.6	7.9	3.0	76.2	10.9	11.6	4.7	9.0	4.1	76.1	12.2	12.2	2.4	0
3	9.3	10.6	3.4	7.8	2.9	76.2	10.9	12.0	5.0	9.4	4.1	76.1	12.2	12.2	2.8	0
4	8.9	10.7	3.4	7.8	2.9	76.2	10.5	12.2	5.0	9.4	4.1	76.1	12.2	12.2	3.0	0
5	9.8	10.3	3.7	7.6	3.2	76.2	11.8	12.1	4.7	9.2	4.4	76.1	12.5	12.5	3.6	0
6	9.3	11.3	4.0	8.3	3.5		11.0	12.2	4.8	8.9	4.4		12.8	12.8	3.0	0
7	9.5	10.7	3.6	7.9	3.7		12.2	12.0	5.0	9.2	4.4		10.9	10.9	1.6	0
8	9.6	10.6	3.4	7.6	3.2		11.0	12.0	4.7	9.2	4.3		12.5	12.5	3.0	0
Mean	**9.4**	**10.6**	**3.6**	**7.8**	**3.2**	**76.2**	**11.1**	**11.9**	**4.8**	**9.2**	**4.2**	**76.1**	**12.2**	**12.2**	**2.7**	**0**

Table B5 – Weld Measurements for Specimen T22-2

Meas. Number	Pre-Test Weld Measurements												Post-Test Weld Measurements			
	Front Face						Back Face						Failure Face			
	Shear Leg (mm)	Tension Leg (mm)	45° Measurements Upper (mm)	45° Measurements Throat (mm)	45° Measurements Lower (mm)	Weld Length (mm)	Shear Leg (mm)	Tension Leg (mm)	45° Measurements Upper (mm)	45° Measurements Throat (mm)	45° Measurements Lower (mm)	Weld Length (mm)	Shear Leg After Fracture (mm)	Fracture Surface (mm)	Weld Root Penetration (mm)	Fracture Angle (°)
1	9.9	9.4	2.9	7.0	3.2	76.1	10.5	11.4	4.8	8.7	3.8	76.1	12.4	12.4	2.5	0
2	10.5	10.5	3.6	7.9	3.8	76.1	11.3	11.4	4.8	8.9	4.3	76.1	13.2	13.2	2.7	0
3	10.2	10.1	3.1	7.6	3.8	76.1	11.2	11.3	4.8	9.0	4.3	76.1	12.4	12.4	2.2	0
4	8.5	10.2	3.4	8.1	3.0	76.1	11.0	11.6	4.8	9.0	3.8	76.1	10.3	10.3	1.9	0
5	10.4	10.0	3.2	8.3	3.7	76.1	11.9	10.9	4.8	8.9	4.3	76.1	13.2	13.2	2.7	0
6	9.7	9.9	3.1	8.4	3.2		10.2	11.9	5.1	9.2	3.7		12.0	12.0	2.3	0
7	11.4	10.0	3.4	8.4	3.7		10.6	11.6	5.0	8.9	3.8		13.7	13.7	2.3	0
8	12.2	10.4	3.4	8.6	4.3		9.9	11.9	4.8	9.0	3.8		14.4	14.4	2.3	0
Mean	**10.3**	**10.0**	**3.3**	**8.0**	**3.6**	**76.1**	**10.8**	**11.5**	**4.9**	**9.0**	**4.0**	**76.1**	**12.7**	**12.7**	**2.4**	**0**

Table B6 – Weld Measurements for Specimen T22-3

Meas. Number	Pre-Test Weld Measurements												Post-Test Weld Measurements			
	Front Face						Back Face						Failure Face			
	Shear Leg (mm)	Tension Leg (mm)	45° Measurements Upper (mm)	45° Measurements Throat (mm)	45° Measurements Lower (mm)	Weld Length (mm)	Shear Leg (mm)	Tension Leg (mm)	45° Measurements Upper (mm)	45° Measurements Throat (mm)	45° Measurements Lower (mm)	Weld Length (mm)	Shear Leg After Fracture (mm)	Fracture Surface (mm)	Weld Root Penetration (mm)	Fracture Angle (°)
1	11.7	9.7	3.2	8.3	4.6	76.0	10.0	11.6	4.4	8.3	3.2	76.1	14.2	14.2	2.5	0
2	11.5	10.4	3.7	8.4	4.6	76.0	10.7	11.1	4.0	8.3	3.5	76.1	13.8	13.8	2.3	0
3	11.6	10.3	3.4	8.4	4.3	76.0	10.1	11.4	4.2	7.9	3.3	76.1	13.9	13.9	2.3	0
4	9.5	10.6	3.4	8.1	3.2	76.1	9.5	11.5	4.5	8.6	3.0	76.2	11.5	11.5	2.0	0
5	11.1	9.9	3.1	8.1	4.0	76.1	10.2	11.7	4.0	8.4	3.2	76.1	13.0	13.0	1.9	0
6	10.6	9.6	3.2	8.3	4.1		9.5	11.1	4.5	8.1	3.2		11.9	11.9	1.3	0
7	10.4	9.8	3.4	9.0	4.3		10.3	12.0	4.8	9.0	3.7		11.4	11.4	1.0	0
8	12.3	10.6	3.4	8.4	4.4		10.9	12.1	4.7	9.0	3.7		13.9	13.9	1.5	0
Mean	**11.1**	**10.1**	**3.4**	**8.4**	**4.2**	**76.0**	**10.1**	**11.6**	**4.4**	**8.5**	**3.3**	**76.1**	**12.9**	**12.9**	**1.8**	**0**

Table B7 – Weld Measurements for Specimen T26-1

Meas. Number	Pre-Test Weld Measurements												Post-Test Weld Measurements			
	Front Face						Back Face						Failure Face			
	Shear Leg (mm)	Tension Leg (mm)	45° Measurements Upper (mm)	45° Measurements Throat (mm)	45° Measurements Lower (mm)	Weld Length (mm)	Shear Leg (mm)	Tension Leg (mm)	45° Measurements Upper (mm)	45° Measurements Throat (mm)	45° Measurements Lower (mm)	Weld Length (mm)	Shear Leg After Fracture (mm)	Fracture Surface (mm)	Weld Root Penetration (mm)	Fracture Angle (°)
1	12.2	11.7	4.4	9.8	4.6	76.0	13.7	10.8	4.2	9.0	4.9	76.2	16.5	10.9	2.8	24
2	12.9	11.5	4.5	9.5	4.9	76.0	13.7	10.7	3.7	8.7	4.8	76.2	15.7	9.5	2.0	27
3	12.2	11.9	4.8	9.4	4.8	76.0	13.1	10.7	3.6	9.0	4.6	77.0	14.4	9.3	1.3	25
4	13.1	11.7	4.8	9.5	5.1	76.0	13.2	10.4	3.6	9.2	4.6	76.0	15.1	10.0	1.8	22
5	12.6	11.4	5.0	9.4	5.1	76.0	12.0	10.5	3.4	9.0	4.4	76.1	14.3	9.9	2.3	21
6	11.7	11.9	5.0	9.7	4.9		13.1	10.6	3.7	9.0	4.8		15.3	10.1	2.1	22
7	12.2	11.6	4.8	9.4	4.9		13.4	10.7	3.6	9.0	5.1		15.4	10.0	2.0	23
8	12.4	11.4	4.7	9.4	4.8		13.4	10.2	3.7	8.6	5.4		14.9	8.9	1.6	30
Mean	**12.4**	**11.6**	**4.8**	**9.5**	**4.9**	**76.0**	**13.2**	**10.6**	**3.7**	**9.0**	**4.8**	**76.3**	**15.2**	**9.8**	**2.0**	**24**

Table B8 – Weld Measurements for Specimen T26-2

Meas. Number	Pre-Test Weld Measurements												Post-Test Weld Measurements			
	Front Face						Back Face						Failure Face			
	Shear Leg (mm)	Tension Leg (mm)	45° Measurements Upper (mm)	45° Measurements Throat (mm)	45° Measurements Lower (mm)	Weld Length (mm)	Shear Leg (mm)	Tension Leg (mm)	45° Measurements Upper (mm)	45° Measurements Throat (mm)	45° Measurements Lower (mm)	Weld Length (mm)	Shear Leg After Fracture (mm)	Fracture Surface (mm)	Weld Root Penetration (mm)	Fracture Angle (°)
1	11.5	11.6	4.8	9.5	4.8	75.9	12.6	11.3	4.5	9.4	5.1	76.2	15.1	11.7	3.6	23
2	12.9	11.9	4.8	9.4	4.9	75.9	13.0	11.2	4.5	9.2	5.1	76.1	16.7	11.7	3.8	23
3	13.0	12.0	5.0	9.4	5.1	75.9	12.4	10.9	4.2	9.0	4.9	76.1	16.8	11.4	3.8	23
4	11.2	11.5	4.8	9.5	4.8	76.0	11.7	11.0	4.0	9.0	4.3	76.2	14.7	11.6	3.5	23
5	12.7	12.2	5.0	9.7	5.1	75.9	13.0	10.8	4.2	9.2	4.8	76.2	15.4	11.1	2.8	23
6	13.5	12.2	5.0	9.5	5.2		12.4	11.3	4.5	9.4	4.6		17.3	11.7	3.8	22
7	12.3	11.9	4.8	9.7	5.1		12.9	11.5	4.5	9.4	4.8		14.9	11.3	2.6	23
8	12.3	11.7	4.8	9.5	4.9		13.6	11.7	4.5	9.2	5.1		15.1	11.3	2.9	21
Mean	**12.4**	**11.9**	**4.9**	**9.5**	**5.0**	**75.9**	**12.7**	**11.2**	**4.4**	**9.2**	**4.8**	**76.1**	**15.8**	**11.4**	**3.3**	**23**

Table B9 – Weld Measurements for Specimen T26-3

Meas. Number	Pre-Test Weld Measurements												Post-Test Weld Measurements			
	Front Face						Back Face						Failure Face			
	Shear Leg (mm)	Tension Leg (mm)	45° Measurements Upper (mm)	45° Measurements Throat (mm)	45° Measurements Lower (mm)	Weld Length (mm)	Shear Leg (mm)	Tension Leg (mm)	45° Measurements Upper (mm)	45° Measurements Throat (mm)	45° Measurements Lower (mm)	Weld Length (mm)	Shear Leg After Fracture (mm)	Fracture Surface (mm)	Weld Root Penetration (mm)	Fracture Angle (°)
1	12.2	11.5	4.2	9.4	4.6	76.2	12.1	12.3	5.0	9.2	4.8	76.2	14.9	10.2	2.7	24
2	12.7	11.6	4.2	9.2	4.6	76.1	13.1	11.7	4.5	9.2	4.9	76.2	15.1	10.6	2.4	20
3	12.6	11.5	4.2	9.0	4.9	76.2	13.3	11.3	4.4	9.2	4.8	76.2	14.8	10.0	2.2	24
4	13.7	11.6	4.8	9.5	5.2	76.1	13.0	11.3	4.4	9.5	5.1	76.3	16.8	11.9	3.1	22
5	13.0	11.9	4.5	9.4	5.1	76.2	13.2	11.3	4.4	9.5	5.1	76.2	15.3	9.9	2.3	24
6	13.1	11.7	4.5	9.2	5.1		13.6	11.7	4.4	9.7	5.1		14.5	9.8	1.3	23
7	12.8	11.7	4.8	9.2	5.2		12.9	11.4	4.2	9.2	4.9		14.5	9.8	1.7	25
8	13.8	11.9	5.1	9.5	5.7		13.0	11.5	4.2	9.0	5.2		16.4	10.6	2.6	26
Mean	**13.0**	**11.7**	**4.6**	**9.3**	**5.1**	**76.2**	**13.0**	**11.6**	**4.4**	**9.3**	**5.0**	**76.2**	**15.3**	**10.3**	**2.3**	**24**

Table B10 – Weld Measurements for Specimen T32-1

Meas. Number	Pre-Test Weld Measurements												Post-Test Weld Measurements			
	Front Face						Back Face						Failure Face			
	Shear Leg (mm)	Tension Leg (mm)	45° Measurements Upper (mm)	45° Measurements Throat (mm)	45° Measurements Lower (mm)	Weld Length (mm)	Shear Leg (mm)	Tension Leg (mm)	45° Measurements Upper (mm)	45° Measurements Throat (mm)	45° Measurements Lower (mm)	Weld Length (mm)	Shear Leg After Fracture (mm)	Fracture Surface (mm)	Weld Root Penetration (mm)	Fracture Angle (°)
1	12.5	11.3	4.0	9.0	4.4	76.0	12.6	12.7	4.5	8.6	4.6	76.2	15.9	10.2	3.4	25
2	12.5	11.0	4.0	9.0	4.3	76.0	12.9	12.7	4.7	8.6	4.6	76.2	16.3	10.2	3.4	25
3	12.7	11.4	4.2	8.9	4.4	76.0	12.8	12.4	4.7	8.9	4.6	76.2	16.5	10.7	3.6	25
4	12.0	11.7	4.2	8.7	4.0	76.0	12.0	12.6	5.0	9.2	4.3	76.2	15.4	11.3	3.4	25
5	12.3	11.4	4.0	7.9	4.3	76.0	11.5	12.3	4.8	9.4	4.3	76.2	13.8	10.6	2.3	25
6	12.2	11.7	4.0	8.7	4.6		12.4	13.2	5.3	9.0	4.3		15.8	11.5	3.5	25
7	12.3	10.1	3.9	9.0	4.3		12.0	13.1	4.7	8.7	4.4		16.3	10.2	4.3	23
8	11.6	11.2	4.0	8.7	4.4		11.5	12.4	4.4	8.7	4.4		15.4	10.3	3.9	25
Mean	**12.3**	**11.2**	**4.1**	**8.8**	**4.3**	**76.0**	**12.2**	**12.7**	**4.8**	**8.9**	**4.4**	**76.2**	**15.7**	**10.6**	**3.5**	**25**

Table B11 – Weld Measurements for Specimen T32-2

Meas. Number	Pre-Test Weld Measurements												Post-Test Weld Measurements			
	Front Face						Back Face						Failure Face			
	Shear Leg (mm)	Tension Leg (mm)	45° Measurements Upper (mm)	45° Measurements Throat (mm)	45° Measurements Lower (mm)	Weld Length (mm)	Shear Leg (mm)	Tension Leg (mm)	45° Measurements Upper (mm)	45° Measurements Throat (mm)	45° Measurements Lower (mm)	Weld Length (mm)	Shear Leg After Fracture (mm)	Fracture Surface (mm)	Weld Root Penetration (mm)	Fracture Angle (°)
1	12.1	11.8	4.0	8.9	4.6	76.0	12.1	12.6	4.5	9.4	4.8	76.1	15.0	10.7	2.9	21
2	11.1	11.6	4.4	9.0	4.6	76.1	11.8	11.9	4.5	9.4	4.4	76.1	14.6	10.5	2.8	21
3	12.1	11.5	4.0	9.0	4.8	76.1	12.7	12.2	4.5	9.2	4.8	76.1	15.9	10.7	3.2	21
4	11.4	10.4	4.2	9.4	4.6	76.1	11.7	13.6	4.7	8.9	4.6	76.1	15.1	10.5	3.4	22
5	10.8	12.4	4.7	9.4	4.6	76.1	13.0	12.7	5.0	9.2	4.8	76.1	16.3	10.5	3.3	22
6	11.1	11.8	4.8	9.7	4.6		11.7	12.3	5.0	9.2	4.8		15.1	10.2	3.4	23
7	11.1	11.7	4.7	8.7	4.6		11.8	12.7	4.8	8.6	4.9		15.3	9.8	3.5	26
8	11.3	12.3	4.7	8.6	4.4		11.7	13.2	4.8	8.4	4.6		15.0	8.7	3.3	31
Mean	**11.4**	**11.7**	**4.4**	**9.1**	**4.6**	**76.1**	**12.1**	**12.7**	**4.7**	**9.0**	**4.7**	**76.1**	**15.3**	**10.2**	**3.2**	**23**

Table B12 – Weld Measurements for Specimen T32-3

Meas. Number	Pre-Test Weld Measurements												Post-Test Weld Measurements			
	Front Face						Back Face						Failure Face			
	Shear Leg (mm)	Tension Leg (mm)	45° Measurements Upper (mm)	45° Measurements Throat (mm)	45° Measurements Lower (mm)	Weld Length (mm)	Shear Leg (mm)	Tension Leg (mm)	45° Measurements Upper (mm)	45° Measurements Throat (mm)	45° Measurements Lower (mm)	Weld Length (mm)	Shear Leg After Fracture (mm)	Fracture Surface (mm)	Weld Root Penetration (mm)	Fracture Angle (°)
1	10.8	12.7	5.3	10.5	4.4	76.0	11.6	11.6	3.9	8.7	4.1	76.1	14.8	11.6	4.0	12
2	11.6	13.9	5.3	9.0	4.6	76.0	12.7	11.4	3.9	8.4	4.4	76.1	15.7	11.9	4.1	14
3	10.6	12.1	5.1	9.0	4.0	76.0	12.6	11.1	3.9	8.6	4.6	76.0	14.3	10.2	3.7	17
4	10.0	13.7	4.8	7.9	3.8	76.0	12.6	11.1	4.2	8.7	4.6	76.1	13.0	9.6	3.0	16
5	9.9	12.6	4.8	8.4	4.0	76.0	12.4	11.6	4.7	9.5	4.9	76.1	13.7	13.7	3.8	0
6	10.4	12.2	4.8	8.4	4.3		12.3	12.0	4.8	9.5	4.8		13.8	13.7	3.4	0
7	10.1	12.8	4.8	7.9	3.8		11.4	12.8	4.8	9.4	4.6		13.2	12.2	3.1	0
8	10.3	13.0	4.8	8.6	4.1		11.8	12.4	4.8	9.2	4.8		13.2	9.3	2.9	20
Mean	**10.5**	**12.9**	**5.0**	**8.7**	**4.1**	**76.0**	**12.2**	**11.8**	**4.4**	**9.0**	**4.6**	**76.1**	**13.9**	**11.5**	**3.5**	**10**

Table B13 – Weld Measurements for Specimen F1-1

Meas. Number	Pre-Test Weld Measurements								Post-Test Weld Measurements			
	Front Face				Back Face				Failure Face			
	Shear Leg (mm)	Tension Leg (mm)	45° Meas. (mm)	Weld Length (mm)	Shear Leg (mm)	Tension Leg (mm)	45° Meas. (mm)	Weld Length (mm)	Shear Leg After Fracture (mm)	Fracture Surface (mm)	Weld Root Penetration (mm)	Fracture Angle (°)
1	11.6	10.2	8.1	72.9	9.9	10.8	7.8	72.8	16.4	12.7	4.8	15
2	10.5	10.6	9.4	74.6	12.2	10.2	8.1	72.3	15.1	11.9	4.6	14
3	12.5	10.9	9.0		12.6	11.0	8.1		16.9	11.6	4.4	26
4	12.4	11.0	8.9		12.7	11.0	8.7		13.2	9.4	0.8	28
5	10.5	11.6	8.9		11.2	11.6	9.5		12.0	9.1	1.6	20
6	10.4	10.4	8.1		12.5	11.5	9.5		12.8	10.7	2.4	20
Mean	**11.3**	**10.8**	**8.7**	**73.7**	**11.8**	**11.0**	**8.6**	**72.5**	**14.4**	**10.9**	**3.1**	**20**

Table B14 – Weld Measurements for Specimen F1-2

Meas. Number	Pre-Test Weld Measurements								Post-Test Weld Measurements			
	Front Face				Back Face				Failure Face			
	Shear Leg (mm)	Tension Leg (mm)	45° Meas. (mm)	Weld Length (mm)	Shear Leg (mm)	Tension Leg (mm)	45° Meas. (mm)	Weld Length (mm)	Shear Leg After Fracture (mm)	Fracture Surface (mm)	Weld Root Penetration (mm)	Fracture Angle (°)
1	9.6	9.6	7.1	69.9	9.1	8.2	6.8	73.1	11.7	9.2	2.0	16
2	10.4	9.6	7.3	71.6	10.9	9.6	7.0	73.0	12.8	9.5	2.4	16
3	10.3	9.1	7.6	71.5	12.1	9.1	7.6	74.2	11.1	8.2	0.8	24
4	9.3	9.3	6.5		11.3	9.8	7.9		10.5	8.7	1.2	19
5	9.9	9.9	6.7		11.2	10.9	7.9		13.0	9.6	3.1	20
6	10.0	9.5	7.3		10.8	10.6	7.3		12.7	9.2	2.8	22
Mean	**9.9**	**9.5**	**7.1**	**71.0**	**10.9**	**9.7**	**7.4**	**73.4**	**12.0**	**9.1**	**2.0**	**20**

Table B15 – Weld Measurements for Specimen F1-3

Meas. Number	Pre-Test Weld Measurements								Post-Test Weld Measurements			
	Front Face				Back Face				Failure Face			
	Shear Leg (mm)	Tension Leg (mm)	45° Meas. (mm)	Weld Length (mm)	Shear Leg (mm)	Tension Leg (mm)	45° Meas. (mm)	Weld Length (mm)	Shear Leg After Fracture (mm)	Fracture Surface (mm)	Weld Root Penetration (mm)	Fracture Angle (°)
1	8.8	9.5	7.8	70.5	12.7	9.7	7.9	74.7	11.3	8.0	2.5	31
2	9.3	9.7	7.9	73.1	11.0	10.1	7.9	73.4	11.1	8.9	1.7	30
3	10.3	10.4	8.1	71.7	11.1	10.2	8.3		10.9	7.7	0.6	32
4	10.3	10.1	8.4		10.8	10.0	8.4		10.8	8.1	0.5	26
5	9.1	10.2	7.9		11.0	11.0	8.7		11.4	8.7	2.3	25
6	9.1	10.0	8.1		9.7	11.2	8.3		11.3	9.4	2.3	12
Mean	**9.5**	**10.0**	**8.0**	**71.7**	**11.1**	**10.4**	**8.3**	**74.0**	**11.1**	**8.4**	**1.6**	**26**

Table B16 – Weld Measurements for Specimen F2-1

Meas. Number	Pre-Test Weld Measurements								Post-Test Weld Measurements			
	Front Face				Back Face				Failure Face			
	Shear Leg (mm)	Tension Leg (mm)	45° Meas. (mm)	Weld Length (mm)	Shear Leg (mm)	Tension Leg (mm)	45° Meas. (mm)	Weld Length (mm)	Shear Leg After Fracture (mm)	Fracture Surface (mm)	Weld Root Penetration (mm)	Fracture Angle (°)
1	8.7	11.4	7.6	73.3	9.7	12.3	6.7	71.7	12.7	8.6	3.9	62
2	8.7	9.6	7.1	70.3	10.4	11.9	7.9	70.0	12.6	9.3	3.9	63
3	9.8	9.8	7.3		9.7	11.1	7.9		14.5	9.3	4.8	64
4	9.8	10.1	7.9		9.7	10.6	7.6		14.2	9.3	4.4	66
5	9.8	9.6	7.9		10.0	11.5	7.8		13.8	10.6	4.0	20
6	10.4	10.3	7.9		9.9	11.3	7.6		13.9	10.7	3.5	14
Mean	**9.5**	**10.1**	**7.6**	**71.8**	**9.9**	**11.4**	**7.6**	**70.8**	**13.6**	**9.6**	**4.1**	**48**

Table B17 – Weld Measurements for Specimen F2-2

Meas. Number	Pre-Test Weld Measurements								Post-Test Weld Measurements			
	Front Face				Back Face				Failure Face			
	Shear Leg (mm)	Tension Leg (mm)	45° Meas. (mm)	Weld Length (mm)	Shear Leg (mm)	Tension Leg (mm)	45° Meas. (mm)	Weld Length (mm)	Shear Leg After Fracture (mm)	Fracture Surface (mm)	Weld Root Penetration (mm)	Fracture Angle (°)
1	9.5	11.9	7.6	73.6	10.2	11.2	8.3	69.9	16.9	11.0	6.8	55
2	10.6	11.6	8.3	71.7	9.7	11.1	7.9	72.2	16.0	10.5	6.3	62
3	10.7	11.0	8.1		11.1	10.9	8.4		16.4	12.0	5.3	16
4	11.1	10.8	8.4		9.4	11.1	8.6		12.8	9.5	3.4	16
5	11.5	11.3	8.4		10.9	10.7	8.3		14.2	9.9	3.3	16
6	11.1	10.8	7.8		10.6	11.0	7.9		14.9	10.5	4.4	12
Mean	**10.7**	**11.2**	**8.1**	**72.7**	**10.3**	**11.0**	**8.2**	**71.0**	**15.2**	**10.6**	**4.9**	**29**

Table B18 – Weld Measurements for Specimen F2-3

Meas. Number	Pre-Test Weld Measurements								Post-Test Weld Measurements			
	Front Face				Back Face				Failure Face			
	Shear Leg (mm)	Tension Leg (mm)	45° Meas. (mm)	Weld Length (mm)	Shear Leg (mm)	Tension Leg (mm)	45° Meas. (mm)	Weld Length (mm)	Shear Leg After Fracture (mm)	Fracture Surface (mm)	Weld Root Penetration (mm)	Fracture Angle (°)
1	9.4	10.9	7.1	72.7	11.3	11.4	8.1	75.5	11.6	8.3	2.3	33
2	9.7	11.2	7.6	68.5	10.9	11.4	7.9	75.7	12.1	9.2	2.4	27
3	8.6	11.4	7.6		11.3	11.2	8.1		10.8	8.4	2.2	32
4	9.3	11.0	7.3		11.0	11.1	8.3		11.7	9.1	2.4	29
5	8.9	10.6	7.5		10.7	10.3	7.9		12.0	9.3	3.1	26
6	9.9	11.0	8.1		10.7	10.2	8.1		13.9	10.8	4.0	22
Mean	**9.3**	**11.0**	**7.5**	**70.6**	**11.0**	**11.0**	**8.1**	**75.6**	**12.0**	**9.2**	**2.7**	**28**

Table B19 – Weld Measurements for Specimen F3-1

Meas. Number	Pre-Test Weld Measurements								Post-Test Weld Measurements			
	Front Face				Back Face				Failure Face			
	Shear Leg (mm)	Tension Leg (mm)	45° Meas. (mm)	Weld Length (mm)	Shear Leg (mm)	Tension Leg (mm)	45° Meas. (mm)	Weld Length (mm)	Shear Leg After Fracture (mm)	Fracture Surface (mm)	Weld Root Penetration (mm)	Fracture Angle (°)
1	9.8	12.4	9.2	67.9	10.3	13.9	9.0	70.8	12.6	9.2	2.8	25
2	9.4	11.4	9.2	71.3	10.5	13.3	9.4	71.6	12.1	9.0	2.7	25
3	9.9	12.4	9.2	71.4	10.3	13.4	9.0	71.0	14.0	9.0	4.1	37
4	10.0	11.9	8.6		10.7	13.1	9.5		13.1	9.1	3.0	24
5	10.5	13.5	8.7		10.7	13.0	7.9		14.4	9.7	4.0	28
6	10.6	12.5	8.1		10.7	13.5	7.9		14.1	9.3	3.5	30
Mean	**10.0**	**12.3**	**8.8**	**70.2**	**10.5**	**13.4**	**8.8**	**71.1**	**13.4**	**9.2**	**3.3**	**28**

Table B20 – Weld Measurements for Specimen F3-2

Meas. Number	Pre-Test Weld Measurements								Post-Test Weld Measurements			
	Front Face				Back Face				Failure Face			
	Shear Leg (mm)	Tension Leg (mm)	45° Meas. (mm)	Weld Length (mm)	Shear Leg (mm)	Tension Leg (mm)	45° Meas. (mm)	Weld Length (mm)	Shear Leg After Fracture (mm)	Fracture Surface (mm)	Weld Root Penetration (mm)	Fracture Angle (°)
1	8.9	11.0	7.6	69.4	9.8	11.2	6.8	70.5	16.0	9.9	6.2	28
2	9.3	10.4	7.6	73.4	9.7	11.7	7.5	73.4	12.8	9.9	3.1	20
3	10.7	10.2	7.3	72.5	9.6	12.5	7.6	74.2	12.4	9.3	2.8	19
4	10.9	11.0	8.3		9.1	11.4	8.3		11.2	7.7	2.0	24
5	10.9	11.2	7.9		9.3	11.0	7.6		11.5	7.8	2.2	30
6	11.3	10.2	7.1		9.3	11.4	7.9		12.0	9.3	2.7	50
Mean	**10.3**	**10.7**	**7.6**	**71.8**	**9.5**	**11.5**	**7.6**	**72.7**	**12.6**	**9.0**	**3.2**	**28**

Table B21 – Weld Measurements for Specimen F3-3

	Pre-Test Weld Measurements								Post-Test Weld Measurements			
	Front Face				Back Face				Failure Face			
Meas. Number	Shear Leg (mm)	Tension Leg (mm)	45° Meas. (mm)	Weld Length (mm)	Shear Leg (mm)	Tension Leg (mm)	45° Meas. (mm)	Weld Length (mm)	Shear Leg After Fracture (mm)	Fracture Surface (mm)	Weld Root Penetration (mm)	Fracture Angle (°)
1	9.5	10.8	7.8	71.7	8.7	12.1	9.0	67.3	Fracture in Reinforced Weld			
2	9.1	11.9	7.5	72.2	9.8	12.4	9.2	71.2				
3	8.2	13.4	6.8	72.4	9.6	13.1	8.9	71.9				
4	9.5	13.5	7.3		9.4	13.9	7.9					
5	9.3	13.1	7.8		9.7	14.0	8.9					
6	9.7	12.8	8.6		9.8	12.9	7.8					
Mean	**9.2**	**12.6**	**7.6**	**72.1**	**9.5**	**13.0**	**8.6**	**70.1**	—	—	—	—

Table B22 – Weld Measurements for Specimen L1-1

Meas. Number	Pre-Test Weld Measurements															
	Front Face								Back Face							
	Weld 1				Weld 2				Weld 3				Weld 4			
	Main Plate Leg (mm)	Lap Plate Leg (mm)	45° Meas. (mm)	Weld Length (mm)	Main Plate Leg (mm)	Lap Plate Leg (mm)	45° Meas. (mm)	Weld Length (mm)	Main Plate Leg (mm)	Lap Plate Leg (mm)	45° Meas. (mm)	Weld Length (mm)	Main Plate Leg (mm)	Lap Plate Leg (mm)	45° Meas. (mm)	Weld Length (mm)
1	10.8	11.4	4.0	49.8	8.7	9.1	7.1	50.4	9.6	10.4	8.1	49.0	10.0	9.9	7.1	47.7
2	11.7	11.4	6.7	49.7	9.1	9.1	7.8	50.4	11.2	11.2	8.7	49.2	10.2	11.6	7.8	47.7
3	10.2	11.2	4.4	49.6	8.2	9.4	7.1	50.6	10.5	11.1	8.7	49.3	9.1	11.6	7.8	47.9
4	10.3	11.4	7.0	49.6	8.6	10.1	7.0	50.7	10.4	10.4	8.3	49.4	10.4	11.0	7.6	48.1
5	10.2	11.4	7.5	49.6	9.2	9.4	7.1	51.1	11.0	9.8	8.4	49.8	10.3	11.2	7.6	48.2
Mean	**10.6**	**11.4**	**5.9**	**49.6**	**8.7**	**9.4**	**7.2**	**50.6**	**10.5**	**10.6**	**8.4**	**49.3**	**10.0**	**11.0**	**7.6**	**47.9**

Meas. Number	Post-Test Weld Measurements							
	Weld 3				Weld 4			
	Main Plate Leg After Fracture (mm)	Fracture Surface (mm)	Weld Root Penetration (mm)	Fracture Angle (°)	Main Plate Leg After Fracture (mm)	Fracture Surface (mm)	Weld Root Penetration (mm)	Fracture Angle (°)
1	10.6	7.6	1.0	31	10.7	7.1	0.6	36
2	11.9	7.9	0.7	31	11.4	7.3	1.2	39
3	11.0	7.9	0.4	29	10.4	8.1	1.3	35
4	10.3	6.9	-0.1	31	10.8	7.2	0.4	36
5	11.4	6.6	0.4	44	11.6	8.0	1.3	33
Mean	**11.0**	**7.4**	**0.5**	**33**	**11.0**	**7.5**	**1.0**	**36**

Table B23 – Weld Measurements for Specimen L1-2

Meas. Number	Pre-Test Weld Measurements															
	Front Face								Back Face							
	Weld 1				Weld 2				Weld 3				Weld 4			
	Main Plate Leg (mm)	Lap Plate Leg (mm)	45° Meas. (mm)	Weld Length (mm)	Main Plate Leg (mm)	Lap Plate Leg (mm)	45° Meas. (mm)	Weld Length (mm)	Main Plate Leg (mm)	Lap Plate Leg (mm)	45° Meas. (mm)	Weld Length (mm)	Main Plate Leg (mm)	Lap Plate Leg (mm)	45° Meas. (mm)	Weld Length (mm)
1	12.2	10.8	7.8	49.5	10.8	10.2	7.8	50.0	10.7	8.9	7.3	50.5	10.9	8.3	7.3	49.5
2	11.3	11.1	7.9	49.8	11.6	10.6	8.1	49.9	11.5	9.2	7.6	50.4	9.4	9.4	7.1	49.5
3	11.3	11.9	7.8	50.0	11.7	10.8	8.1	50.2	10.1	10.0	7.9	50.4	10.1	9.3	7.6	49.6
4	11.9	11.9	7.6	50.0	12.3	10.0	7.6	50.0	11.3	9.8	7.8	50.4	12.0	10.5	7.8	49.7
5	9.6	11.7	8.1	50.4	12.1	10.5	7.5	50.2	11.2	10.1	7.5	50.4	12.1	9.3	7.1	49.8
Mean	**11.3**	**11.5**	**7.8**	**49.9**	**11.7**	**10.4**	**7.8**	**50.0**	**11.0**	**9.6**	**7.6**	**50.4**	**10.9**	**9.4**	**7.4**	**49.6**

Meas. Number	Post-Test Weld Measurements							
	Weld 1				Weld 2			
	Main Plate Leg After Fracture (mm)	Fracture Surface (mm)	Weld Root Penetration (mm)	Fracture Angle (°)	Main Plate Leg After Fracture (mm)	Fracture Surface (mm)	Weld Root Penetration (mm)	Fracture Angle (°)
1	13.2	7.5	1.0	38	13.5	9.6	2.7	18
2	12.2	7.2	0.9	38	13.6	9.3	2.0	21
3	11.9	7.1	0.6	38	13.2	8.2	1.5	26
4	12.6	8.7	0.7	37	13.3	8.9	1.0	23
5	11.5	8.2	1.9	32	14.0	9.2	1.9	30
Mean	**12.3**	**7.7**	**1.0**	**37**	**13.5**	**9.0**	**1.8**	**23**

Table B24 – Weld Measurements for Specimen L1-3

Meas. Number	Pre-Test Weld Measurements															
	Front Face								Back Face							
	Weld 1				Weld 2				Weld 3				Weld 4			
	Main Plate Leg (mm)	Lap Plate Leg (mm)	45° Meas. (mm)	Weld Length (mm)	Main Plate Leg (mm)	Lap Plate Leg (mm)	45° Meas. (mm)	Weld Length (mm)	Main Plate Leg (mm)	Lap Plate Leg (mm)	45° Meas. (mm)	Weld Length (mm)	Main Plate Leg (mm)	Lap Plate Leg (mm)	45° Meas. (mm)	Weld Length (mm)
1	11.6	11.2	7.5	48.1	9.1	10.3	6.7	50.8	10.6	9.6	8.1	49.3	9.7	9.7	7.3	49.9
2	10.2	12.4	8.7	48.3	9.3	11.0	6.8	50.8	10.6	9.6	6.5	49.4	11.0	10.5	7.0	49.4
3	10.4	12.8	7.9	48.4	9.8	10.9	6.4	50.8	11.4	10.4	7.9	49.6	11.0	10.8	6.5	49.4
4	10.2	10.2	6.8	48.4	9.1	10.6	6.8	50.7	10.7	10.3	7.3	49.6	9.4	10.6	7.6	49.4
5	11.6	10.9	9.2	48.4	9.6	10.7	7.8	50.9	10.7	10.5	7.9	49.8	10.5	10.5	7.9	49.5
Mean	**10.8**	**11.5**	**8.0**	**48.3**	**9.4**	**10.7**	**6.9**	**50.8**	**10.8**	**10.1**	**7.6**	**49.5**	**10.3**	**10.4**	**7.3**	**49.5**

Meas. Number	Post-Test Weld Measurements							
	Weld 1				Weld 2			
	Main Plate Leg After Fracture (mm)	Fracture Surface (mm)	Weld Root Penetration (mm)	Fracture Angle (°)	Main Plate Leg After Fracture (mm)	Fracture Surface (mm)	Weld Root Penetration (mm)	Fracture Angle (°)
1	13.3	8.6	1.8	26	10.8	7.9	1.8	28
2	11.0	8.5	0.8	27	11.4	8.6	2.1	28
3	11.1	7.9	0.7	36	10.7	6.9	1.0	38
4	12.4	6.1	2.2	44	10.9	8.2	1.7	32
5	13.2	9.7	1.6	25	11.3	7.7	1.7	31
Mean	**12.2**	**8.2**	**1.4**	**31**	**11.0**	**7.9**	**1.7**	**31**

Table B25 – Weld Measurements for Specimen L2-1

Meas. Number	Pre-Test Weld Measurements															
	Front Face								Back Face							
	Weld 1				Weld 2				Weld 3				Weld 4			
	Main Plate Leg (mm)	Lap Plate Leg (mm)	45° Meas. (mm)	Weld Length (mm)	Main Plate Leg (mm)	Lap Plate Leg (mm)	45° Meas. (mm)	Weld Length (mm)	Main Plate Leg (mm)	Lap Plate Leg (mm)	45° Meas. (mm)	Weld Length (mm)	Main Plate Leg (mm)	Lap Plate Leg (mm)	45° Meas. (mm)	Weld Length (mm)
1	10.1	12.2	9.5	47.4	9.8	11.0	7.9	49.4	10.5	10.8	8.3	49.2	11.5	11.0	6.8	49.6
2	10.4	12.5	8.9	47.8	11.0	11.1	8.3	49.6	10.7	11.1	8.4	49.2	11.5	11.1	7.1	49.7
3	10.8	12.3	8.9	48.1	11.1	11.3	7.8	49.6	11.2	11.4	8.4	49.5	11.5	11.2	7.3	49.4
4	11.7	11.5	9.5	48.2	11.3	11.7	8.4	49.8	11.3	11.6	8.1	49.6	11.8	11.4	7.9	49.3
5	11.3	11.3	9.0	48.4	10.2	11.7	8.4	50.1	10.4	11.5	6.8	50.3	11.7	11.3	7.3	49.4
Mean	**10.9**	**12.0**	**9.2**	**48.0**	**10.7**	**11.4**	**8.2**	**49.7**	**10.8**	**11.3**	**8.0**	**49.6**	**11.6**	**11.2**	**7.3**	**49.5**

Meas. Number	Post-Test Weld Measurements			
	Weld 2			
	Main Plate Leg After Fracture (mm)	Fracture Surface (mm)	Weld Root Penetration (mm)	Fracture Angle (°)
1	12.0	9.3	2.2	26
2	13.3	10.0	2.4	25
3	13.0	9.1	1.9	31
4	13.9	9.9	2.6	25
5	12.9	9.5	2.7	28
Mean	**13.0**	**9.6**	**2.3**	**27**

Table B26 – Weld Measurements for Specimen L2-2

Meas. Number	Pre-Test Weld Measurements															
	Front Face								Back Face							
	Weld 1				Weld 2				Weld 3				Weld 4			
	Main Plate Leg (mm)	Lap Plate Leg (mm)	45° Meas. (mm)	Weld Length (mm)	Main Plate Leg (mm)	Lap Plate Leg (mm)	45° Meas. (mm)	Weld Length (mm)	Main Plate Leg (mm)	Lap Plate Leg (mm)	45° Meas. (mm)	Weld Length (mm)	Main Plate Leg (mm)	Lap Plate Leg (mm)	45° Meas. (mm)	Weld Length (mm)
1	10.0	10.1	6.7	49.3	9.9	10.1	7.1	50.1	13.0	10.4	7.9	50.2	9.2	11.2	6.0	49.8
2	11.0	11.3	6.5	48.9	9.4	10.2	7.0	50.3	12.0	10.7	7.8	50.0	10.1	11.9	7.0	48.7
3	10.4	11.3	6.8	48.9	9.8	9.9	6.7	50.0	11.9	11.5	7.9	49.9	9.6	11.7	6.4	48.7
4	10.2	10.9	7.3	48.7	10.7	9.7	6.7	49.9	12.9	11.1	7.6	49.8	10.2	11.9	6.7	48.6
5	9.8	11.2	7.0	48.7	10.2	10.6	6.4	49.9	11.9	11.3	7.3	49.8	9.7	11.5	6.4	48.5
Mean	**10.3**	**11.0**	**6.9**	**48.9**	**10.0**	**10.1**	**6.8**	**50.0**	**12.3**	**11.0**	**7.7**	**49.9**	**9.8**	**11.6**	**6.5**	**48.9**

Meas. Number	Post-Test Weld Measurements			
	Weld 2			
	Main Plate Leg After Fracture (mm)	Fracture Surface (mm)	Weld Root Penetration (mm)	Fracture Angle (°)
1	12.3	8.4	3.0	27
2	12.0	8.3	1.9	27
3	10.3	6.4	0.7	36
4	11.6	8.1	1.4	32
5	12.4	8.9	2.7	29
Mean	**11.7**	**8.0**	**1.9**	**30**

Table B27 – Weld Measurements for Specimen L2-3

Meas. Number	Pre-Test Weld Measurements															
	Front Face								Back Face							
	Weld 1				Weld 2				Weld 3				Weld 4			
	Main Plate Leg (mm)	Lap Plate Leg (mm)	45° Meas. (mm)	Weld Length (mm)	Main Plate Leg (mm)	Lap Plate Leg (mm)	45° Meas. (mm)	Weld Length (mm)	Main Plate Leg (mm)	Lap Plate Leg (mm)	45° Meas. (mm)	Weld Length (mm)	Main Plate Leg (mm)	Lap Plate Leg (mm)	45° Meas. (mm)	Weld Length (mm)
1	11.1	11.5	8.9	50.0	9.7	11.2	7.5	49.9	9.3	11.1	7.8	46.7	10.2	10.8	8.1	49.1
2	11.6	11.8	9.0	49.9	9.1	11.3	7.3	50.1	9.8	11.4	7.8	46.6	11.1	10.7	7.9	49.3
3	11.5	11.9	9.2	49.8	9.9	11.0	7.3	49.9	11.4	11.8	8.4	46.4	11.1	11.2	7.9	49.3
4	11.1	12.3	9.0	49.8	10.4	11.2	7.3	49.7	10.7	12.4	8.1	46.6	10.2	11.1	7.6	49.3
5	10.8	12.0	9.0	49.5	10.1	11.5	7.1	49.3	11.4	12.5	8.7	46.5	10.0	11.3	8.1	49.2
Mean	**11.2**	**11.9**	**9.0**	**49.8**	**9.8**	**11.2**	**7.3**	**49.8**	**10.5**	**11.8**	**8.2**	**46.6**	**10.5**	**11.0**	**7.9**	**49.2**

Meas. Number	Post-Test Weld Measurements			
	Weld 2			
	Main Plate Leg After Fracture (mm)	Fracture Surface (mm)	Weld Root Penetration (mm)	Fracture Angle (°)
1	12.6	9.2	3.3	24
2	12.5	8.9	2.7	25
3	14.2	9.8	2.8	23
4	11.9	7.9	1.3	26
5	14.6	9.5	3.2	24
Mean	**13.2**	**9.1**	**2.7**	**24**

Table B28 – Weld Measurements for Specimen L3-1

Meas. Number	Pre-Test Weld Measurements															
	Front Face								Back Face							
	Weld 1				Weld 2				Weld 3				Weld 4			
	Main Plate Leg (mm)	Lap Plate Leg (mm)	45° Meas. (mm)	Weld Length (mm)	Main Plate Leg (mm)	Lap Plate Leg (mm)	45° Meas. (mm)	Weld Length (mm)	Main Plate Leg (mm)	Lap Plate Leg (mm)	45° Meas. (mm)	Weld Length (mm)	Main Plate Leg (mm)	Lap Plate Leg (mm)	45° Meas. (mm)	Weld Length (mm)
1	9.8	11.2	9.2	49.5	10.1	10.4	9.7	51.1	9.3	10.1	8.3	49.3	9.1	10.6	8.4	50.9
2	10.5	11.7	9.5	49.4	10.5	11.3	9.5	50.6	9.5	10.4	7.9	49.2	8.7	10.6	7.9	50.5
3	9.3	12.6	9.4	49.2	10.3	11.5	10.0	50.3	10.1	10.5	7.6	49.0	8.9	11.1	7.9	50.2
4	9.8	12.0	9.4	49.1	10.7	10.5	9.8	50.3	10.0	11.1	8.3	48.8	9.2	11.2	8.1	49.8
5	10.5	11.9	8.3	49.2	10.1	10.4	9.5	50.3	10.0	11.4	7.9	48.3	9.1	9.8	8.4	49.1
Mean	**10.0**	**11.9**	**9.1**	**49.3**	**10.3**	**10.8**	**9.7**	**50.5**	**9.8**	**10.7**	**8.0**	**48.9**	**9.0**	**10.7**	**8.2**	**50.1**

Meas. No.	Post-Test Weld Measurements															
	Weld 1				Weld 2				Weld 3				Weld 4			
	Shear Leg After Fracture (mm)	Fracture Surface (mm)	Weld Root Penetration (mm)	F. A.† (°)	Shear Leg After Fracture (mm)	Fracture Surface (mm)	Weld Root Penetration (mm)	F. A.† (°)	Shear Leg After Fracture (mm)	Fracture Surface (mm)	Weld Root Penetration (mm)	F. A.† (°)	Shear Leg After Fracture (mm)	Fracture Surface (mm)	Weld Root Penetration (mm)	F. A.† (°)
1	12.3	9.1	2.5	37	11.6	8.4	1.5	42	12.1	8.5	2.9	58	11.6	10.2	2.6	16
2	12.2	9.1	1.7	36	11.7	9.4	1.2	48	12.8	9.7	3.3	51	11.8	12.0	3.1	21
3	11.4	9.2	2.1	29	11.7	9.8	1.4	50	13.0	9.8	2.8	54	11.2	9.4	2.3	21
4	11.6	9.1	1.9	32	12.8	10.7	2.1	49	11.8	9.3	1.9	57	12.1	10.2	2.9	22
5	12.3	9.1	1.8	32	13.2	10.9	3.1	44	14.4	11.0	4.3	60	12.8	10.4	3.7	19
Mean	**12.0**	**9.1**	**2.0**	**33**	**12.2**	**9.8**	**1.9**	**46**	**12.8**	**9.7**	**3.0**	**56**	**11.9**	**10.4**	**2.9**	**20**

† F. A. = Fracture Angle

Table B29 – Weld Measurements for Specimen L3-2

Meas. Number	Pre-Test Weld Measurements															
	Front Face								Back Face							
	Weld 1				Weld 2				Weld 3				Weld 4			
	Main Plate Leg (mm)	Lap Plate Leg (mm)	45° Meas. (mm)	Weld Length (mm)	Main Plate Leg (mm)	Lap Plate Leg (mm)	45° Meas. (mm)	Weld Length (mm)	Main Plate Leg (mm)	Lap Plate Leg (mm)	45° Meas. (mm)	Weld Length (mm)	Main Plate Leg (mm)	Lap Plate Leg (mm)	45° Meas. (mm)	Weld Length (mm)
1	9.6	12.3	7.9	48.8	10.6	10.9	6.8	50.0	9.6	11.6	8.3	50.8	9.8	9.9	6.5	49.5
2	9.6	13.3	7.5	48.4	11.0	11.4	6.5	49.6	10.2	11.9	7.5	50.4	10.3	10.8	7.1	49.5
3	9.9	11.3	7.0	48.2	9.6	11.2	6.8	49.6	9.7	11.7	9.0	50.3	9.5	12.1	7.9	49.9
4	8.6	11.8	7.1	48.2	9.1	11.5	6.7	49.5	9.0	12.6	8.6	50.2	10.4	11.5	7.6	48.8
5	9.9	12.3	8.3	47.9	8.3	11.8	7.1	49.4	9.6	12.3	7.9	49.9	9.8	11.4	7.8	48.6
Mean	**9.5**	**12.2**	**7.6**	**48.3**	**9.7**	**11.4**	**6.8**	**49.6**	**9.6**	**12.0**	**8.3**	**50.3**	**10.0**	**11.1**	**7.4**	**49.2**

Meas. Number	Post-Test Weld Measurements			
	Weld 2			
	Main Plate Leg After Fracture (mm)	Fracture Surface (mm)	Weld Root Penetration (mm)	Fracture Angle (°)
1	13.7	9.6	3.0	26
2	14.3	9.2	3.4	26
3	12.8	9.2	3.2	30
4	12.2	9.2	3.1	26
5	12.2	9.4	3.9	27
Mean	**13.0**	**9.3**	**3.3**	**27**

Table B30 – Weld Measurements for Specimen L3-3

Meas. Number	Pre-Test Weld Measurements															
	Front Face								Back Face							
	Weld 1				Weld 2				Weld 3				Weld 4			
	Main Plate Leg (mm)	Lap Plate Leg (mm)	45° Meas. (mm)	Weld Length (mm)	Main Plate Leg (mm)	Lap Plate Leg (mm)	45° Meas. (mm)	Weld Length (mm)	Main Plate Leg (mm)	Lap Plate Leg (mm)	45° Meas. (mm)	Weld Length (mm)	Main Plate Leg (mm)	Lap Plate Leg (mm)	45° Meas. (mm)	Weld Length (mm)
1	9.4	9.1	7.0	51.2	11.2	11.6	9.2	51.4	9.6	9.5	8.6	52.6	9.7	9.2	7.9	50.6
2	9.7	11.8	7.8	51.0	12.2	11.1	8.3	51.2	11.1	9.7	8.7	52.3	9.1	8.9	7.9	50.4
3	9.7	12.3	7.0	50.9	12.1	12.0	8.7	51.2	9.8	10.7	8.6	51.9	9.6	10.0	8.6	50.1
4	9.4	11.9	7.6	50.7	11.6	11.2	9.2	51.1	11.1	10.0	8.4	51.9	9.4	10.5	8.3	50.0
5	8.6	11.7	7.9	50.6	11.3	11.4	9.0	50.8	11.8	11.2	8.9	51.7	10.8	10.8	8.1	50.0
Mean	**9.3**	**11.3**	**7.5**	**50.9**	**11.7**	**11.5**	**8.9**	**51.1**	**10.7**	**10.2**	**8.6**	**52.1**	**9.7**	**9.8**	**8.2**	**50.2**

Meas. Number	Post-Test Weld Measurements			
	Weld 2			
	Main Plate Leg After Fracture (mm)	Fracture Surface (mm)	Weld Root Penetration (mm)	Fracture Angle (°)
1	11.4	8.2	2.1	35
2	11.4	9.0	1.7	30
3	11.0	7.9	1.3	35
4	11.6	8.6	2.2	29
5	10.6	8.0	2.1	31
Mean	**11.2**	**8.3**	**1.9**	**32**

Table B31 – Gauge Lengths Used for Determining Strain

Specimen Designation	LVDT 1 (mm)	LVDT 2 (mm)	LVDT 3 (mm)	LVDT 4 (mm)
T20-1	12.9	13.9	14.3	12.5
T20-2	13.2	12.6	13.6	13.6
T20-3	13.5	13.7	13.9	12.5
T22-1	9.5	9.7	11.4	10.9
T22-2	10.5	10.2	10.5	11.1
T22-3	12.1	11.5	10.1	10.4
T26-1	11.9	12.5	13.2	13.7
T26-2	12.4	12.9	12.7	12.8
T26-3	12.3	13.3	12.9	12.9
T32-1	12.3	12.2	11.9	12.5
T32-2	11.4	11.0	12.0	12.4
T32-3	10.7	9.7	11.8	12.5
F1-1	16.9	14.7	16.0	18.0
F1-2	14.6	14.5	15.1	15.2
F1-3	12.9	13.4	16.3	15.8
F2-1	12.8	13.8	13.8	13.5
F2-2	13.6	15.6	12.5	14.6
F2-3	12.8	13.7	15.4	14.9
F3-1	12.3	15.4	14.2	15.1
F3-2	12.8	15.5	13.6	13.0
F3-3	13.3	13.3	13.1	13.6
L1-1	10.6	8.7	10.5	10.0
L1-2	11.3	11.7	11.0	10.9
L1-3	10.8	9.4	10.8	10.3
L2-1	10.9	10.7	10.8	11.6
L2-2	10.3	10.0	12.3	9.8
L2-3	11.2	9.8	10.5	10.5
L3-1	10.0	10.3	9.8	9.0
L3-2	9.5	9.7	9.6	10.0
L3-3	9.3	11.7	10.7	9.7

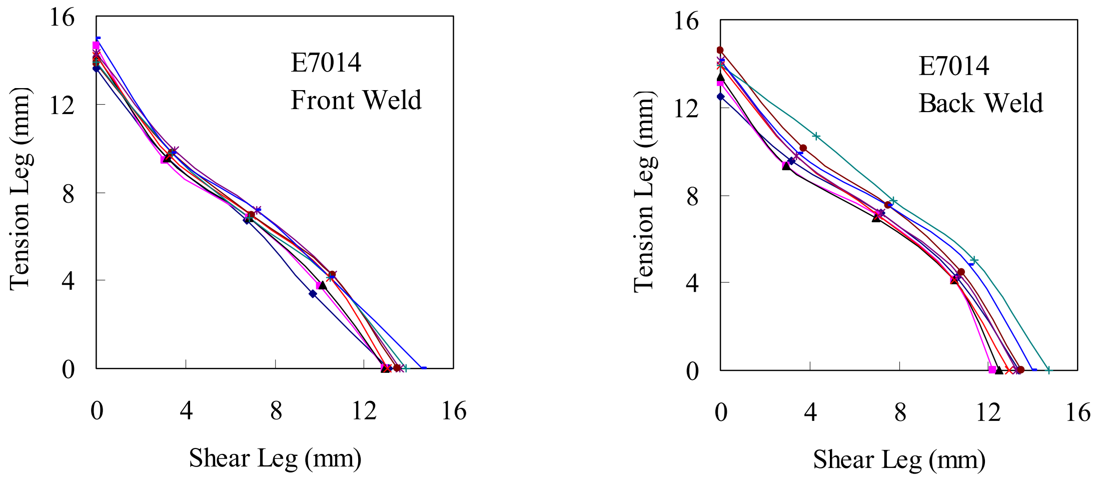

Figure B3 – Weld Profile for Specimen T20-1

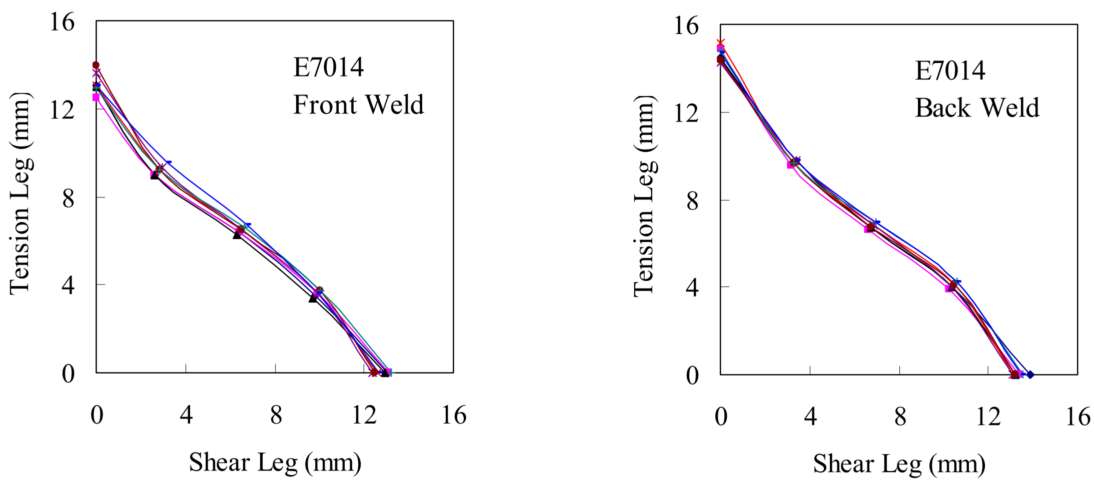

Figure B4 – Weld Profile for Specimen T20-2

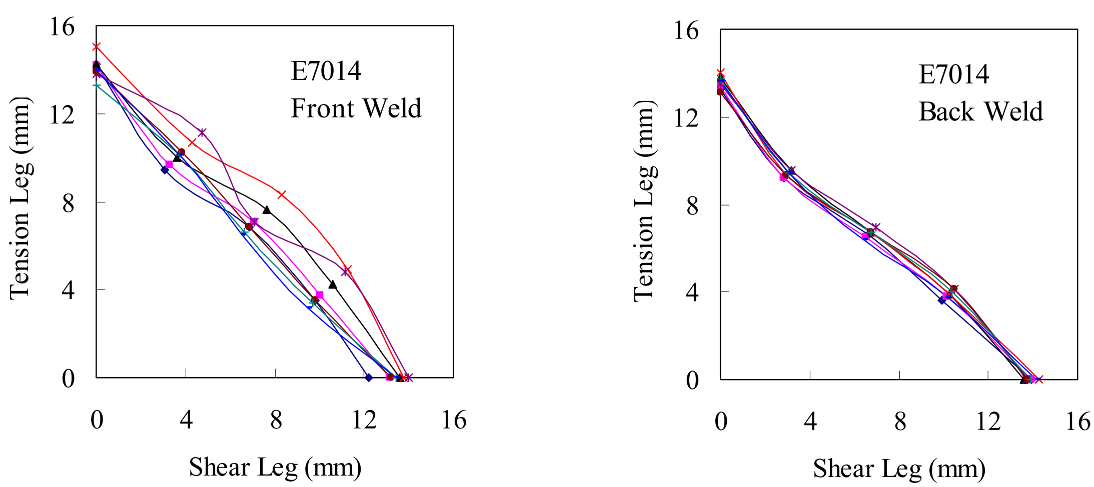

Figure B5 – Weld Profile for Specimen T20-3

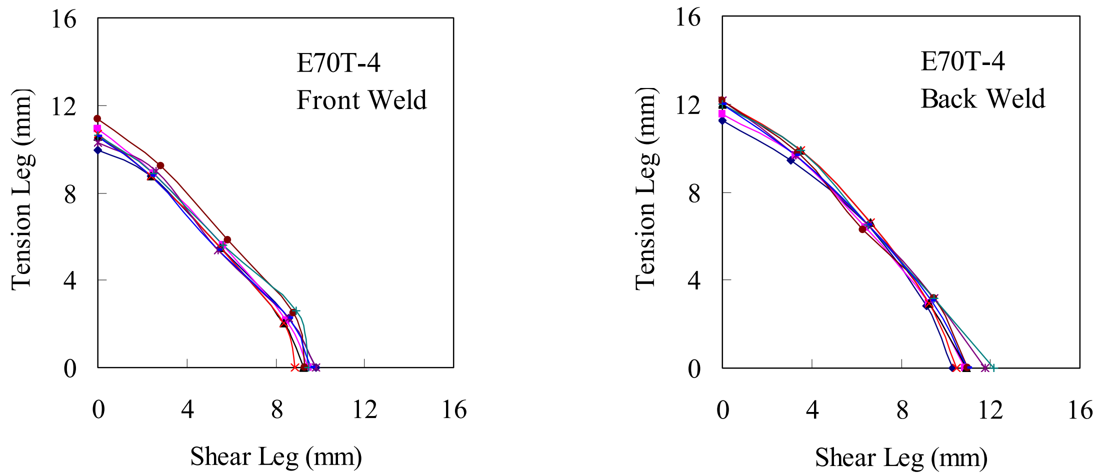

Figure B6 – Weld Profile for Specimen T22-1

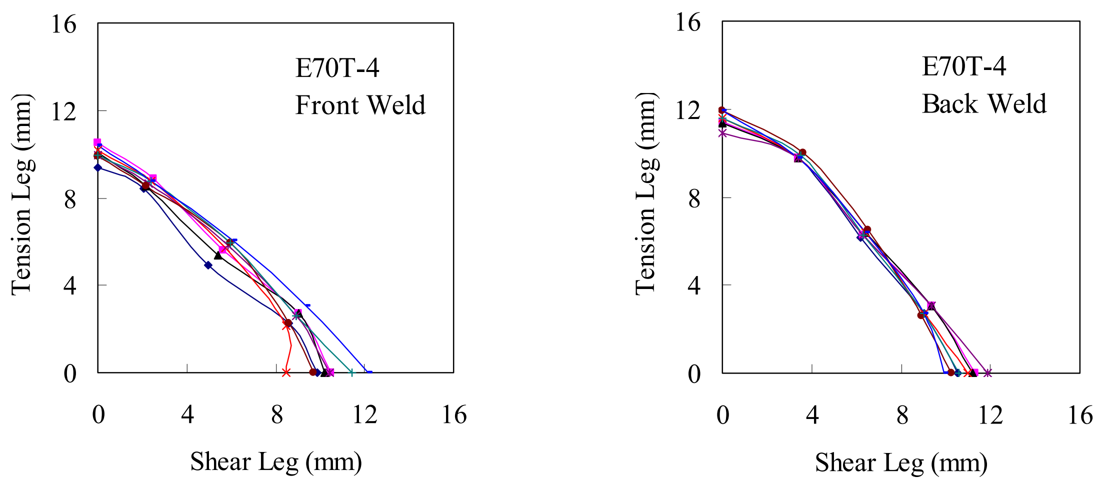

Figure B7 – Weld Profile for Specimen T22-2

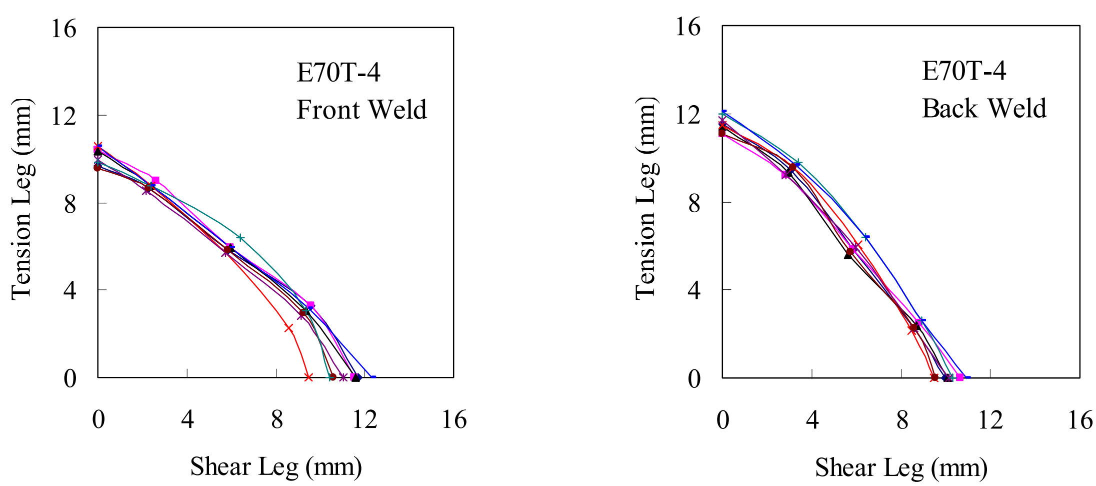

Figure B8 – Weld Profile for Specimen T22-3

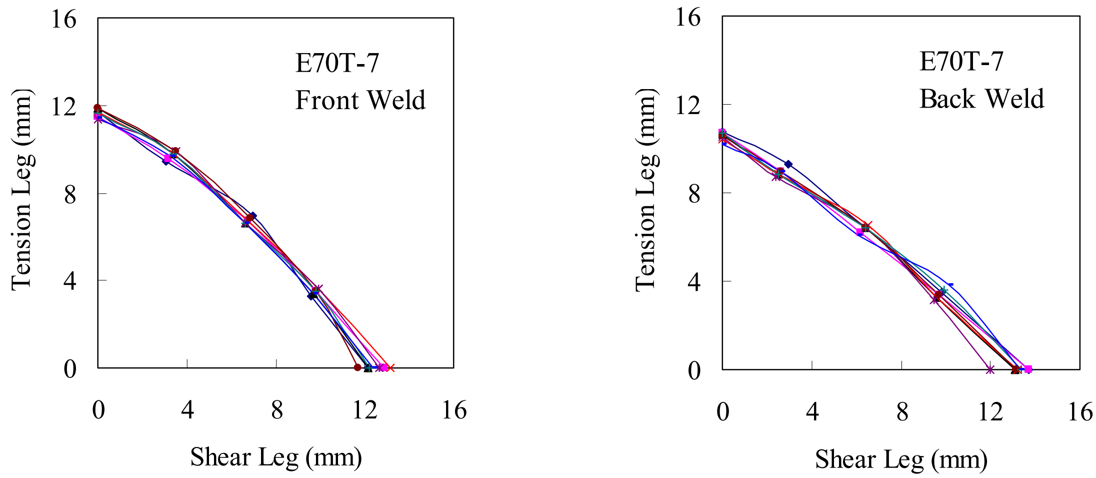

Figure B9 – Weld Profile for Specimen T26-1

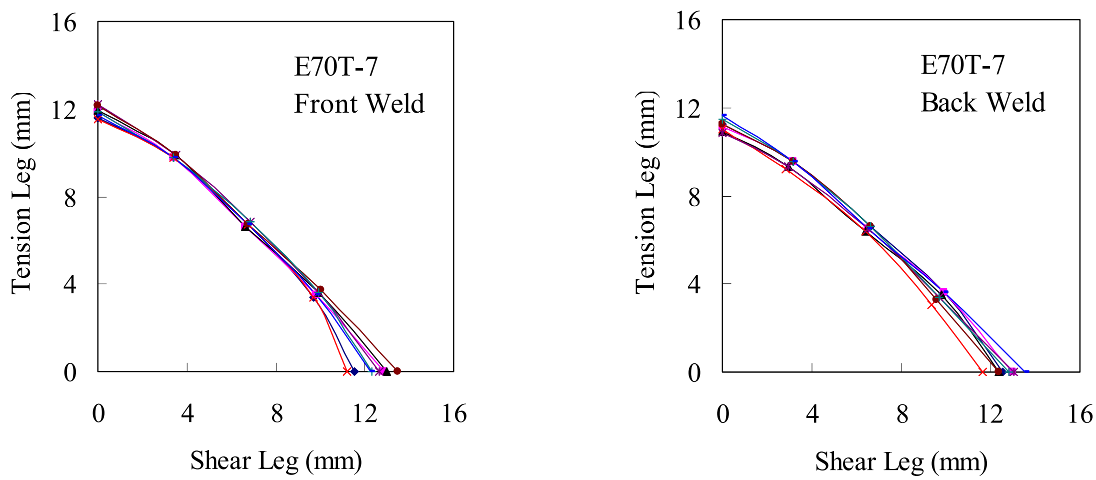

Figure B10 – Weld Profile for Specimen T26-2

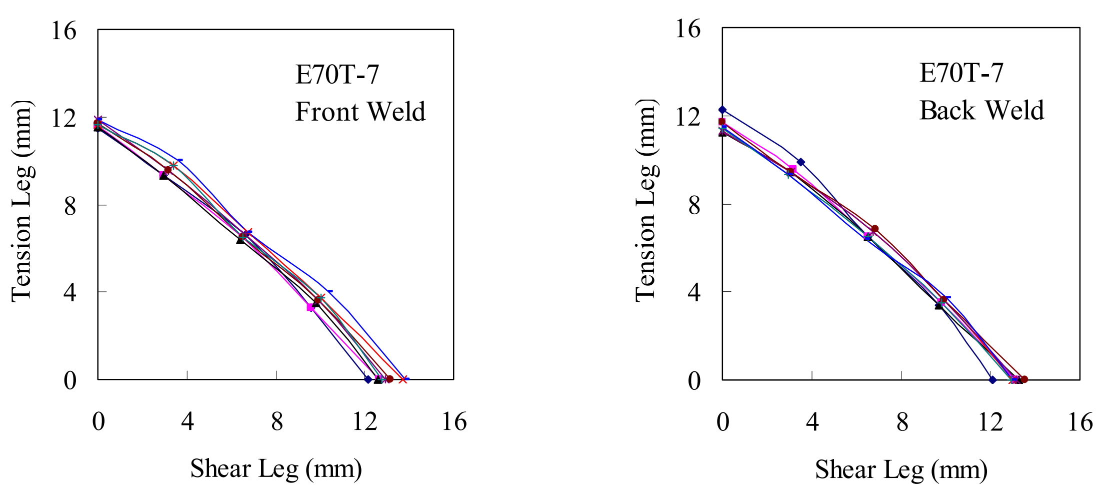

Figure B11 – Weld Profile for Specimen T26-3

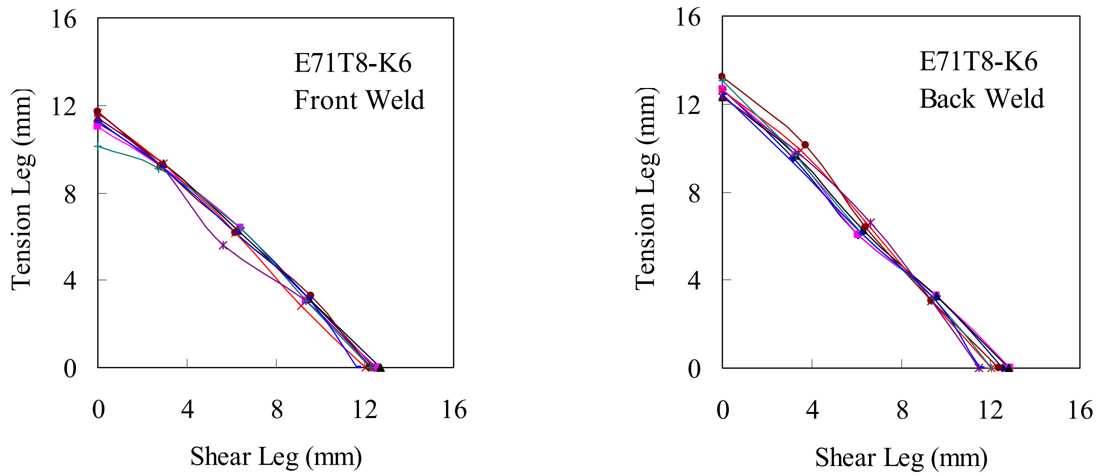

Figure B12 – Weld Profile for Specimen T32-1

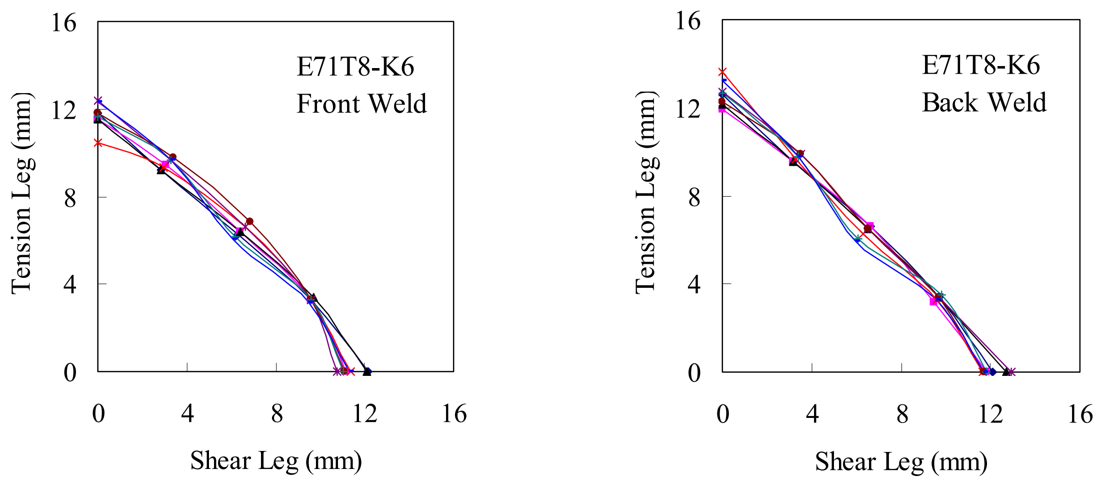

Figure B13 – Weld Profile for Specimen T32-2

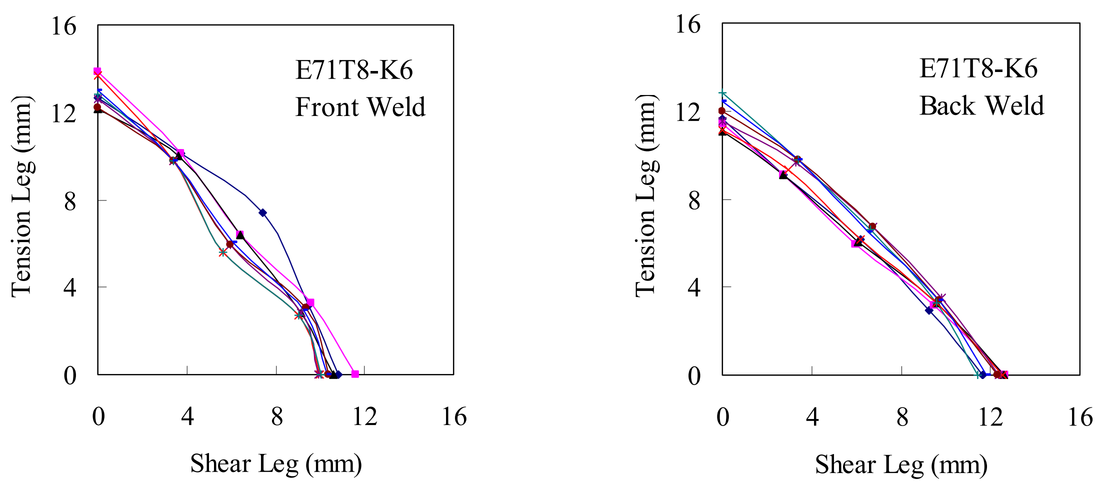

Figure B14 – Weld Profile for Specimen T32-3

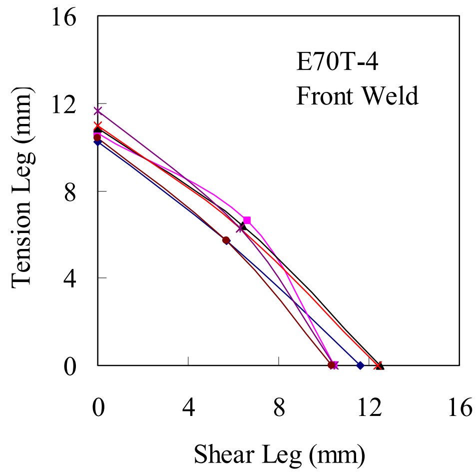

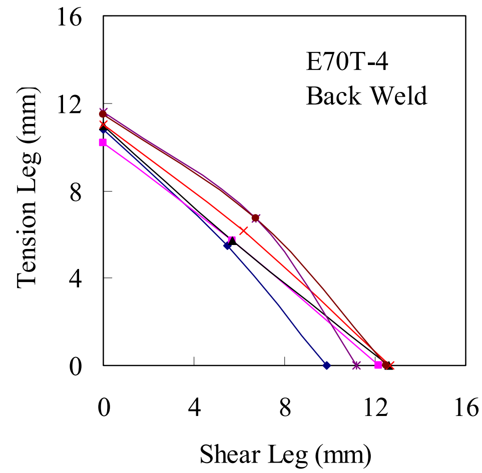

Figure B15 – Weld Profile for Specimen F1-1

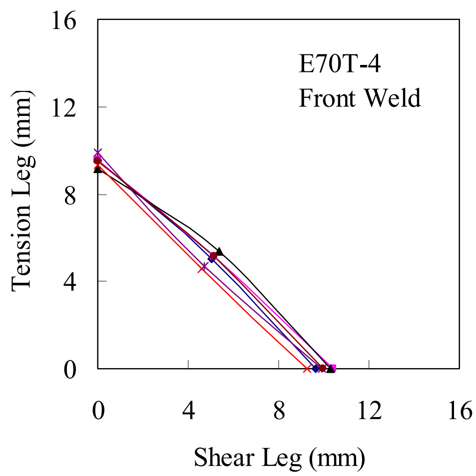

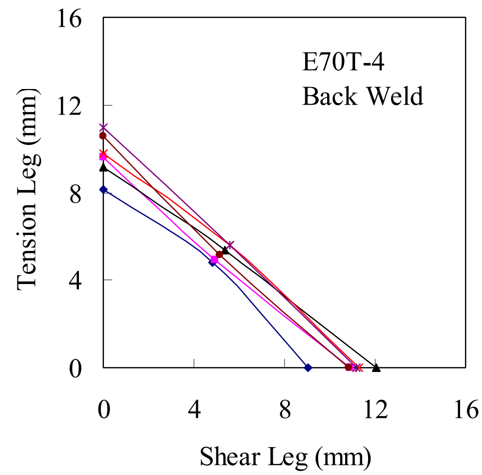

Figure B16 – Weld Profile for Specimen F1-2

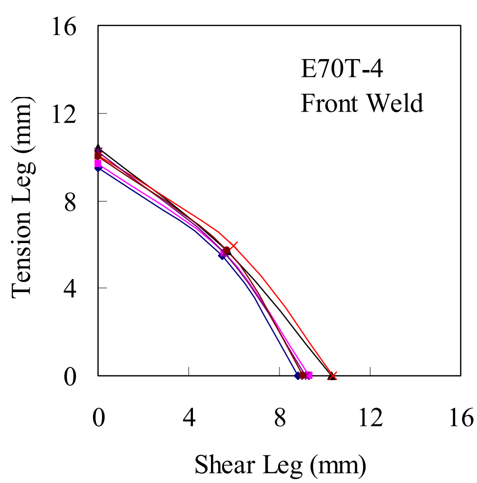

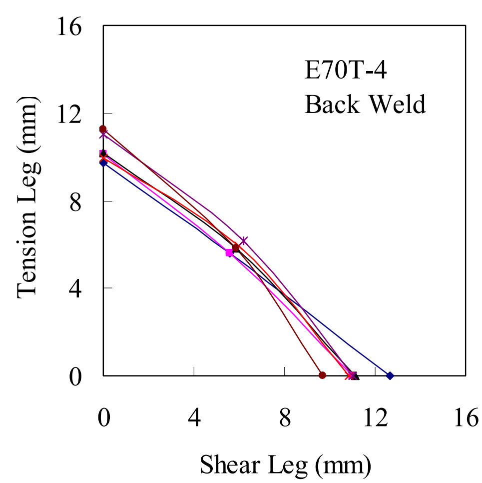

Figure B17 – Weld Profile for Specimen F1-3

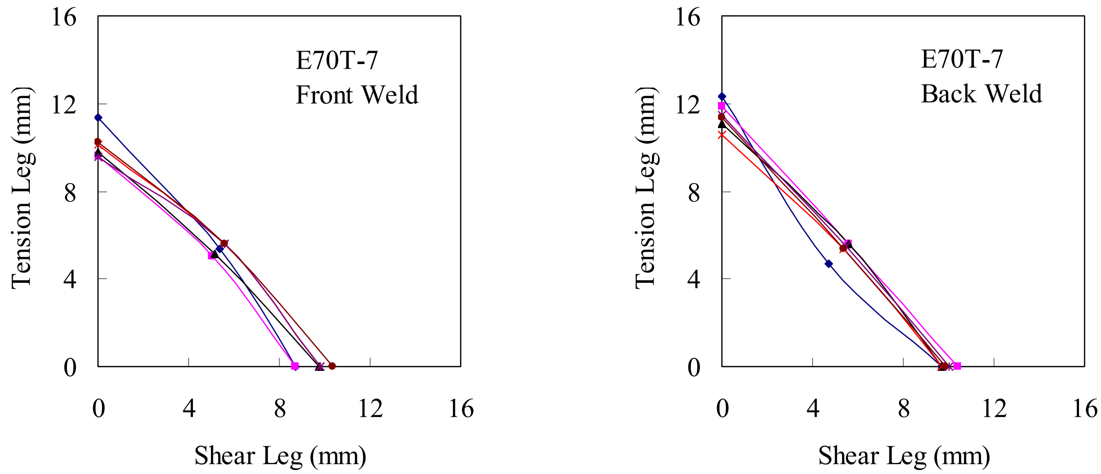

Figure B18 – Weld Profile for Specimen F2-1

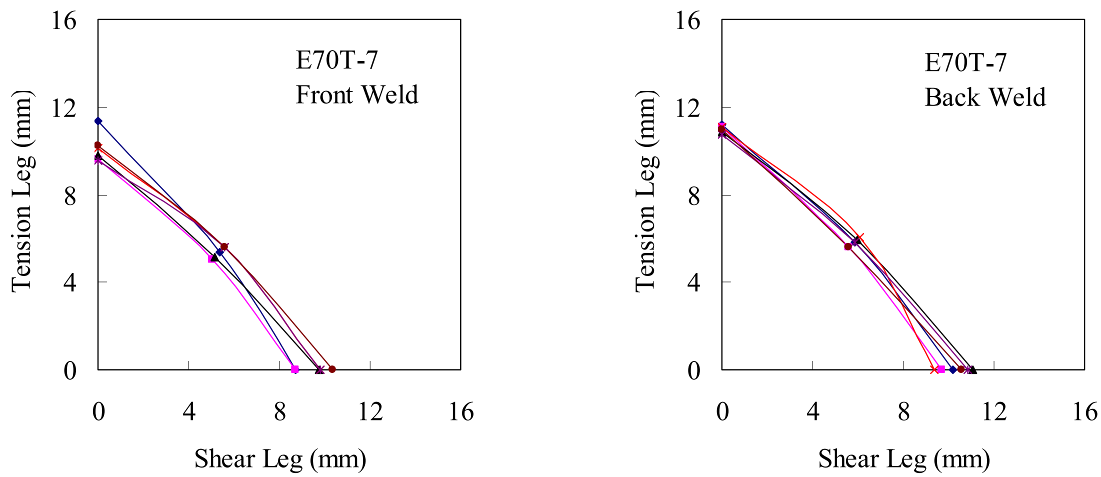

Figure B19 – Weld Profile for Specimen F2-2

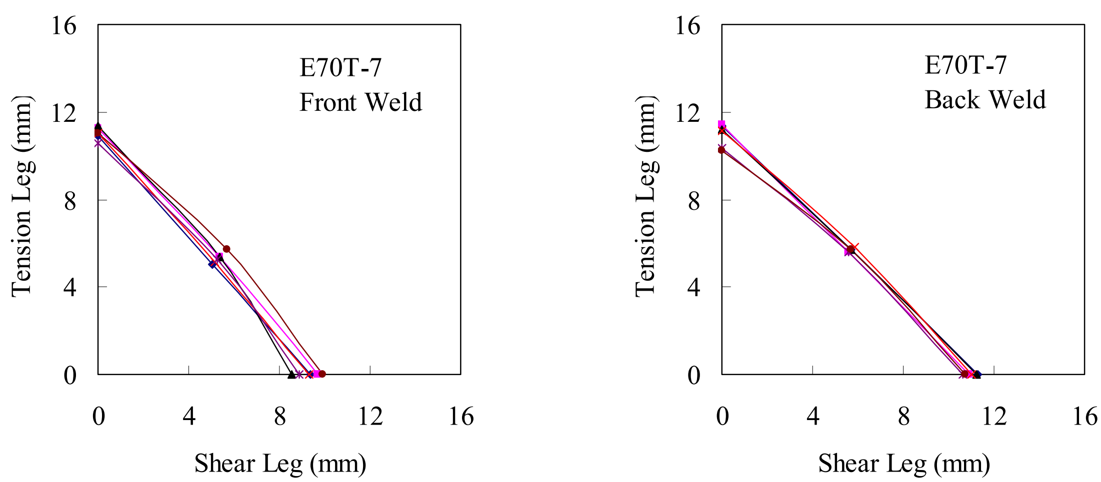

Figure B20 – Weld Profile for Specimen F2-3

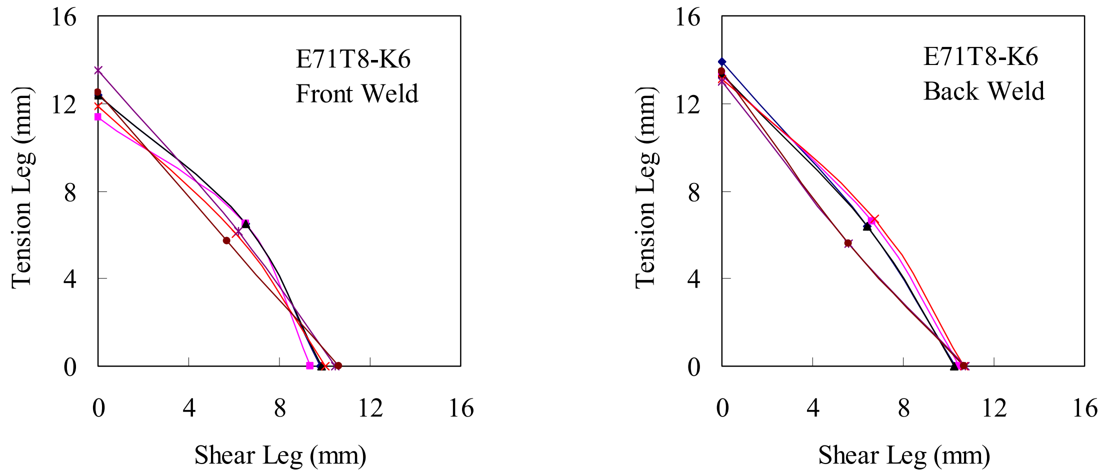

Figure B21 – Weld Profile for Specimen F3-1

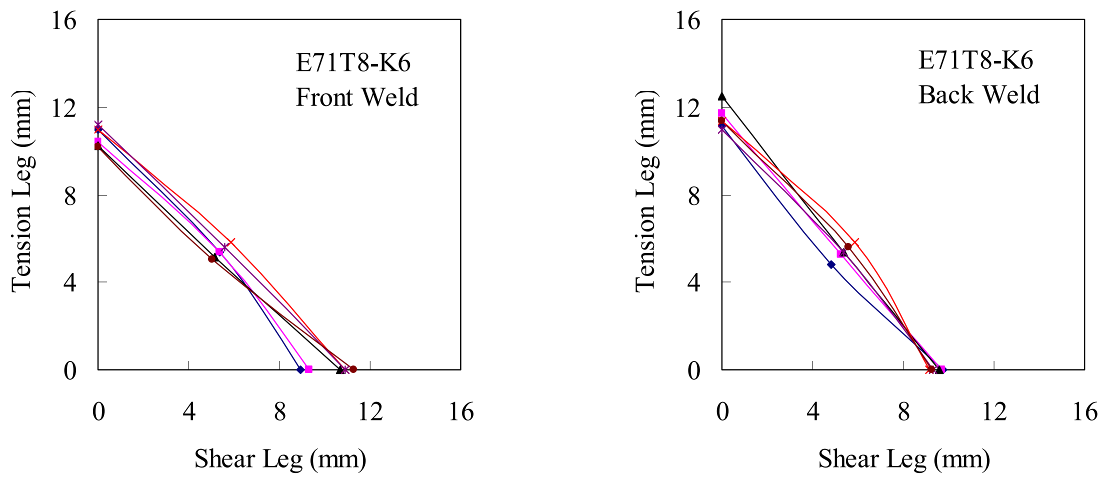

Figure B22 – Weld Profile for Specimen F3-2

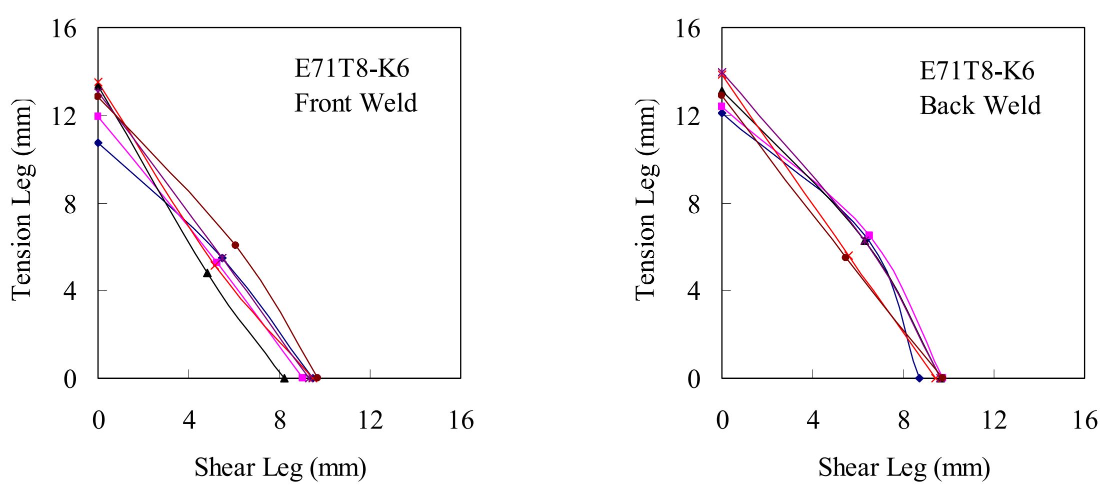

Figure B23 – Weld Profile for Specimen F3-3

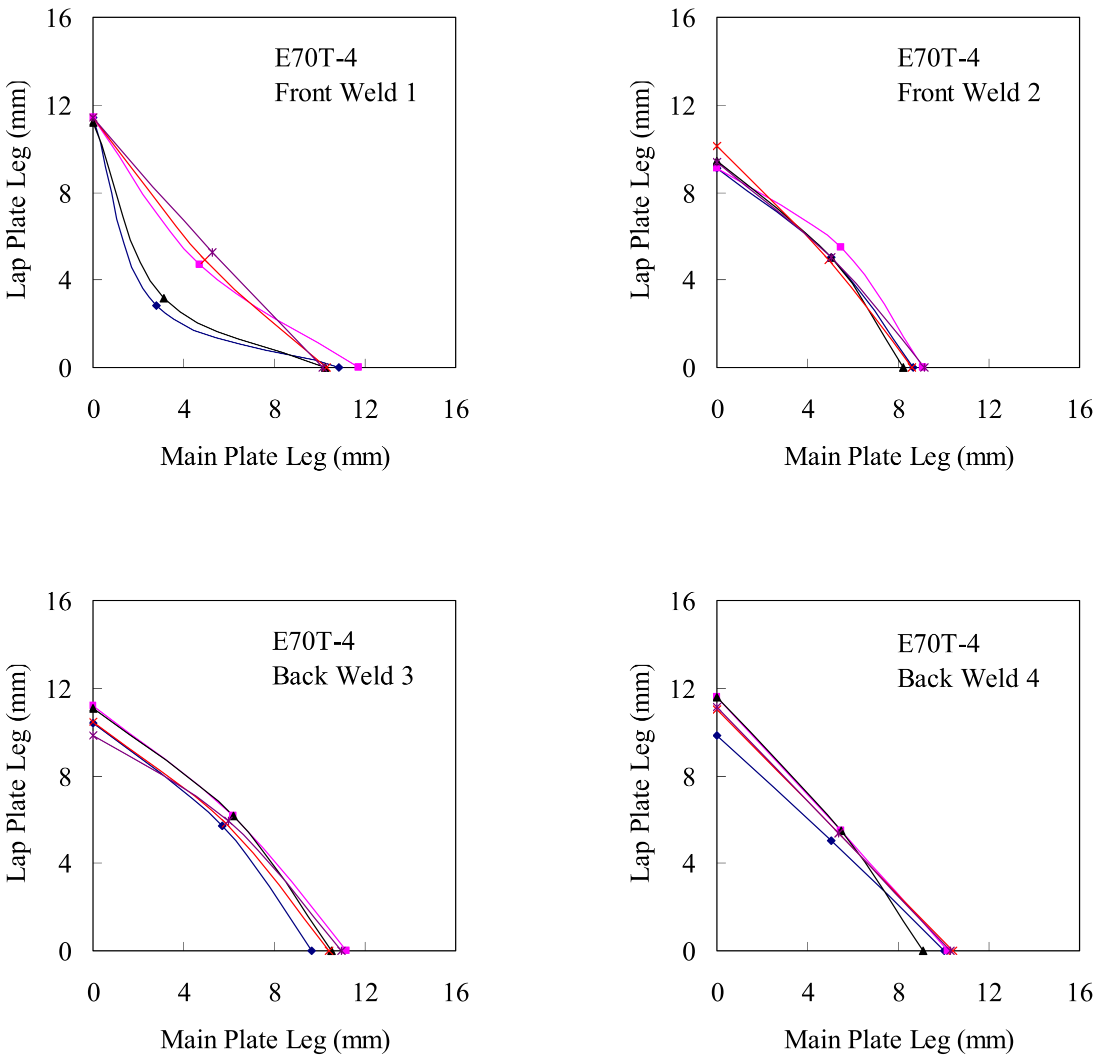

Figure B24 – Weld Profile for Specimen L1-1

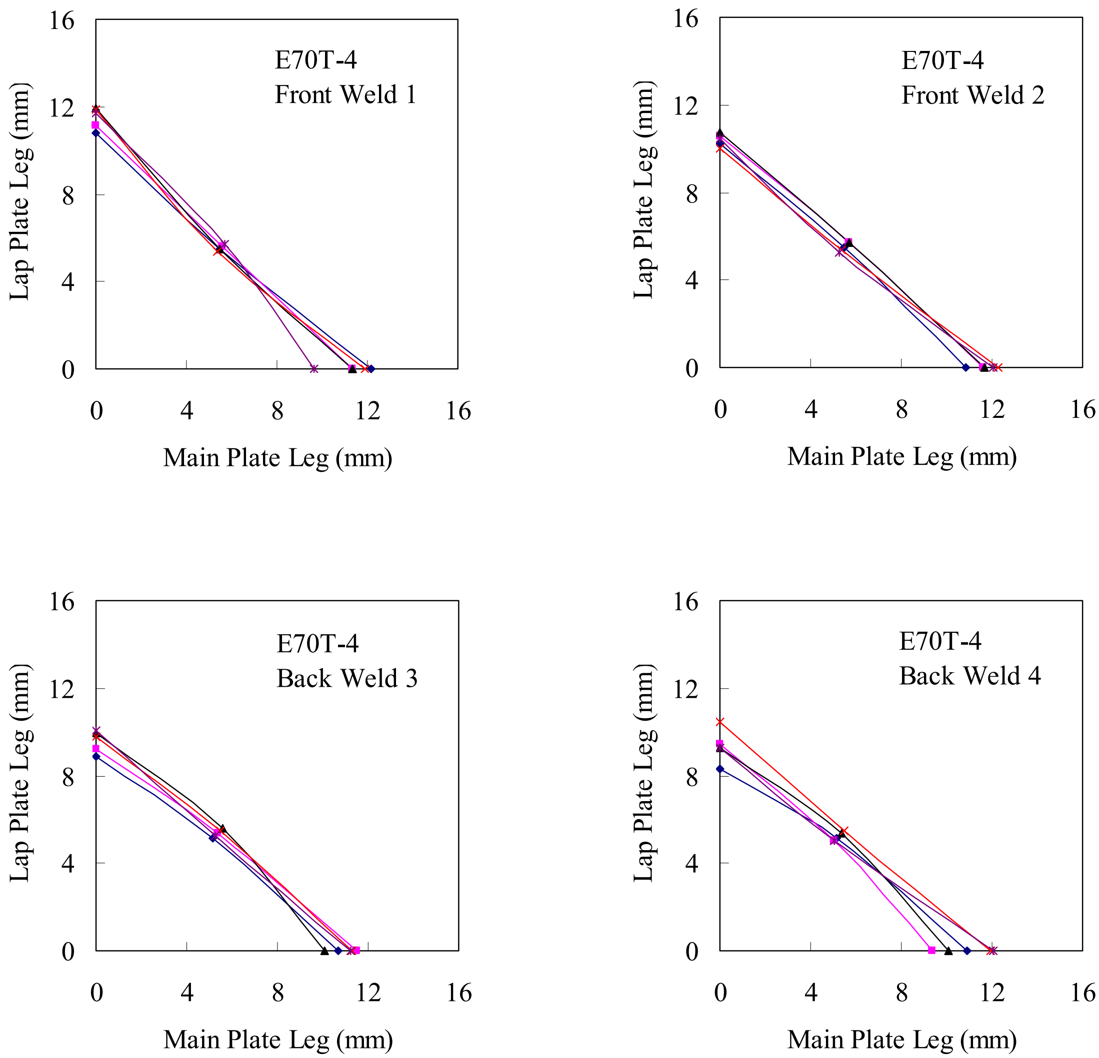

Figure B25 – Weld Profile for Specimen L1-2

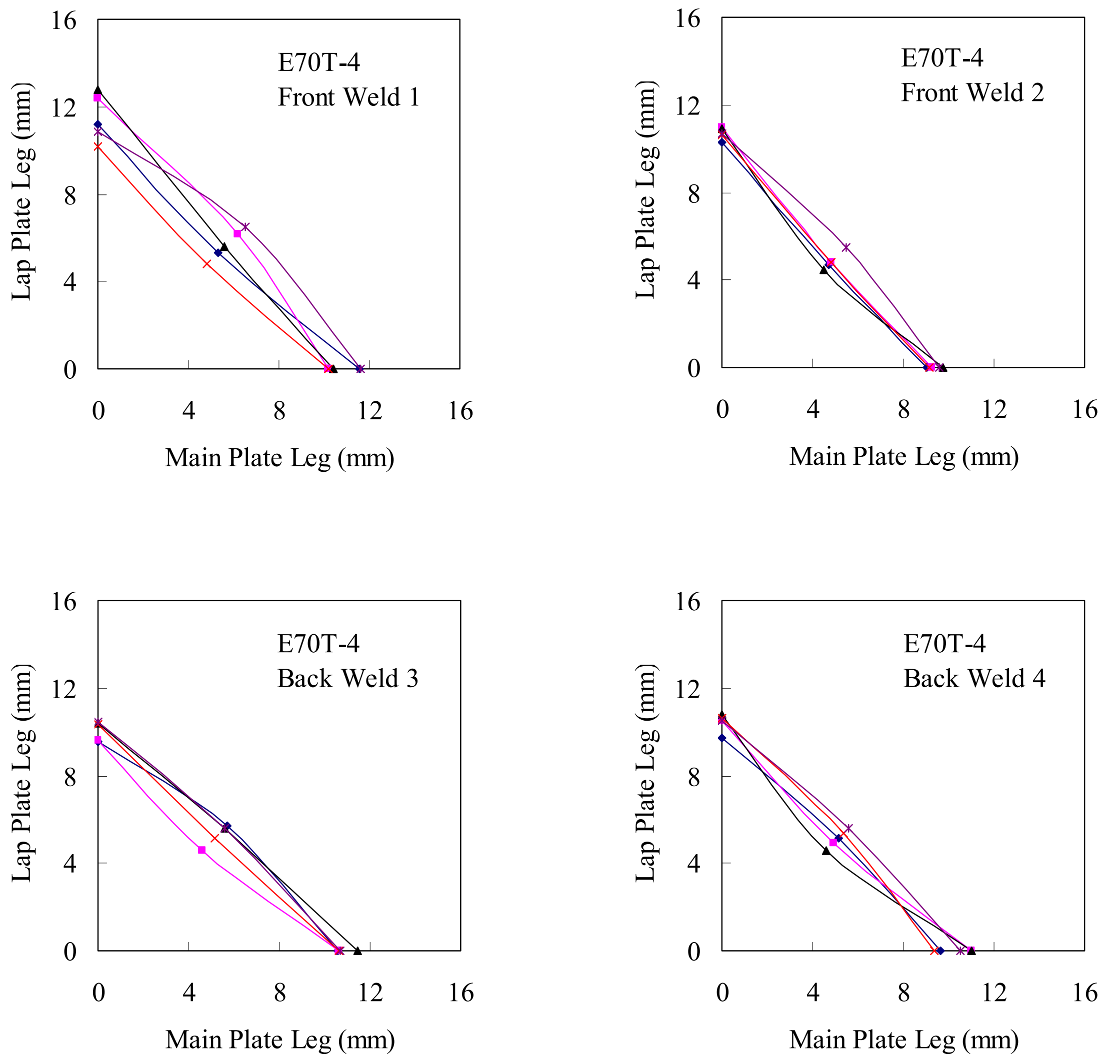

Figure B26 – Weld Profile for Specimen L1-3

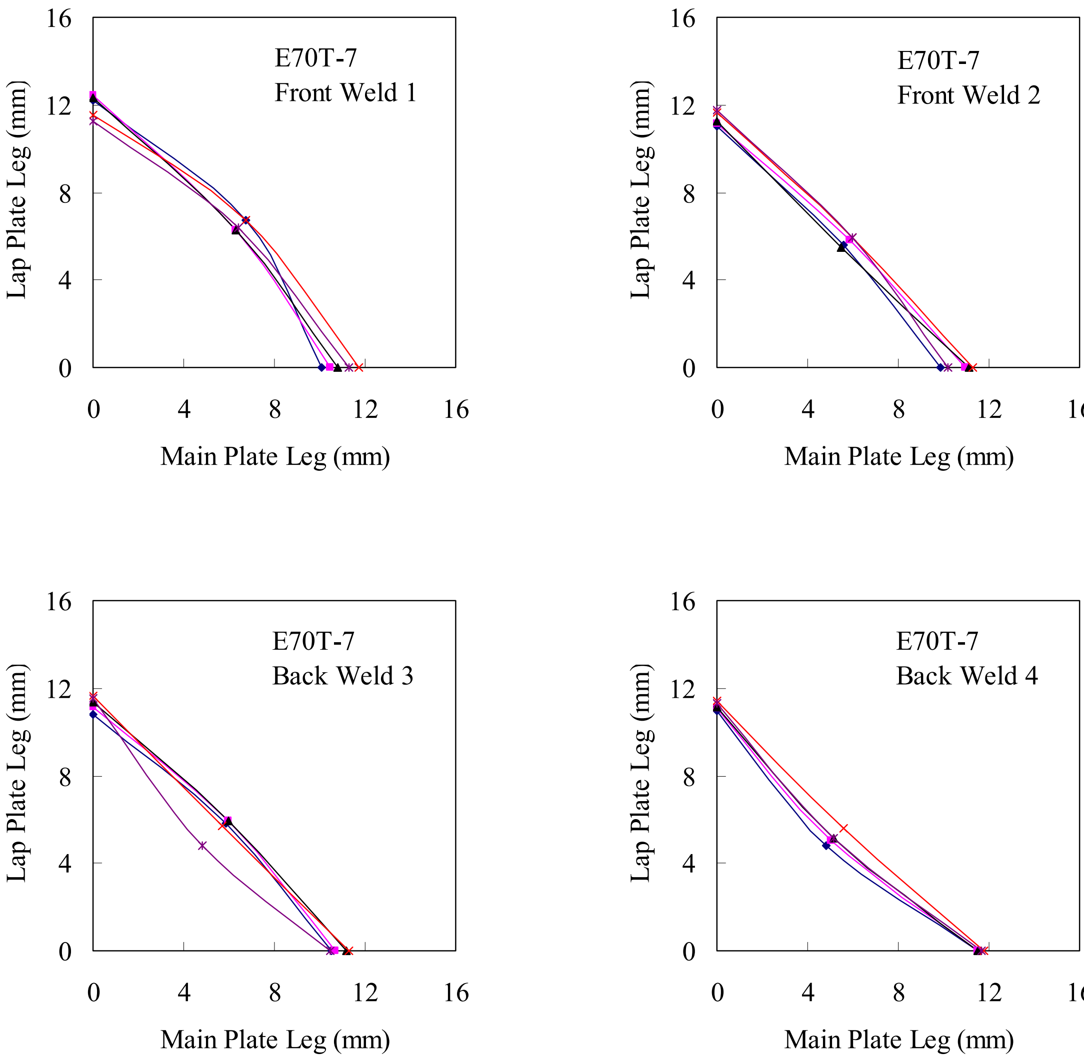

Figure B27 – Weld Profile for Specimen L2-1

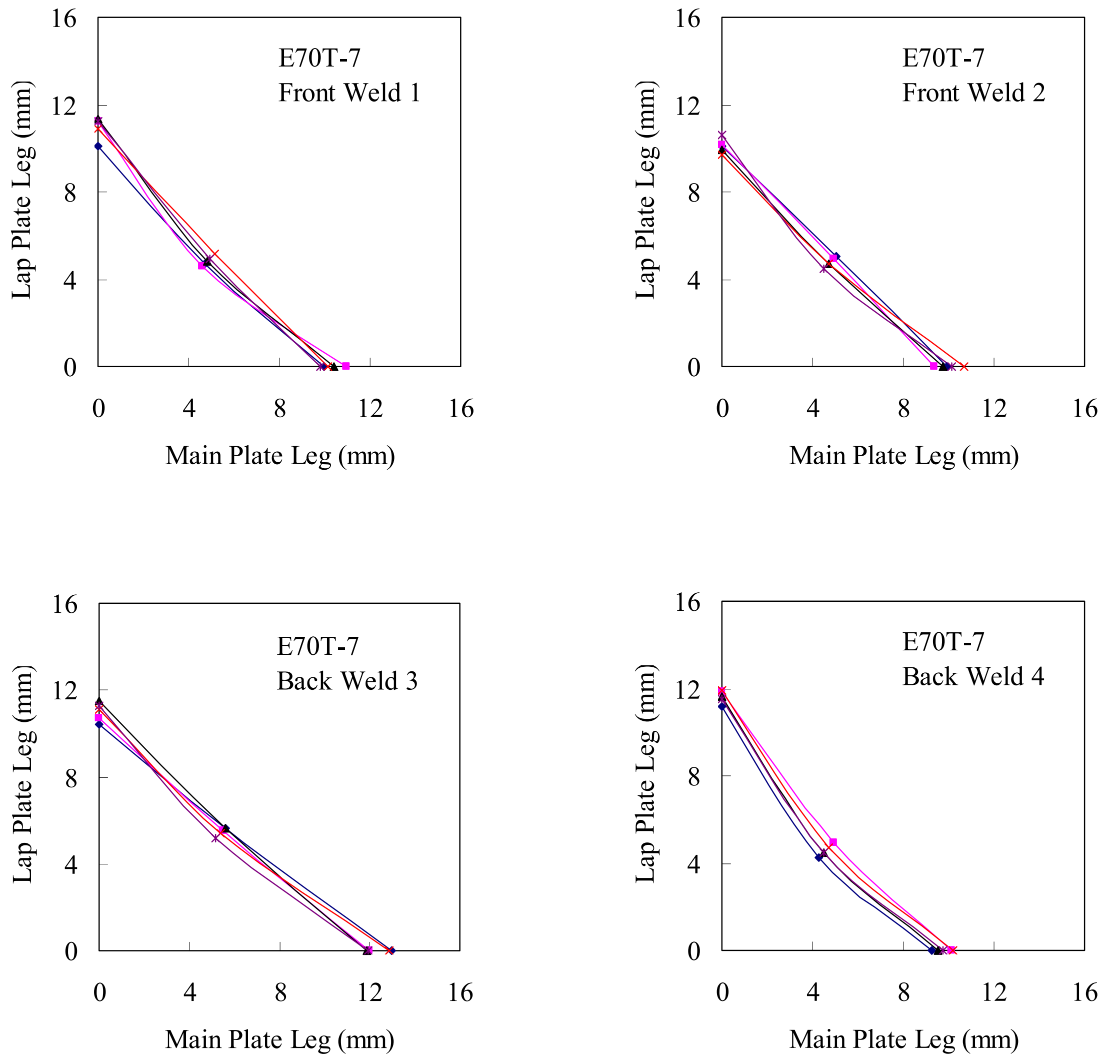

Figure B28 – Weld Profile for Specimen L2-2

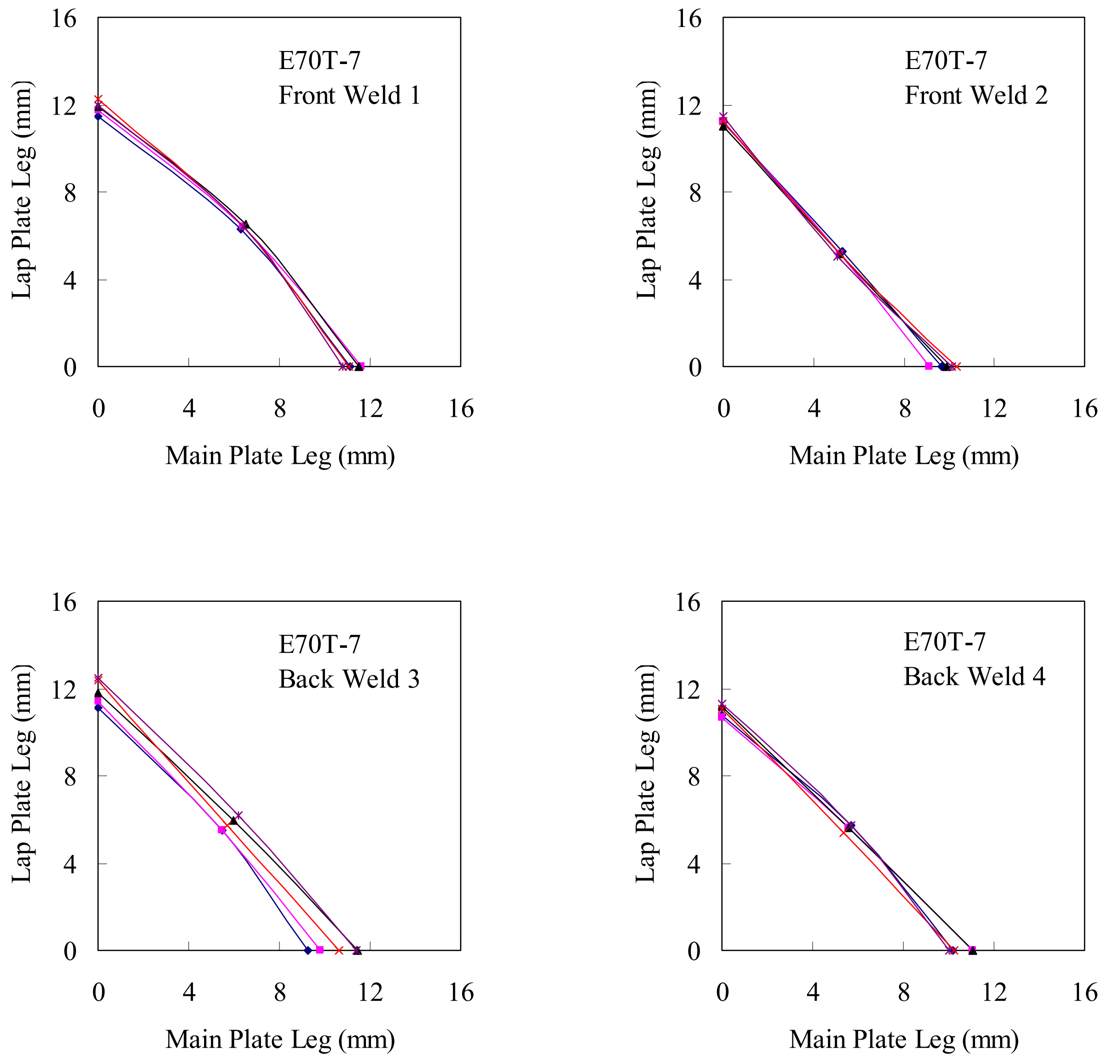

Figure B29 – Weld Profile for Specimen L2-3

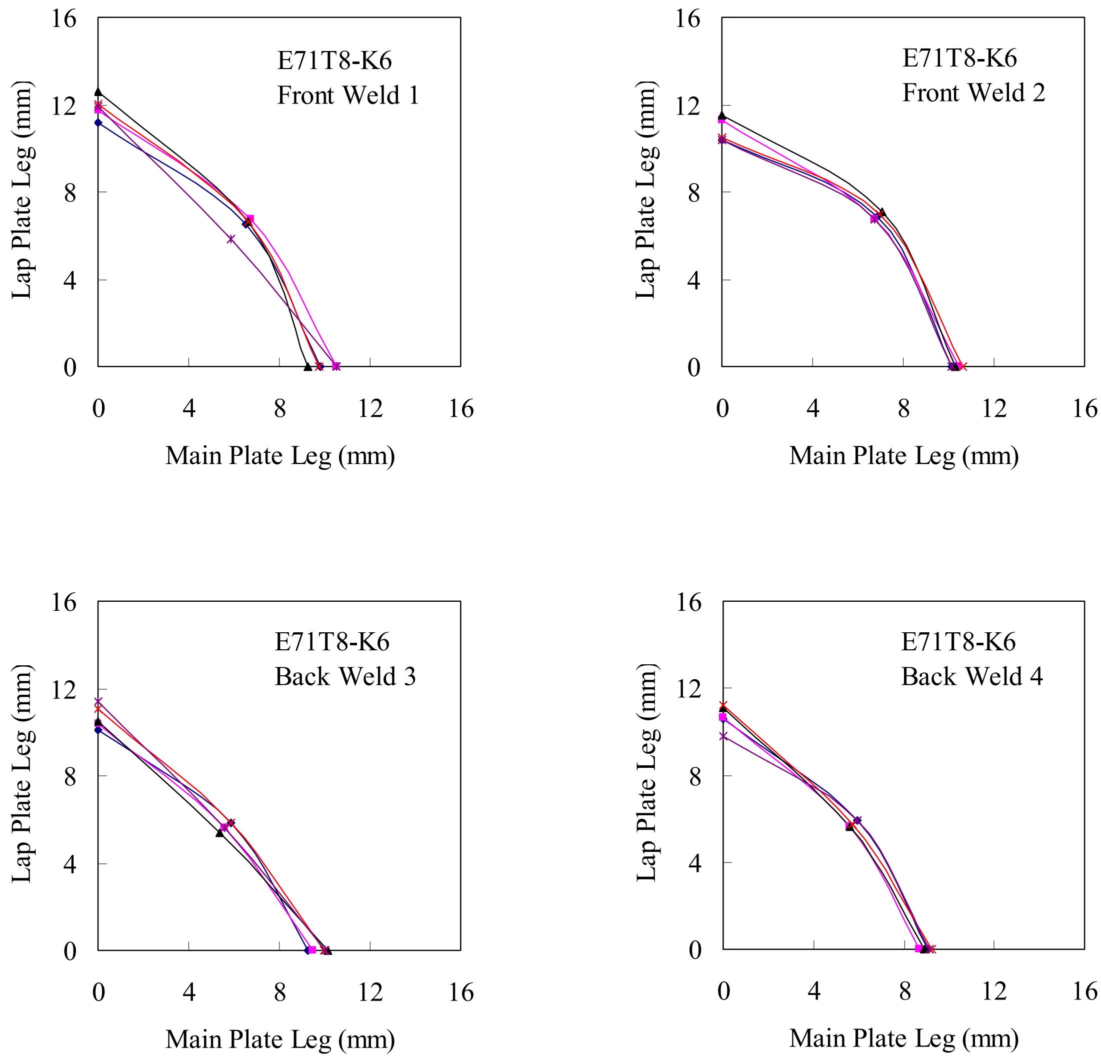

Figure B30 – Weld Profile for Specimen L3-1

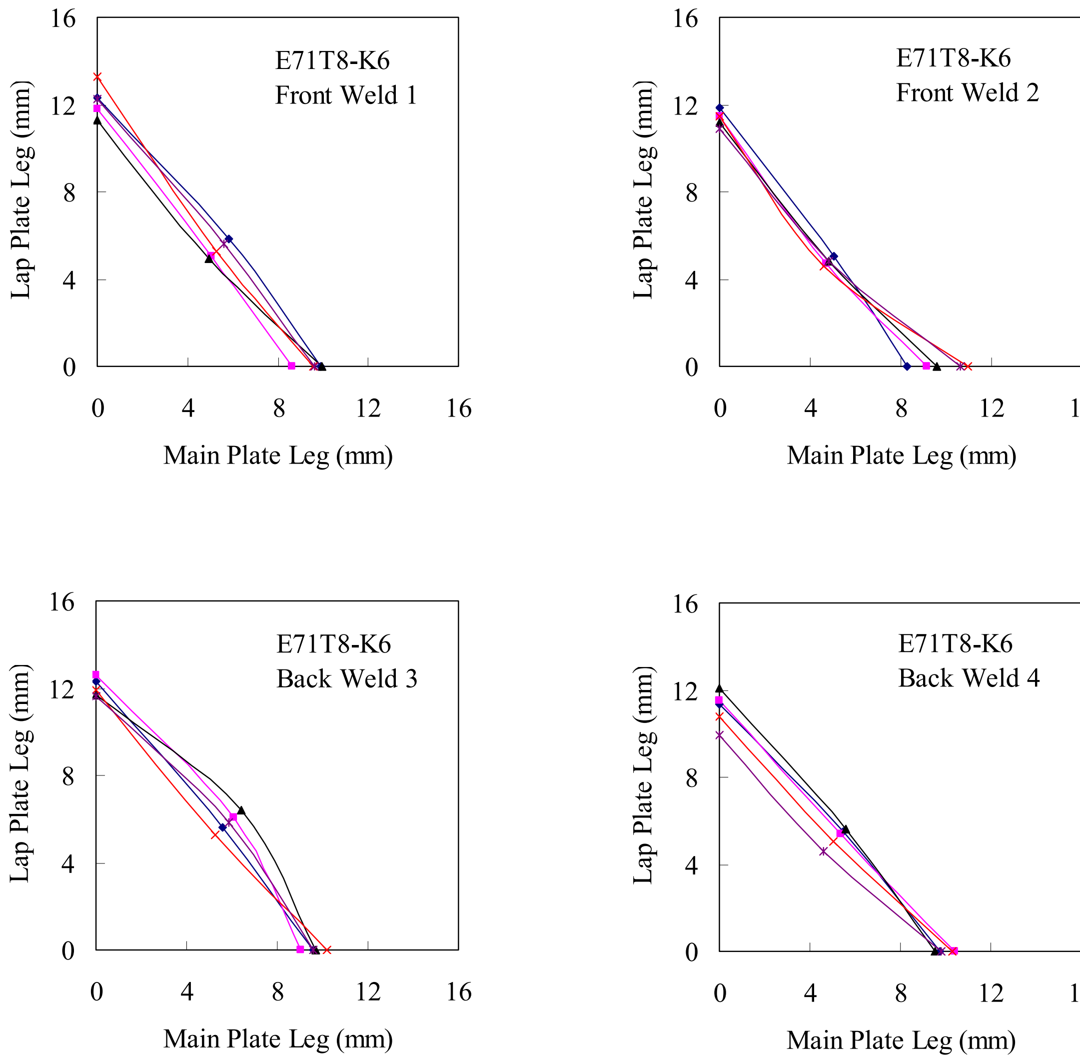

Figure B31 – Weld Profile for Specimen L3-2

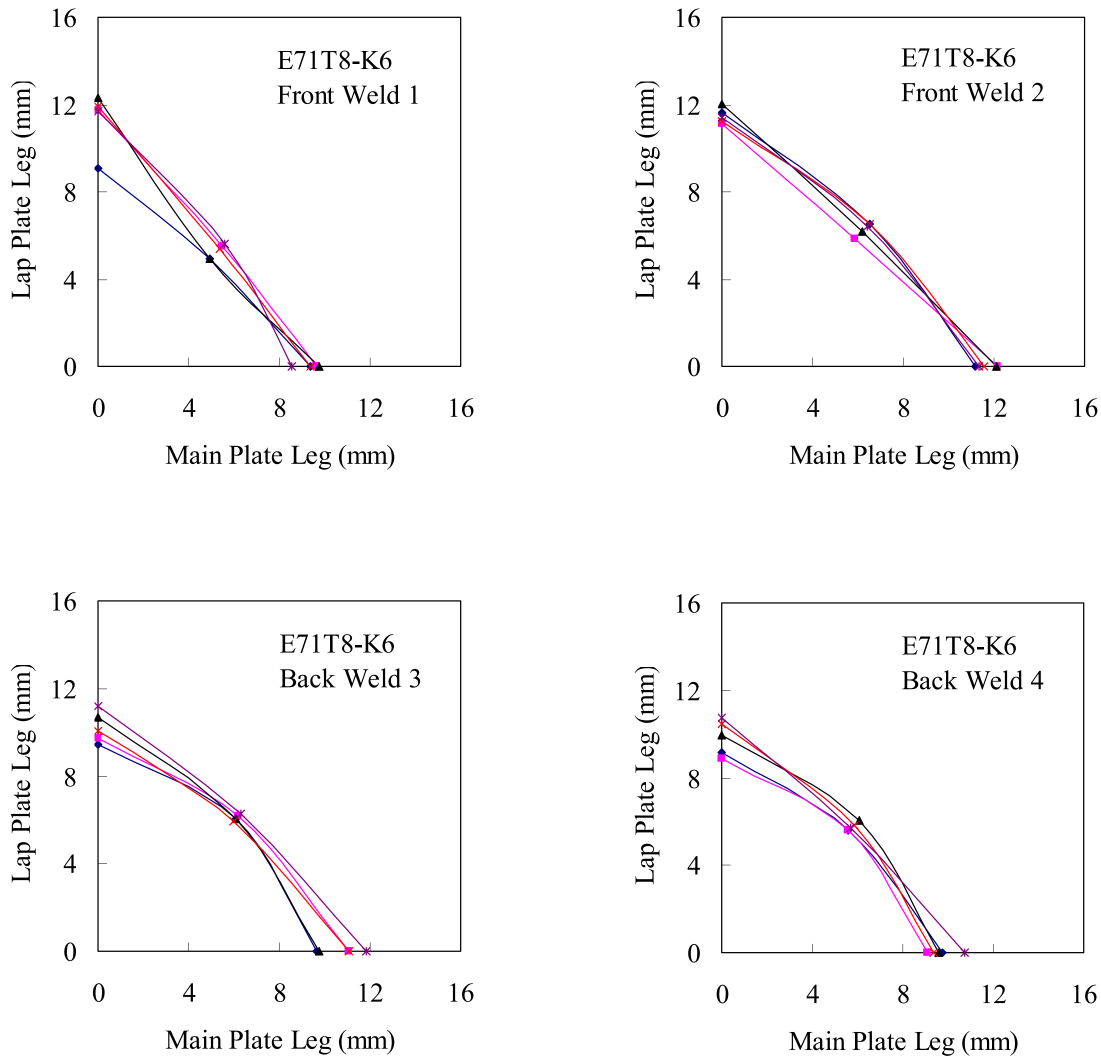

Figure B32 – Weld Profile for Specimen L3-3

APPENDIX C

Material Tension Coupon Test Results

Appendix C – Material Tension Coupon Test Results

The material tension coupon tests were performed in Phase I of this project; therefore, the results presented in this appendix are also provided in Ng *et al*. (2002). The elongations for all coupons were measured over a 50 mm gauge length, and the yield strengths were determined using the 0.2% offset method.

Two different manufacturers produced the filler metals, and two different steel fabricators prepared the weld assemblies from which the weld metal tension coupons were cut. All electrodes were manufactured by Hobart Brothers Corporation except for the SMAW electrode, which was manufactured by Lincoln Electric Company. The weld assemblies from which the E70T-4 and E71T8-K6 weld metal tension coupons were cut were prepared by Supreme Steel while the ones from which the E7014 and E70T-7 weld metal coupons were cut were prepared by Waiward. An identifier has been created to simplify this information in Table C2. A description of this identifer is given in Figure C1.

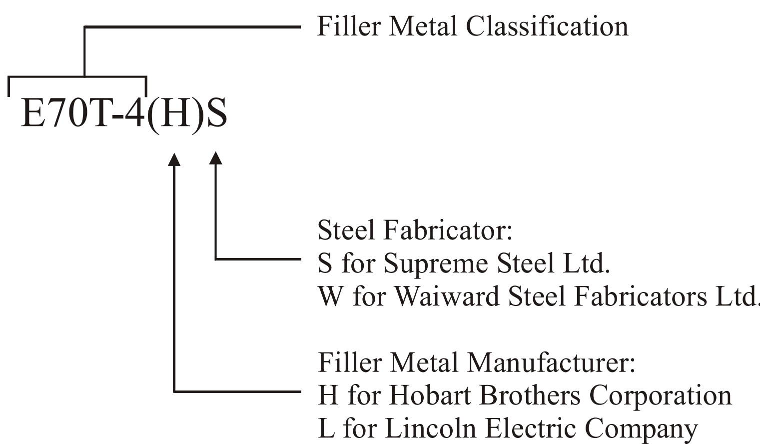

Figure C1 – Description of the Identifier for the Weld Metal Tension Coupons

Table C1 – Base Metal Tension Coupon Test Results for the 350W Steel Plates

Nominal Thickness	Coupon Number	Static Yield Strength (1) (MPa)	Static Tensile Strength (MPa)	Modulus of Elasticity (MPa)	Elongation (2) (%)	Reduction of Area (%)
15.9 mm	1	347	466	202 700	38.2	66.6
	2	347	465	200 100	38.2	67.2
	Mean	**347**	**466**	**201 400**	**38.2**	**66.9**
25.4 mm	1	388	538	201 800	40.9	62.8
	2	385	538	201 300	40.9	64.1
	Mean	**386**	**538**	**201 600**	**40.9**	**63.4**

(1) Measured at 0.2% offset
(2) Measured on 50 mm gauge length

Table C2 – Weld Metal Tension Coupon Tests

Identifier	Coupon Number	Static Yield Strength (1) (MPa)	Static Tensile Strength (MPa)	Modulus of Elasticity (MPa)	Elongation (2) (%)	Reduction of Area (%)
E7014(L)W	1	448	517	200 400	20.6	51.7
	2	456	523	221 000	22.8	54.5
	Mean	**452**	**520**	**210 700**	**21.7**	**53.1**
E70T-4(H)S	1	470	630	206 100	21.1	36.5
	2	473	631	191 100	23.4	51.0
	Mean	**472**	**631**	**198 600**	**22.3**	**43.8**
E70T-7(H)W	1	465	609	201 300	23.6	49.2
	2	471	600	200 200	22.5	49.4
	Mean	**468**	**605**	**200 750**	**23.1**	**49.3**
E71T8-K6(H)S	1	409	495	207 800	25.9	59.0
	2	395	491	206 900	30.8	74.1
	Mean	**402**	**493**	**207 400**	**28.4**	**66.6**

(1) Measured at 0.2% offset
(2) Measured on 50 mm gauge length

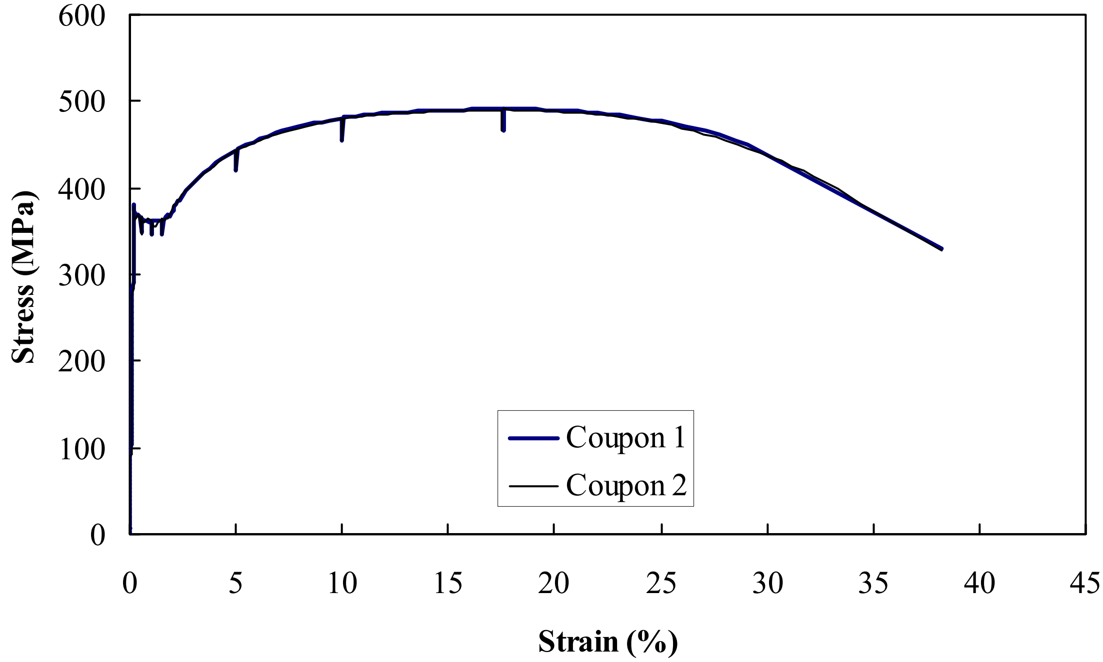

Figure C2 – Stress vs. Strain Curves for 15.9 mm Plate

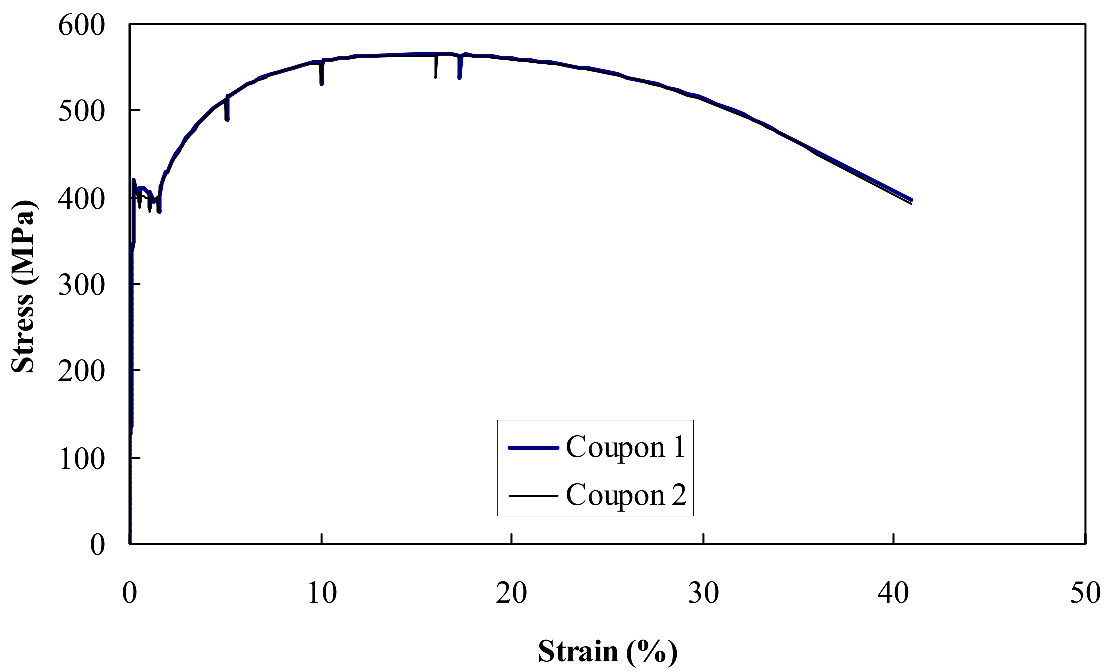

Figure C3 – Stress vs. Strain Curves for 25.4 mm Plate

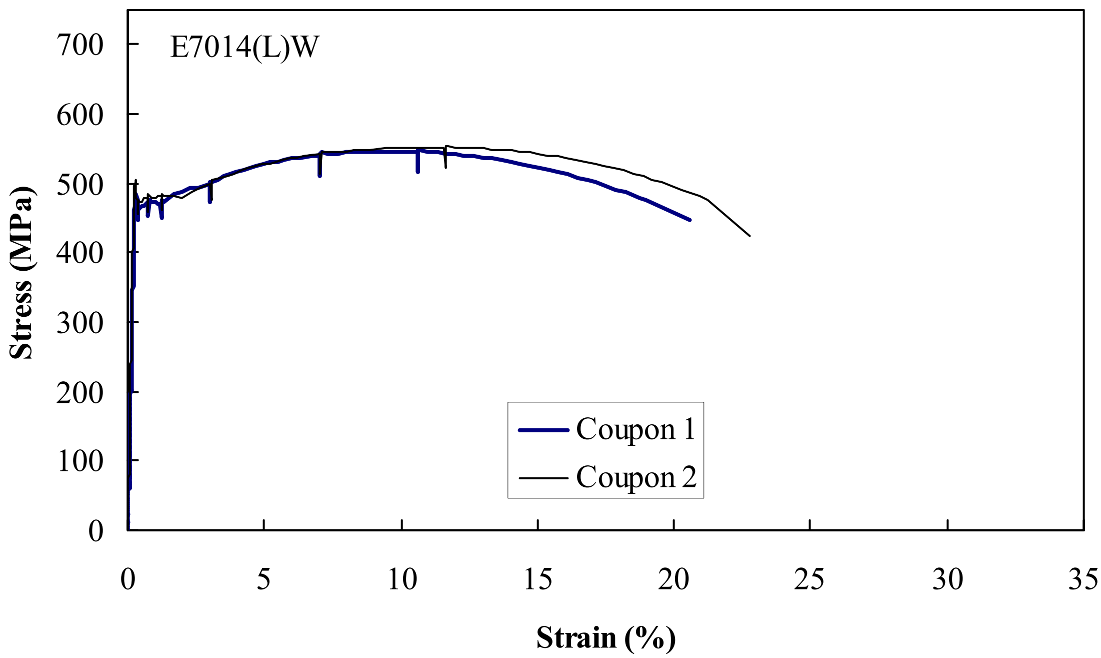

Figure C4 – Stress vs. Strain Curves for Weld Metal E7014

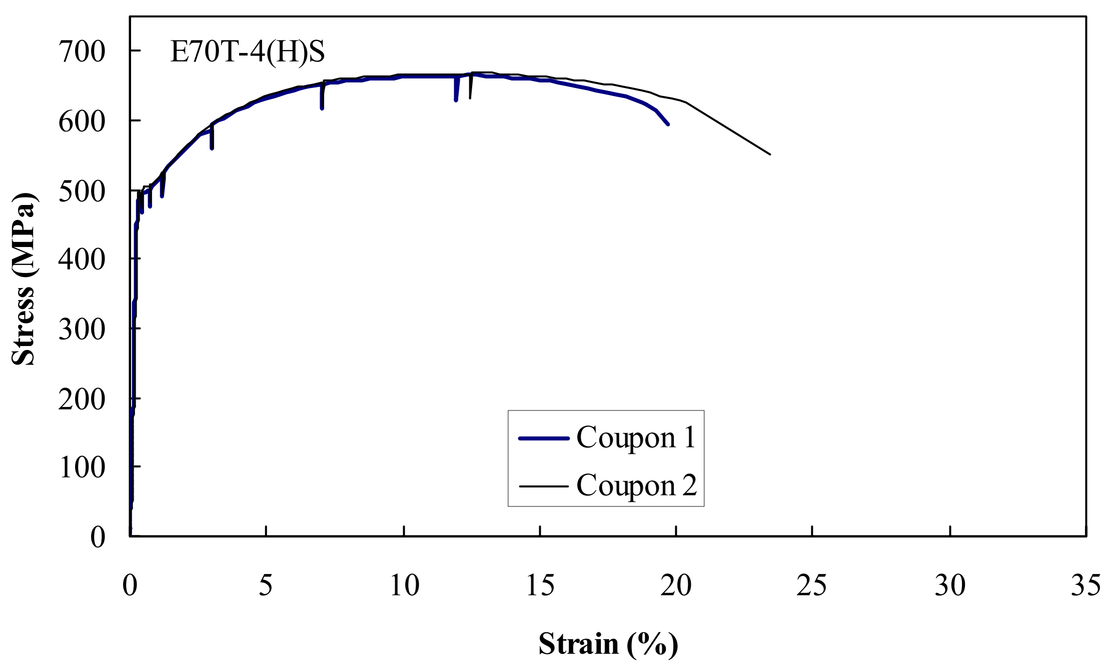

Figure C5 – Stress vs. Strain Curves for Weld Metal E70T-4

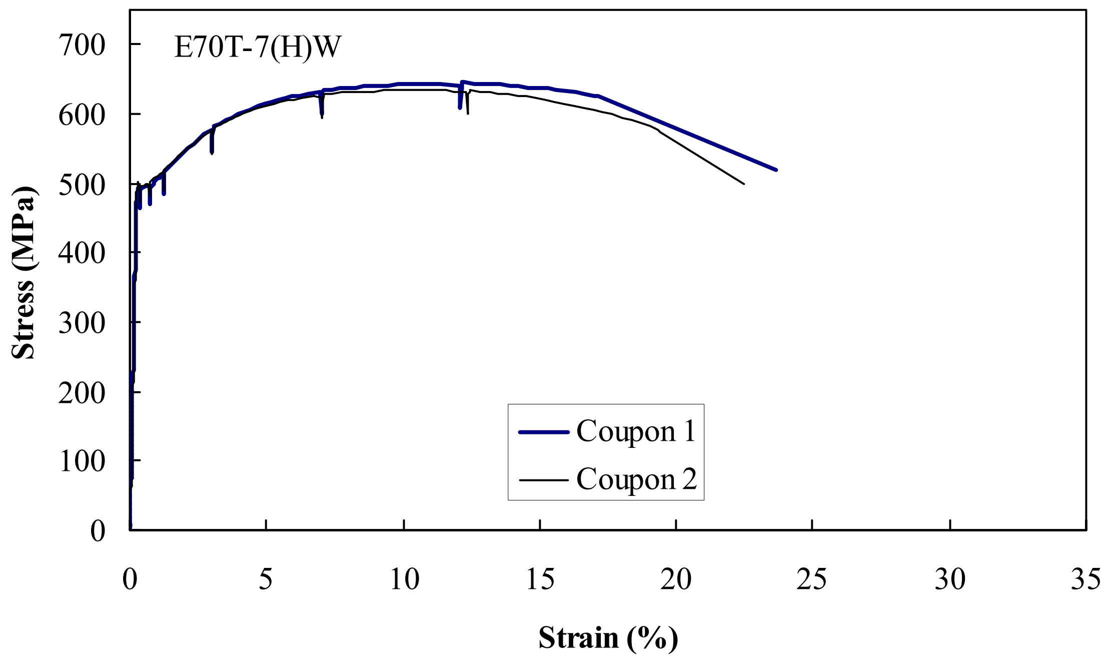

Figure C6 – Stress vs. Strain Curves for Weld Metal E70T-7

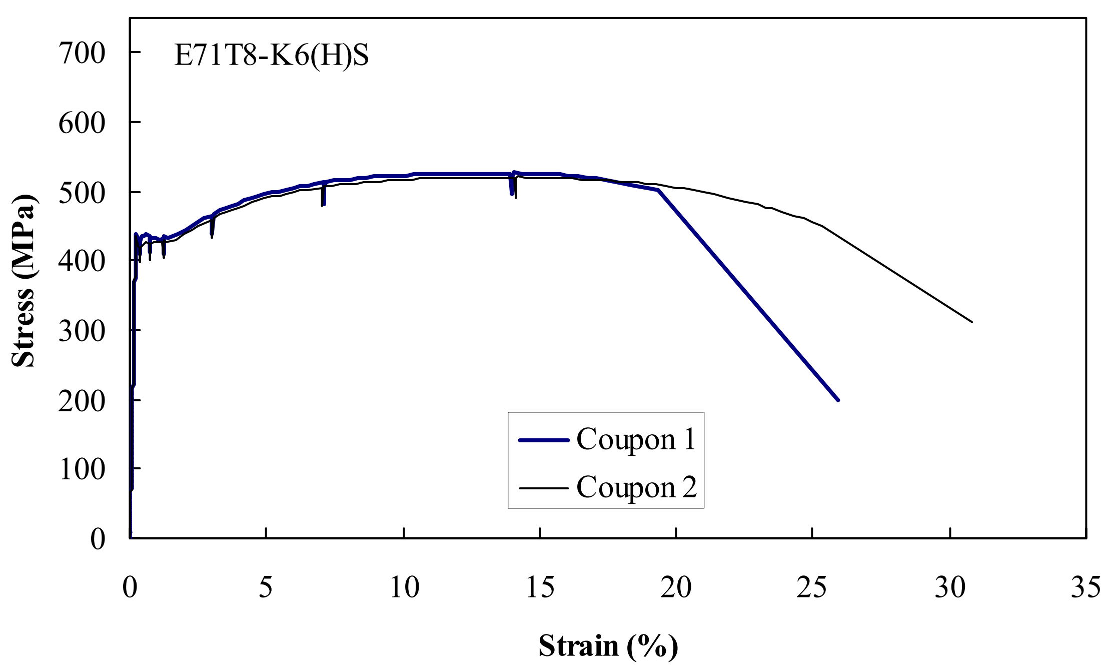

Figure C7 – Stress vs. Strain Curves for Weld Metal E71T8-K6

APPENDIX D

Test Results

Appendix D – Test Results

The weld measurements and the data collected from the tests have been manipulated to produce results suitable for analysing weld strength and ductility. A description of the results presented in the tables of this appendix is given below.

1. Test-to-predicted ratios were determined using the measured ultimate loads and the predictions of CSA–S16–01 (CSA, 2001) fillet weld design equation. Two types of test-to-predicted ratios are provided. The first used the predictions calculated with the weld strengths measured from the weld metal tension coupon tests while the second used the predictions calculated with the nominal weld strengths.

2. The Theoretical Throat Area was determined from the measured weld length and the theoretical weld throat calculated from the mean measured dimensions of the two weld legs.

3. The Ultimate P/A_{throat} is the quotient between the portion of the measured ultimate load carried by the weld and the Theoretical Throat Area of that weld. The welds on each specimen were assumed to resist the applied loaded equally.

4. The Fracture Surface Area is the mean measured width of the fractured surface area multiplied by the measured weld length.

5. The $P/A_{fracture}$ is the quotient between the portion of the measured ultimate load carried by the weld and the Fracture Surface Area. The welds on each specimen were assumed to resist the applied loaded equally.

6. The strains at two different instances in the weld response are given: the strain at ultimate load and the strain at weld fracture. Both were calculated by taking the weld deformation at those instances and dividing by the appropriate measured gauge length. In the case of the transverse and longitudinal weld specimens where there were two strain results per weld, the average of the two strains is given.

7. The fracture angle reported is the mean of the fracture angle measurements made. The fracture angle was measured as the angle between the main plate surface and the weld fracture surface.

Table D1 – Transverse Weld Specimen Test Results (also published in Ng *et al.*, 2002)

Specimen Designation	AWS Classification	Ultimate Load P_u (kN)	Weld Location	Test/Predicted Ratio: Measured Weld Strength	Test/Predicted Ratio: Nominal Weld Strength	Theoretical Throat Area A_{throat} (mm^2)	Ultimate P/A_{throat} (MPa)	Fracture Surface Area, $A_{fracture}$ (mm^2)	$P/A_{fracture}$ (MPa)	Mean Strain at P_u	Mean Fracture Strain	Fracture Angle (°)
T20-1	E7014	782	Front	1.01	1.09	741	528	767	510	0.134	0.154	27
			Back	1.03	1.12	724	540	—	—	0.053	0.057	—
T20-2	E7014	949	Front	1.30	1.41	697	681	1040	456	0.171	0.190	7
			Back	1.21	1.31	749	633	—	—	0.126	0.130	—
T20-3	E7014	878	Front	1.14	1.24	736	596	946	464	0.132	0.147	7
			Back	1.14	1.23	740	594	—	—	0.090	0.094	—
T22-1	E70T-4	912	Front	1.34	1.76	538	847	928	491	0.129	0.150	0
			Back	1.17	1.53	617	739	—	—	0.076	0.078	—
T22-2	E70T-4	903	Front	1.30	1.71	548	824	966	467	0.114	0.131	0
			Back	1.19	1.56	601	752	—	—	0.078	0.079	—
T22-3	E70T-4	994	Front	1.38	1.81	568	875	983	506	0.157	0.167	0
			Back	1.35	1.78	580	857	—	—	0.143	0.144	—
T26-1	E70T-7	1060	Front	1.35	1.70	645	822	—	—	0.170	0.170	—
			Back	1.39	1.74	630	842	749	708	0.167	0.167	24
T26-2	E70T-7	1068	Front	1.35	1.70	651	821	868	615	0.201	0.213	23
			Back	1.38	1.73	639	836	—	—	0.161	0.163	—
T26-3	E70T-7	1062	Front	1.32	1.67	661	804	787	675	0.225	0.225	24
			Back	1.33	1.67	658	807	—	—	0.131	0.131	—
T32-1	E71T8-K6	1044	Front	1.67	1.72	630	829	—	—	0.206	0.206	—
			Back	1.57	1.62	670	779	811	644	0.227	0.230	25
T32-2	E71T8-K6	1049	Front	1.71	1.75	620	846	—	—	0.268	0.279	—
			Back	1.59	1.64	664	789	776	676	0.238	0.257	23
T32-3	E71T8-K6	1022	Front	1.67	1.72	617	829	876	583	0.297	0.306	10
			Back	1.60	1.65	643	794	—	—	0.184	0.186	—

Table D2 – Forty-Five Degree Weld Specimen Test Results

Specimen Designation	AWS Classification	Ultimate Load P_u (kN)	Weld Location	Test/Predicted Ratio Measured Weld Strength	Test/Predicted Ratio Nominal Weld Strength	Theoretical Throat Area Athroat (mm^2)	Ultimate P/A_{throat} (MPa)	Fracture Surface Area, $A_{fracture}$ (mm^2)	$P/A_{fracture}$ (MPa)	Mean Strain at Pu	Mean Fracture Strain	Fracture Angle (°)
F1-1	E70T-4	789	Front	1.25	1.64	575	686	—	—	0.074	0.080	—
			Back	1.23	1.62	584	675	791	499	0.093	0.104	20
F1-2	E70T-4	763	Front	1.43	1.88	487	783	643	593	0.082	0.087	20
			Back	1.31	1.72	532	717	—	—	0.054	0.056	—
F1-3	E70T-4	745	Front	1.38	1.81	493	755	606	615	0.110	0.110	26
			Back	1.21	1.59	560	665	—	—	0.073	0.073	—
F2-1	E70T-7	813	Front	1.55	1.96	498	816	691	588	0.125	0.125	48
			Back	1.46	1.84	530	766	—	—	0.063	0.063	—
F2-2	E70T-7	840	Front	1.42	1.79	564	745	—	—	0.050	0.057	—
			Back	1.50	1.89	534	787	751	559	0.100	0.116	29
F2-3	E70T-7	823	Front	1.56	1.96	502	820	649	634	0.141	0.143	28
			Back	1.34	1.68	586	702	—	—	0.069	0.069	—
F3-1	E71T8-K6	755	Front	1.61	1.66	546	691	647	583	0.143	0.172	28
			Back	1.50	1.54	588	642	—	—	0.125	0.146	—
F3-2	E71T8-K6	725	Front	1.59	1.63	533	681	—	—	0.092	0.103	—
			Back	1.59	1.64	531	683	653	555	0.119	0.140	28
F3-3	E71T8-K6	790	Front	—	—	535	—	—	Reinforced	—	—	—
			Back	—	—	538	—	—	Weld Failed	—	—	—

Figure D3 – Longitudinal Weld Specimen Test Results

Specimen Designation	AWS Classification	Ultimate Load P_u (kN)	Weld Location	Test/Predicted Ratio		Theoretical Throat Area A_{throat} (mm^2)	Ultimate P/A_{throat} (MPa)	Fracture Surface Area, $A_{fracture}$ (mm^2)	$P/A_{fracture}$ (MPa)	Mean Strain at P_u	Mean Fracture Strain	Fracture Angle (°)
				Measured Weld Strength	Nominal Weld Strength							
L1-1	E70T-4	731	Weld 1	1.12	1.47	386	474	—	—	0.115	0.145	—
			Weld 2	1.33	1.75	324	563	—	—	0.140	0.176	—
			Weld 3	1.17	1.54	369	496	363	503	0.173	0.234	33
			Weld 4	1.22	1.60	355	515	361	506	0.182	0.247	36
L1-2	E70T-4	762	Weld 1	1.12	1.47	402	474	386	493	0.156	0.253	37
			Weld 2	1.16	1.52	389	489	452	421	0.150	0.243	23
			Weld 3	1.24	1.63	364	524	—	—	0.146	0.206	—
			Weld 4	1.28	1.68	352	541	—	—	0.146	0.208	—
L1-3	E70T-4	740	Weld 1	1.15	1.51	380	487	395	469	0.140	0.222	31
			Weld 2	1.22	1.61	358	517	399	463	0.161	0.256	31
			Weld 3	1.20	1.58	365	507	—	—	0.139	0.205	—
			Weld 4	1.21	1.58	363	509	—	—	0.146	0.215	—
L2-1	E70T-7	830	Weld 1	1.33	1.67	386	538	—	—	0.147	0.295	—
			Weld 2	1.32	1.67	387	536	475	437	0.149	0.300	27
			Weld 3	1.32	1.66	388	535	—	—	0.152	0.277	—
			Weld 4	1.29	1.62	398	521	—	—	0.142	0.259	—
L2-2	E70T-7	805	Weld 1	1.36	1.71	366	550	—	—	0.129	0.207	—
			Weld 2	1.40	1.76	355	566	—	—	0.132	0.213	—
			Weld 3	1.21	1.53	410	491	—	—	0.100	0.183	—
			Weld 4	1.36	1.71	365	551	391	514	0.127	0.231	30
L2-3	E70T-7	802	Weld 1	1.22	1.53	406	494	—	—	0.100	0.195	—
			Weld 2	1.34	1.69	368	545	—	—	0.114	0.223	—
			Weld 3	1.35	1.70	366	548	422	475	0.154	0.285	24
			Weld 4	1.32	1.67	374	536	—	—	0.154	0.286	—

Figure D3 – Longitudinal Weld Specimen Test Results (Cont.)

Specimen Designation	AWS Classification	Ultimate Load P_u (kN)	Weld Location	Test/Predicted Ratio		Theoretical Throat Area A_{throat} (mm^2)	Ultimate P/A_{throat} (MPa)	Fracture Surface Area, $A_{fracture}$ (mm^2)	$P/A_{fracture}$ (MPa)	Mean Strain at P_u	Mean Fracture Strain	Fracture Angle (°)
				Measured Weld Strength	Nominal Weld Strength							
L3-1	E71T8-K6	743	Weld 1	1.49	1.53	376	493	450	413	0.224	0.584	33
			Weld 2	1.49	1.53	377	492	497	373	0.217	0.564	46
			Weld 3	1.59	1.64	353	526	473	393	0.188	0.574	56
			Weld 4	1.63	1.67	345	539	523	355	0.204	0.623	20
L3-2	E71T8-K6	700	Weld 1	1.46	1.50	362	483	—	—	0.151	0.418	—
			Weld 2	1.44	1.48	367	477	462	379	0.148	0.410	27
			Weld 3	1.40	1.44	378	463	—	—	0.179	0.483	—
			Weld 4	1.45	1.49	366	479	—	—	0.173	0.466	—
L3-3	E71T8-K6	750	Weld 1	1.55	1.59	367	511	423	443	0.198	0.421	32
			Weld 2	1.36	1.39	418	448	—	—	0.159	0.337	—
			Weld 3	1.48	1.52	385	488	—	—	0.181	0.350	—
			Weld 4	1.64	1.68	347	540	—	—	0.198	0.385	—

APPENDIX E

Fillet Weld Stress vs. Strain Response

Appendix E – Fillet Weld Stress vs. Strain Response

Stress vs. strain curves showing the behaviour of the fillet welds on each specimen are presented in this appendix. The information that is given in these plots is highlighted in Figure E1 and described below.

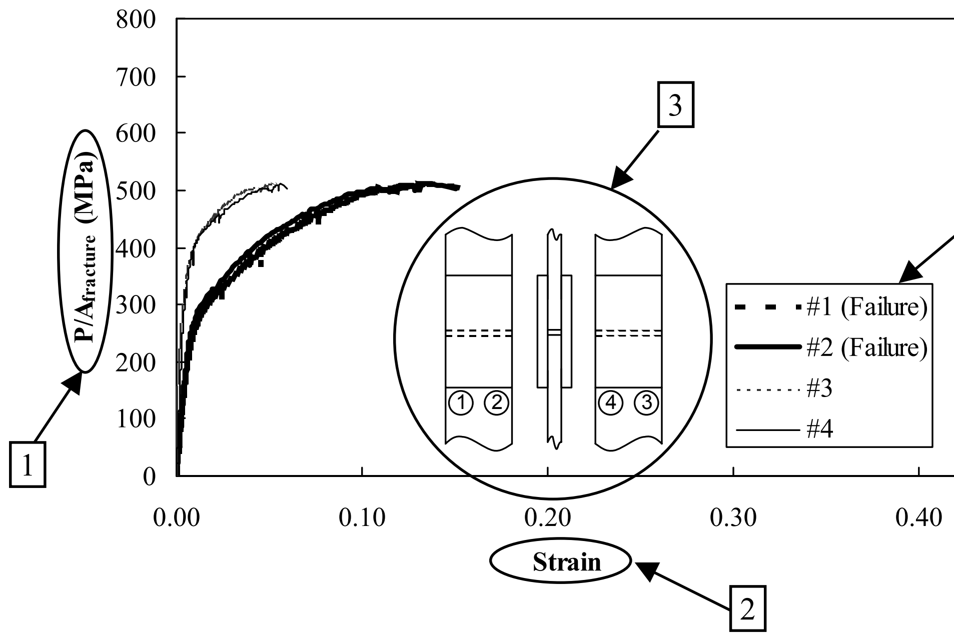

Figure E1 – Sample Stress vs. Strain Curve

1. The fillet weld stresses plotted are the stresses that were calculated using the measured fracture area. For those specimens in which more than one weld fractured, the average fracture area was used. Each weld was assumed to carry one-quarter of the applied load in the longitudinal weld specimens and half the applied load in the transverse and 45-degree weld specimens. It was also assumed that the welds that did not fracture would have had approximately the same fracture surface area as those that did fracture. For the one specimen that did not fail in the test welds (F3-3), the stresses calculated on the theoretical throat area, which was determined using the mean measured weld leg dimensions, are plotted instead.

2. The plotted weld strains were calculated in the following fashion:

    a. For the transverse welds, the measured weld displacements were divided by the average of the weld leg size measurements performed at the two punch marks made for each LVDT to hold the LVDT bracket in place.

    b. For the 45-degree welds, the measured weld displacements were divided by the gauge length. This gauge length was determined by averaging the weld leg size measurements performed at the two LVDT punch marks and then adjusting the average to obtain the weld portion that was parallel to the direction of loading.

    c. For the longitudinal welds, the displacements were divided by the average measured size of the weld shear leg on the main plate. This means that the strains plotted are the shear strains. The deformations measured over the full length of the welds were used.

3. This diagram shows the location of each LVDT within the specimen. The circled numbers represent the LVDTs.

4. The legend identifies for each curve the location where the displacements were measured and indicates where fracture took place.

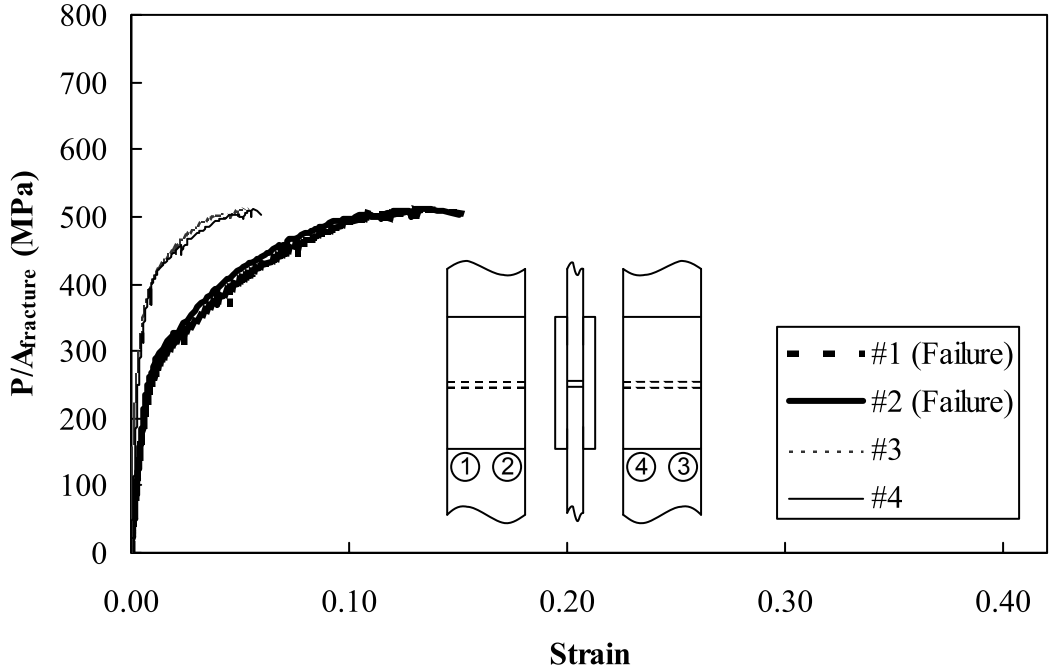

Figure E1 – Specimen T20-1 with Transverse Welds from E7014 Filler Metal

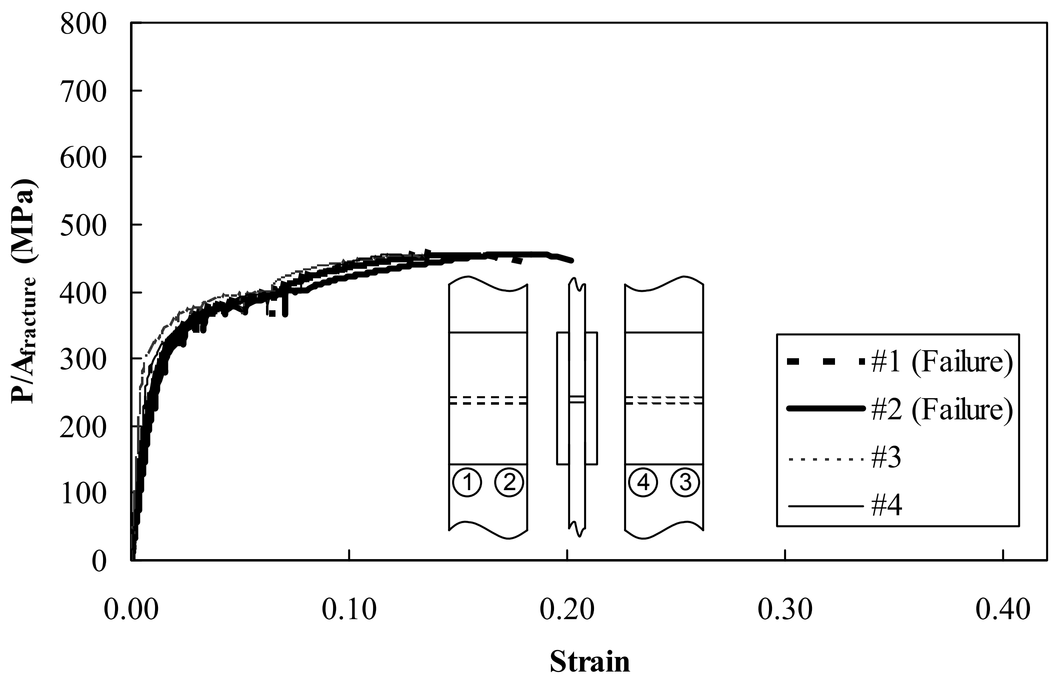

Figure E2 – Specimen T20-2 with Transverse Welds from E7014 Filler Metal

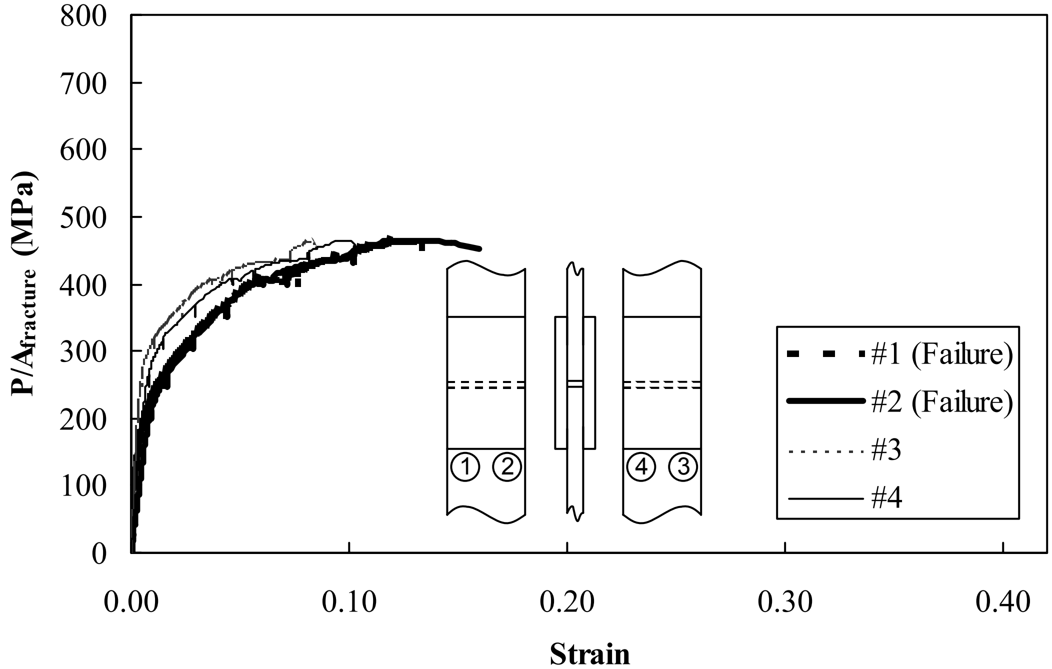

Figure E3 – Specimen T20-3 with Transverse Welds from E7014 Filler Metal

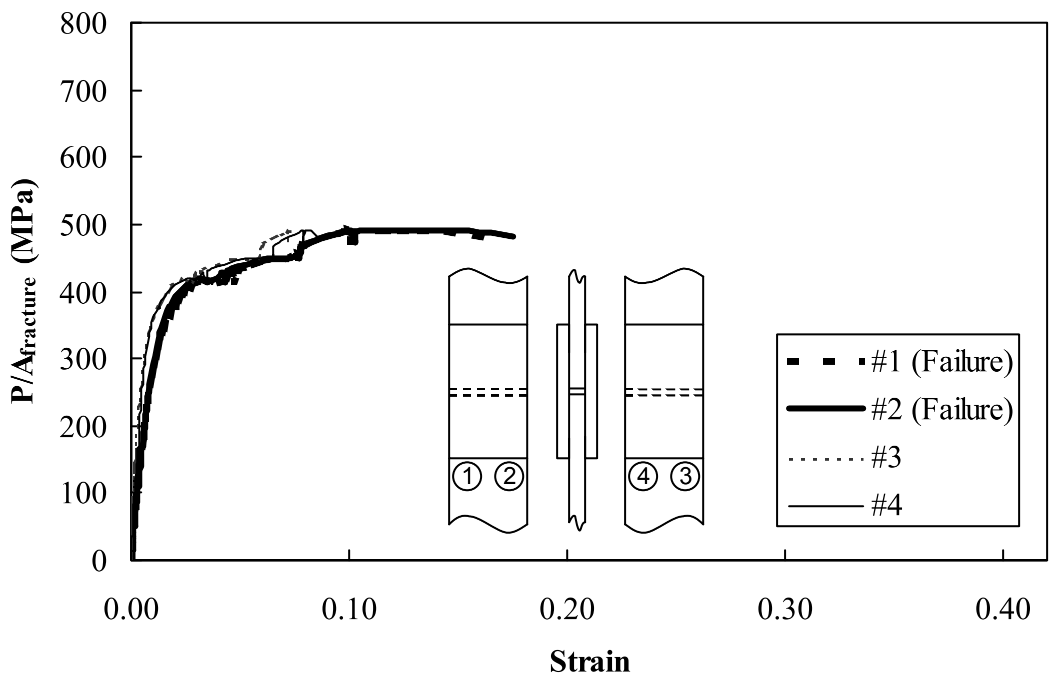

Figure E4 – Specimen T22-1 with Transverse Welds from E70T-4 Filler Metal

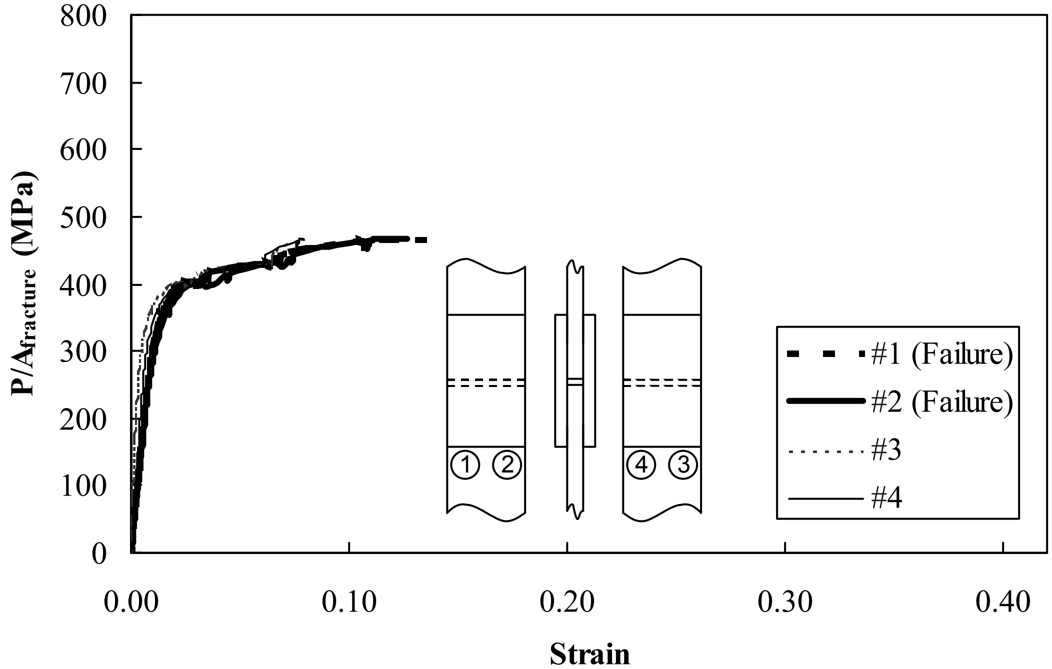

Figure E5 – Specimen T22-2 with Transverse Welds from E70T-4 Filler Metal

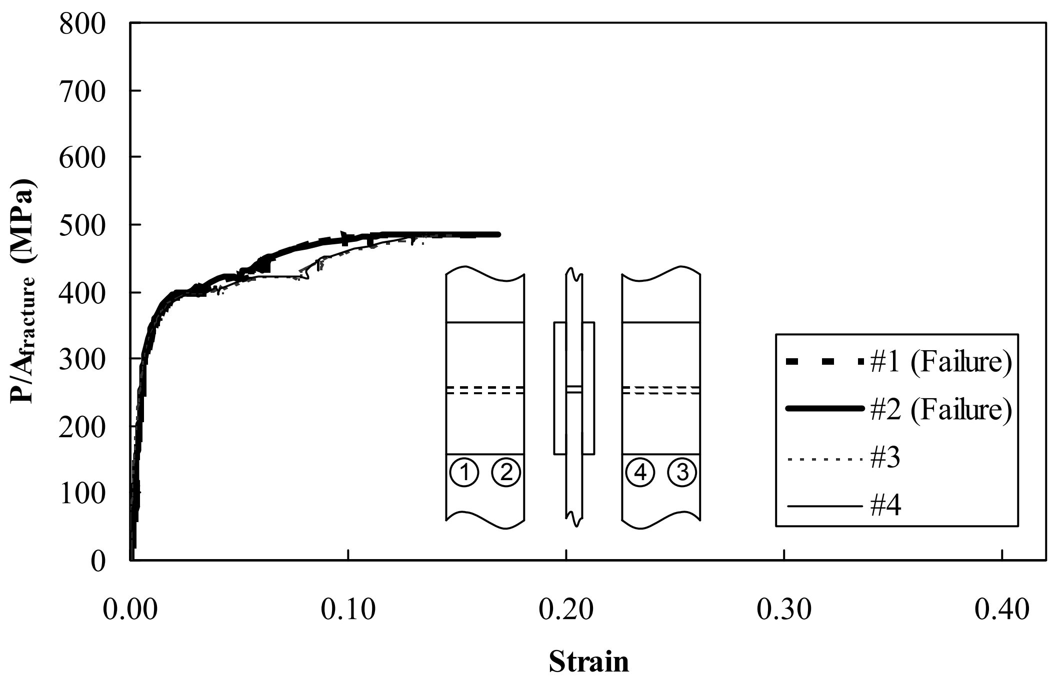

Figure E6 – Specimen T22-3 with Transverse Welds from E70T-4 Filler Metal

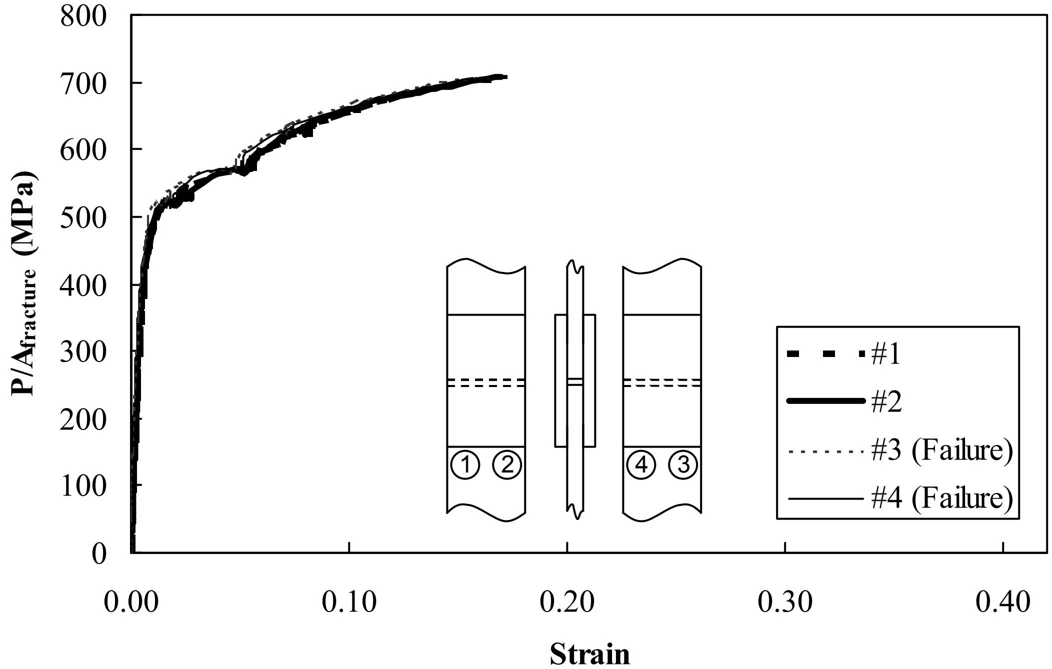

Figure E7 – Specimen T26-1 with Transverse Welds from E70T-7 Filler Metal

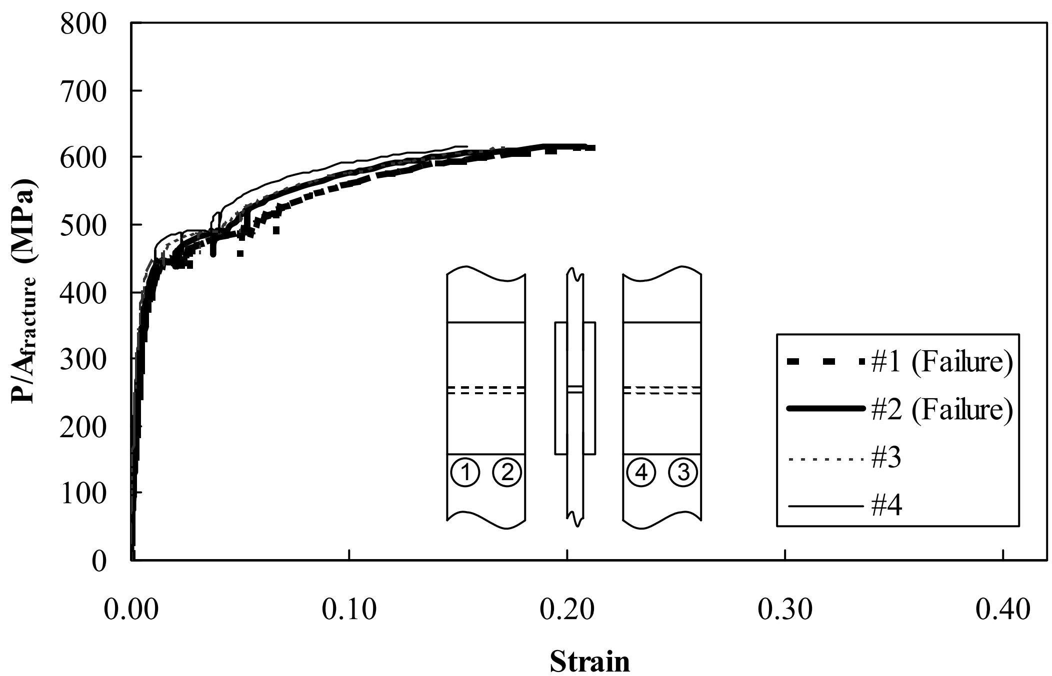

Figure E8 – Specimen T26-2 with Transverse Welds from E70T-7 Filler Metal

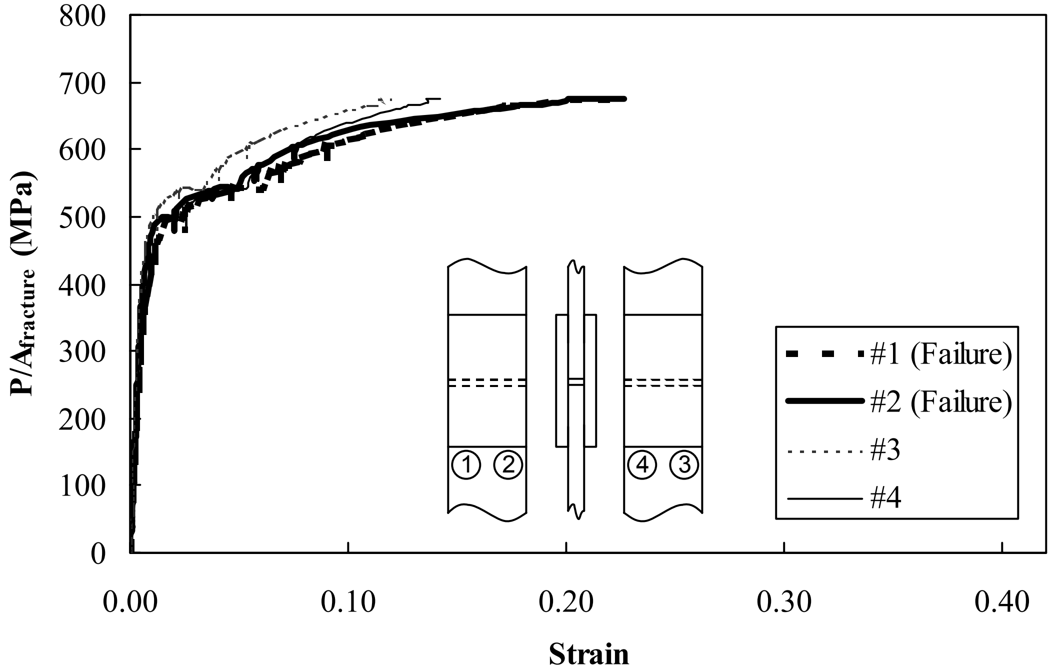

Figure E9 – Specimen T26-3 with Transverse Welds from E70T-7 Filler Metal

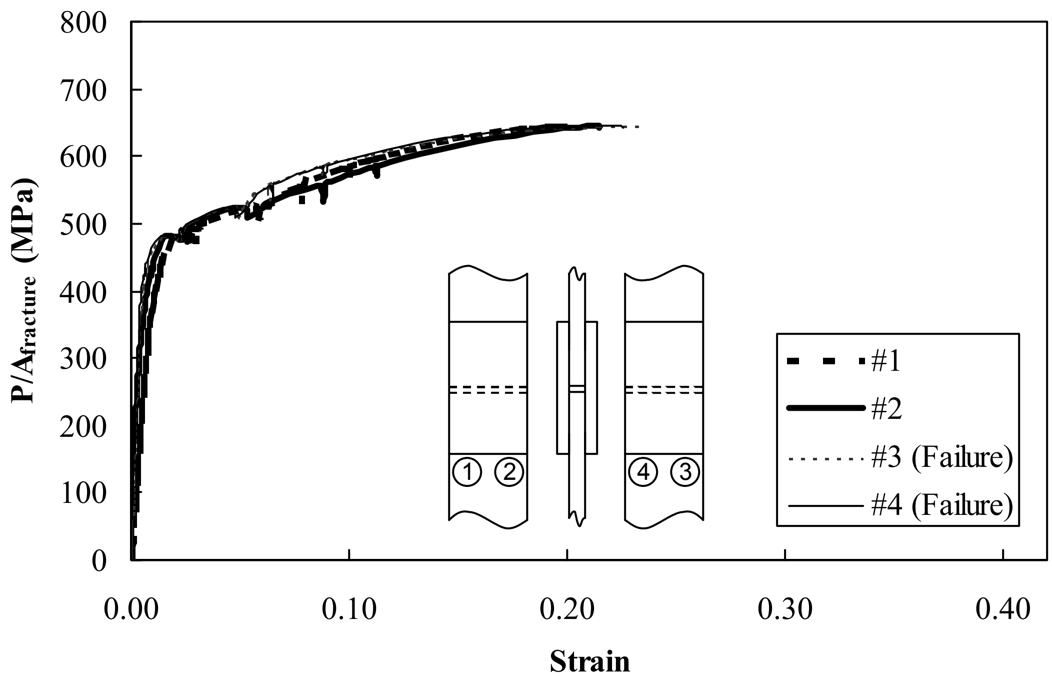

Figure E10 – Specimen T32-1 with Transverse Welds from E71T8-K6 Filler Metal

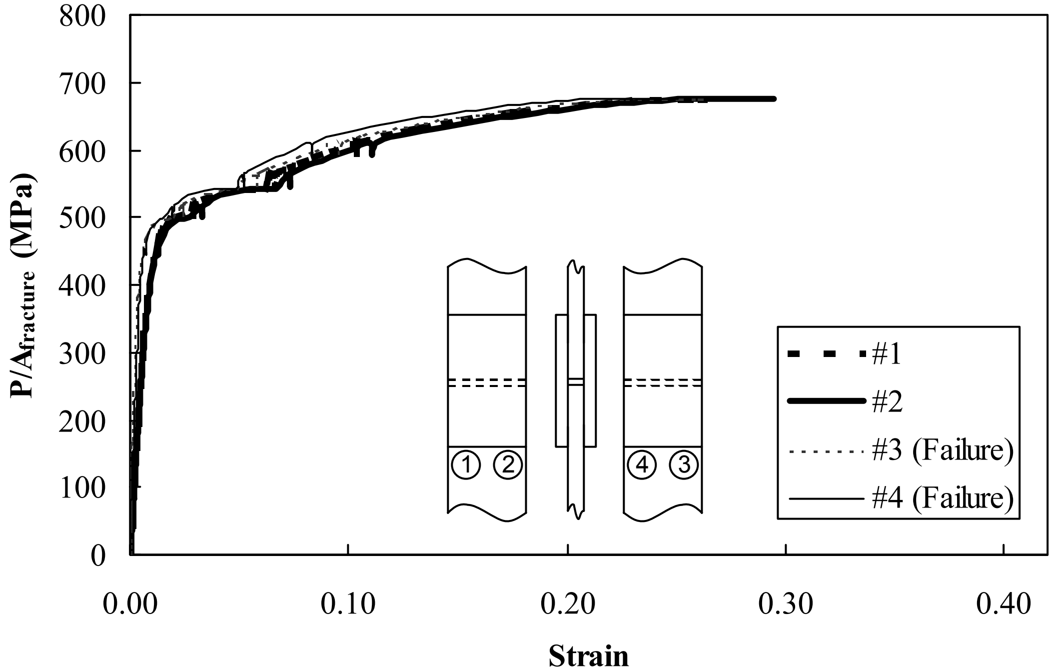

Figure E11 – Specimen T32-2 with Transverse Welds from E71T8-K6 Filler Metal

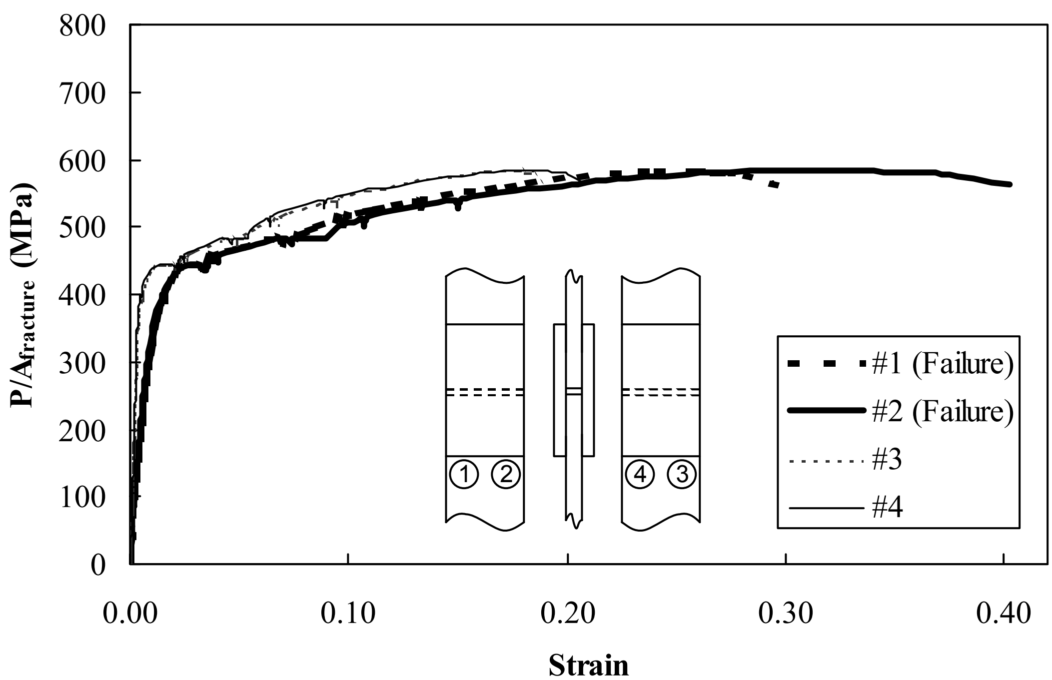

Figure E12 – Specimen T32-3 with Transverse Welds from E71T8-K6 Filler Metal

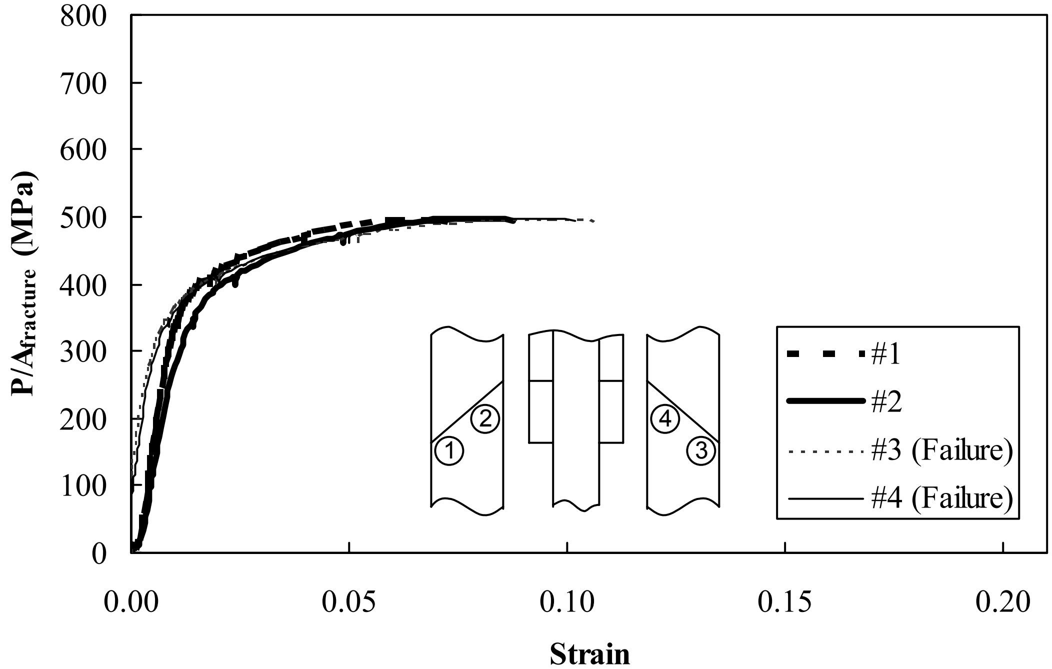

Figure E13 – Specimen F1-1 with 45-Degree Welds from E70T-4 Filler Metal

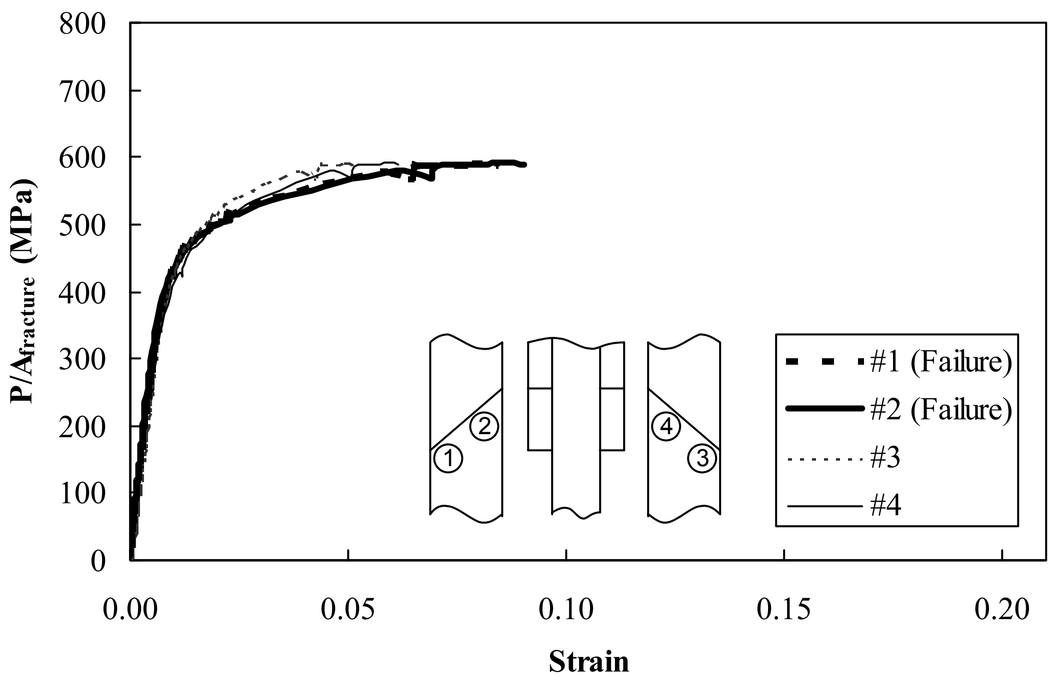

Figure E14 – Specimen F1-2 with 45-Degree Welds from E70T-4 Filler Metal

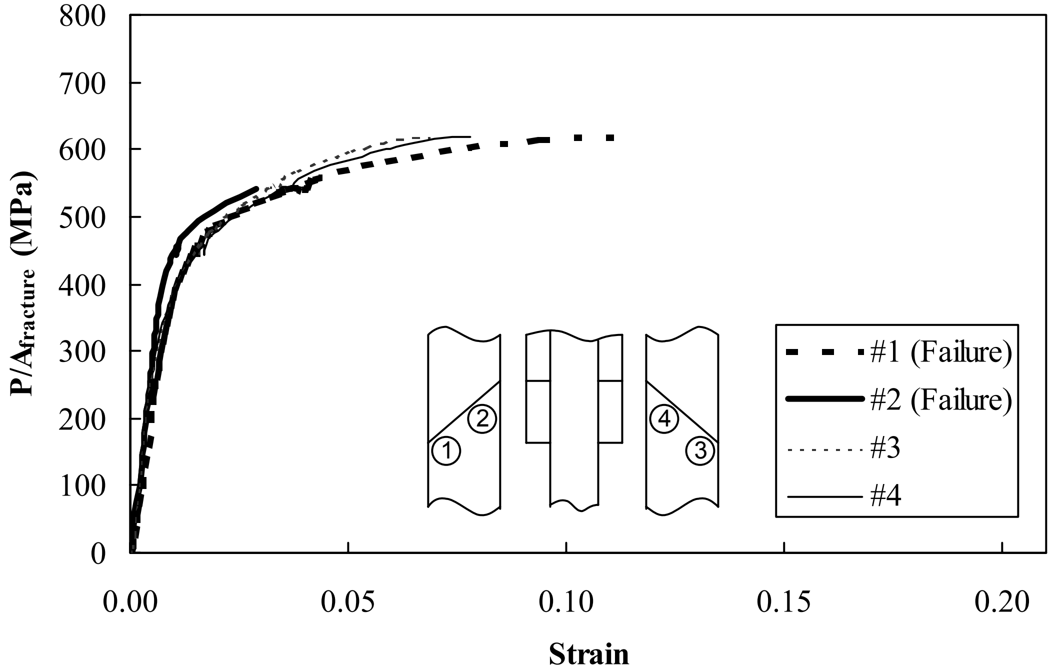

Figure E15 – Specimen F1-3 with 45-Degree Welds from E70T-4 Filler Metal

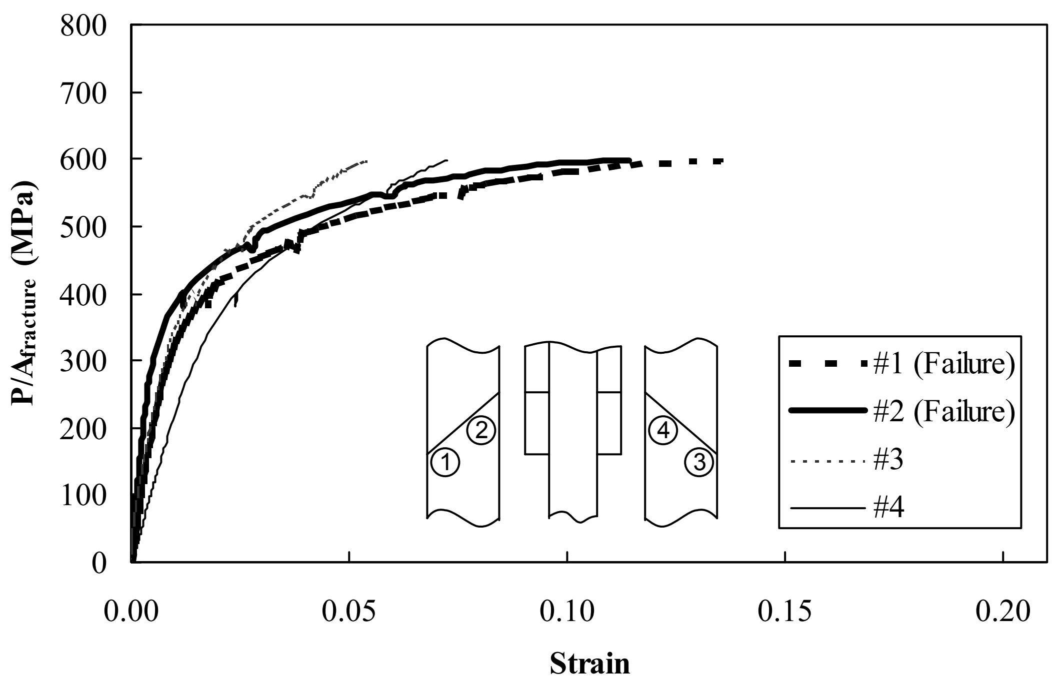

Figure E16 – Specimen F2-1 with 45-Degree Welds from E70T-7 Filler Metal

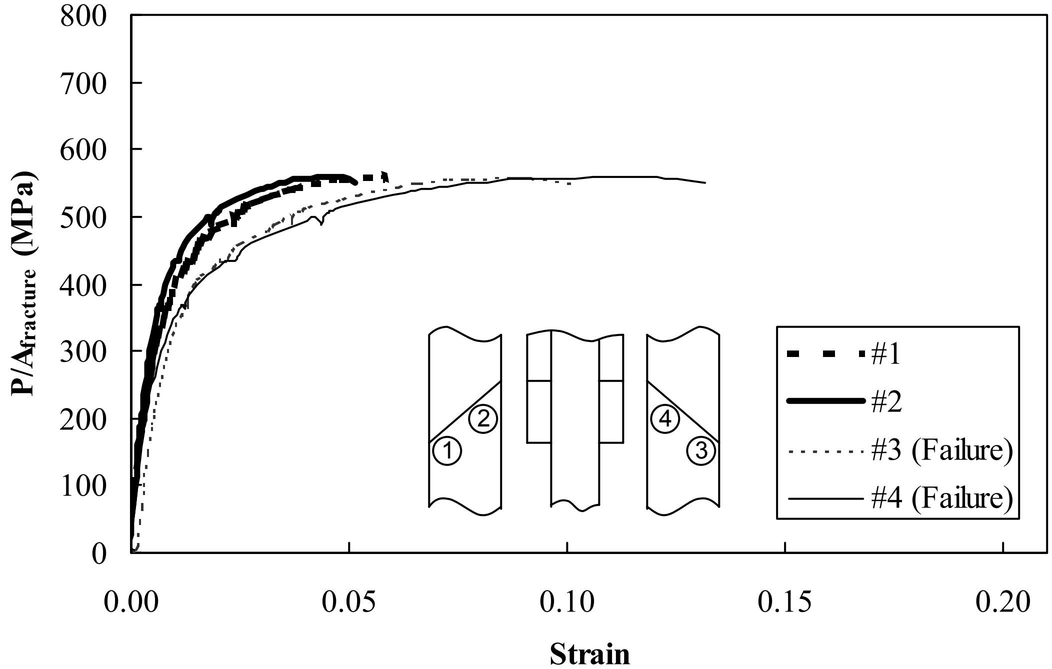

Figure E17 – Specimen F2-2 with 45-Degree Welds from E70T-7 Filler Metal

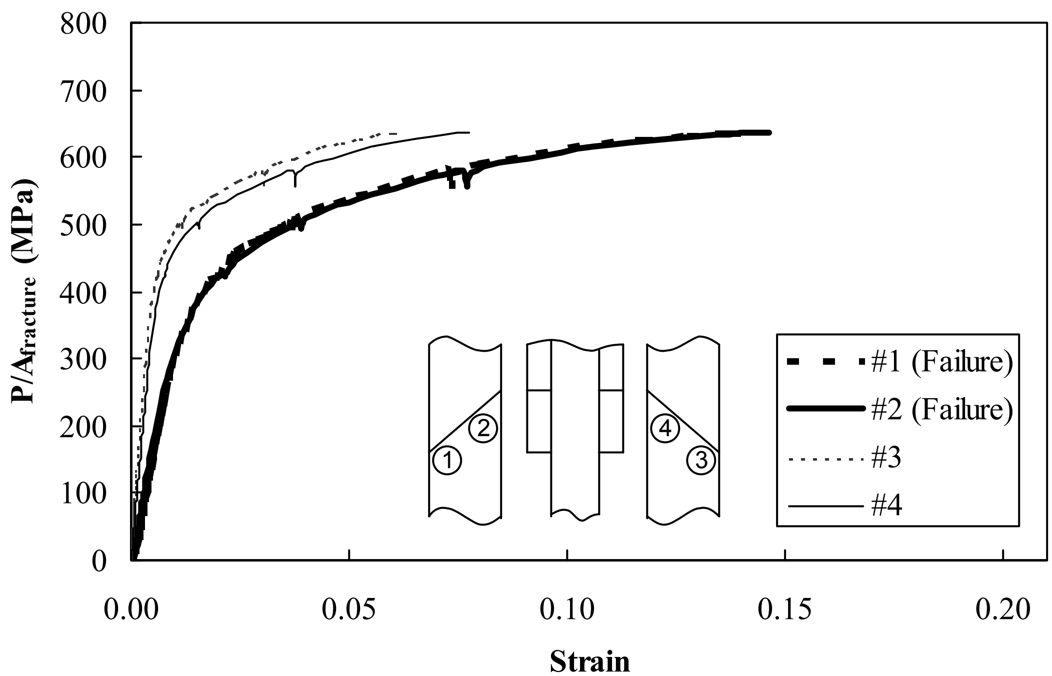

Figure E18 – Specimen F2-3 with 45-Degree Welds from E70T-7 Filler Metal

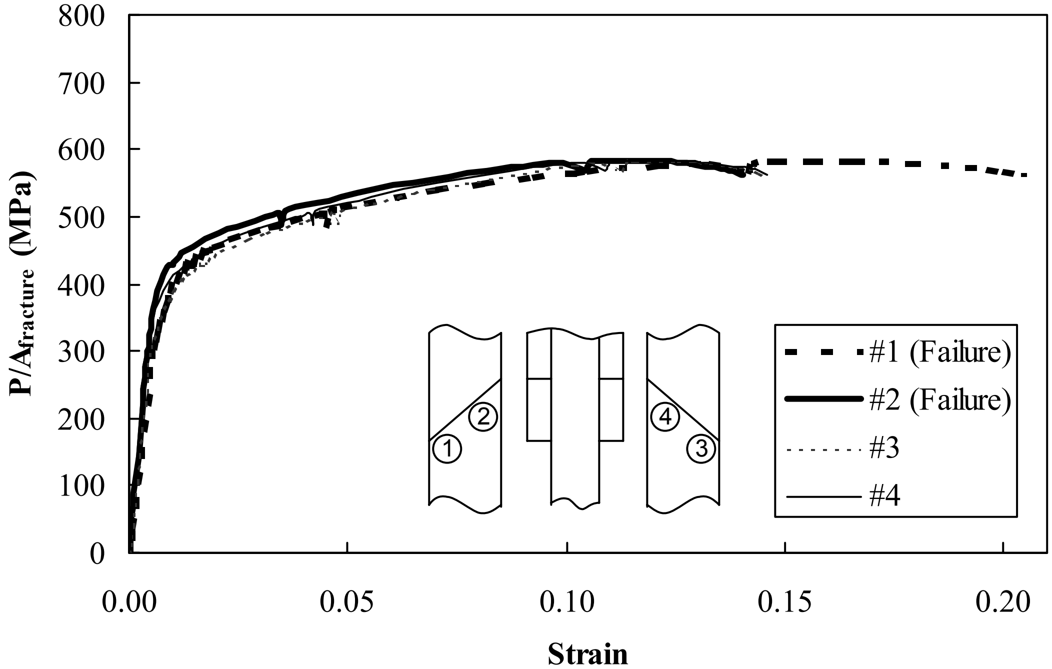

Figure E19 – Specimen F3-1with 45-Degree Welds from E71T8-K6 Filler Metal

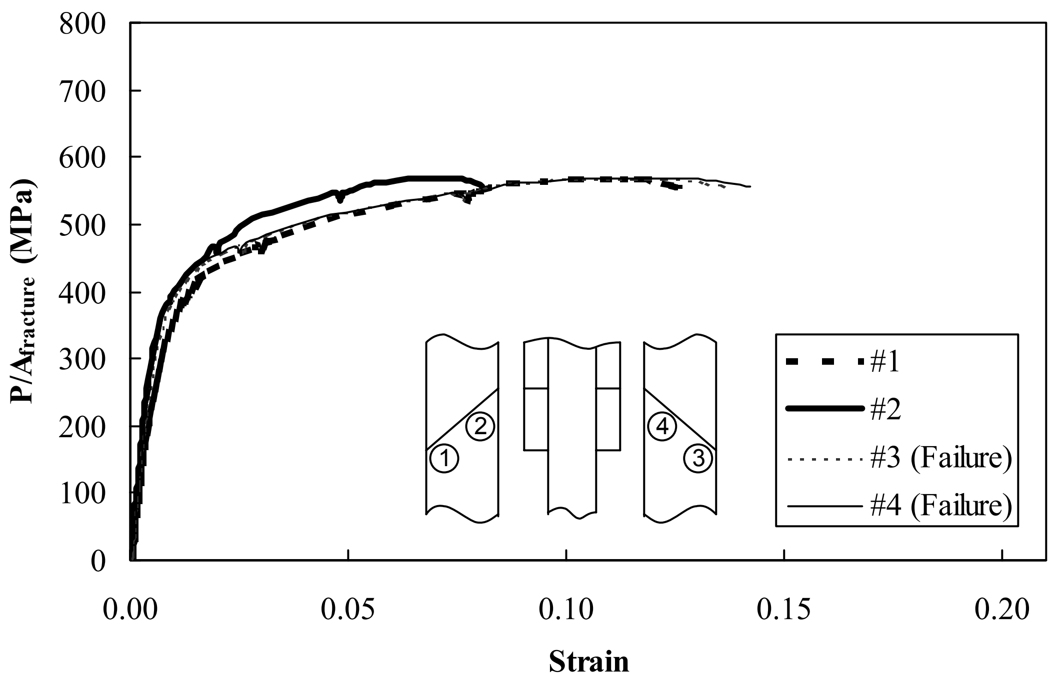

Figure E20 – Specimen F3-2 with 45-Degree Welds from E71T8-K6 Filler Metal

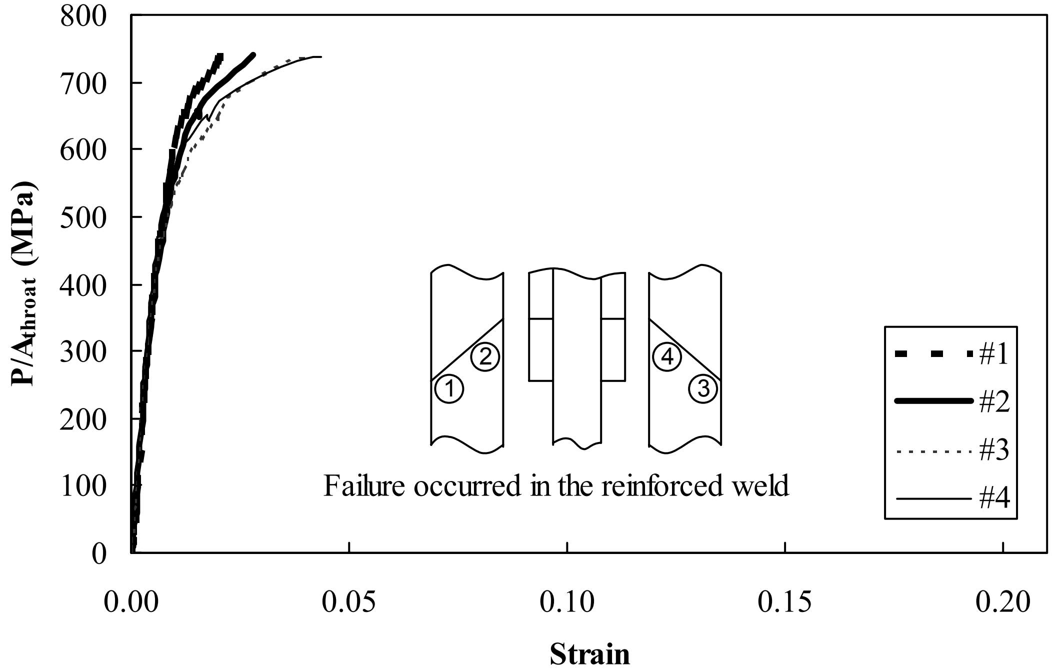

Figure E21 – Specimen F3-3 with 45-Degree Welds from E71T8-K6 Filler Metal

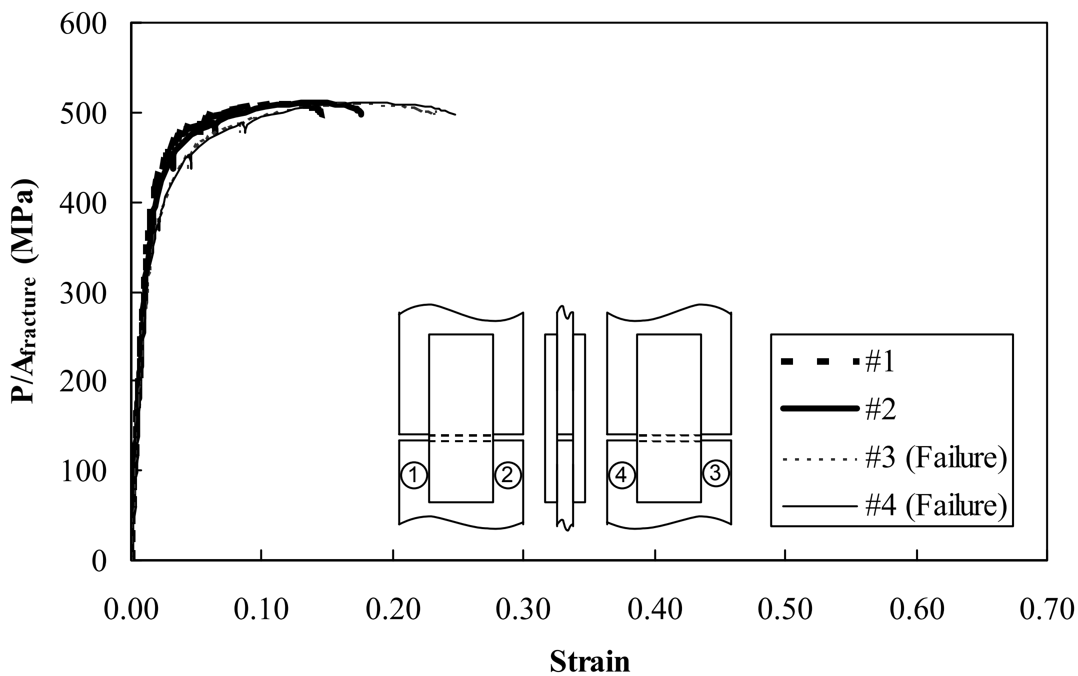

Figure E22 – Specimen L1-1 with Longitudinal Welds from E70T-4 Filler Metal

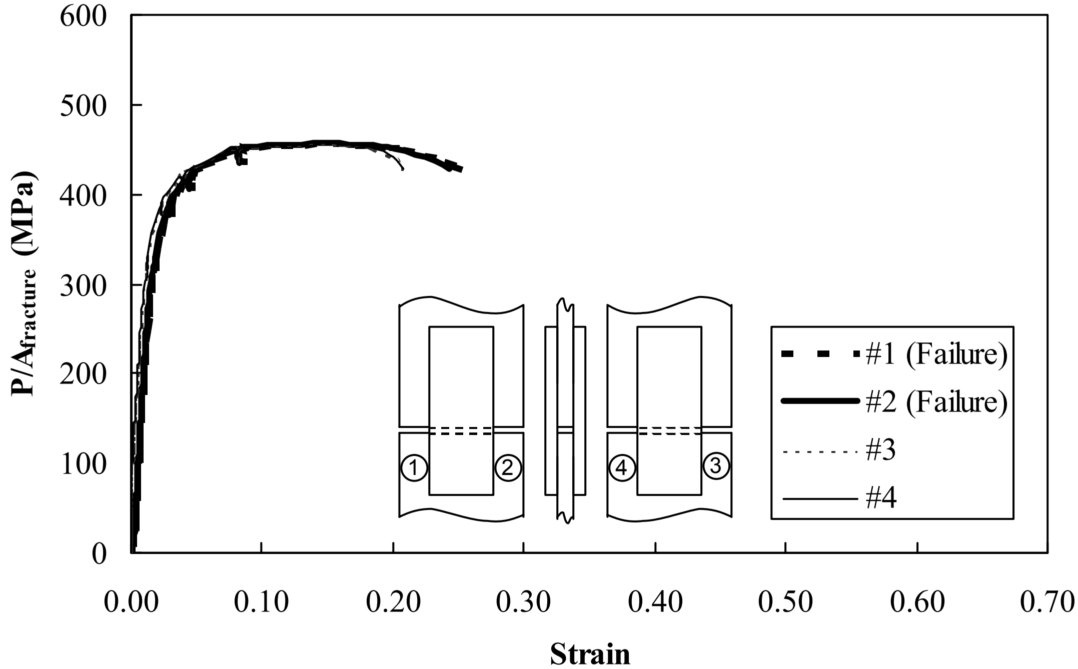

Figure E23 – Specimen L1-2 with Longitudinal Welds from E70T-4 Filler Metal

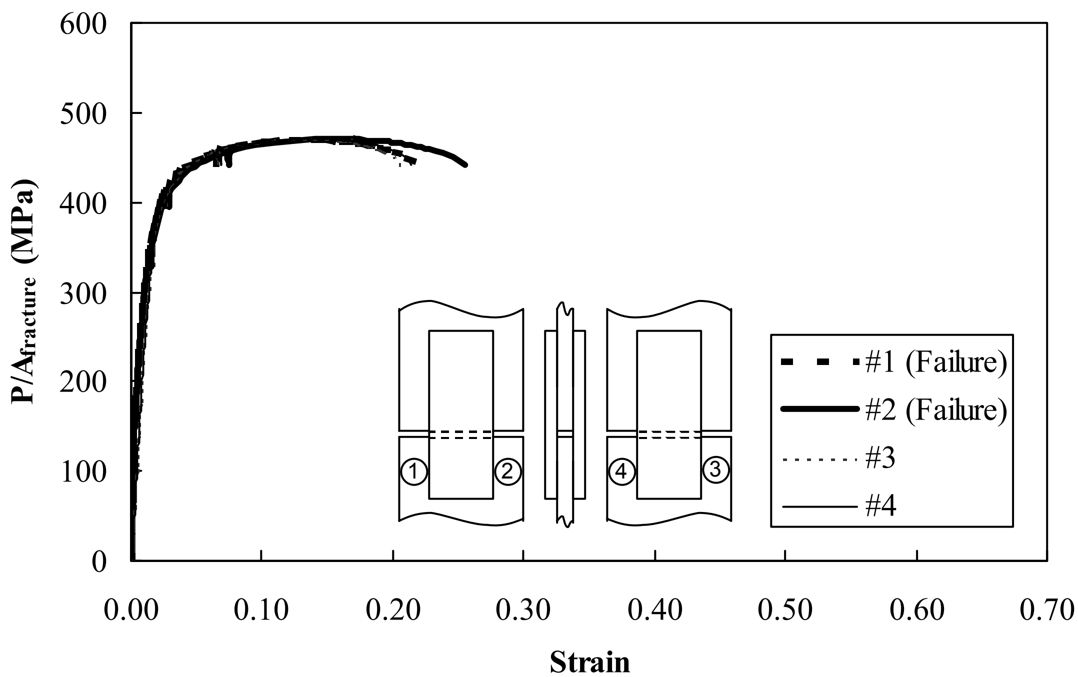

Figure E24 – Specimen L1-3 with Longitudinal Welds from E70T-4 Filler Metal

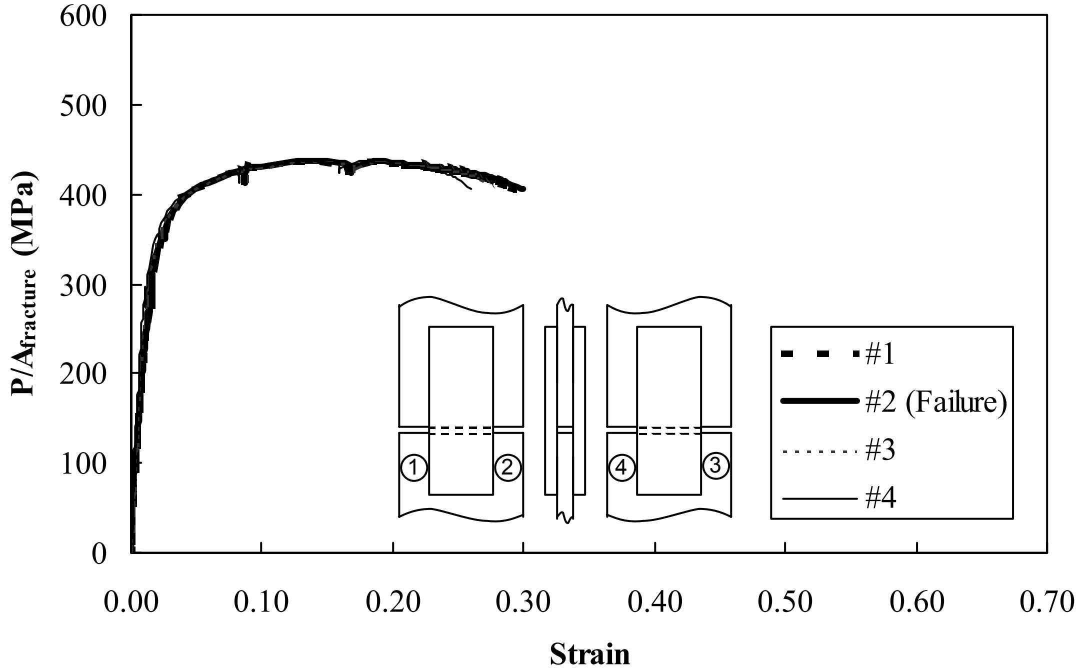

Figure E25 – Specimen L2-1 with Longitudinal Welds from E70T-7 Filler Metal

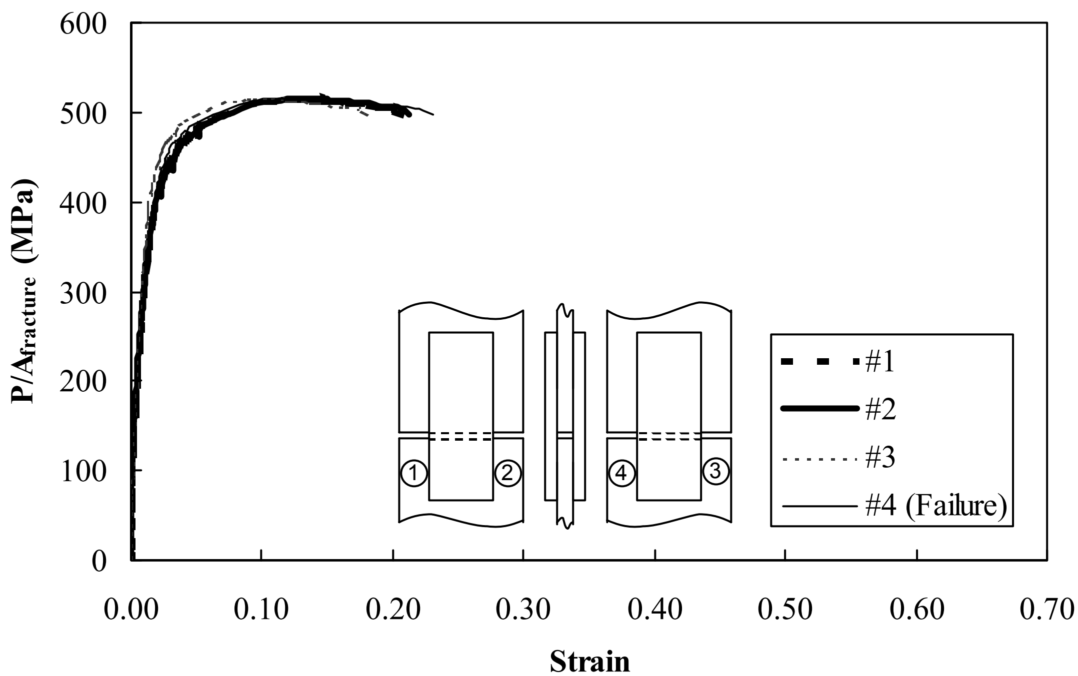

Figure E26 – Specimen L2-2 with Longitudinal Welds from E70T-7 Filler Metal

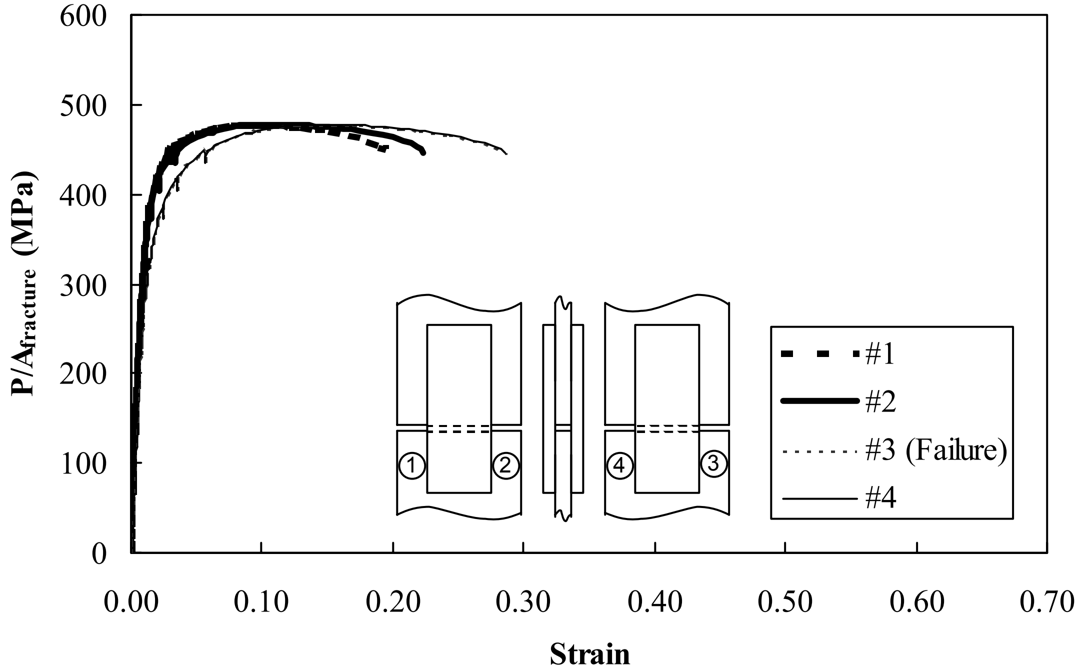

Figure E27 – Specimen L2-3 with Longitudinal Welds from E70T-7 Filler Metal

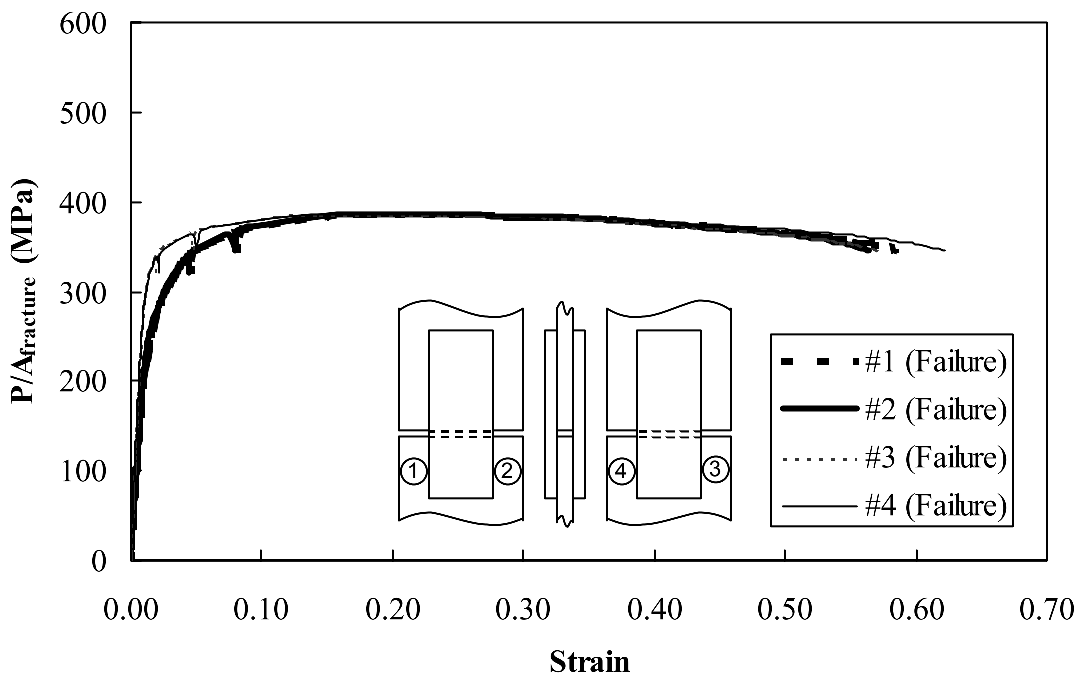

Figure E28 – Specimen L3-1 with Longitudinal Welds from E71T8-K6 Filler Metal

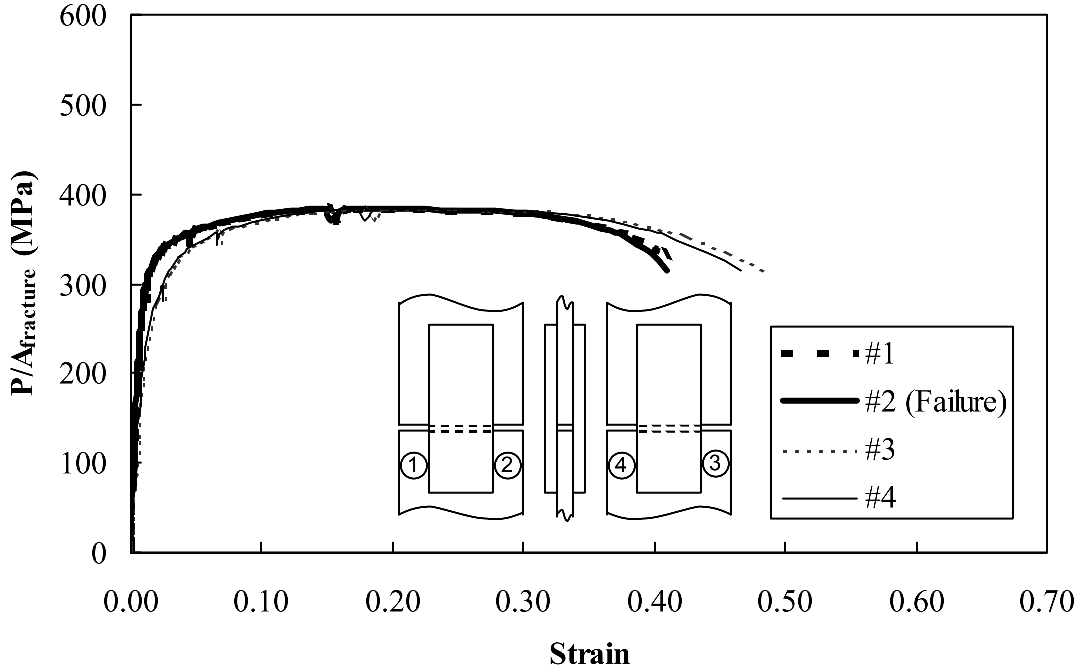

Figure E29 – Specimen L3-2 with Longitudinal Welds from E71T8-K6 Filler Metal

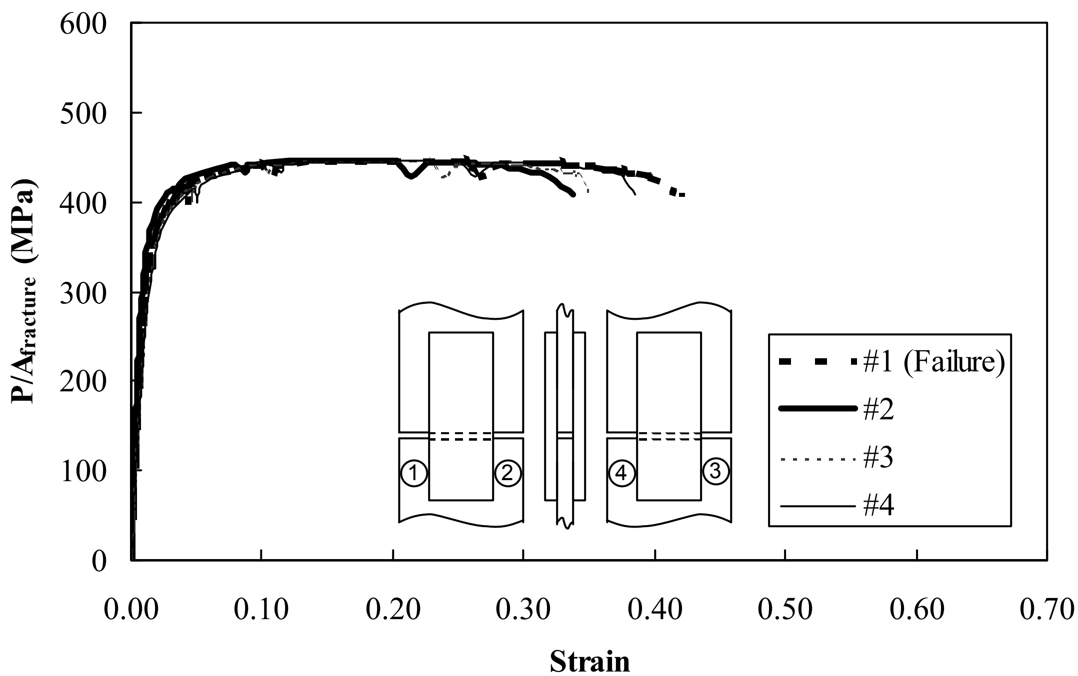

Figure E30 – Specimen L3-3 with Longitudinal Welds from E71T8-K6 Filler Metal

APPENDIX F

Photomicrographs of Weld Fracture Surface

Appendix F – Photomicrographs of Weld Fracture Surface

The fracture surfaces of several specimens of each weld orientation were examined under a scanning electron microscope. Because of space constraints within the machine, samples of approximately 3 mm in length were cut from the fracture surface for this purpose. The photomicrographs taken during the examination are presented in this appendix.

Fracture surfaces of transverse weld specimens that failed at the shear leg and at 23° are shown in Figures F1 and F2, respectively. Both surfaces had elongated microvoids, which indicate ductile failure caused predominately by shear. This type of failure explains the large fracture strains exhibited by specimen T32-2.

Specimens F1-2 and F2-3 failed at an angle of 20° and 28°, respectively, to the main plate. Both fracture surfaces (Figures F3 and F5) contained slightly elongated microvoids, indicating ductile fracture. On the sample from specimen F1-2, inclusions along the weld root were also found (Figure F4), which might account for the lower fracture strain (up to 27% smaller) of this specimen as compared to the other E70T-4 specimens.

The failure angle of specimen F2-1 varied from 14° at one end to 66° at the other end. The fracture surface at the location of the larger failure angle (Figure F6) showed equiaxed microvoids, which are formed from ductile failure in tension. The fracture surface at the location of the smaller failure angle (Figure°F7) showed elongated microvoids, which are formed from ductile failure in which shear played a larger role. Some porosity, not shown in these photos, was also observed on the fracture surface. This porosity did not appear to affect the strength and ductility of the weld.

Specimen F3-1 failed at an angle of 28°. Part of the fracture surface contained equiaxed microvoids indicating ductile failure in tension as displayed in Figure F8, but approximately 70% of the surface showed areas of cleavage fracture such as that shown in Figure F9. There was good penetration on this specimen, but some porosity was present near the weld root. Despite the porosity and the fact that the fracture was mostly brittle, the strength and ductility was still similar to that of the other E71T8-K6 weld specimen (the third specimen failed at the reinforced weld). This is attributable to the small size of the fracture surface examined; the 3 mm sample length may not be representative of the entire fracture surface, which is 50 mm in length.

The failure angles of specimens L1-2 and L2-3 were approximately 23°. As shown in Figures F10 to F13, the fracture surfaces of both specimens contained similar features. Although it is unexpected in longitudinal welds, which are anticipated to fail in shear, the microvoids were not very elongated. The lack of fusion at the weld root as revealed in

Figures F11 and F13 may have caused some of this unexpected behaviour by weakening the welds.

In contrast to the last two specimens, the fracture surface of L3-1 depicted in Figure F14 is more typical of what is expected of longitudinal welds. The microvoids were considerably elongated, indicating ductile shear failure. The failure angle of this specimen was 33°.

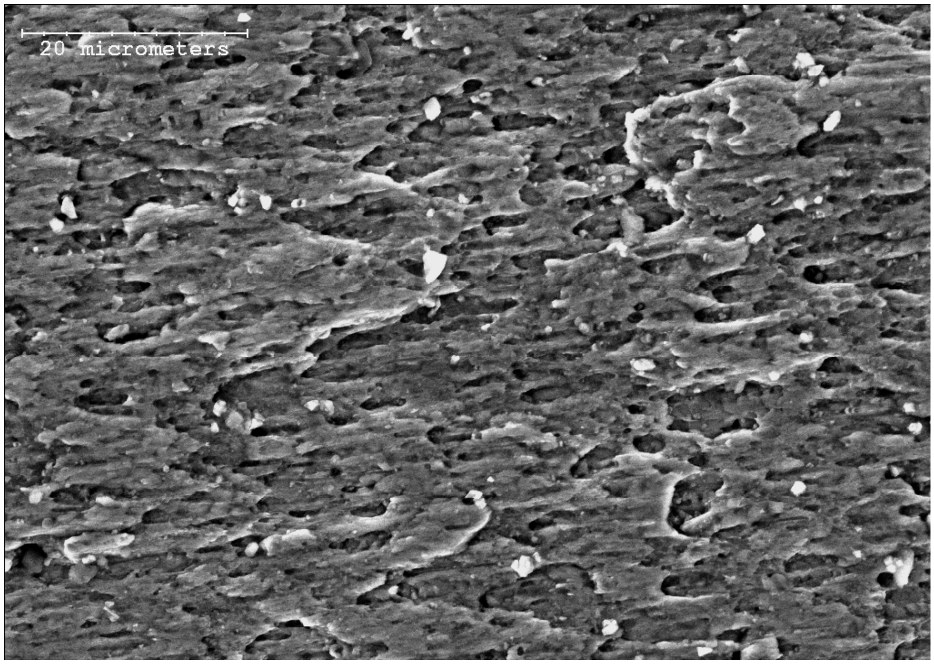

Figure F1 – Elongated Microvoids on Fracture Surface of Specimen T22-2

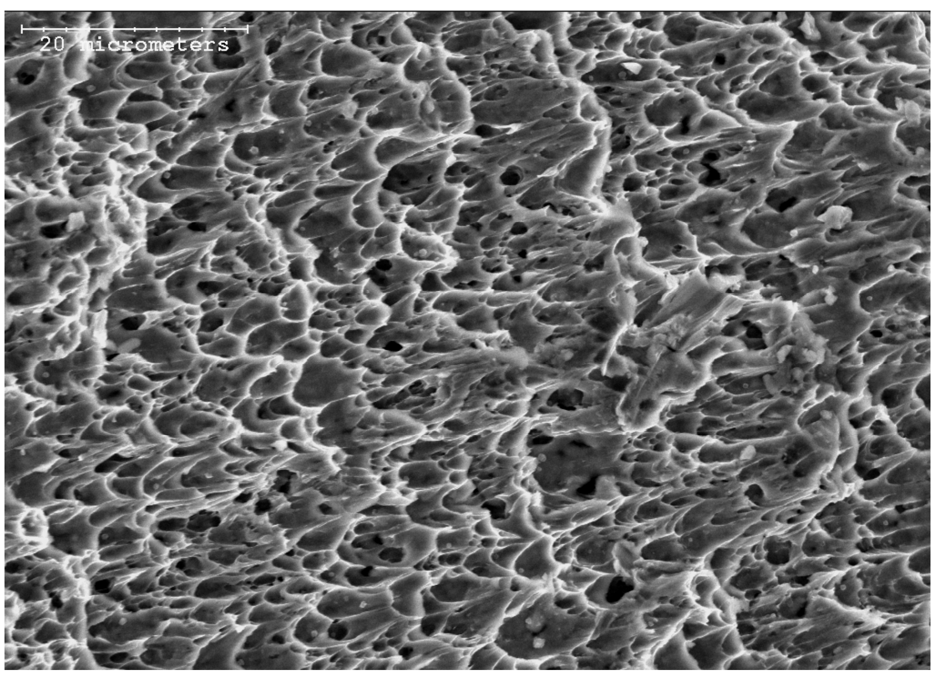

Figure F2 – Elongated Microvoids on Fracture Surface of Specimen T32-2

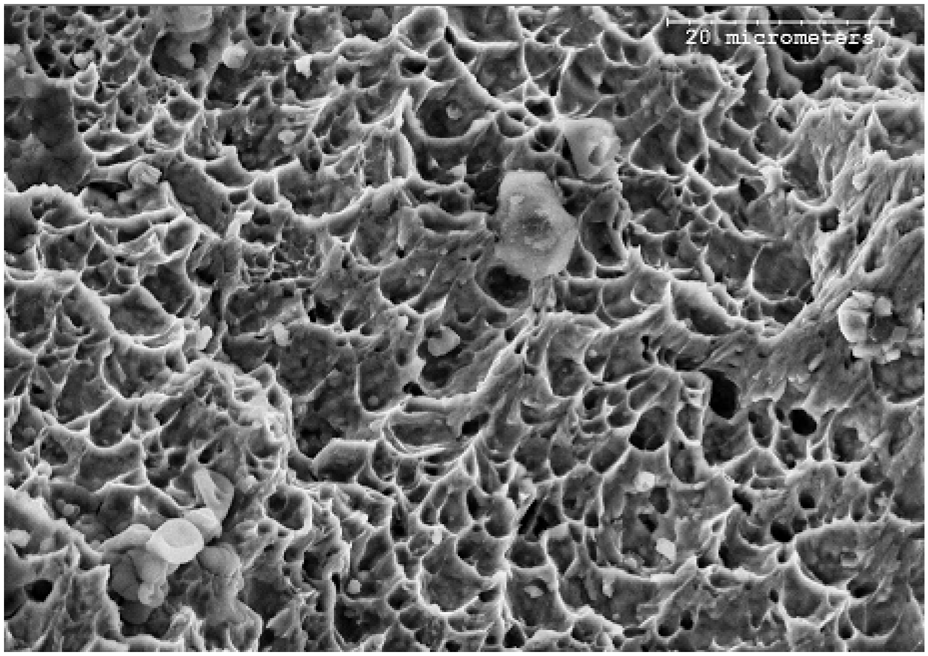

Figure F3 – Equiaxed and Elongated Microvoids on Fracture Surface of Specimen F1-2

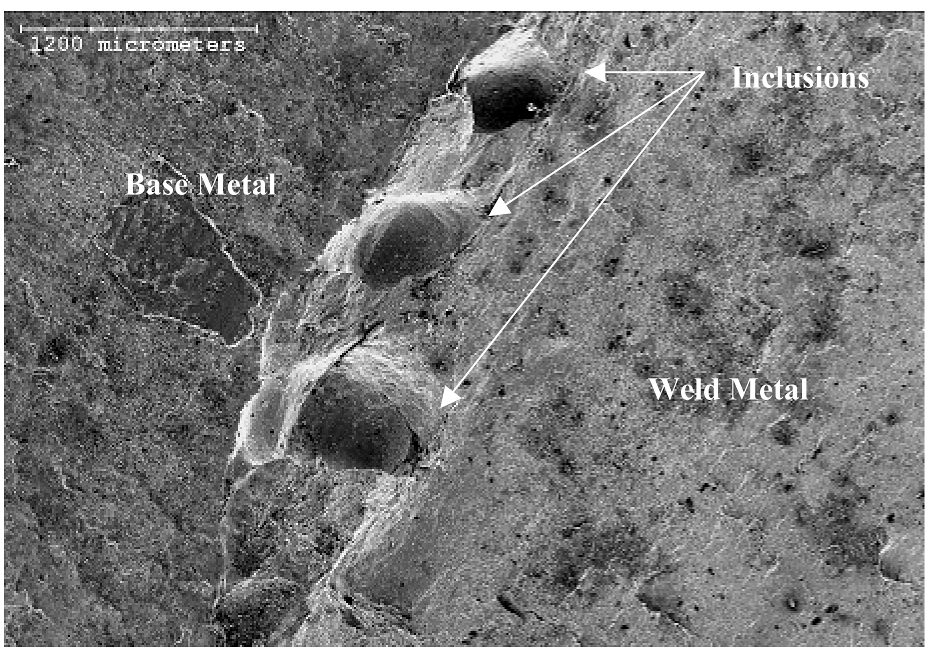

Figure F4 – Inclusions at the Weld Root of Specimen F1-2

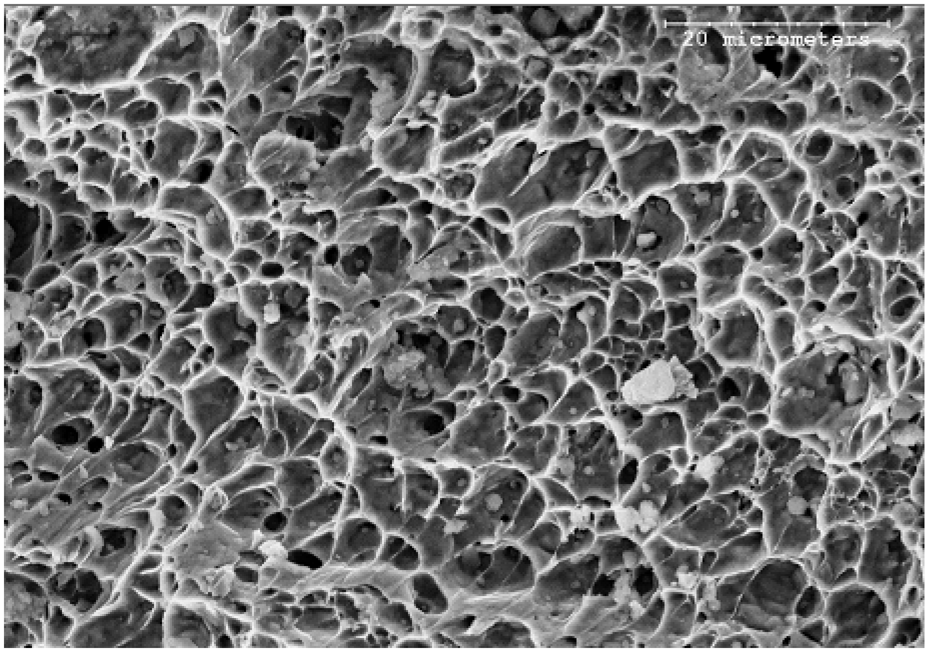

Figure F5 – Elongated Microvoids on Fracture Surface of Specimen F2-3

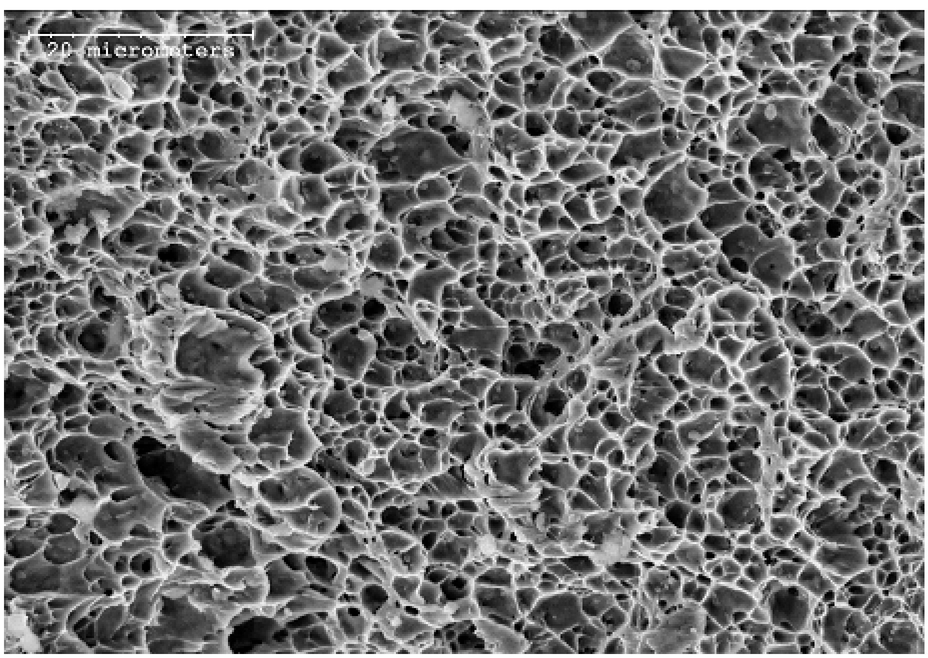

Figure F6 – Microvoids on Fracture Surface of Specimen F2-1

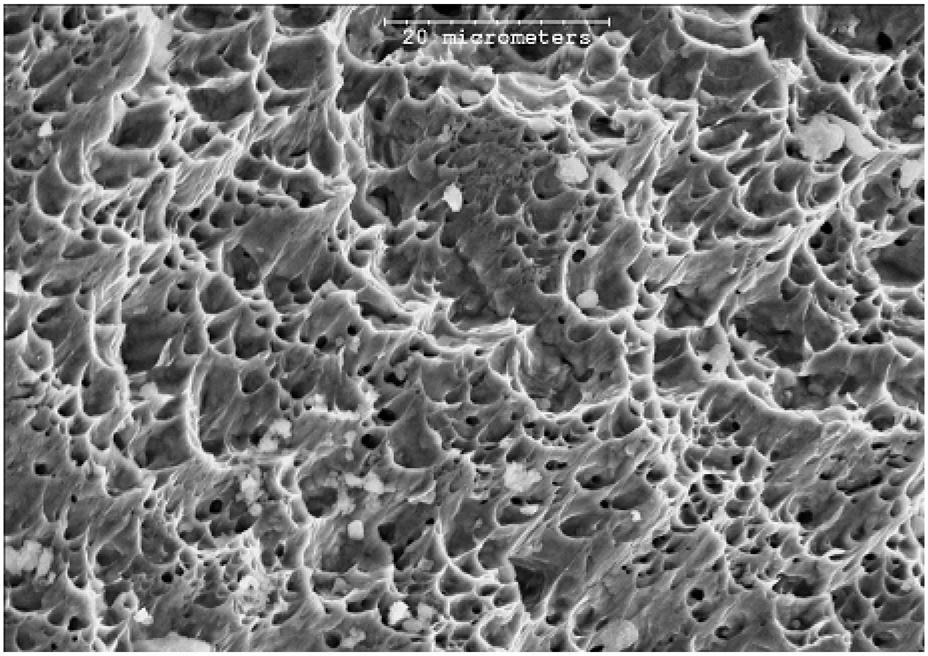

Figure F7 – Elongated Microvoids on Fracture Surface of Specimen F2-1

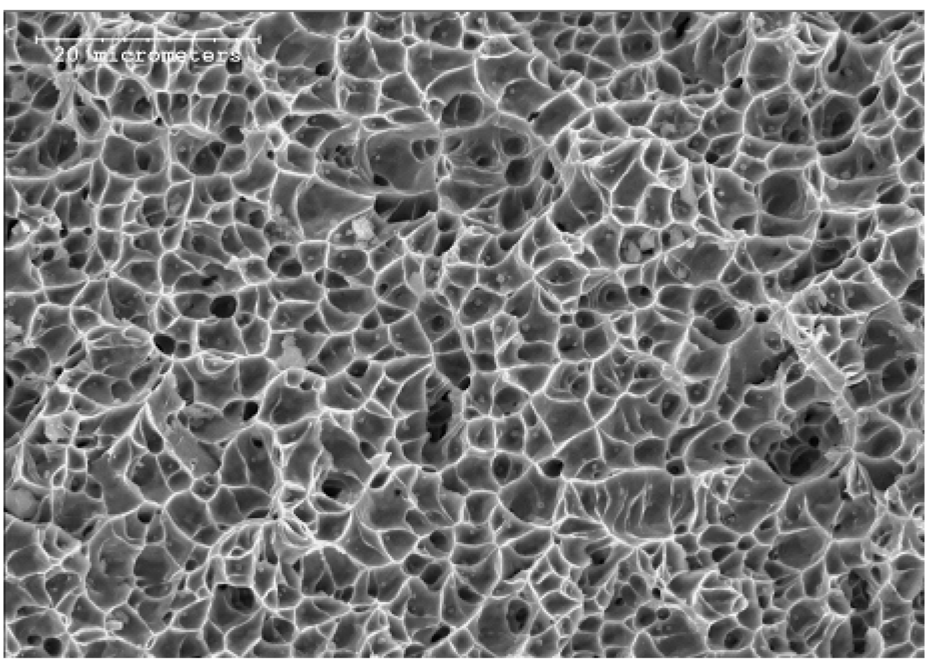

Figure F8 – Microvoids on Fracture Surface of Specimen F3-1

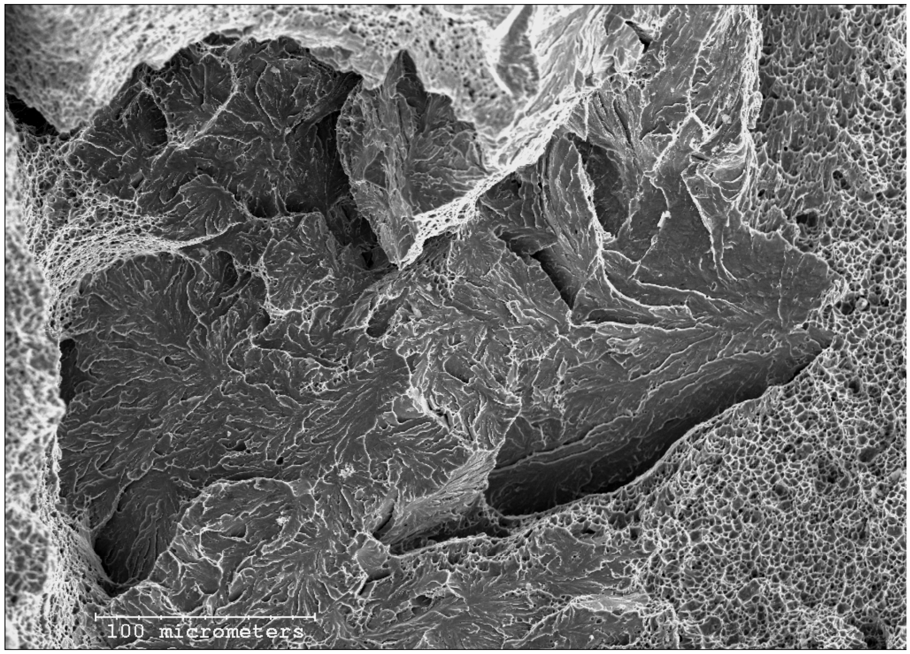

Figure F9 – Cleavage Fracture Surface of Specimen F3-1

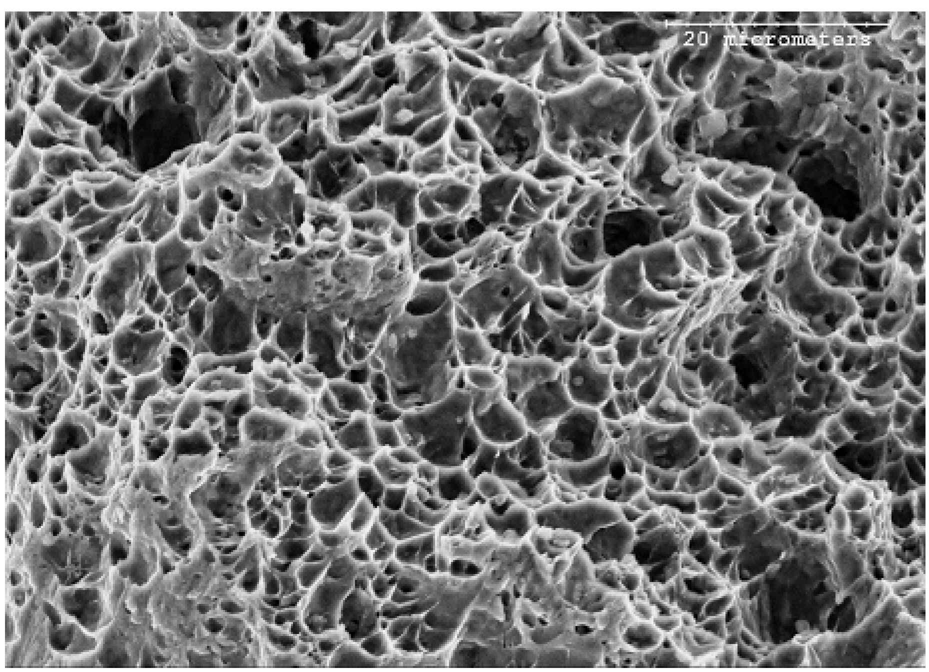

Figure F10 – Microvoids on Fracture Surface of Specimen L1-2

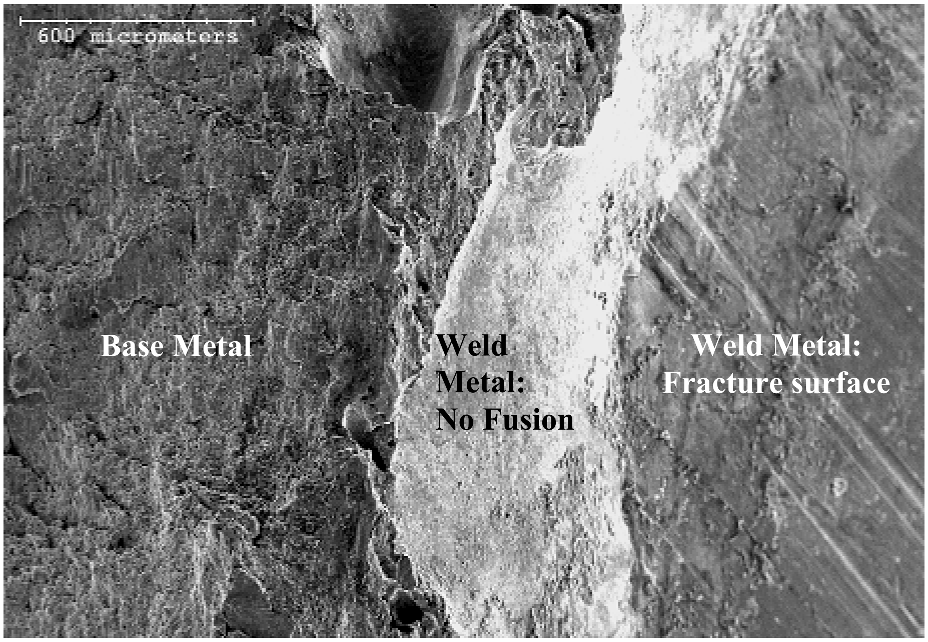

Figure F11 – Lack of Fusion at the Weld Root of Specimen L1-2

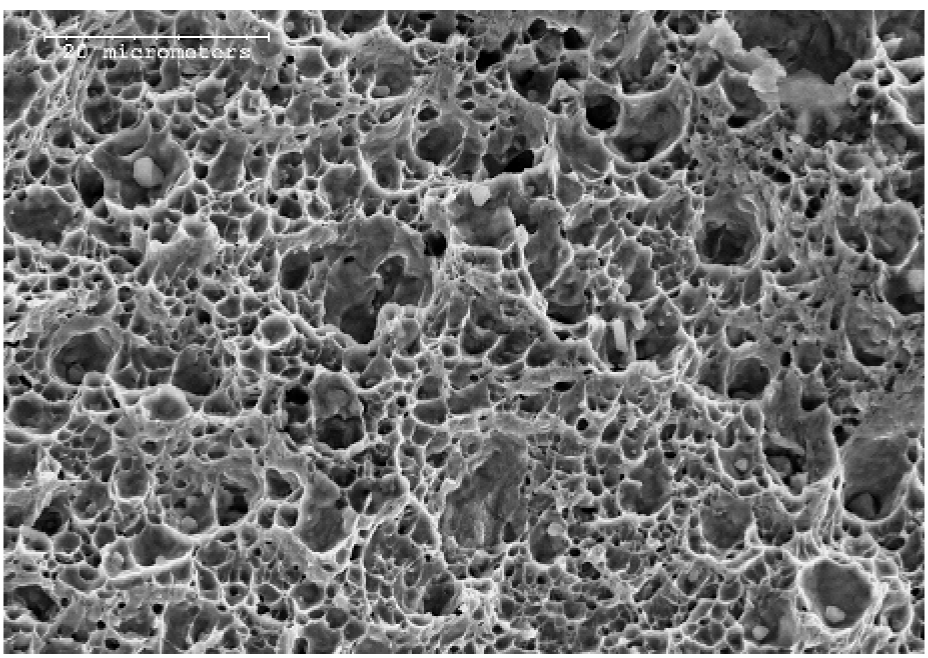

Figure F12 – Microvoids on Fracture Surface of Specimen L2-3

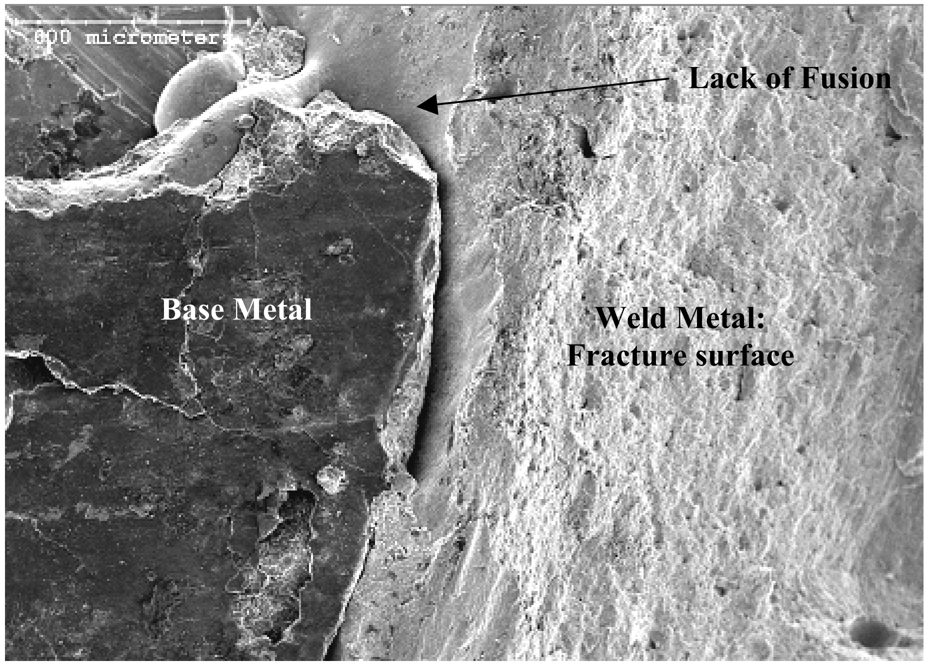

Figure F13 – Lack of Fusion at the Weld Root of Specimen L2-3

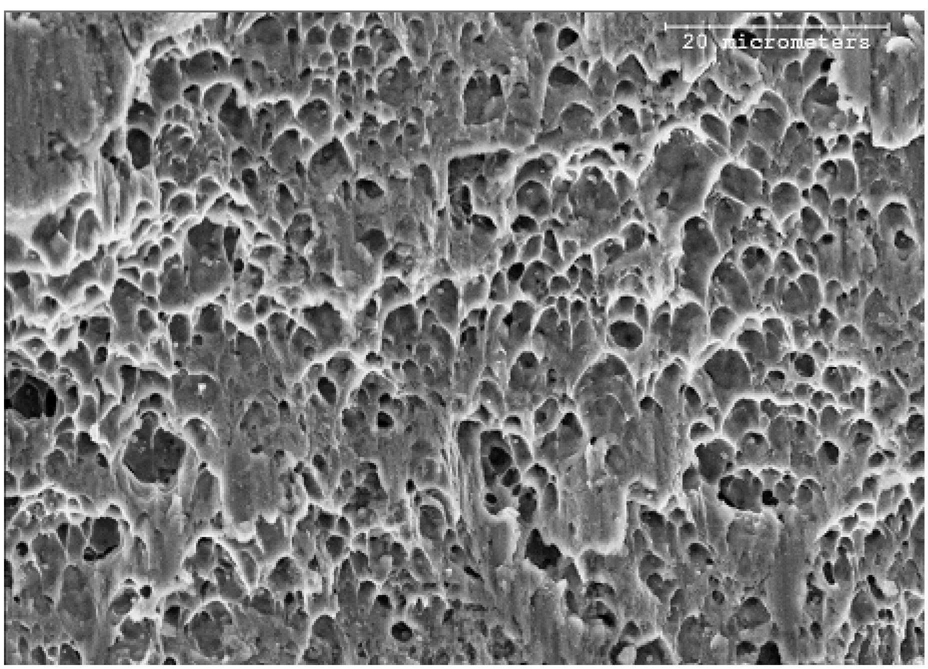

Figure F14 – Elongated Microvoids on Fracture Surface of Specimen L3-1

STRUCTURAL ENGINEERING REPORTS

225. *An Analysis of the Cyclic Behaviour of Steel Gusset Plate Connections* by Scott S. Walbridge, Gilbert Y. Grondin, and J.J. Roger Cheng, September 1998.

226. *Rehabilitation of Unreinforced Masonry Walls with Externally Applied Fiber Reinforced Polymers* by Michael L. Albert, J.J. Roger Cheng, and A.E. Elwi, October, 1998.

227. *Fatigue of Bearing-Type Shear Splices* by Georg Josi, G.Y. Grondin, and G.L. Kulak, April, 1999.

228. *Out-of-Plane Cyclic Behavior of Masonry Walls Reinforced Externally with GFRP* by Marc D. Kuzik, A.E. Elwi, and J.J. Roger Cheng, August 1999.

229. *Cyclic Behavior of Stiffened Gusset Plate–Brace Member Assemblies* by Trina Nast, G.Y. Grondin, and J.J.R. Cheng, November 1999.

230. *Behaviour of Sleeper-supported Line Pipe* by Jeffrey D. DiBattista, J.J.R. Cheng, and D.W. Murray, April 2000.

231. *Field Assessment of Crowchild Trail Bridge* by Kong K. Taing, J.J.R. Cheng, and S. Afhami, January 2000.

232. *Ductile Fracture of Steel* by Heng Aik Khoo, J.J. Roger Cheng, and T.M. Hrudey, August 2000.

233. *Shear Lag in Bolted Cold-Formed Steel Angles and Channels in Tension* by Amy Sin-Man Yip and J.J. Roger Cheng, September 2000.

234. *Behaviour of Reinforced Concrete Beams Strengthened in Shear with FRP Sheets* by Christophe Deniaud and J.J. Roger Cheng, October 2000.

235. *Behaviour of Distortion-Induced Fatigue Cracks in Bridge Girders* by R. Fraser, G.Y. Grondin, and G.L. Kulak, December 2000.

236. *Stiffener Tripping in Stiffened Steel Plates* by I.A. Sheikh, A.E. Elwi and G.Y. Grondin, January 2001.

237. *Critical Buckling Strains for Energy Pipelines* by A.B. Dorey, J.J.R. Cheng and D.W. Murray, April 2001.

238. *Local buckling and Fracture Behaviour of Line Pipe under Cyclic Loading* by Brian Myrholm, J.J.R. Cheng and D.W. Murray, May 2001.

239. *Behaviour of Welded Cold-Formed Steel Tension* Members by Alvaro Lemenhe and J.J.R. Cheng, July 2001.

240. *Behaviour and Rehabilitation of Distortion-Induced Fatigue Cracks in Bridge Girders* by M. D'Andrea, G.Y. Grondin, and G.L. Kulak, September 2001.

241. *Punching Shear Capacity of Slab-Column Connections with Steel-Fibre reinforcement under Lateral Cyclic Loading* by Sascha K. Schreiber and Scott D.B. Alexander, September 2001.

242. *Behaviour of Slabs with Fibre-Reinforced Polymer Reinforcement* by Carlos E. Ospina, Roger J.J. Cheng, and Scott D.B. Alexander, October 2001.

243. *Behaviour of Slab-Column Connections with Partially Debonded Reinforcement under Cyclic Lateral Loading* by M.A. Ali and S.D.B. Alexander, January 2002.

244. *Block Shear Behaviour of Coped Steel Beams* by Cameron R. Franchuk, Robert G. Driver, and Gilbert Y. Grondin, September 2002.

245. *Behaviour of Transverse Fillet Welds* by Anthony K.F. Ng, Robert G. Driver, and Gilbert Y. Grondin, October 2002.

246. *Analysis of Buried Pipelines with Thermal Applications* by Nader Yoosef-Ghodsi, and D.W. Murray, October 2002.

247. *Fracture of Wrinkled Energy Pipelines* by Das, S., Cheng, J.J.R., Murray, D.W., November 2002.

248. *Block Shear Behaviour of Bolted Gusset Plates* by Bino Baljit Singh Huns, Gilbert Y. Grondin, and Robert G. Driver, December 2002.

249. *Numerical Solutions for Pipeline Wrinkling* by Song, X., Cheng, J.J.R., Murray, D.W., January 2003.

250. *Behaviour of Steel Columns Reinforced with Welded Steel Plates* by Ziqi Wu and Gilbert Y. Grondin, February 2003.

251. *Effect of Loading Angle on the Behaviour of Fillet Welds* by Kam Deng, Gilbert Y. Grondin, and Robert G. Driver, March 2003.